

**DIAMINO DIAMIDE COPPER COMPLEXES  
as ANTI-ARTHRITIC AGENTS**

A thesis submitted to the

**UNIVERSITY of CAPE TOWN**

in fulfilment of the requirements for the degree of

**DOCTOR of PHILOSOPHY**

by

**ALEXANDER VOYÉ**

**M.Sc. (UCT)**

Department of Chemistry  
University of Cape Town  
Rondebosch 7700  
South Africa

**July 1993**

The University of Cape Town has been given  
the right to reproduce this thesis in whole  
or in part, without charge, for the author.

The copyright of this thesis vests in the author. No quotation from it or information derived from it is to be published without full acknowledgement of the source. The thesis is to be used for private study or non-commercial research purposes only.

Published by the University of Cape Town (UCT) in terms of the non-exclusive license granted to UCT by the author.

**To My Parents**

## ACKNOWLEDGEMENTS

I would like to express my most sincere thanks and appreciation to my supervisors, Professor Peter W. Linder and Professor Graham E. Jackson. In particular I would like to thank them for their tremendous support, encouragement and friendship that I have enjoyed throughout the many years of this research.

I would also like to extend my thanks to the following:

- ⇒ Professor Mino R. Caira and Dr Margaret Niven for their invaluable assistance with the X-ray crystallographic work.
- ⇒ Dr Ralph G. Torrington and Mr Leonard Barbour for helping with many of the computing aspects.
- ⇒ Dr Mike Byrne and Professor Gerry Blekkenhorst from the UCT Nuclear Medicine and Radiotherapy Units for assistance with the animal study.
- ⇒ Karen van der Meulen for her moral support and never-ending encouragement.
- ⇒ The University of Cape Town and the Foundation for Research and Development for financial assistance.

## ABSTRACT

This thesis describes the investigation of a series of diamino diamide copper(II) complexes with respect to their potential as anti-inflammatory agents in the treatment of rheumatoid arthritis. Several physico-chemical techniques were employed in the investigation including glass electrode potentiometry, UV/VIS spectroscopy, molecular mechanics calculations, speciation modelling as well as X-ray crystallography. Animal experiments were also carried out.

Stability constants were determined at 25°C in 0.15 mol dm<sup>-3</sup> (Na)[Cl] and are reported for the ligands N,N' bis [2-(dimethylamino)ethyl] ethanediamide (5UM), N,N' bis [2-(diethylamino)ethyl] ethanediamide (5UE), N,N' bis [2-(dimethylamino)ethyl] propanediamide (6UM) and N,N' bis [3-(dimethylamino)propyl] ethanediamide (656UM) with copper(II). The complexes ML, MLH<sub>1</sub> and MLH<sub>2</sub> were common to all four systems, with the oxamide derivatives forming the additional binuclear complex, M<sub>2</sub>LH<sub>2</sub>. Two other unique complexes, i.e. M<sub>2</sub>LH<sub>3</sub> and MLH<sub>3</sub>, were formed by the ligands 5UM and 656UM respectively. The order of stability of the uncharged MLH<sub>2</sub> species, which are of particular interest as possible *in vivo* copper(II) mobilizers, was found to be 5UM > 5UE > 6UM > 656UM. This was rather unexpected based on the analogous series of tetramine ligands.

In the UV/VIS investigation, absorption wavelengths corresponding to the extinction maxima of the individual species in aqueous solution were determined. These results indicated that for the major binary complexes, an increasing number of liganding nitrogen atoms are present in the coordination sphere of the copper(II) ions. Thus the ML, MLH<sub>1</sub> and MLH<sub>2</sub> species of all four ligands have 2, 3 and 4 copper to nitrogen bonds respectively.

The structures of the complexes in solution could therefore be determined and their strain energy was subsequently investigated by molecular mechanics calculations. Due to difficulties associated with molecular mechanics calculations involving coordination compounds, use was made of an innovative approach in which the energy changes on MLH<sub>2</sub> complexation of the methyl substituted ligands with copper(II) were compared. It was found that these results could successfully explain the anomalous order of stability.

The crystal structure of [C<sub>11</sub>H<sub>24</sub>O<sub>2</sub>N<sub>4</sub>Cl<sub>2</sub>]<sub>2</sub> (Cu<sub>4</sub>OCl<sub>10</sub>), which incorporates the hexa- $\mu_2$ -chloro- $\mu_4$ -oxo-tetra[chlorocuprate(II)] anion, was solved by Patterson and difference Fourier heavy-atom direct methods. The crystals are monoclinic with unit cell dimensions of  $a = 14.405 \text{ \AA}$ ,  $b = 15.805 \text{ \AA}$ ,  $c = 20.644 \text{ \AA}$  and  $\beta = 99.61^\circ$  and a space group of C2/c with  $Z = 4$ . Refinement was carried out by full-matrix least-squares calculations including anisotropic thermal parameters for all non-hydrogen atoms. The final weighted  $R$  factor was 0.059.

Finally, animal experiments were carried out, in which the tissue distribution of radio-active <sup>67</sup>Cu in white mice was determined following interperitoneal administration of the copper(II) complexes of 5UM, 3,6,9,12-tetra-azatetradecanedioic acid (TTDA) and 3,6,9-triazaundecanedioic acid (DTDA), respectively. The results indicate that the 5UM complex is not sufficiently stable *in vivo* and hence rapidly dissociates, resulting in a tissue distribution similar to that of <sup>67</sup>CuCl<sub>2</sub>. The latter two ligands, although forming stable complexes *in vivo*, were rapidly excreted in the urine and are therefore also not of much use as anti-inflammatory agents.

## TABLE OF CONTENTS

	page no.
Acknowledgements	i
Abstract	ii
Table of Contents	iv
List of Symbols and Abbreviations	vi
Structural Formulae	x
<b>CHAPTER ONE : GENERAL INTRODUCTION</b>	
1.1 Rheumatoid Arthritis (RA)	1
1.2 Drugs Used in the Treatment of RA	7
1.3 The Involvement of Copper	11
<b>CHAPTER TWO : LIGANDS</b>	
2.1 Complexation and the Chelate Effect	15
2.2 Ligand Requirements	17
2.3 Choice of Ligands	19
2.4 The Aims of this Study	23
<b>CHAPTER THREE : EXPERIMENTAL</b>	
3.1 Introduction	24
3.2 Potentiometric Theory	27
3.2.1 Complex Formation	27
3.2.2 Computational Considerations	41
3.3 Experimental Procedure	45
3.4 Results and Observations	50
3.4.1 Protonation	51
3.4.2 Complexation with Copper(II)	55
3.4.2.1 N,N' bis [2-(dimethylamino)ethyl] ethanediamide (5UM)	57
3.4.2.2 N,N' bis [2-(diethylamino)ethyl] ethanediamide (5UE)	64

3.4.2.3 N,N' bis [2-(dimethylamino)ethyl] propanediamide (6UM)	66
3.4.2.4 N,N' bis [3-(dimethylamino)propyl] ethanediamide (656UM)	70
3.5 UV/VIS Analysis	73
3.5.1 Theory and Procedure	73
3.5.2 Results	79
3.6 Discussion	85
<b>CHAPTER FOUR : COMPUTER MODELLING</b>	
4.1 Introduction	98
4.2 Theory	101
4.3 Computational Procedure	111
4.3.1 Choice of Program	114
4.3.2 Force-Field Parametrization	115
4.3.3 Model Validation	119
4.3.3.1 Structural Comparisons	119
4.3.3.2 Energetic Comparisons	129
4.4 Results and Discussion	135
<b>CHAPTER FIVE : ANIMAL EXPERIMENTS</b>	
5.1 Introduction	145
5.2 Experimental Procedure	146
5.3 <i>In Vivo</i> Modelling	147
5.4 Results and Discussion	148
<b>CHAPTER SIX : CONCLUDING REMARKS</b>	
153	
APPENDIX A : Ligand Synthesis	156
APPENDIX B : Molecular Mechanics Force-Field	164
APPENDIX C : Crystal Structure Determination	171
<b>REFERENCES</b>	

## LIST OF SYMBOLS

<b>A</b>	: Debye-Hückel constant, equa. 3.5
<b>a</b>	: activity, defined by equa. 3.3
$\hat{a}_i$	: ionic size parameter of the <i>i</i> th ion, equa. 3.5
<b>B</b>	: Debye-Hückel constant, equa. 3.5
$\beta_{pqr}$	: overall stoichiometric formation constant, equa. 3.4
${}^T\beta_{pqr}$	: thermodynamic formation constant, equa. 3.1
<b>C</b>	: empirical constant, equa. 3.5
$c_i$	: concentration of the <i>i</i> th ion ( $\text{mol dm}^{-3}$ ), equa. 3.6
$\gamma$	: molar activity coefficient, equa. 3.3
$\gamma_i$	: activity coefficient of the <i>i</i> th ion, equa. 3.5
<b>D</b>	: dielectric constant, equa. 4.7
$\delta$	: NMR chemical shift (ppm)
<b>E</b>	: measured EMF of the cell (volt), equa. 3.11
$E^\circ$	: electrode response intercept (volt), equa. 3.11
$E_b$	: bond angle bending potential, equa. 4.2
$E_{elec}$	: electrostatic potential, equa. 4.7
$E_{hb}$	: hydrogen bonding potential, equa. 4.8
$E_{opb}$	: out-of-plane bending potential, equa. 4.2
$E_{sb}$	: bond stretching, angle bending potential, equa. 4.6
$E_{vdw}$	: van der Waals potential, equa. 4.5
$E_\omega$	: torsion angle potential, equa. 4.3
$\epsilon$	: molar absorption coefficient ( $\text{mol}^{-1} \text{dm}^3 \text{cm}^{-1}$ )
<b>F</b>	: Faraday constant
$\Delta G^\circ$	: standard Gibbs free energy change of reaction ( $\text{kJ mol}^{-1}$ )
$g_i$	: degeneracy of the <i>i</i> th energy level
$hkl$	: crystallographic Miller indexes
$\Delta H^\circ$	: standard enthalpy change of reaction ( $\text{kJ mol}^{-1}$ ), equa. 3.8
<b>I</b>	: ionic strength ( $\text{mol dm}^{-3}$ ), equa. 3.6
<b>J</b>	: NMR coupling constant (Hz)
$K_i$	: stepwise stoichiometric formation constant
${}^TK_i$	: stepwise thermodynamic formation constant, equa. 3.2

$K_w$	: dissociation constant of water
$k$	: Boltzman constant
$k_b$	: angle bending force constant, equa. 4.2
$k_{opb}$	: out-of-plane bending force constant, equa. 4.3
$k_s$	: bond stretching force constant, equa. 4.1
$k_{sb}$	: stretch-bend force constant, equa. 4.6
$l$	: bond length (Ångström)
$l^\circ$	: strain-free or natural bond length (Ångström), equa. 4.1
$l$	: path-length (cm), equa. 3.26
$\lambda$	: wavelength (nm)
$\bar{n}$	: complexation function defined by equa. 3.18 & 3.19
$\bar{n}_H$	: protonation function defined by equa. 3.14 & 3.15
$\bar{n}_H^*$	: protonation function defined by equa. 3.21
$n_p$	: number of parameters to be optimized, equa. 3.22
p.m.i.	: plasma mobilization index
$Q_\gamma$	: quotient of activity coefficients
$\bar{Q}$	: deprotonation function defined by equa. 3.20
$q$	: partial atomic charge, equa. 4.7
$\theta^\circ$	: strain-free bond angle (degrees), equa. 4.2
$R$	: natural gas constant ( $JK^{-1} mol^{-1}$ ), equa. 3.8
$R^H$	: Hamilton R-factor, defined by equa. 3.24
$R_{lim}$	: limit of the Hamilton R-factor
$R$	: crystallographic R-factor, Table C1
$R_w$	: crystallographic weighted R-factor
$r^*$	: sum of the van der Waals radii (Ångström), equa. 4.5
$S$	: Nernstian slope, equa. 3.11
$\Delta S^\circ$	: standard entropy change of reaction ( $J mol^{-1}$ ), equa. 3.8
$\sigma$	: standard deviation, equa. 3.23
$T$	: absolute temperature (Kelvin), equa. 3.8
$T_H$	: total proton concentration ( $mol dm^{-3}$ ), equa. 3.13
$T_H^*$	: calculated total proton concentration ( $mol dm^{-3}$ ), equa. 3.20
$T_L$	: total ligand concentration ( $mol dm^{-3}$ ), equa. 3.9 & 3.16
$T_M$	: total metal concentration ( $mol dm^{-3}$ )

U	: Boltzman mean strain energy (kJ mol <sup>-1</sup> )
U <sub>obj</sub>	: objective function defined by equa. 3.22
w	: crystallographic weighting scheme, Table C1
w <sub>n</sub>	: titration point weighting defined by equa. 3.23
ω	: torsion angle (degrees), equa. 4.4
z <sub>i</sub>	: charge on the ith ion, equa. 3.5
ζ*	: potential energy-well depth, equa. 4.5

*Ligand Abbreviations used in this Study*

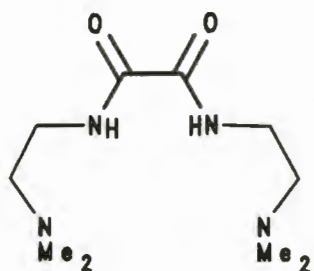
5tet	: 3,6-diazaoctanediamine
656tet	: 4,7-diazadecanediamine
6tet	: 3,7-diazanonanediamine
55tri	: 3-azapentanediamine
56tri	: 3-azaheptanediamine
66tri	: 4-azaoctanediamine
5DH	: 3,6-diazaheptanediamide
656DH	: 4,7-diazadecanediamide
6DH	: 3,7-diazaoctanediamide
5UE	: N,N' bis [2-(diethylamino)ethyl] ethanediamide
5UH	: N,N' bis [aminoethyl] ethanediamide
5UM	: N,N' bis [2-(dimethylamino)ethyl] ethanediamide
656UH	: N,N' bis [aminopropyl] ethanediamide
656UM	: N,N' bis [3-(dimethylamino)propyl] ethanediamide
6UE	: N,N' bis [2-(diethylamino)ethyl] propanediamide
6UH	: N,N' bis [aminoethyl] propanediamide
6UM	: N,N' bis [2-(dimethylamino)ethyl] propanediamide
5MH	: 2,7-dioxa-3,6-diazaoctanediamine
bipy	: 2,2'-bipyridine
DTDA	: 3,6,9-triazaundecanedioic acid
DTPA	: diethylenetriamine-N,N,N',N'',N''-pentaacetic acid
EDTA	: ethylenediaminetetraacetic acid
en	: ethylenediamine
glyalaNH <sub>2</sub>	: glycyl-β-alanine amide

glyglyNH <sub>2</sub>	:	glycylglycine amide
mono5UM	:	N [2-(dimethylamino)ethyl] ethanediamide
TETA	:	1,4,8,11-tetra-azacyclotetradecane-N,N',N'',N'''-tetraacetic acid
tn	:	trimethylenediamine
trien	:	triethylenetetramine (see 5tet)
TTDA	:	3,6,9,12-tetra-azatetradecanedioic acid

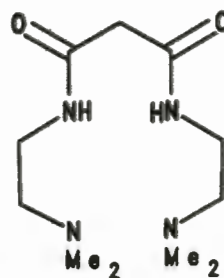
*Other Abbreviations used in this Study*

AZA	:	Azathioprine
CDCl <sub>3</sub>	:	Deuterated Chloroform
CSD	:	Cambridge Structural Database
DCI	:	Deuterium Chloride
DMARDS	:	Disease-Modifying Antirheumatic Drugs
D <sub>2</sub> O	:	Deuterium Oxide
Et	:	Ethyl Group
GI	:	Gastrointestinal
HSA	:	Human Serum Albumin
HSAB	:	Hard and Soft Acids and Bases
IgG	:	Immunoglobulin G
MCMM	:	Monte Carlo Multiple conformer energy Minimization
Me	:	Methyl Group
MeCN	:	Acetonitrile
MTX	:	Methotrexate
NMR	:	Nuclear Magnetic Resonance
NSAIDS	:	Nonsteroidal Anti-Inflammatory Drugs
PG	:	Prostaglandin
PMN	:	Polymorphonuclear Neutrophil
RA	:	Rheumatoid Arthritis
RF	:	Rheumatoid Factor
SOD	:	Superoxide Dismutase
SSZ	:	Sulfasalazine
THF	:	Tetrahydrofuran
UV	:	Ultra Violet
VIS	:	Visible

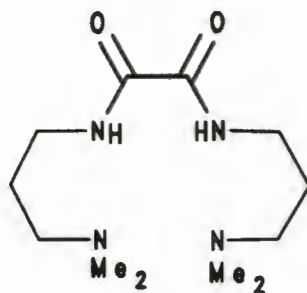
STRUCTURAL FORMULAE OF LIGANDS  
INVESTIGATED IN THIS STUDY



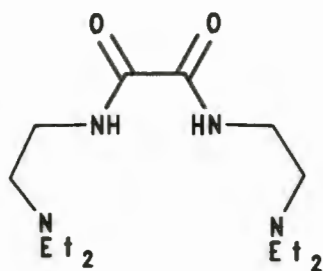
5UM



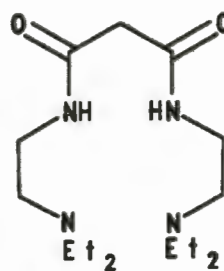
6UM



656UM

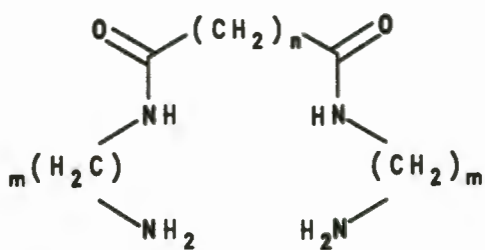


5UE



6UE

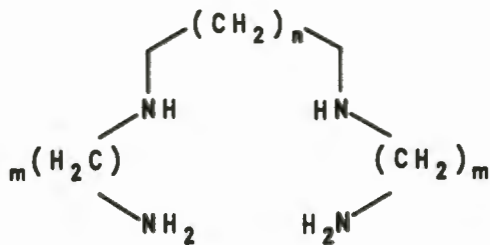
*Structural Formulae of Additional Ligands Discussed in this Study*



5UH :  $n=0$ ;  $m=2$

6UH :  $n=1$ ;  $m=2$

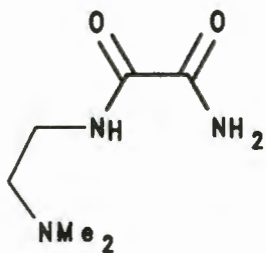
656UH :  $n=0$ ;  $m=3$



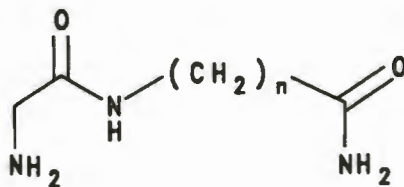
5tet :  $n=0$ ;  $m=2$

6tet :  $n=1$ ;  $m=2$

656tet :  $n=0$ ;  $m=3$

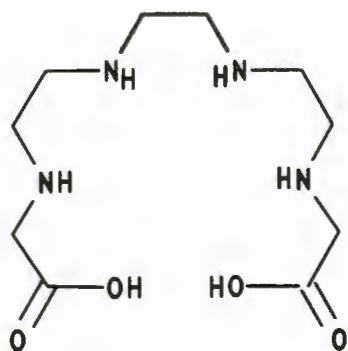


mono5UM

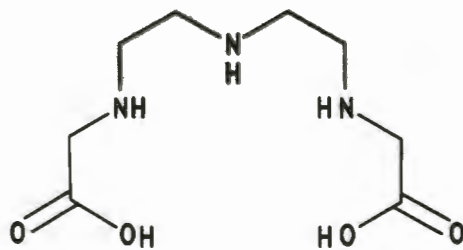


glyglyNH<sub>2</sub> :  $n=1$

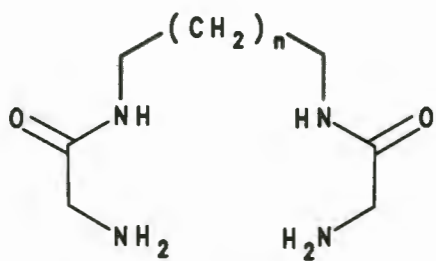
glyalaNH<sub>2</sub> :  $n=2$



TTDA

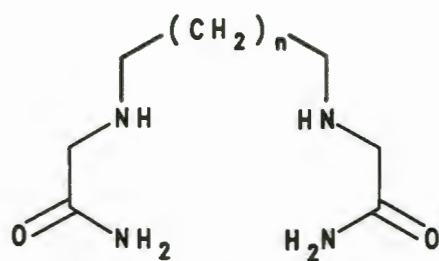


DTDA



5MH : n=0

6MH : n=1



5DH : n=0

6DH : n=1

**CHAPTER ONE**  
**INTRODUCTION**

## 1.1 RHEUMATOID ARTHRITIS (RA)

Rheumatoid Arthritis (RA) is probably the best known of the autoimmune rheumatic diseases (which include Systemic lupus erythematosus, Scleroderma and Polymyositis amongst others) afflicting between 0.3 and 1.5% of the worlds population [1]. Some reports have even suggested the incidence of RA to be as high as 5% [2]. Women are affected two to three times more often than men and although the incidence of RA generally increases with advancing years reaching a peak between 40 and 60, the disease can occur at any age [1].

Although the skin and the lungs can also be involved, RA primarily manifests itself as a painful inflammation of the synovial joints, often causing considerable erosion of the cartilage and bone. Much of this articular damage is irreversible and can be extremely debilitating, leading to a substantial decrease in the quality of life of patients with unremitting chronic RA [3]. Although the effects are not considered to be fatal in the same way as cancer, there is an increased mortality associated with the disease which justifies the ongoing research.

However, despite many decades of intensive investigation the aetiology of RA remains obscure and the pathogenesis is only poorly understood [3, 4]. Virtually everything that is known about this disease has been extensively covered in the literature, with a number of in-depth medical textbooks dedicated exclusively to the subject [2, 3, 4, 5, 6, 7]. A detailed review of RA is far beyond the scope of this thesis and therefore only a short overview of some of the salient features will be given here.

Hopes are waning for the discovery of a single aetiology for RA due to the failure of finding a specific exogenous or endogenous agent of causation [8]. Various hypotheses have been proposed for the aetiology of this chronic disease. No evidence exists to suggest

that RA is caused by nutritional factors, metabolic errors, endocrine abnormalities, cold, damp or even injuries [9]. However, as polyarthritis occurs during many bacterial, spirochetal and viral infections, added to the fact that various forms of arthritis and synovitis can be experimentally induced in laboratory animals, much interest is currently centered on infectious aetiologies [1].

Thus mycoplasma and bacterial antigens have been used in animal models as synovial inciters, whereas systemic administration of bacterial peptidoglycans resulting in chronic destructive inflammatory synovitis is an example of a remote inciter [1, 10]. It has also been shown that type II collagen can cause arthritis in rats, mice and even primates [8]. Of greater current interest however, are possible viral infections acting as triggering mechanisms of RA. Thus it is known that lentiviruses cause a deforming arthritis in goats and sheep. Furthermore an inflammatory polyarthritis in humans is sometimes brought about by the rubella virus as well as the human B19 strain of parvovirus. The rubella virus even has a propensity for localization in cartilage when injected systemically.

Viruses could act as triggering agents in a number of different ways. The first hypothesis involves sequestration of the virus in the articular cartilage leading to a localized immune response. The second proposition relies on the fact that acute synovitis often results from circulating immune complexes which happen to accompany most viral infections. The third hypothesis, possibly implicating the Epstein-Barr virus, consists of viral alteration of the immune system causing the production of potentially harmful autoantibodies such as rheumatoid factors (RFs) [1]. Thus, although the precise aetiology remains unknown, it seems most likely that several micro-organisms may serve as triggering events of RA, in association with genetic predisposition of the host [3, 8, 10].

Whatever the cause of RA it is generally accepted that the initial effect is a breakdown of the local immune system, for instance due to defective B-lymphocyte

function or T-cell regulatory suppression. It has been suggested that this causes production of autoantibodies directed against antigenic determinants on native or denatured/altered immunoglobulin G (IgG). Immunoglobulins are antibodies themselves and form a major part of the normal immune response. Thus 'self' recognition has occurred and therefore RA is known as an autoimmune disorder. Several hypotheses have been advanced to explain how IgG could become immunogenic [8]. One proposition is that the conformation of IgG is altered by a thiol-disulphide interchange reaction [11].

These antiglobulins or autoantibodies are known as Rheumatoid factors and are found in the serum and joint fluid of most patients. The RFs are nonspecific and interact with a number of immunoglobulin types in the synovial fluid, to form extravascular immune complexes. This activates the complement system and causes polymorphonuclear neutrophils (PMNs) to migrate into the joint. The  $\gamma$ -globulin immune complexes are subsequently phagocytosed by the PMNs. This process is associated with a release of lysosomal enzymes (proteinases) and considerably increased production of oxygen radicles, thereby amplifying the Rheumatoid synovitis. The lysosomal proteinases have the potential to digest collagen, cartilage matrix and elastic tissue thereby creating more antigenic material and perpetuating the inflammation. The oxygen radicles, such as the superoxide anion, are highly reactive entities and can directly cause tremendous cellular injury. They are thus normally rapidly eliminated by superoxide dismutase (SOD), a copper and zinc dependent enzyme, by the following reaction.



Accompanying the activation of PMNs is an increased mobilization of membrane phospholipids, resulting in release of arachidonic acid and its subsequent oxidation by cyclo-oxygenase to form proinflammatory prostaglandins (PGs).

Other body components can also act as autoantigens, e.g. collagen. However it is not thought that these constitute the primary lesion in RA but are a secondary reaction well suited to propagate tissue injury. Joints are however predisposed to injury and inflammation as they are moving, load bearing structures and therefore subject to microtrauma almost constantly. Thus a breakdown of the normal immune system involved in tissue repair is also an attractive theory.

Figure 1.1 is a schematic representation of a normal joint [12]. Its ability to function properly as a load bearing structure depends on the integrity and correct alignment of the opposing surfaces of articular cartilage, as well as the thickness and pattern of the subchondral bone. The functional characteristics of the connective tissues in the joints are determined by their chemical composition. These tissues consist mainly of proteoglycans, collagen and glycoproteins.

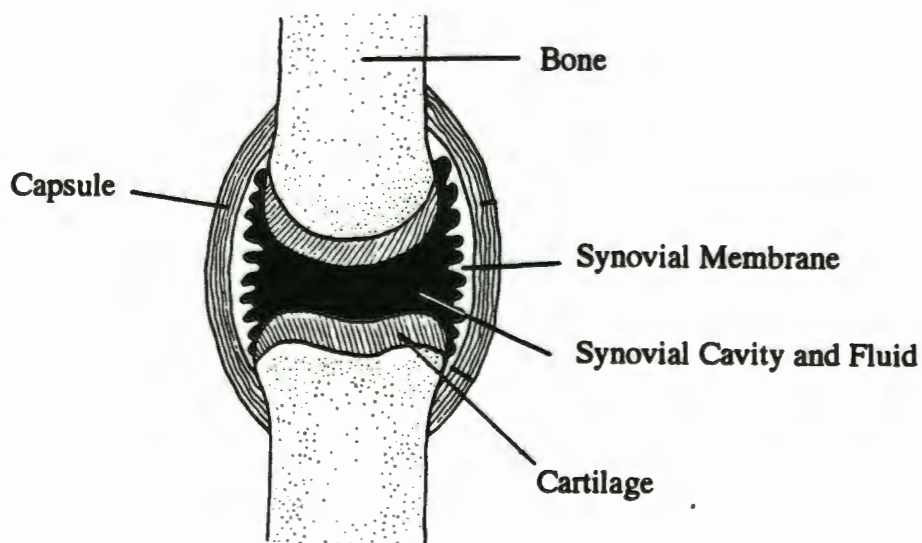


**Figure 1.1 :** Schematic representation of a normal joint.

Following the primary inflammatory reactions described above, proliferation of synovial granulation tissue (pannus) now occurs at the periphery of the cartilage in areas where the bone is unprotected. The cartilage is exposed to destructive enzymes from two sources, 1. the synovial fluid and 2. the pannus, which readily cleave and thereby remove proteoglycans from the cartilage. This removal, albeit reversible, diminishes the capacity of the cartilage to resist deformation under mechanical load [13].

Collagen in its native triple-helical form is resistant to degradation by common proteolytic enzymes. However, collagenases derived from PMNs and macrophages can denature the collagen polypeptide chains causing irreversible damage of the cartilage. Bone collagen, however, is further protected from enzymatic degradation by the presence of the calcium phosphate mineral phase. Its destruction thus requires prior demineralization, which could be brought about by a local decrease in pH. Direct bone resorption initiated by cells in the pannus may also occur, a process in which osteoclasts and prostaglandins, particularly PGE<sub>2</sub>, have been implicated [13].

Finally, it has been suggested that immune complexes deposited in the superficial layers of the cartilage may act as chemoattractants for the synovial pannus, causing the granulomatous response to spread throughout the joint [8]. Thus the presence of cartilage itself, together with immune complexes, may be responsible for the chronicity and persistence of rheumatoid inflammation.

This therefore constitutes the mechanism of joint destruction leading to erosion of articular cartilage and subchondral bone, as shown in Figure 1.2, resulting in the permanent and debilitating structural damage that is associated with chronic unremitting RA.

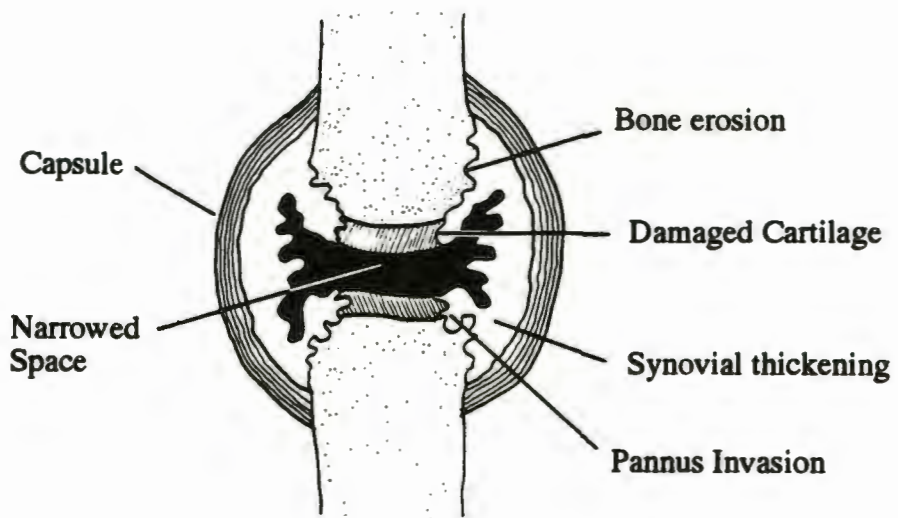


**Figure 1.2** : Schematic representation of a rheumatoid arthritic joint at an advanced stage of destruction.

## 1.2 DRUGS USED IN THE TREATMENT OF RA

The desired medical approach to treatment of any illness is, in decreasing order of importance : 1. removal of the causal agent(s), 2. disruption of the pathological mechanism and 3. as a last resort with little prospects of disease remission, alleviation of the symptoms. Since the aetiology of RA is unknown the primary cause of the disease cannot be the putative target of the therapeutic strategy. However control of the disease may be affected by immunosuppressives and the symptoms alleviated by anti-inflammatories, i.e. treatment targeting points two and three above.

The following are some of the most important agents currently used by most rheumatologists according to a recent review by Sanz and Alboukrek [14]. These can be conveniently classified into three categories, i.e. 1. nonsteroidal anti-inflammatory drugs (NSAIDS), 2. glucocorticosteroids and 3. disease-modifying antirheumatic drugs (DMARDS).

The NSAIDS include salicylates such as Aspirin and a large number of non-salicylates which are generally weak carboxylic or enolic acid derivatives. These have analgesic, antipyretic and anti-inflammatory properties and are thought to function by inhibition of the cyclo-oxygenase pathway of PG synthesis. Several other PG-independent mechanisms of action have also been proposed such as inhibition of collagenase, stabilization of lysosomal membranes and disruption of membrane-associated enzymatic functions which generate the superoxide radicle [14, 15]. Despite the fact that several of the anti-inflammatory actions mentioned above may play a role in the pathogenesis of RA, NSAIDS are not considered to be remission-inducing agents. Furthermore a high incidence of skin reactions, adverse renal side effects and gastrointestinal (GI) toxicity have become major complications in the long-term treatment of chronic RA using NSAIDS.

The glucocorticosteroids are potent, fast-acting anti-inflammatory agents and include compounds such as cortisone, prednisone and dexamethasone amongst others. They have numerous metabolic and physiological effects, affecting lymphocytes, granulocytes, macrophages and cell membranes as well as inhibiting the immune system [15]. Corticosteroids are, however, not considered to have disease-remitting potential, although this has recently been questioned since protection against joint erosion has been reported [14]. Due to the multifactorial pathogenesis of RA and the multiple effects of steroids on cell functions, their precise method of action has yet to be determined. One hypothesis is that their activity lies in their ability to decrease recruitment of neutrophils and macrophages to the sites of inflammation. They are also known to be potent inhibitors of arachidonic acid metabolism by preventing the acids release from phospholipids, resulting in the non-synthesis of PG [14]. Other possible modalities include inhibition of collagen synthesis and stabilization of lysosomal membranes [15].

Their use in the treatment of RA is indicated in order to improve symptoms and maintain functional status when 1st line treatment with NSAIDS has failed and DMARDS have not yet begun to act. However many serious side effects are associated with the use of corticosteroids, especially their effects on bone and the GI tract. Other complications include glucose intolerance, increased susceptibility to infections and impaired wound healing. Furthermore it is difficult to discontinue their use as some patients may develop a steroid-dependence.

The final group of anti-arthritic agents are loosely known as the DMARDS, and include sulfasalazine (SSZ), D-penicillamine, various antimalarial and gold compounds, as well as the more recent immunoregulators cyclophosphamide, azathioprine (AZA) and methotrexate (MTX). These drugs are rather slow acting. Some have been used for a number of decades in RA treatment, yet their mechanisms of action remain unknown.

Briefly, SSZ is thought to modify lymphocyte functions and inhibit RF synthesis as well as cyclo-oxygenase and proteolytic enzyme activity. The antimalarials affect several basic cellular processes such as thiol-disulphide interchange, the collagenase enzyme reaction and nucleoprotein interactions. They also exhibit anti-inflammatory properties, such as inhibition of PG synthesis and superoxide release by neutrophils, as well as stabilizing lysosomal membranes and suppressing phagocytosis. In addition they possess several immunoregulatory effects, for instance the inhibition of immune complex formation. Many disputed hypothesis surround the method of action of gold compounds. It has however been shown that gold affects complement activation and decreases serum concentrations of immunoglobulins through an effect on macrophages and B lymphocytes. D-penicillamine, which is a structural analogue of cysteine, is thought to exhibit anti-rheumatic activity due to a number of different reactions, for example, by inhibiting the release of oxygen radicles and lysosomal enzymes. Furthermore it has been suggested that D-penicillamine also has immunosuppressive properties due to its selective inhibition of T lymphocyte function.

Unfortunately all of the above agents exhibit adverse reactions related mainly to the GI tract. Other side reactions include ocular toxicity of the antimalarials, effects on the central nervous system by SSZ and high incidences of dermatitis, stomatitis, renal and hematologic side effects by the gold compounds. Apart from these negative side reactions the main reason for discontinuing their use in the treatment of RA is a lack of continued clinical response.

More rapid improvement and somewhat better long-term efficacy has been achieved by the use of the cytotoxic, immunosuppressive agent, MTX, which has a profound effect on the biosynthesis of nucleic acids. Apart from numerous immunological effects, the most important probably being decreased immunoglobulin and antibody production, it also displays anti-inflammatory activity. Unfortunately this promising drug

has several quite serious adverse reactions affecting the liver, lungs and GI tract, as well as the renal, reproductive and central nervous systems. Thus the main reason for discontinuing the use of MTX is its toxicity, which is in contrast to the DMARDS previously discussed. The drug AZA was until recently the only cytotoxic agent approved for clinical use. Similarly to MTX it has both anti-inflammatory and immunoregulatory activity, inhibiting monocyte production, B cell proliferation and  $\gamma$ -globulin synthesis. However, significant GI intolerance, bone marrow depression and infections are associated with its use. Cyclophosphamide, an alkylating agent that inhibits DNA replication, acts by affecting B cell functions which result in decreased immunoglobulin production. It also suppresses antibody responses and reduces serum immunoglobulins. Complications include infection and malignancies.

It is therefore evident from the above that, as has recently been stated, ... *current modalities of treatment are suboptimal in controlling symptoms, and their disease-modifying potential is limited at best ... and that ... the toxicity associated with the use of conventional agents is substantial ...* [14]. Thus there is a great need for continued research into the development of new drugs with disease remitting characteristics.

A striking omission, however, from the above list of pharmaceuticals, are drugs consisting of trace metal complexes, in particular those involving copper. This is symptomatic of most medical texts [2, 3, 6, 7] in which virtually no mention is made of copper for the treatment of RA, although many articles have appeared in the greater scientific literature advocating the use of this metal, having proven its efficacy [11, 15, 16, 17, 18].

### 1.3 THE INVOLVEMENT OF COPPER

Copper is widely distributed in nature as the metal or, in one of its two most important oxidation states i.e. Cu(I) and Cu(II), as sulphides, oxides and carbonates. In its metal form it is malleable, ductile and a good conductor of heat and electricity, second only to silver [19]. It is a major constituent of most alloys and has been termed one of mans' most important metals, the ore having been mined for over 5000 years.

In 1928 copper was shown to be an essential trace metal in animal nutrition, although amounts in excess are toxic. Following iron and zinc, it is in fact the third most abundant metallic element in the human body [20]. The body of a normal adult contains between 75 and 150 mg of copper, the average person consuming about 3 mg daily. Foods with a high copper content include liver, crustaceans, nuts and chocolate [21].

Dietary copper is readily absorbed in the stomach and small intestine, from where it is transported to the liver by the blood as a serum albumin complex. In the liver, which is the principal copper processing organ, it is stored as a metallothionin complex or converted into ceruloplasmin and released back into the blood to meet normal metabolic needs. Excess copper is excreted via the bile where it is complexed to bilirubin, thereby preventing reabsorption in the gut [22].

About 95% of plasma copper is inertly bound to ceruloplasmin, an oxidase enzyme containing 6 to 8 atoms of the metal and earning its name from the characteristically intense blue colour [20, 23]. The remaining copper is present as the labile complexes of 1. human serum albumin (HSA) and 2. low molecular weight amino acid anions, especially histidinate and cystinate [24], including also ternary complexation [25]. Copper is also present in red blood cells, where it is bound to erythrocuprein. Thus, due to the large

affinity of plasma proteins for this metal, the free cupric ion concentration is exceedingly small and has been estimated to be as low as  $10^{-18}$  mol dm<sup>-3</sup> [17].

Copper is widely distributed throughout the body. Its concentration correlates well with the amount of copper dependent metabolic activity occurring in a particular organ. Thus the heart and brain contain more copper than all other body tissues, apart from the storage and excretory organs. A large number of copper dependent enzymes catalyzing very diverse metabolic reactions have been distinguished, underlining the importance of this metal. These include amongst others [26]:

1. Various oxidases, e.g. cytochrome C and ceruloplasmin, required for cellular utilization of oxygen during energy production,
2. Dopamine- $\beta$ -hydroxylase, for conversion of dopamine to norepinephrine which is a neural hormone important in the transmission of nerve impulses,
3. Tyrosinase, for the synthesis of dihydroxyphenylalanine which is subsequently transformed to melanin, required for pigmentation,
4. Superoxide dismutase, the main copper-containing enzyme in the cytosol of leucocytes and erythrocytes, for inactivation of oxide radicles,
5. Amine oxidase, for removal of amine by-products by conversion to aldehydes and
6. Lysyl oxidase, for oxidation of terminal lysine amine groups of tropocollagen to the corresponding aldehydes. These condense spontaneously with free amine groups on adjacent molecules to form imine bonds. This represents the intermolecular cross-linking required for collagen maturation.

Copper was believed to be of therapeutic value as long ago as 1000 years B.C. and many folklore remedies for RA such as high copper containing diets and the wearing of copper bracelets abound. In defence of the latter, results by Walker *et al* have in fact indicated that dermal assimilation of copper can be significant [27, 28]. Furthermore much pharmacologic evidence suggests the use of copper complexes to be beneficial in the alleviation and treatment of RA and that these compounds have disease remitting qualities [16, 18, 26]. Thus it was demonstrated by Sorenson [16] that the anti-inflammatory activity of various drugs was increased when these were administered as their copper complexes. Furthermore various non-active ligands showed anti-inflammatory activity when administered together with copper, which was also observed by Lewis *et al* [29]. Sorenson [26] thus concluded that ... *the activity of the parent ligand, if it has any, must be due to the formation of its copper complex in vivo.*

It has, however, been observed that serum levels of copper are significantly increased during acute phases of RA inflammation, returning to normal with remission [18]. Considering the results of copper administration, this seems a bit paradoxical. Although controversial in the past, it now appears that this rise in serum copper is due to an increase in ceruloplasmin concentration [23, 30, 31, 32] and represents a physiological response to inflammation [18, 23]. Ceruloplasmin has until recently been described as *a protein in search of a function* [23]. It binds copper irreversibly and is thus not thought to be involved in its transport, as this would require denaturation of the protein at the user site. It has however been shown that ceruloplasmin is a powerful antioxidant and could thus provide protection against cellular destruction, which may be the reason for its increased synthesis [23]. This would however bring about a decrease in the concentration of serum albumin copper, as well as of the labile low molecular weight copper complexes. It has been shown by computer calculations that these are virtually all uncharged [33] and they are thus thought to be involved in the transport of copper across membranes to biological binding sites.

Although the mechanism of action by which copper exhibits anti-inflammatory activity is not yet understood, several possibilities exist. Of the copper dependent enzyme reactions listed above superoxide dismutation and lysyl oxidation are directly implicated in the response to rheumatoid inflammation and may require copper for their induction. The copper complexes of D-penicillamine and salicylate, amongst others, have also been shown to exhibit good *in vitro* SOD like activity [15, 34] and could thus have a direct anti-inflammatory effect. Other possible mechanisms of action include copper stimulation of ceruloplasmin production [15], stabilization of lysosomal membranes, modulation of PG synthesis and T-lymphocyte responses [18] and formation of a hystidine-cystine-copper complex which inhibits the denaturation of joint fluid IgG [11, 35].

Administered copper complexes could thus either have a direct effect on RA due to their SOD mimetic activity, or could act indirectly by increasing the labile low molecular weight (l.m.w.) pool of copper thereby inducing the enzyme reactions or mediating the other possible effects mentioned above.

Whatever its mode of action, the importance of copper at the site of inflammation has been sufficiently established and hence its manipulation by pharmaceuticals is essential. This therefore represents the justification for studying copper(II) complexes, particularly with respect to their copper mobilizing ability. The initial aim of this study is therefore to choose a series of potential copper(II) mobilizing agents.

**CHAPTER TWO**  
**LIGANDS**

## 2.1 COMPLEXATION AND THE CHELATE EFFECT

Metal ion mobilizing agents are essentially organic molecules or inorganic ions which can form complexes with the metal ion of interest, thereby keeping it in solution. However, prior to choosing a particular series of complexing agents for their potential copper(II) mobilizing ability, as suggested for the treatment of RA, various concepts involved in metal ion complexation should be discussed.

In the simplest case, when metal ions are dissolved in aqueous solution they are essentially already complexed since they do not exist as discrete entities, but are present in the form of aqua ions. Complexation by other monodentate ligands (defined as Lewis bases capable of donating an electron pair) can then be thought of as the stepwise displacement of these water molecules and is limited only by the thermodynamic stability of the species and ultimately by the coordination number of the particular metal ion. The stability constants, also known as formation or equilibrium constants, associated with this competitive process will be discussed in greater detail in the following chapter.

If the ligands are bidentate, complexation can occur in which chelate rings are formed. The name is derived from the Latin word *chele* meaning claw. Associated with these chelate rings is an enhanced stability compared to that of similar complexes involving only monodentate binding. This is known as the chelate effect, which is usually entropy driven and is in some cases very pronounced [20]. For example, the bis ethylenediamine copper(II) complex,  $[\text{Cu}(\text{en})_2]^{2+}$ , is nearly  $10^7$  times more stable than  $[\text{Cu}(\text{NH}_3)_4]^{2+}$  [36], ignoring for the moment the dependence of the magnitude of the chelate effect on the chosen standard state. Increasing the number of chelate rings also enhances the stability. Thus the tetradentate triethylenetetramine copper(II) complex,  $[\text{Cu}(\text{trien})]^{2+}$ , consisting of three contiguous or fused 5-membered rings, is a further  $10^{0.6}$  times more stable than  $[\text{Cu}(\text{en})_2]^{2+}$ .

This leads to the question of the optimum chelate ring size. Apart from one or two exceptions, it has been found that 5-membered chelate rings are the most stable. For instance, the  $[\text{Cu}(\text{en})_2]^{2+}$  complex is nearly 1000 times more stable than the bis 6-membered trimethylenediamine copper(II) complex,  $[\text{Cu}(\text{tn})_2]^{2+}$ . Thus the chelate effect decreases with increasing ring size, until a limit is reached where the chelates prefer to act as monodentate ligands. This can lead to the possible bridging of metal ions as in binuclear species. On the other hand, 4-membered chelate rings are generally less stable than 6 or even 7-membered rings.

Although 5-membered rings are generally the most stable in the case of first-row transition metal complexes, it has been found that systems containing two contiguous or fused rings are often more stable if one of these is a 6-membered chelate ring. Thus the order of stability of 5,6 > 5,5 > 6,6 contiguous ring systems for the copper(II) triamine complexes has been established [37]. This effect is even more pronounced in the case of systems containing three contiguous rings, where it has been found that the stability of copper(II) tetramine complexes is greatly enhanced by the introduction of 6-membered rings especially if this is in the central position. This effect has been attributed to relief of steric strain caused by the presence of the fused ring systems [38]. Thus the stability order of 5,6,5 > 6,5,6 > 5,5,5 > 6,6,6 contiguous rings has been established for these systems [39, 40].

Finally, just as an  $n$ -dentate chelating ligand leads to more stable complexes than  $n$  monodentate ligands of a similar type, so an  $n$ -dentate macrocyclic ligand gives even more stable complexes than the  $n$ -dentate open chain chelate. This is known as the macrocyclic effect and can further enhance complex stability by several orders of magnitude [20].

## 2.2 LIGAND REQUIREMENTS

In order to achieve successful metal ion administration and subsequent mobilization in the body fluids, several general requirements have to be fulfilled. The most important of these are the following :

1. The ligand must be a strong chelator in order to form thermodynamically stable complexes with the metal ion at physiological conditions of temperature and pH, thus minimizing loss to competing serum proteins.
2. The complex must however be sufficiently kinetically labile to be able to give up the metal ion at the biologically active site.
3. The ligand must be as specific to the metal of interest as possible, in order that other metal ion equilibria, essential for correct body function, are not disturbed and that the complex is not disrupted.
4. The complex must be formally uncharged and hence lipophilic to enable transport across cell membranes and prevent urinary excretion. In fact, it is not only essential for the complex to have a neutral charge but it must also be relatively nonpolar, since it was found by Jackson and Kelly that complexes which were too hydrophilic were rapidly excreted in the urine of laboratory animals [41, 42].
5. Lastly, if the complex is to be orally administered an additional requirement of stability at the low pHs encountered in stomach fluids must also be satisfied.

Ligands can be used to either mobilize copper from endogenous reserves or exogenous sources, thereby increasing the low molecular weight (l.m.w.) fraction of copper complexes in the body fluids. Unfortunately, ceruloplasmin, which is the major copper storage protein accounting for more than 90% of serum copper, binds this metal

irreversibly and would thus need to be denatured in order to make its copper accessible [24]. Essentially therefore, endogenous copper is only available from serum albumin (SA) which is the main copper transport protein in the blood. However, since the concentration of ceruloplasmin increases in response to the development of RA, so the concentration of SA is reduced and its function therefore already impaired. The only realistic means of increasing the body pool of labile uncharged l.m.w. copper(II) complexes is thus by exogenous copper administration.

## 2.3 CHOICE OF LIGANDS

In order to be able to meet the above requirements for metal ion mobilization, potential ligands must possess several thermodynamically desirable characteristics. These vary according to the particular metal ion being considered. Unfortunately enhanced stability is not the only criterion for successful mobilization, but selectivity as well as other physical attributes of the complex play an important role.

There are several different ways of achieving selective thermodynamic binding [43]. Of these the most important for controlling the selection of copper(II) are the type of liganding donor atoms, the preferential co-ordination geometry and the metal ion to ligand size fit. According to HSAB principles, the 'soft' nitrogen and sulphur donor atoms are selective for a number of the 'borderline' 2+ metal ions, i.e. iron(II), nickel(II), copper(II) and zinc(II). However copper(II) shows a remarkable ability to form bonds at pH  $\approx$  7 to peptide and amide nitrogens in their ionized state, giving it a selectivity factor of copper / zinc of about 10000 [43]. Sulphur could be considered a useful liganding donor atom but is in fact preferred by the 'softer' copper(I) ion. Furthermore, in the form of the thiol group, sulphur actually brings about reductive chelation of copper(II) and is notoriously toxic.

Selectivity for copper(II) is further enhanced by utilizing this ion's preference for a tetragonal environment, which is due to the ligand-field Jahn-Teller effect. This is in contrast to the tetrahedral copper(I) and zinc(II) and octahedral nickel(II) and iron(II) preferences. Both these effects are exemplified by the binding site of the copper carrying plasma protein serum albumin, incorporating ionized peptide nitrogen to copper bonds and a roughly square planar, four nitrogen chelate environment [43].

These thermodynamic requirements are readily exhibited by a number of dianionic macrocyclic ligands. However the copper(II) complexes thus formed are generally not sufficiently labile and ligands of this type were therefore not considered.

Jackson and Kelly, in a computer simulation study, determined that linear diphenolate, dicarboxylate or dialkyl phosphate substituted polyamines had the thermodynamically most desirable characteristics of several potential copper(II) mobilizing agents examined [24]. Ligands with amide nitrogen donors were however, not included in their study. Two representative ligands, i.e. 3,6,9,12-tetra-azatetradecanedioic acid (TTDA) and 3,6,9-triazaundecanedioic acid (DTDA), were thus subsequently synthesized and investigated [41]. Although these formed very stable, formally uncharged copper(II) complexes *in vitro* as well as *in vivo*, they were found to be rapidly excreted in the urine due to their hydrophilicity [42] and would therefore not be of much use as anti-inflammatory agents.

It was therefore decided to investigate a series of linear tetradentate chelate ligands, a prerequisite for enhanced stability (see previously), incorporating two ionizable amide nitrogens in order to achieve the desired copper(II) ion selectivity. Dissociation of the amide protons would furthermore fulfill the requirement of electrical neutrality, as well as probably forming a more nonpolar complex than those studied by Jackson and Kelly. This is due to the charge being embedded inside the structure. From the above discussion, it is evident that the other two ligand donor atoms should also be nitrogens, although present in the form of amines, in particular as the dimethyl and diethyl substituted tertiary amines. The effect of different electron donating groups can therefore be determined and complex stability further enhanced. Thus it was decided to investigate the following ligands: 1. N,N' bis [2-(dimethylamino)ethyl] ethanediamide (5UM), 2. N,N' bis [2-(dimethylamino)ethyl] propanediamide (6UM), 3. N,N' bis [3-(dimethylamino)propyl] ethanediamide (656UM), 4. N,N' bis [2-(diethylamino)ethyl] ethanediamide (5UE) and 5.

N,N' bis [2-(diethylamino)ethyl] propanediamide (6UE). (see structural formulae at the beginning of the thesis) The arrangement of functional groups is in the order amine-amide-amide-amine in each case. This series of ligands thus varies only in the number of methylene groups present in the chain, which has the effect of changing the dimensions of the chelate rings that can potentially be formed. An optimum ligand to metal size fit can therefore also be established.

Ligands similar to the ethanediamides (i.e. oxamides) have elicited much interest in the past, mainly because of their ability to bridge metal ions thereby forming binuclear complexes [44]. In fact, the 1 to 1 complexes have been termed *metal chelate ligands* by some workers [45]. Changing the arrangement of the functional groups such that the amides are in terminal positions results in a series of ligands based on alkyldiamines, which have also been widely studied by a number of workers [46, 47, 48]. The interest in the diamino diamide ligands is however largely due to their obvious biological significance as models of the peptide bonds of proteins [49, 50, 51, 52, 53].

Of special significance to this study is the suggestion that peptide molecules such as diglycyl-L-histidine can be used to mimic the copper(II) transport site of serum albumin [54, 55]. It has been proposed that the specific binding site occurs at the NH<sub>2</sub>-terminal peptide segment of HSA, and consists of the amino acid sequence, aspartine-alanine-histidine... [56]. In the case of bovine serum albumin the sequence is thought to be aspartine-threonine-histidine... [57].

Although the imine nitrogen of the imidazole ring is possibly the most basic heterocyclic nitrogen atom known, having a pK<sub>a</sub> of 6.95 [58], Jackson and Kelly found that ligands containing an imidazole residue were not particularly good at mobilizing copper(II) *in vivo* [24]. This is rather surprising in view of the wide biological involvement of histidine as a chelating agent. It is therefore hoped that by replacing the

imidazole functional group of the histidine residue by another, more electron donating amine nitrogen, the copper(II) complex stability will be increased. If it is found that one of the diamino diamide ligands can indeed effectively compete with HSA for copper(II), then successful *in vivo* mobilization of this metal ion is a distinct possibility.

Samples of the ligands 5UM and 5UE were obtained from K.Voyi. Thus only the remaining ligands, i.e. 6UM, 6UE and 656UM, were synthesized in this study. The synthetic procedures, together with microanalytical and NMR results, are presented in Appendix A.

## 2.4 THE AIMS OF THIS STUDY

Based on the needs for research into RA and new anti-inflammatory drugs outlined in the preceding chapter, a series of copper(II) specific ligands that are potentially useful anti-arthritic agents has been established. The further objectives of this study are therefore the following:

1. To measure the stability of the complexes formed between this series of ligands and various physiologically important trace metals, in particular copper(II), using glass electrode potentiometry. These results will then be used to determine the probable speciation of the metal ion in solution.
2. Following this, to ascertain the specific structures of these complexes in solution by an applicable spectroscopic technique.
3. To measure the partition coefficients between aqueous and organic solvents, thereby determining the ability of the complexes to pass through lipid membranes.
4. To investigate the copper(II) mobilizing potential of the complexes by computer modelling of the speciation in blood plasma.
5. Lastly, to perform animal experiments in order to determine the tissue distribution and verify the *in vivo* stability of the complexes, as well as possibly evaluate their anti-arthritic effect.

It is realized that a comprehensive study of all the objectives listed above is probably beyond the scope of just one thesis, especially if, as is anticipated, other interesting aspects emerge which would require further investigation.

**CHAPTER THREE**  
**EXPERIMENTAL**

### 3.1 INTRODUCTION

The aim in this experimental section was to determine the stability and type of complexes formed in solution under physiological conditions between the metal ion, copper(II), and the series of ligands previously described.

Several experimental methods can be utilized to investigate the chemical species that can potentially form in solution, for example, ultra filtration, calorimetry, solvent extraction, potentiometry, reaction kinetics, polarography, as well as nuclear magnetic resonance, Raman, UV/VIS and infrared spectroscopy. [59, 60] Of these potentiometry is probably the most extensively used owing to its sensitivity and reproducibility, making it one of the most precise and accurate non-invasive techniques available and was therefore the method of choice in this study [59].

In general the potentiometric technique consists of performing a series of titrations involving the ligand, metal ion and protons (or hydroxyl ions) and determining the free concentration of at least one of these components at each point during the titration by means of a suitable reversible ion sensitive electrode. The formation constants of the species present in solution can then be obtained by some graphical method or, as is more usual nowadays, by an iterative computational optimization procedure such as ESTA [61], MINQUAD [62] or SUPERQUAD [63].

In order to determine protonation constants, titrations of only the ligand with either acid or base are carried out. Comparing these data with those obtained from titrations including the metal ion allows the strength of complexation to be determined. Ideally it would be desirable to directly determine as many free ion activities in solution as possible in order to obtain a greater degree of reliability and accuracy. This, however, is not always practical or necessary and usually only one activity is measured. Anion or metal ion

selective electrodes can be used but often give unstable readings, exhibit poor reversibility and reproducibility, have slow response times and/or are subject to interference by other ions. Frequently they are not commercially available and in some instances such as in the case of zinc have not been developed.

Hydrogen ion sensitive glass electrodes on the other hand are less affected by the above problems resulting in measurements with excellent reproducibility. [64] Furthermore, virtually all equilibrium processes in aqueous solutions involve hydrogen and hydroxyl ions either directly or indirectly and therefore it is this free ion activity that is generally measured in a potentiometric investigation.

Only if the ligand is one which cannot be protonated or does not have any dissociable protons that can be displaced on complexation with a metal, is the use of a metal ion or other ion selective electrode essential. As this was not the case for the ligands in this study, hydrogen ion sensitive glass electrodes were used throughout.

In deciding upon the titration conditions, use of the very high background electrolyte concentration resulting in a  $3.0 \text{ mol dm}^{-3}$  ionic strength was considered in order to minimize the effects of activity coefficient and liquid-junction potential changes that occur during the course of a titration.

However, the experimental conditions should essentially resemble the biological environment as closely as possible, and because of the fact that the program ESTA can take the above-mentioned effects into account to some extent, an ionic strength more pertinent to physiological conditions of  $.15 \text{ mol dm}^{-3}$  was chosen instead. As high concentrations of NaCl are present in most body fluids, NaCl was therefore chosen as the supporting background electrolyte to make up this ionic strength.

The correct temperature for work applicable to biological systems is obviously 37°C. This does however present some practical difficulties such as evaporation from the test solution and condensation on the roof of the titration vessel. As most potentiometric determinations are carried out at 25°C it was decided to perform all experiments at this temperature thus avoiding the problem of having to completely insulate the titration setup and being able to directly compare the results with those reported in the literature.

Finally, some other complementary experimental technique will have to be applied to the systems under investigation in order to determine the sites and type of metal ion coordination, as potentiometry alone cannot provide this information definitively. A suitable spectroscopic technique was therefore chosen to study the various systems once the potentiometric investigation had been completed.

## 3.2 THEORY

### 3.2.1 COMPLEX FORMATION

The general theory of complex formation and the potentiometric determination of stability constants has been dealt with in the literature quite extensively. [59, 64, 65, 66] Thus only a broad outline of the reactions, equations and assumptions that are applicable will be given here.

In any solution containing metal ions M, ligands L and protons/hydroxyl ions H, the formation of a variety of different complexes can occur. This process can be described by the following general equilibrium reaction



where p, q and r are the stoichiometric coefficients pertaining to M, L and H respectively. When r = -1 this refers to proton removal or hydroxyl ion addition. Ionic charges have been omitted for simplicity.

This general reaction can therefore take into account formation of mononuclear binary, protonated or hydroxo, polynuclear as well as oligonuclear species. The extent of formation is governed by the stability of the individual complexes and the relative total concentrations of each component. Applying the law of mass action to the general equilibrium reaction, the overall thermodynamic stability constant can be expressed as

$${}^T\beta_{pqr} = \{M_pL_qH_r\} / \{M\}^p\{L\}^q\{H\}^r \quad 3.1$$

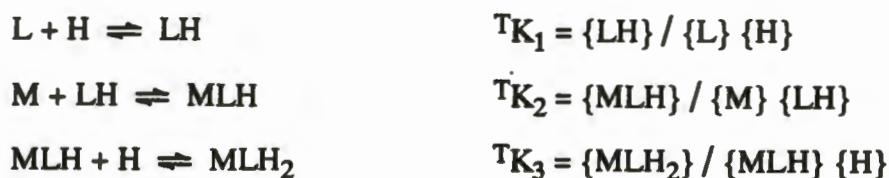
where the stoichiometric coefficients used in this study are in the order specified, in accordance with IUPAC [67] and { } denote activities.

By convention, unless otherwise specified, equilibria in this study are defined as the formation of complexes from their constituent components, as opposed to dissociation, which is also indicated by the particular direction in which the general reaction has been written. Thus the stability or equilibrium constants are formation constants, the term complexation constant relating to metal-ligand and metal-ligand-proton/hydroxyl interactions, whereas the term protonation constant is reserved for ligand-proton interactions only.

Most investigations of complex equilibria are carried out in either polar aprotic or polar protic solvents. In such solutions the metal ions, protons and charged ligands are solvated and complexation can therefore be regarded as the successive displacement of solvent molecules from the coordination sphere of the metal ion. In the case of aqueous solutions the general reaction should thus be extended to include water as one of the components and therefore the activity of water should also appear in the expression of the thermodynamic stability constant [65]. However in most studies performed in dilute solutions, it is usually assumed that the activity of water is effectively constant. This is especially true on keeping the ionic strength and thereby the activity coefficient constant by means of a supporting electrolyte. The activity of water can therefore be omitted leading to the simpler and more elegant expression for the conventional stability constants given above. [59, 65] This simplification can however be misleading on comparing ligands that coordinate through a different number of sites to the metal ion.

The notion of successive stepwise formation of complexes has given rise to another description of the equilibria in solution, i.e. the stepwise formation constants [68] which

can be illustrated by the following possible set of reactions and equations for the formation of  $MLH_2$  as an example:



These constants are related to the overall formation constant by the general expression

$${}^T \beta_{pqr} = \prod_i^n {}^T K_i \quad 3.2$$

i.e. the overall stability constant for the formation of  $MLH_2$  is the product of all  $n$  stepwise constants  ${}^T K_i$ .

Different experimental techniques measure different properties of the observable that is varying on complexation. Thus spectroscopic techniques determine the concentration of particular species in solution whereas most electrochemical and distribution methods provide a measure of their activity, i.e. their effective concentration. Activities are related to concentration by the expression

$$a = (c / c^\circ) \times \gamma \quad 3.3$$

where  $a$  is the activity

$c$  is the molar concentration,

$c^\circ$  is the molar standard concentration and

$\gamma$  is the molar activity coefficient.

However, because it is impossible to determine single ion activity coefficients and due to the fact that it is not the activity  $a_{\text{obs}}$  but the activity product  $(a_{\text{obs}} \times a_x)^{0.5}$  (where  $a_x$  relates to the counterion of the supporting background electrolyte) that is measured in a potentiometric investigation using ion sensitive electrodes, stability constants are generally expressed in terms of concentration.

Thus it is customary to use the overall stoichiometric or concentration constant for the general reaction as given by

$$\beta_{\text{pqr}} = [\text{M}_p\text{L}_q\text{H}_r] / [\text{M}]^p[\text{L}]^q[\text{H}]^r \quad 3.4$$

where [ ] denote concentrations.

All stability constants quoted in this study are defined in terms of the above expression. This is related to the thermodynamic constant  ${}^T\beta_{\text{pqr}}$  by the equation

$$\beta_{\text{pqr}} = {}^T\beta_{\text{pqr}} \times Q_\gamma$$

where  $Q_\gamma$  is the quotient of activity coefficients of the species involved in the equilibrium given by

$$Q_\gamma = (\gamma_{\text{M}})^p (\gamma_{\text{L}})^q (\gamma_{\text{H}})^r / \gamma_{\text{M}_p\text{L}_q\text{H}_r}$$

In order to carry out a meaningful determination of the formation constants, i.e. one in which  $\beta_{\text{pqr}}$  remains constant throughout the course of the experiment, it is necessary only for  $Q_\gamma$  to be kept unchanged albeit that its absolute value is not known.

However, activity coefficients and therefore  $Q_\gamma$  are functions of ionic strength as can be seen from the extended form of the Debye-Hückel equation

$$-\log \gamma_i = [ A z_i^2 I^{0.5} / ( 1 + B \hat{a}_i I^{0.5} ) ] + C I \quad 3.5$$

where A and B are constants characteristic of a particular solvent and the

temperature (for water at 25°C, A = 0.509 and B = 0.328)

$z_i$  is the charge of the  $i^{\text{th}}$  ion

I is the ionic strength

$\hat{a}$  is the ionic size parameter in Ångström, estimates for which

have been given by Kielland [69], and

C is an empirical constant.

As the concentrations of the species in solution change on complexation during the experiment so in the absence of a supporting electrolyte, the ionic strength which can be given by

$$I = 1/2 \sum_1^n c_i z_i^2 \quad 3.6$$

also varies, and this in turn affects the activity coefficients and thereby  $Q_\gamma$ . Hence in order to satisfy the requirement of a constant activity quotient, a constant ionic strength needs to be maintained. This is achieved by carrying out the investigation in a large excess of inert background electrolyte thereby masking the effects of concentration changes of the reacting species.

Furthermore the stability constants vary with temperature according to the following expression

$$d \ln K / d (1/T) = - \Delta H^\circ / R \quad 3.7$$

obtained by differentiation of the relationship

$$\ln K = -\Delta H^\circ / RT + \Delta S^\circ / R \quad 3.8$$

where  $\Delta H^\circ$  and  $\Delta S^\circ$  are the standard enthalpy and entropy changes of the complexation reaction,

T is the absolute temperature in Kelvin and

R is the natural gas constant in  $\text{JK}^{-1} \text{mol}^{-1}$ .

The above equation is derived from the expression

$$\Delta G^\circ = -R T \ln K$$

where  $\Delta G^\circ$  is the standard Gibbs free energy change of reaction and is given by the well-known thermodynamic relationship

$$\Delta G^\circ = \Delta H^\circ - T \Delta S^\circ$$

in terms of the standard enthalpy and entropy changes of the reaction.

The stability constants are therefore strictly only applicable to the ionic strength, temperature and the medium in which they have been determined and should not be transferred to other systems if at all possible. Equation 3.5 has however been found useful as a basis for the extrapolation of stability constants to different ionic strengths [70] and was thus also used here in order to compare results from this study with those reported in the literature for different conditions. This equation was also used to make corrections in the computational analysis of the experimental data (see below). Equally, knowing values for  $\Delta H^\circ$ , equilibrium constants determined at one temperature can be used to calculate values at another temperature, by integration of equation 3.7 and making the assumption that  $\Delta H^\circ$  is constant over the usually small temperature interval employed.

A further important point that can be made on considering the above two expressions is that complex formation is promoted by a negative enthalpy and a positive entropy change.

The single most important group of expressions for completely describing complex equilibrium systems are the mass balance equations which relate the total concentration of each component to the sum of the concentrations of the individual species incorporating that component. As the concentration of each species can be expressed in terms of the free concentration, the stability constant and the stoichiometric coefficients using equation 3.4, so the following mass balance equation for the ligand, for example, can be derived.

$$\begin{aligned}
 T_L &= [L] + [LH] + \dots + [ML] + 2[ML_2] + \dots + [MLH] + \dots + q[M_pL_qH_r] \\
 &= \sum_{-R}^R \sum_0^Q \sum_0^P q \beta_{pqr} [M]^p [L]^q [H]^r \quad 3.9
 \end{aligned}$$

Similarly the mass balance equations for the metal and the proton are given by

$$\begin{aligned}
 T_M &= \sum_{-R}^R \sum_0^Q \sum_1^P p \beta_{pqr} [M]^p [L]^q [H]^r \text{ and} \\
 T_H &= \sum_{-R}^R \sum_0^Q \sum_0^P r \beta_{pqr} [M]^p [L]^q [H]^r
 \end{aligned}$$

making up the set of simultaneous equations to be solved for the unknown stability constants and free concentrations. The above expressions can be set equal to the total analytical or real total concentrations which can be determined from the experimental variables at each point of the titration by the following equation for the ligand as an example

$$T_L^{\text{Real}} = [c_L^v \times V^o + c_L^b \times v^b] / [V^o + v^b] \quad 3.10$$

where  $c_L^v$  is the initial concentration of ligand in the titration vessel

$V^o$  is the initial volume in the vessel

$c_L^b$  is the concentration of ligand in the burette and

$v^b$  is the volume added from the burette.

Similarly expressions for  $T_M^{\text{Real}}$  and  $T_H^{\text{Real}}$  can be derived.

Thus for the set of simultaneous equations there are  $n_b$  unknown stability constants and, at each point of the titration,  $n_c$  unknown free component concentrations. If the total number of mass balance equations given by

$$m = n_{\text{mbe}} \times n_p$$

where  $n_p$  equals the number of titration points, is greater than the total number of unknown parameters given by

$$n_b + n_c \times n_p$$

then the system can essentially be solved. Clearly the above requirement is not satisfied as  $n_{\text{mbe}} = n_c$ . However the solution of the simultaneous equations is easily effected on experimentally determining just one of the free component concentrations at each point in the titration. Thus the number of unknowns reduces to

$$n_b + (n_c - 1) \times n_p$$

which for even quite complex chemical systems becomes less than  $m$  as the number of data points increases.

It can be shown [71] that the experimental variable determined in a potentiometric investigation measuring the potential between a hydrogen ion sensitive glass electrode and a calomel reference electrode as in this study, is the activity product  $a_{\text{H}^+} \times a_{\text{Cl}^-}$  (NaCl being used as the background electrolyte). Since the chloride concentration is known, the measured emf yields a value of  $a_{\text{H}^+} \times \gamma_{\text{Cl}^-}$ .

The electrode response can be given by a Nernstian relationship defined by the following equation

$$E = E^\circ + S \log [\text{H}^+] \quad 3.11$$

where  $E^\circ$  is the electrode response intercept

$S$  is the Nernstian slope =  $RTF^{-1} \ln 10$

( $R$  being the natural gas constant,  $T$  the absolute temperature and  $F$  the Faraday constant)

and the operational pH is therefore defined as

$$\text{pH} = -\log [\text{H}^+] \quad 3.12$$

It should be noted that  $E$  is defined in terms of the hydrogen ion concentration. This is permissible as the electrode response intercept,  $E^\circ$ , incorporates not only the liquid-junction, interfering ion and glass membrane potentials but also the hydrogen and chloride ion activity coefficients in the form of  $S \log \gamma_{\text{H}^+}$  and  $S \log \gamma_{\text{Cl}^-}$  respectively.

In order to keep these terms constant throughout the titration a constant ionic strength is maintained by means of a supporting electrolyte as was previously discussed. However in the case of work carried out under physiologically applicable conditions it is

not always possible for the supporting electrolyte to be in the required large excess and variations in ionic strength can therefore occur on complexation. Allowance was thus made for the concomitant changes in activity coefficients by means of equation 3.5 for instance.

Furthermore, not only are stability constants temperature dependent (see previously), but as is indicated by equation 3.11, the measured potential is also affected by temperature. Thus for the same reasons as for keeping a constant ionic strength, a constant temperature (within about  $\pm 0.05$  Kelvin) needs to also be maintained throughout the titration [59].

The titrations described in this thesis were generally carried out in a pH range from 2 to 12 in which the diffusion potential difference due to the mobile  $H^+$  and  $OH^-$  ions is negligible [64]. Furthermore, as the salt bridge of the calomel reference electrode was filled with the same electrolyte used to make up the inert background the liquid-junction potential was justifiably assumed to be constant. Similarly, interference by alkaline metal ions was also assumed to be negligible. However, to obtain meaningful values of the hydrogen ion concentration from the measured potentials, values for  $E^\circ$  need to be determined and hence calibration of the electrodes is required. Since the above mentioned factors together with the standard potential of the glass membrane may vary from day to day and are difficult to control, calibration against standard buffer solutions is inadequate. In order to reduce the influence of these effects it is therefore desirable to carry out an internal calibration of the electrodes involving refinement of the  $E^\circ$  values in the test solution itself.

Various graphical and computational methods have been developed for the analysis of potentiometric data in order to determine formation constants depending on the requirements of the system under study [59, 72]. To visualize the experimental data and

identify the major complexes present in order to choose an initial model for refinement, use was made of the two secondary concentration variables, the so-called formation and deprotonation functions,  $\bar{n}$  [73] and  $\bar{Q}$  [74]. These were also used to decide upon the final chemical model by comparison of the experimental functions with those calculated using the corresponding set of refined constants.

The variable  $\bar{n}_H$  is defined as the average number of protons bound to the ligand

$$\therefore \bar{n}_H = \frac{\text{conc. of protons bound to the ligand}}{\text{total ligand conc.}}$$

The total proton concentration in a system involving mononuclear binary formation of ligands and protons is given by the expression

$$T_H = [H] - [OH] + [LH] + 2[LH_2] + \dots + j[LH_j] + \dots + N[LH_N]$$

$$\therefore T_H = [H] - K_w [H]^{-1} + [L] \sum_1^N j \beta_{01j} [H]^j \quad 3.13$$

where  $[L] \sum_1^N j \beta_{01j} [H]^j$  is the concentration of protons bound to the ligand and is equal to

$T_H - [H] + K_w [H]^{-1}$  with  $K_w$  being the dissociation constant of water. Therefore in terms of experimental variables

$$\bar{n}_H = [T_H - [H] + K_w [H]^{-1}] / T_L \quad 3.14$$

which is known as  $\bar{n}_H^{\text{observed}}$ . Having measured the free proton concentration,  $\bar{n}_H$  can be determined and plotted against  $-\log [H]$  to give the observed protonation curve.

The total ligand concentration in this system is given by

$$T_L = [L] + [LH] + [LH_2] + \dots + [LH_N] = [L] \sum_0^N \beta_{01j} [H]^j$$

Combining this with the last term of equation 3.13 into expression 3.14, one of the concentration variables can be eliminated resulting in an alternative expression for  $\bar{n}_H$  in terms of  $\beta_{01j}$  and the free hydrogen ion concentration i.e.

$$\bar{n}_H = \frac{\sum_1^N j \beta_{01j} [H]^j}{\sum_0^N \beta_{01j} [H]^j} \quad 3.15$$

known as  $\bar{n}_H^{\text{calculated}}$ . Having determined the  $\beta_{01j}$ 's this then gives rise to the calculated protonation curve.

In the case of mononuclear binary complexation involving ligands and metal ions, the variable  $\bar{n}$  is defined, similarly to  $\bar{n}_H$ , as the average number of ligands bound to the metal.

$$\therefore \bar{n} = \text{conc. of ligands bound to the metal} / \text{total metal conc.}$$

For mononuclear binary species formation in a system containing metals, ligands and protons, the total ligand concentration is given by

$$\begin{aligned} T_L &= ([L] \sum_0^N \beta_{01j} [H]^j) + \beta_{110} [M] [L] + 2 \beta_{120} [M] [L]^2 + \dots + N \beta_{1N0} [M] [L]^N \\ &= [L] \sum_0^N \beta_{01j} [H]^j + [M] \sum_1^N j \beta_{1j0} [L]^j \end{aligned} \quad 3.16$$

where  $[M] \sum_1^N j \beta_{1j0} [L]^j$  is the concentration of ligand bound to metal and is equal to  $T_L - [L] \sum_0^N \beta_{01j} [H]^j$ .

$$\therefore \bar{n} = (T_L - [L] \sum_0^N \beta_{01j} [H]^j) / T_M$$

Rearranging equation 3.15 and substituting into the above gives

$$\bar{n} = (T_L - ([L] \sum_1^N \beta_{01j} [H]^j) / \bar{n}_H) / T_M \quad 3.17$$

As  $[L] \sum_1^N \beta_{01j} [H]^j$  is equal to  $T_H - [H] + K_w [H]^{-1}$  from equation 3.13

$$\therefore \bar{n} = (T_L - (T_H - [H] + K_w [H]^{-1}) / \bar{n}_H) / T_M \quad 3.18$$

in terms of experimental variables and is known as  $\bar{n}^{\text{observed}}$ . It can be shown that equation 3.15 applies equally in the three component system. Therefore, since  $\bar{n}_H$  is known,  $\bar{n}$  can be determined and plotted against the free ligand concentration (determined by rearranging equation 3.17) to give the observed complexation curve. Superimposable curves for different titrations give an indication of the reproducibility of the system and the precision of the measurements. Any deviation from this overlapping pattern, especially for a set of titrations with different metal to ligand ratios, is usually an indication of the presence of not only mononuclear binary complexes but also other types of complexes such as protonated, hydroxo and polynuclear species which have not been included in the formal definition of  $\bar{n}$ . Thus a fan like appearance is indicative of protonated or hydroxo metal ligand complexes, whereas parallel plots suggest polynuclear formation. It is therefore essential that titrations are performed at different metal to ligand ratios and, in the case of the protonation investigation, at various ligand concentrations.

If mononuclear binary complexes predominate, as is usually the case for plots of  $\bar{n}_H$ , rough estimates of the stepwise formation constants can be obtained from the pH and pL values corresponding to the half integral values of  $\bar{n}_H$  and  $\bar{n}$  respectively, using the Bjerrum half  $\bar{n}$  method.

The total metal concentration is given by

$$T_M = [M] + [ML] + [ML_2] + \dots + [ML_N]$$

$$= [M] \sum_0^N \beta_{1j0} [L]^j$$

Combining this expression with the last term of equation 3.16 in the definition of  $\bar{n}$ , one of the concentration variables is again eliminated resulting in the alternative expression for  $\bar{n}$  in terms of  $\beta_{1j0}$ 's and the free ligand concentration

$$\bar{n} = \frac{\sum_1^N j \beta_{1j0} [L]^j}{\sum_0^N \beta_{1j0} [L]^j} \quad 3.19$$

known as  $\bar{n}^{\text{calculated}}$ . On determining the set of  $\beta_{1j0}$ 's,  $\bar{n}^{\text{calc}}$  can be plotted against the free ligand concentration giving the calculated complexation curve.

The deprotonation function,  $\bar{Q}$ , is defined as the average number of protons released per metal ion due to complexation and is given by

$$\bar{Q} = (T_H^* - T_H) / T_M \quad 3.20$$

where  $T_H^*$  is the calculated total proton concentration in the system at the observed pH ignoring the presence of any metal complexes and  $T_H$  is the total analytical proton concentration.  $T_H^*$  is calculated from the observed free proton concentration by the expression

$$T_H^* = [H] - K_w [H]^{-1} + \sum_{-R}^R \sum_0^Q \sum_0^P r \beta [M]^p [L]^q [H]^r$$

with the proviso that  $p = 0$ ,

whereas  $T_H$  is determined from experimental variables using an equation similar to 3.10. Furthermore, another formation function  $\tilde{n}_H^*$  is defined similarly to  $\tilde{n}_H$ , which is given by

$$\tilde{n}_H^* = (T_H^* - [H] + K_w [H]^{-1}) / T_L^{\text{Real}} \quad 3.21$$

This variable, together with  $\tilde{Q}$ , is plotted versus  $-\log [H^+]$ , and the relative positions of these curves can then give an indication of the metal to ligand ratio of the predominant species.

### 3.2.2 COMPUTATIONAL CONSIDERATIONS

The two computer programs, MINQUAD [62, 75] and ESTA [61, 76] were mainly used in this study to solve the set of simultaneous mass balance equations and thereby determine the stability constants. These two computer programs do essentially the same thing, both use a generalized Gauss-Newton least-squares method for refinement of parameters, such as formation constants. However ESTA also makes use of a Levenberg-Marquardt method to reduce parameter shifts and modify the vectors towards the direction of steepest descent.

Of the two programs ESTA is the more recent and employs a superior weighting procedure [77]. It also allows for various effects in the electrode equation, mentioned previously, to be quantified [61]. However, as ion interference and liquid-junction potentials were assumed to be constant, (see section 3.2.1), only the feature of correcting for changing activity coefficients was employed here.

Apart from being able to optimize several more parameters than MINQUAD, ESTA also offers the user a choice between two alternative optimization procedures

minimizing either the squares of the residuals in EMF (OBJE) or, similar to MINQUAD, those in total concentrations (OBJT). The program also incorporates modules for the simulation of titration data, previously computed by the programs ZPLOT [73] and PSEUDOPLOT [78], and for the determination of the effects of an error imposition on the optimized parameters. Thus, although MINQUAD was found to be more robust in some instances, ESTA was mainly used in this study and its optimization algorithms will be outlined here.

The objective function to be minimized by the iterative refinement of the set of stability constants is given by

$$U_{\text{obj}} = \sum_1^N w_n (Y_n^{\text{obs}} - Y_n^{\text{cal}})^2 / (N - n_p) \quad 3.22$$

where  $Y_n^{\text{obs}}$  and  $Y_n^{\text{cal}}$  may be either  $\text{EMF}_n$  or  $T_n$

$w_n$  is the weight applied to each point

$N$  is the total number of experimental titration points and

$n_p$  is the number of parameters to be optimized.

The use of weights is essential in order to reduce the adverse effects on optimized parameters arising from errors in values that are kept constant during the calculations, as these errors tend to propagate differently in different regions of the titration [77]. In other words, weighting takes into account the fact that some of the titration points will be more reliable than others and hence relatively greater importance should be placed on these in the optimization process. Thus a large residual of an unreliable data point will not tend to be reduced in favour of increasing other smaller residuals less affected by such errors. Although some of these imposed standard deviations may be for errors in parameters that are systematic in nature, e.g. initial volume, it is their effect on the size of the random errors that is important here. Dealing with systematic errors is an intractable problem and

has been discussed elsewhere [79]. The origin of the errors in the titration data are assumed to be random and their likely effect can therefore be assessed by using a Taylor-series propagation.

The weights  $w_n$ , are calculated at each point from the residuals and the variances  $\sigma^2$ , of all experimental parameters  $p$ , for which errors have been specified, by the expression

$$w_n = [ \sum_p (\partial(Y^{obs} - Y^{calc}) / \partial p)^2 \sigma_p^2 ]^{-1} \quad 3.23$$

as opposed to being calculated from the slope of the titration curve and the variances in titration volumes and emf data only, as is the case in the program SUPERQUAD [63] for instance.

The goodness of fit between experimental data and that calculated from the refined set of  $\beta_{pqr}$ 's is expressed by the Hamilton R-factor

$$R^H = [ U_{obj} / \sum_1^N w_n (Y_n^{obs})^2 ]^{0.5} \quad 3.24$$

This can be compared to  $R_{lim}$  which is an indication of the best possible fit that can be obtained under the conditions that have been imposed by the set of experimental errors. This limit of the R-factor is given by

$$R_{lim} = [ N / \sum_1^N w_n (Y_n^{obs})^2 ]^{0.5}$$

and for a perfect model the R-factor should be equal to  $R_{lim}$ . However since the theory is strictly valid for random errors only, which is often not the case in actual titrations, the R-factor can become less than the  $R_{lim}$  in some instances as has occurred in this study.

To determine whether a statistically significant difference exists at the  $\alpha$  confidence level between the R-factors of two (or more) proposed models use was made of the Hamilton R ratio test [80]. If

$$R_1^H / R_0^H < R_{p, n-p, \alpha} \quad 3.25$$

where  $R_0^H$  and  $R_1^H$  are calculated from equation 3.24 for the models  $H_0$  and  $H_1$ , respectively

$R_{p, n-p, \alpha}$  is taken from tables in reference [81]

$p$  is the number of unknown parameters

$n-p$  is the number of degrees of freedom and

$\alpha$  is the level of confidence

then the alternative hypothesis  $H_1$  is not significantly different to hypothesis  $H_0$  [82]. In this case the simpler model was then chosen on the basis of Ockham's Razor [83].

The choice of the final set of stability constants making up the proposed model that 'best' describes the system under investigation was based on a number of additional criteria. Firstly, the system had to consist of chemically viable species as determined by the number of coordination sites and the denticity of the ligands. Furthermore, models with standard deviations in the logarithm of the stability constants in excess of .03 were rejected. Finally, models were chosen based on the best qualitative fit between the observed and calculated  $\bar{n}$  and  $\bar{Q}$  curves. This graphical method quite often facilitated the distinction between very similar models with statistically insignificantly different R-factors.

### 3.3 EXPERIMENTAL PROCEDURE

The experimental approach used in this study was similar to that of other workers in the field of solution chemistry and essentially involves the potentiometric titration of a series of solutions containing not only different ligand to metal ratios but also, especially in the case without metal present, a range of ligand concentrations in order to test for the presence of polynuclear species formation.

The titrations were performed using a Metrohm automatic burette (Dosimat E635) controlled by a Metrohm automatic titration processor (Titroprocessor E636), which also recorded the experimental readings of volume of titrant added corresponding to emf measured. The data thus obtained together with the analytical concentrations were analyzed according to the procedure outlined in the previous section.

The test solutions were made up in a sealable reaction vessel, thermostated to  $25^{\circ}\text{C} \pm 0.05$  using a Lauda water bath, and contained a thermometer, the glass and calomel reference electrode, a burette tip for the introduction of titrant, fitted with a non-return valve to prevent back-diffusion and a magnetic stirrer bar. Generally the required amount of ligand was weighed out for each titration separately, which results in greater accuracy but is accompanied by a loss in precision. All other reactants were introduced as solutions, using an automatic burette (Dosimat E665). Use of the latter enhanced the accuracy of the measurements as well as the efficiency of preparing titrations covering the required ranges of component concentrations. In order to exclude carbon dioxide and dioxygen from the reaction vessel, an inert atmosphere was maintained throughout the titration by passing dinitrogen over the surface of the solution and subsequently releasing it to the atmosphere via a trap containing the background electrolyte. The high purity gas was obtained by bubbling commercial dinitrogen through a set of wash bottles containing the following solutions:

- i. 50% w/w potassium hydroxide solution to remove carbon dioxide impurities
- ii. Fieser's solution consisting of 20g potassium hydroxide, 2g sodium anthraquinone-2-sulphonate and 15g sodium dithionite in 100 ml water to remove dioxygen
- iii. Excess lead wool in 250 ml of solution containing 50g potassium hydroxide and 2.5g sodium 1,2-naphthaquinone-4-sulphonate to remove trace amounts of dioxygen
- iv. empty
- v. distilled water
- vi. background electrolyte of the correct ionic strength to humidify the inert atmosphere.

The last three traps were thermostated to 25°C in accordance with the titration conditions.

All solutions were made up using Merck Guaranteed Reagents or BDH Aristar grade chemicals in glass distilled deionized water which had been boiled out in order to remove dissolved carbon dioxide. The copper(II) solutions were made up from the dihydrated chloride salt, as chloride was the choice of background electrolyte, and standardized against EDTA solution using Fast Sulphon Black F as indicator according to the procedure given in Vogel [84]. Although the EDTA solution was made up as a primary standard from the dihydrated disodium salt [85], it was standardized against a zinc(II) chloride solution using indicator buffer tablets according to the procedure given in the Merck handbook [86]. The zinc(II) solution was made up as a primary standard by dissolving granulated zinc in concentrated hydrochloric acid. Due to polarization of the metal surface the dissolution was facilitated by the addition of a strip of platinum.

The hydrochloric acid and sodium hydroxide solutions were made up from Merck Titrisol ampoules and standardized potentiometrically against recrystallized borax and potassium hydrogen phthalate, respectively. As a further check, the two solutions were frequently titrated against each other, the results consistently agreeing with those from the solid standardizations to within 0.1%, a discrepancy regarded as satisfactory by even some of the most stringent workers [87]. The basic solutions, although made up under nitrogen in a glove box and stored in a high density polythene bottle fitted with a carbon dioxide soda lime trap, were used for no longer than one week. Apart from the EDTA, all solutions were made up to an ionic strength of  $0.15 \text{ mol dm}^{-3}$  with respect to chloride using the high purity sodium salt.

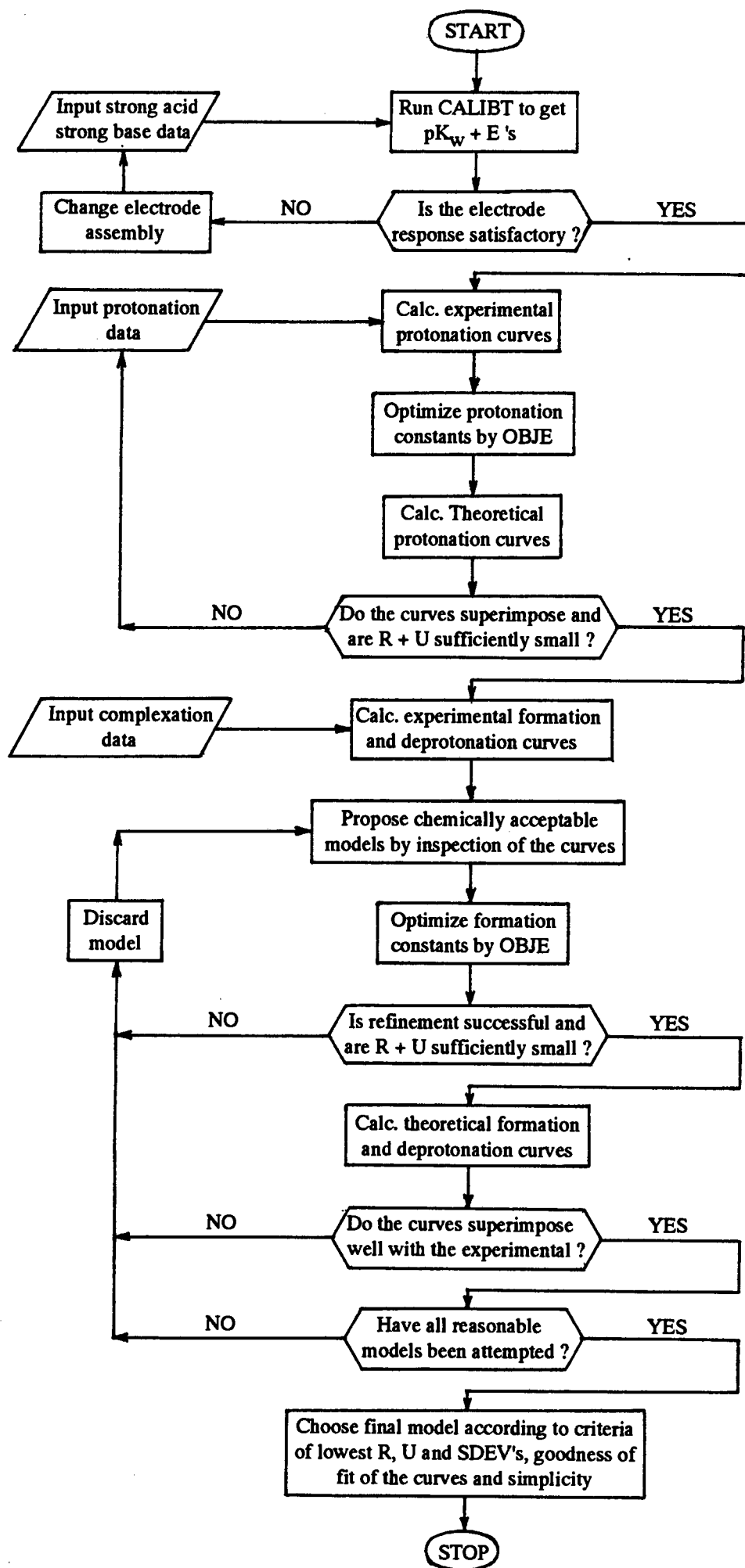
Volumetric flasks were calibrated with deionized water allowing not only for density changes of the water with temperature but also for the volumetric expansion of glass and the Archimedes effect on standard weights [19].

Two hydrogen ion sensitive glass electrodes (EA 109), together with a calomel reference electrode (EA 404), were used alternately, for greater accuracy and electrode recovery, to measure the potential. The reference electrode, which was filled with saturated sodium chloride and allowed to stabilize for several days, was the best one of three chosen on the basis of stable emf readings. The glass electrodes were chosen on the basis of least drift and best electrode response, i.e. adherence of the slope to the theoretical value together with small residuals in emf, as determined from strong acid, strong base titrations using the subroutine CALIBT of the program MAGEC written specifically for this purpose [88]. From this a value for  $pK_w$  applicable to the titration conditions used in this study was also obtained, as well as initial estimates of  $E^\circ$  for the two electrodes. Refined  $E^\circ$  values, used for the protonation analyses, were determined on a weekly basis from potentiometric titrations of the well characterized primary standard, potassium hydrogen phthalate. Due to periodic electrode variations, discussed previously, the emf of

a particular hydrochloric acid solution used throughout, was determined prior to each titration and the  $E^\circ$  values were adjusted according to changes observed in this reading. In the case of the complexation determinations,  $E^\circ$  values were often determined using the data obtained from the protonation titrations of the ligand solution carried out prior to metal ion addition which thus constitutes in situ electrode calibration.

A typical titration sequence for the potentiometric determinations is thus given by the following. Acidic ligand solutions ranging in concentration from about 5 to 20 mmol  $\text{dm}^{-3}$  were titrated with base, followed by a further titration against acid, to determine the reproducibility and reversibility of the system as well as the protonation constants of the particular ligand. Ideally, in the case of the complexation determinations, the initial titration of the ligand was followed by the addition of the required amount of metal ion to the now basic ligand solution. This was then titrated with acid until precipitation occurred as was the case with most of the ligands investigated in this study.

An idealized computational procedure employed for the determination of protonation and complexation constants is represented by the flow diagram on the following page.



### 3.4 RESULTS AND OBSERVATIONS

The results presented are in the form of overall formation constants unless otherwise specified. For convenience concentrations are given in either mol dm<sup>-3</sup> or mmol dm<sup>-3</sup>. The species are defined throughout this section in terms of the three stoichiometric coefficients given in the order M, L and H; for example, 21-2 denotes the species M<sub>2</sub>LH<sub>-2</sub>, whereas 012 denotes the protonated ligand species LH<sub>2</sub>.

A value for pK<sub>w</sub> (i.e. - log K<sub>w</sub>) of 13.73 was obtained from several strong acid, strong base titrations at 0.15 mol dm<sup>-3</sup> using the program MAGEC for analysis of the data. This value is in good agreement with those of Dyrssen *et al*, 13.75 at 0.4 mol dm<sup>-3</sup> [89] and Teder, 13.72 at 0.1 mol dm<sup>-3</sup> [90] and was thus used throughout this study. Since pK<sub>w</sub> is an important parameter especially for work carried out mainly in the basic region, as was the case in this study, a further analysis using ESTA on the protonation data of potassium hydrogen phthalate was performed. This resulted in an identical value of 13.73 for pK<sub>w</sub>.

The titration data were generally analyzed using the program ESTA with the refinement technique, OBJE, as the method of choice. Unfortunately this method of refinement could not be used throughout since frequently only the OBJT procedure would lead to convergence. Whenever possible therefore OBJE results were checked using the OBJT method or the program MINQUAD which, although not identical, usually gave quite similar values.

Standard deviations, used in the weighting procedure, of .05 ml, .10 mV and .005 ml, were imposed on the systems studied, for errors in the parameters of initial vessel volume, emf reading and volume of titrant, respectively.

Debye-Hückel corrections to allow for the effect of changing ionic strength on activity coefficients, and hence formation constants, were initially used in the OBJE refinements. This effect on the constants was however found to be negligible and the feature of ionic strength correction was therefore abandoned as its implementation is rather tedious. Furthermore, since neither OBJT nor MINQUAD allow these corrections to be made, it was decided for consistency not to make use of this feature.

Since most of the ligands were found to be hygroscopic, sometimes to a considerable extent, accurate weighing was fairly difficult. Thus a parameter that was generally refined in addition to the stability constants, was that of the ligand concentration.

### 3.4.1 PROTONATION

All five ligands showed a very similar  $\bar{n}_H$  versus pH dependence with only a slight shift in the position of the curves along the X-axis. Therefore the experimental and theoretical formation curves of only the two ligands, 5UM and 656UM, which were chosen on the basis of having the lowest and highest protonation constants, are presented in Figures 3.3 and 3.4 respectively. For the sake of clarity only a small number of experimental points of a few representative titrations with different initial ligand concentrations have been shown.

The experimental curves coincide very well for different ligand concentrations, which indicates the presence of only mononuclear binary species, as well as a high degree of experimental precision and good reproducibility of the systems. Using the refined  $\log \beta_{01r}$  values given in Table 3.1, together with the relevant titration conditions, theoretical  $\bar{n}_H$  versus pH curves were calculated and plotted as solid lines on the same set of axis in Figures 3.3 and 3.4. These superimpose very well with the experimental plots lending confidence to the values of  $\log \beta_{01r}$  determined in this study.

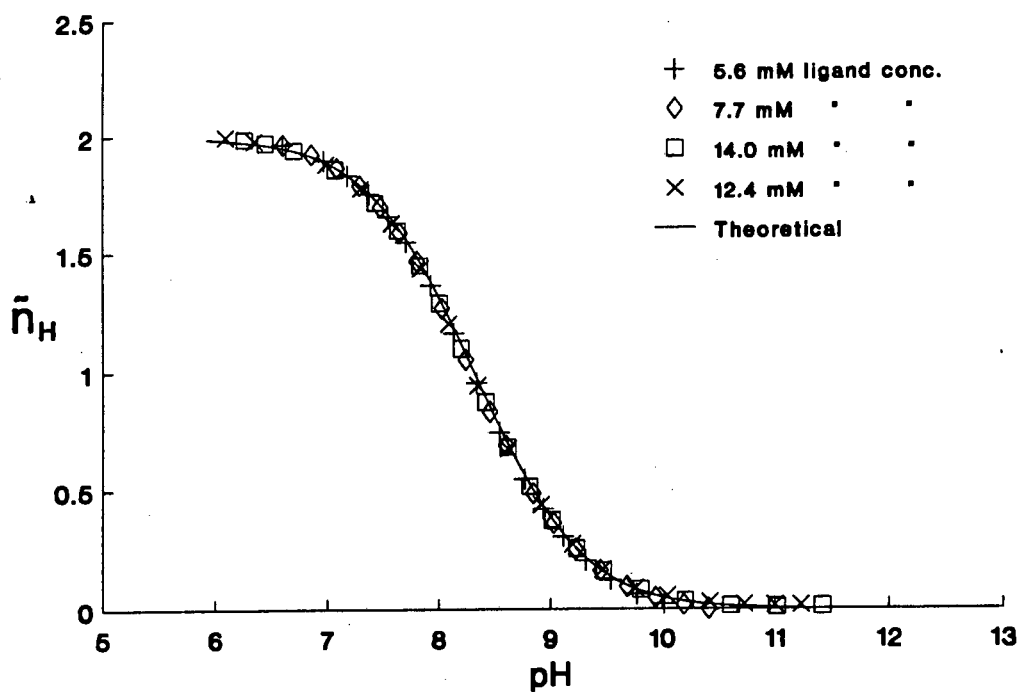


**Figure 3.3 :** Experimental (symbols) and theoretical (solid line) protonation curves for the ligand SUM.

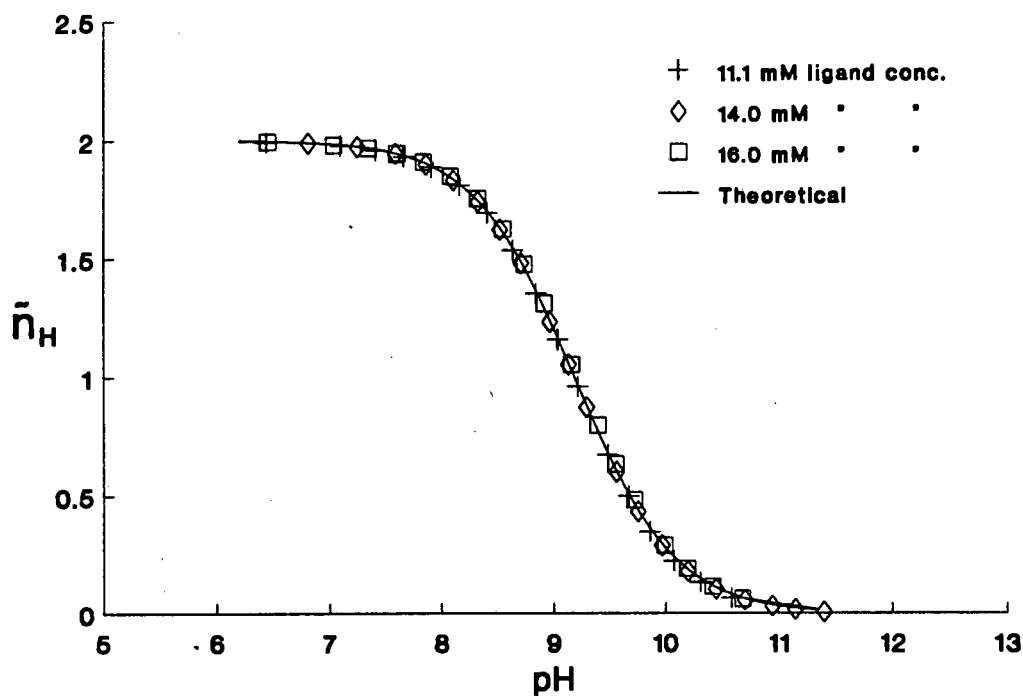
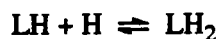


**Figure 3.4 :** Experimental (symbols) and theoretical (solid line) protonation curves for the ligand 656UM.

**Table 3.1** : Logarithms of the overall protonation constants,  $\beta_{01r}$ , for the diamino diamide ligands investigated in this study at 25°C and 0.15 mol dm<sup>-3</sup> (Na)[Cl], together with literature values for the same and related ligands with similar functional groups for the purposes of comparison. A pK<sub>w</sub> of 13.73 was used throughout and the standard deviations have been rounded. n<sub>T</sub> and n<sub>p</sub> refer to the number of titrations and titration points, respectively. Log K<sub>2</sub> is for the reaction



Ligand	Species 0 1 r	log $\beta_{01r}$	SDEV in log $\beta$	log K <sub>2</sub>	n <sub>T</sub>	n <sub>p</sub>	pH range	R <sup>H</sup> , (R <sub>lim</sub> )
5UM	0 1 1	8.72	.002		5	276	5.9 – 10.4	.00567 (.00423)
	0 1 2	16.63	.002	7.91				
6UM	0 1 1	8.83	.001		17	822	5.2 – 11.6	.00534 (.00275)
	0 1 2	16.91	.001	8.07				
656UM	0 1 1	9.52	.002		7	295	5.7 – 11.4	.00785 (.00132)
	0 1 2	18.38	.002	8.86				
5UE	0 1 1	9.23	.001		3	229	6.0 – 11.1	.00199 (.00189)
	0 1 2	17.72	.001	8.49				
6UE	0 1 1	9.51	.002		5	294	6.1 – 11.4	.01127 (.00690)
	0 1 2	18.15	.003	8.64				

Literature Data

Ligand	Species	log $\beta_{01r}$	log K <sub>2</sub>	medium / mol dm <sup>-3</sup>	Reference
5UH	0 1 1	9.31		0.1 KNO <sub>3</sub> , 22°C	[91]
	0 1 2	17.74	8.43		
6UH	0 1 1	9.40		"	"
	0 1 2	18.08	8.68		
656UH	0 1 1	10.15		0.1 – , 25°C	[92]
	0 1 2	19.54	9.39		
5UM	0 1 1	8.93		0.5 KNO <sub>3</sub> , 25°C	[93]
	0 1 2	17.12	8.19		

As can be seen from the protonation curves, the maximum value of  $\bar{n}_H$  is in each case equal to 2, which conforms to the protonation of the two tertiary amine nitrogens of the ligands. Further protonation of the ligands was not expected as the lone pair of electrons on the amide nitrogens are used to stabilize this functional group. Amides are in fact very weak bases being protonated only by strong acids and then only at the carbonyl oxygen and not the nitrogen. On the other hand to form the amide anion requires strong base such as alcoholic KOH. These will therefore not occur under the conditions employed in this study. However if the amide possesses another coordination site at a position that can result in the formation of 5 or 6-membered chelate rings with a metal ion, then the amide proton readily dissociates even under neutral conditions (see later) [44].

Both the protonation constants,  $\log \beta_{011}$  ( $= \log K_1$ ) and  $\log K_2$ , for the various ligands investigated in this study show an increase in basicity in the order 5UM  $\approx$  6UM < 656UM which can be explained by the greater inductive effect of the longer alkyl side chains of the latter ligand, with the longer central alkyl chain of the 6UM ligand having very little effect. Similarly, the constants for both protonation sites of the tetraethyl derivatives show a marked increase in basicity in the order 5UM < 5UE and 6UM < 6UE as expected on the basis of the increasing inductive effect from methyl to ethyl.

Considering the ligand pairs 5UH and 5UM, 6UH and 6UM or 656UH and 656UM, it is seen that the primary amines are more basic than the tertiary amines by roughly half a log unit, in each case. Although the methyl groups are better electron donors than hydrogen, which should result in the tetramethyl ligands being more basic due to the inductive effect, this is found only in the gas phase. It is well known that the expected order in the basicity of amines of  $NRH_2 < NR_2H < NR_3$  as observed in the gas phase is altered to  $NR_3 < NRH_2 < NR_2H$  in solution owing to the varying effect of solvation by water, which is a striking example that solvation energies may confuse the

interpretation of potentiometric results as was previously pointed out [94, 95]. Thus the ligands in this study conform to expectations.

### 3.4.2 COMPLEXATION WITH COPPER(II)

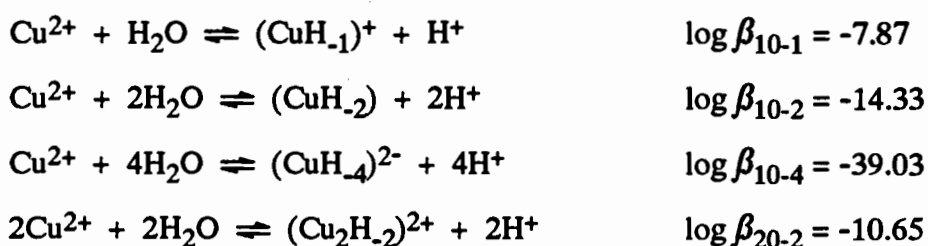
In this section the various formation and deprotonation curves together with the overall complexation constants and the speciation diagrams calculated from these will be presented for each ligand with copper(II). Once again, as the curves for the different ligands all have quite similar features, only representative titrations with a small number of data points for clarity, will be shown for the purposes of illustration. Furthermore, observations which are common to all the systems will only be made once in the following section. For the computational refinements and data visualization of each system the respective protonation constants presented in the previous section were used. As an indication of the possible problems to be encountered in the investigation, the following can be quoted from a paper by Williams *et al* [78] : *'In common with all mathematical treatments of non-simple mononuclear systems we are faced with the qualitative problem of finding the best set of  $\beta$ 's and the quantitative task of assigning values to these  $\beta$ 's. Qualitatively, the possible  $\beta$ 's are limited by the coordination numbers of the metal ions and by the denticity of the ligands.'*

Of the five ligands investigated in this study, 6UE was found to be unable to complex copper effectively resulting in the presence of copper hydroxide precipitate throughout the titrations. Copper(II) complexation with this ligand will therefore not be discussed any further.

An attempt was made to investigate the complexation of the ligand 6UM with zinc(II). This was however unsuccessful due to severe zinc(II) hydroxide precipitation, but acts as an indication of ligand specificity for copper(II).

Each of the four copper(II) diamino diamide ligand systems were found to have the 110, 11-1 and the uncharged 11-2 in common as major species. Furthermore, depending on the distance between the amide groups, the 21-2 complexes were also found to be important for the oxalyl derivatives, but were absent in the malonyl systems. Therefore, as a consequence of these major species in solution, each of the formation curves shows the characteristic back-fanning associated with hydroxo complexation.

As complexation generally occurred in the basic region at a pH greater than 5, the copper(II) hydrolysis equilibria together with their constants (given below) were incorporated in the computational refinements. Values for the constants pertinent to an ionic strength of 0.15 mol dm<sup>-3</sup> were calculated from the equations and data given in Baes and Mesmer [96].



Of possible greater effect on the determined stability constants is the association between copper and the chloride anion, which is after all present in quite high concentrations. This influence can of course be taken into account by also incorporating the copper chloride equilibria, together with their constants in the computational refinement process. Alternatively, allowance could be made for copper(II)-chloride

complexation by multiplying the formation constants given in the following tables by the factor

$$1 + [\text{Cl}^-] \beta_{110} + [\text{Cl}^-]^2 \beta_{120} + [\text{Cl}^-]^3 \beta_{130} + [\text{Cl}^-]^4 \beta_{140}$$

where the  $\beta_{pq0}$  's refer to the various copper chloride species. This was found to have the effect of increasing the value of  $\log \beta_{110}$  for example by an amount of  $0.05 \pm 0.01$  [95]. In line with current practice however, neither of the above methods of correcting for copper chloride association have been employed in this study and it must therefore be borne in mind that the constants are strictly applicable to a  $0.15 \text{ mol dm}^{-3}$  chloride medium only.

As it is evident that various structures could potentially exist for the species in solution, possible coordination sites will be discussed in a following section after further experimental work has been carried out.

#### **3.4.2.1 N,N' bis [2-(dimethylamino)ethyl] ethanediamide (SUM)**

From an experimental point of view this was the easiest of the systems investigated. Titrations of various ligand to metal ratios ranging from 3 : 1 to 1 : 1 were carried out in both directions. These were replicated with identical titration conditions and showed good reproducibility. Even at the low ligand to metal concentrations no copper hydroxide precipitate formation was observed.

However the computational analysis of the potentiometric data presented great difficulty owing to the problem of having to decide on a 'best' model describing the system. Three models came into consideration consisting of the species 110, 11-1, 11-2 and 21-2, plus either 21-3, 21-4 or both of these. Since it was very difficult to decide between the first two models, constants for both have been presented in Table 3.2, together

with values reported in the literature. Attempts to refine constants for species with more than one ligand per metal ion were unsuccessful.

**Table 3.2** : Logarithms of the overall stability constants,  $\beta_{pqr}$ , of copper(II) with SUM for two possible models, determined at 25°C and 0.15 mol dm<sup>-3</sup> (Na)[Cl], together with constants reported in the literature.

Species p q r	log $\beta_{pqr}$	SDEV in log $\beta$	$n_T$	$n_p$	pH range	conc. range mmol dm <sup>-3</sup>	R <sup>H</sup> , (R <sub>lim</sub> )
<u>Model One</u>							
1 1 0	8.33	.02	8	588	4.5 – 10.9	[L]: 4.7 – 10.7	.01088 (.00554)
1 1 -1	1.06	.02				[M]: 2.45 – 7.5	
1 1 -2	-7.06	.01					
2 1 -2	0.79	.01					
2 1 -3	-6.89	.03					
<u>Model Two</u>							
1 1 0	8.44	.01	7	475	4.5 – 10.9	[L]: 4.7 – 10.7	.00898 (.00542)
1 1 -1	1.28	.01				[M]: 2.45 – 7.5	
1 1 -2	-7.24	.01					
2 1 -2	0.74	.01					
2 1 -4	-15.36	.02					
<u>Literature Values</u>							
Calculated from data reported by Zuberbühler and Kaden [93] for 0.5 mol dm <sup>-3</sup> KNO <sub>3</sub> .							
pqr (log $\beta$ ) : 110 (8.26); 11-1 (.55); 11-2 (-7.44); 21-2 (1.49); 21-3 (-7.30); 21-4 (-16.66)							

Model one has a reasonably low R-factor and small standard deviations in log  $\beta_{pqr}$  as well as a very good qualitative correspondence between calculated and observed plots for both  $\bar{n}$  and  $\bar{Q}$  as can be seen from Figures 3.5 and 3.6, respectively.

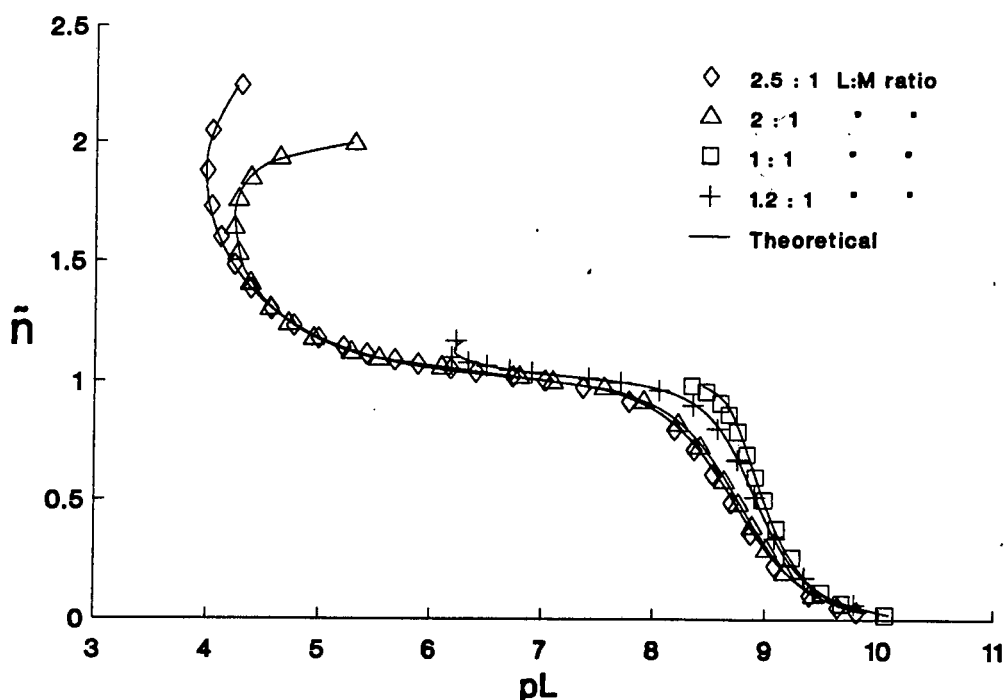


**Figure 3.5** : Experimental (symbols) and theoretical (solid line) complexation curves for various ligand to metal ratios of the copper(II)-5UM system.

The formation curves, particularly those of higher ligand to metal ratios, level off at a value of  $\bar{n}$  equal to 1, indicating the presence of ML as a major species, before fanning-back due to the formation of hydroxo species. The latter are in reality not true hydroxo species but originate from the loss of the amide protons upon metal ion coordination, as has been reported previously by other workers [44, 52, 93]. Essentially the ligand has been defined as having only two dissociable protons, i.e. the amine protons, whereas more than two protons are actually displaced on complexation. This is mathematically indistinguishable from an uptake of hydroxyl ions resulting in the apparent hydroxo complexes  $MLH_{-1}$ ,  $MLH_{-2}$  and  $M_2LH_{-2}$ , i.e. 11-1, 11-2 and 21-2 respectively. As can be seen from Figure 3.5 the various formation curves corresponding to different ligand to metal concentration ratios are split up in the region of  $\bar{n}$  less than one, clearly indicating the presence of polynuclear species.

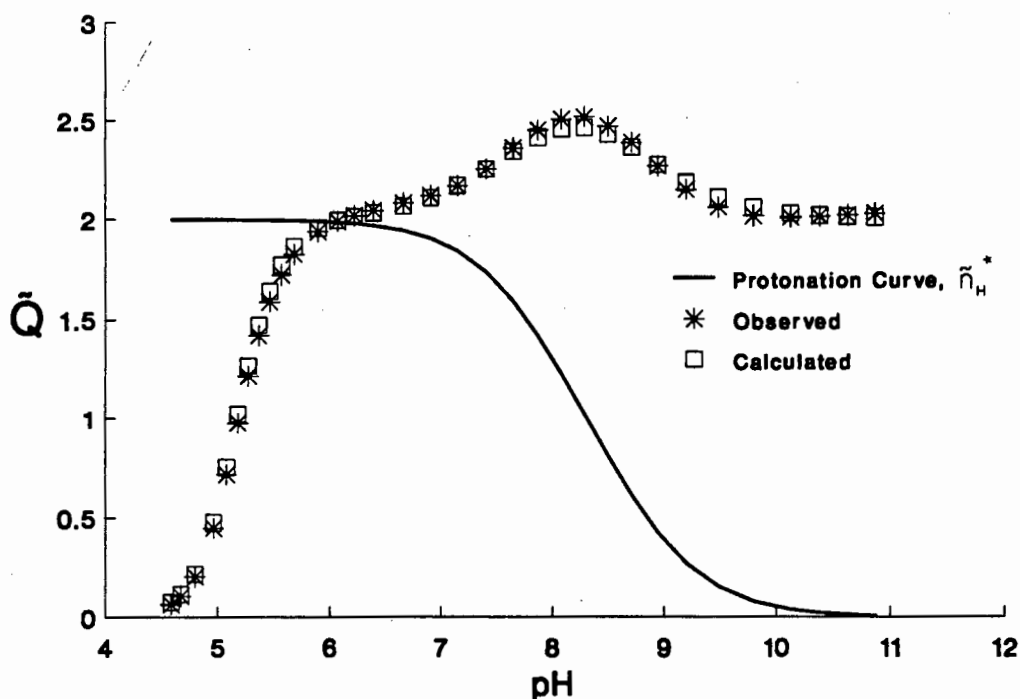


**Figure 3.6** : Observed deprotonation curve for a 2.5 : 1 ligand to metal ratio titration of the copper(II)-5UM system together with the calculated curve using constants from model 1.

The  $\bar{Q}$  deprotonation curves were all quite similar, therefore the observed and calculated plots of only one titration are shown in Figure 3.6. The shape of the curves is also representative of the other ligand systems. Since the  $\bar{Q}$  function has not been as extensively used in the literature as the  $\bar{n}$  function, some of its features will be dealt with here. The solid line in the figure, which starts off at a value of 2, represents the average number of protons bound per ligand according to the measured pH, and is given by  $\bar{n}_H^*$ . This is an indication of the number of protons available for displacement by the metal ion on coordination at a particular pH. As can be seen from the figure the curves of the observed and calculated deprotonation functions  $\bar{Q}$ , rapidly move up to intersect the protonation curve  $\bar{n}_H^*$  at a pH of 6, reaching a maximum value of about 2.5 at pH 8.2. From here on the curves run roughly parallel to the protonation curve and then level off at a value of 2 in the strongly alkaline region. This means that from a pH of about 8.2 onwards two additional protons have been displaced per metal ion on complexation,

resulting in a total of four protons. Since  $\bar{Q}$  is defined as the number of protons displaced per metal ion this could indicate the presence of major species with a 1 : 2 metal to ligand ratio of stoichiometric coefficients, i.e. two ligands per metal ion each with two protons that have been displaced.

However the data are also consistent with the displacement of two additional protons from one ligand molecule again resulting in a loss of four protons per metal ion indicating a major 1 to 1 metal to ligand species, as was found to be the case in this study.

The second model in Table 3.2 has the better R-factor, although based on the Hamilton test this is not statistically significantly different to the first model. It also has smaller standard deviations in  $\log \beta_{pqr}$ . However this model shows a marked discrepancy between the observed and calculated  $\bar{Q}$  curves at high pH as can be seen from Figure 3.7, although the fit in the  $\bar{n}$  curves is indistinguishable from that observed for the first model.

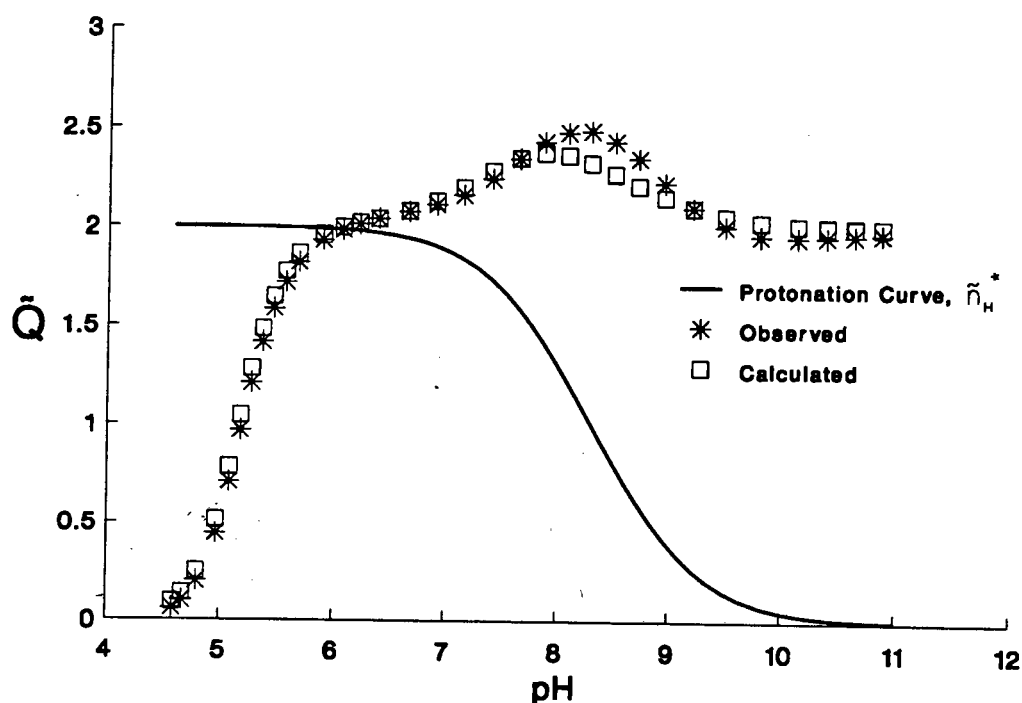


**Figure 3.7** : Observed deprotonation curve for a 2.5 : 1 ligand to metal ratio titration of the copper(II)-5UM system together with the calculated curve using constants from model 2.

This is due to the fact that the function  $\bar{n}$  shows only a small portion of the whole data, being undefined in the basic region from a pH of about 8 onwards for a 2.5 : 1 ligand to metal ratio titration of this particular system. This underlines the importance of the deprotonation function as a means of visualizing the titration data. Calculated and observed titration curves can also be used to visualize all of the data, but this method is unsatisfactory as these plots are rather insensitive to changes in  $\log \beta_{pqr}$ . Another point detracting from model two is that the species don't show a natural stepwise progression, which is always difficult to account for. Thus, for the purposes of further calculations, model one was chosen as providing the best description of the copper(II)-5UM system based mainly on the qualitative criterion of a better fit in the  $\bar{Q}$  curves.

The third model which included both complexes, as was found by Zuberbühler and Kaden [93], had the largest R-factor with a value of .01153 as well as large standard deviations in  $\log \beta_{pqr}$  ranging from .03 to .09. Furthermore a similar discrepancy between the observed and calculated  $\bar{Q}$  was observed as for the second model. As this should theoretically have shown the best statistical fit, since one additional parameter is being optimized, model three was therefore disregarded on the basis of Ockham's razor [83].

Figure 3.8 represents the species distribution of a 2 to 1 ligand to metal titration, calculated by the program ESTA using the constants of model one. From this it can be seen that all five complexes are relatively important, in particular the 11-2 species in the basic region, and the 21-2 binuclear complex in the region of neutral pH between 5 and 7.5. This results in virtually no free copper being present in solution at a pH greater than 6. Apart from the strength of complexation, 21-2 coordination effectively doubles the ligand concentration, which could contribute to the fact that no copper hydroxide precipitation occurred, even in the 1 to 1 ligand to metal titrations.

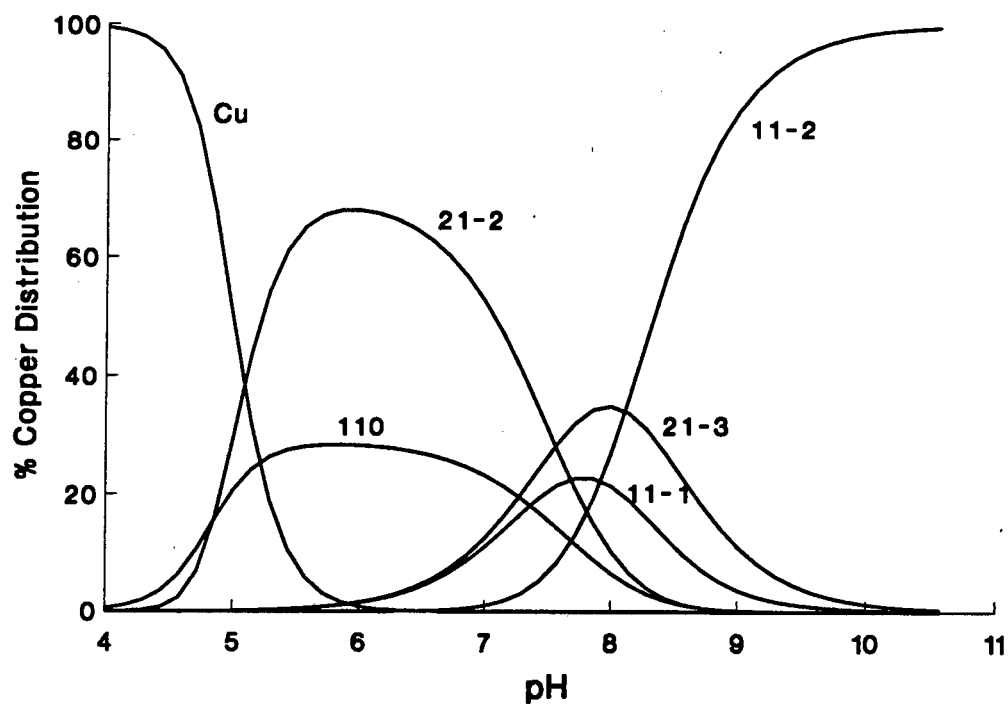


**Figure 3.8** : Species distribution of the copper(II)-5UM system for a 2 : 1 ligand to metal ratio.

A final observation that should be made is about the colour changes of the solutions that took place during the course of the titrations. These proceeded from an intense violet in the strongly alkaline solutions through a dark blue to a very pale, light blue in the mildly acidic region. Thus a change in species distribution with pH, as observed in Figure 3.8, is accompanied by a change in the colour and intensity of the solutions. This is due to the fact that the different species absorb light in different parts of the spectrum according to the number of nitrogen atoms in the coordination sphere of the copper ion, which will be discussed in greater detail in a later section.

### 3.4.2.2 N,N' bis [2-(diethylamino)ethyl] ethanediamide (5UE)

Although this ligand does not exactly fit into the homologous series having N terminal alkyl substituents that are different from those of the other ligands, its complexation with copper(II) was studied in order to determine the consequences of the more strongly inductive effect versus greater steric crowding of the ethyl groups on the strength of binding.

Solutions with ligand to metal ratios ranging from 3.5 : 1 to 1 : 1 were titrated with either acid or base and apart from a slight formation of copper hydroxide precipitate at neutral pH in the low ligand to metal ratio titrations, the investigation of this system was relatively straightforward resulting in the refined constants given in Table 3.3.

**Table 3.3** : Logarithms of the overall stability constants,  $\beta_{pqr}$ , of copper(II) with 5UE, determined at 25°C and 0.15 mol dm<sup>-3</sup> (Na)[Cl].

Species p q r	log $\beta_{pqr}$	SDEV in log $\beta$	$n_T$	$n_p$	pH range	conc. range mmol dm <sup>-3</sup>	R <sup>H</sup> , (R <sub>lim</sub> )
1 1 0	8.16	.01	8	552	4.8 - 11.0	[L] : 5.2 - 17.9	.00891 (.00411)
1 1 -1	0.35	.005				[M] : 2.0 - 5.0	
1 1 -2	-8.49	.01					
2 1 -2	-1.72	.03					

As in the case of the copper(II)-5UM system, a constant for the 21-3 complex could be refined for some of the titrations. However, the R-factors of such models were in fact larger and the fit between the calculated and observed  $\bar{n}$  and  $\bar{Q}$  curves was not any better than for the simpler system reported in the table and therefore on the basis of Ockham's razor these models were not considered. As the  $\bar{Q}$  curves were quite similar to

those of the previous system only the complexation curves of the ligand 5UE with copper(II) are presented in Figure 3.9. The calculated plots are again shown as solid lines.

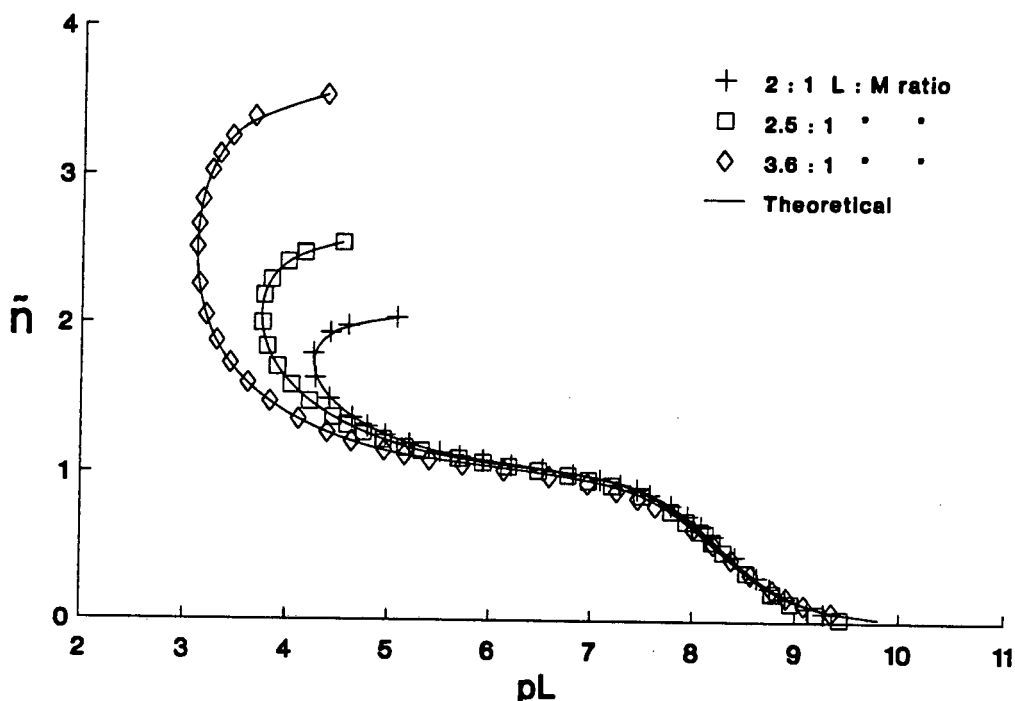


**Figure 3.9** : Experimental (symbols) and theoretical (solid line) complexation curves for various ligand to metal ratios of the copper(II)-5UE system.

In contrast to the copper(II)-5UM system, only a slight splitting of the formation curves for different ligand to metal titration ratios is observed in the region of  $\bar{n}$  less than one, indicating the lesser importance of the polynuclear species. This is also reflected in both the smaller value of the 21-2 constant and in the species distribution plot given in Figure 3.10, with the curve of the 21-2 species lying below that of the 110 complex. The experimental solutions were also less intensely coloured throughout the titrations and not quite as violet in the strongly alkaline region as in the case of the copper(II)-5UM system.

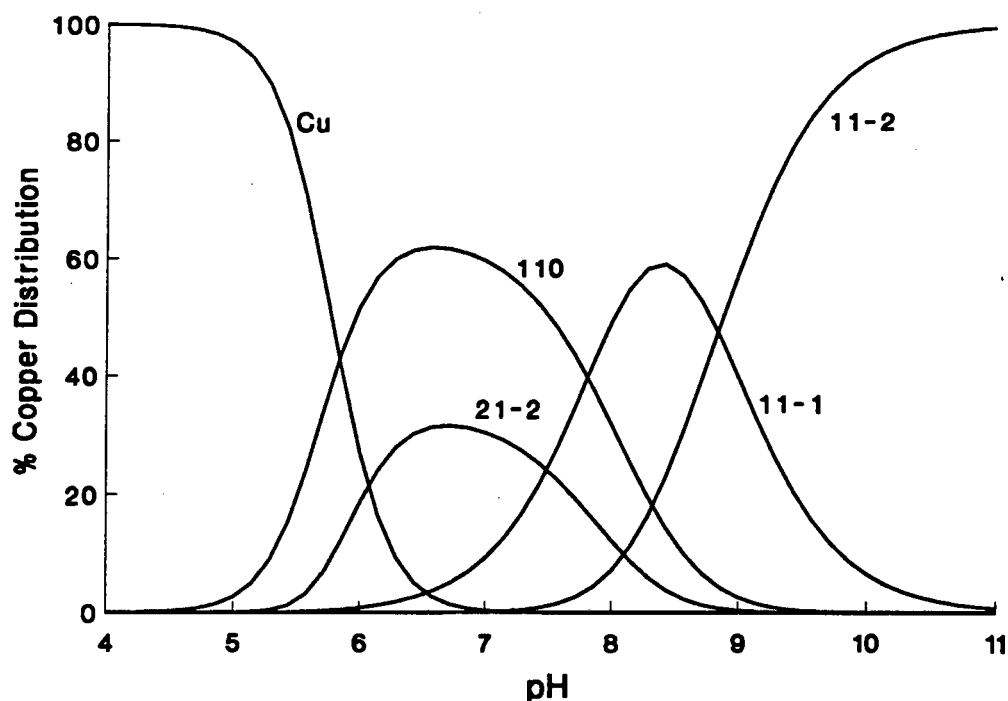


**Figure 3.10** : Species distribution of the copper(II)-5UE system for a 2 : 1 ligand to metal ratio.

### 3.4.2.3 N,N' bis [2-(dimethylamino)ethyl] propanediamide (6UM)

This system presented the greatest experimental difficulties as formation of copper hydroxide precipitate occurred in all titrations, even for very high ligand to metal ratios indicating weak complexation of copper(II) by the ligand 6UM. Based on the analogous series of tetramine ligands this was very surprising as it had been expected that the ligand 6UM would be a stronger metal ion complexor than 5UM. In fact determinations could only be carried out successfully by adding metal ion to very basic solutions of the ligand in large excess, and titrating these with acid until precipitate formation was observed. Carrying out the titration in the opposite direction resulted in a persistent precipitate even in the very alkaline region.

This weak complexation, with precipitation occurring at a pH of about 6.4 for titrations with ligand to metal ratios in excess of 6 : 1, made the computational analysis extremely difficult, not from the point of view of species selection but in the choice of 'best' values for the constants. This required carrying out a considerable amount of computations which is not immediately evident from the results. As can be seen from the formation curve for the copper(II)-6UM system given in Figure 3.11, the value of  $\bar{n}$  does not fall very much below 0.6. The deprotonation function  $\bar{Q}$  given in Figure 3.12 for a 4.5 : 1 ligand to metal ratio does also not reach the pH-axis.

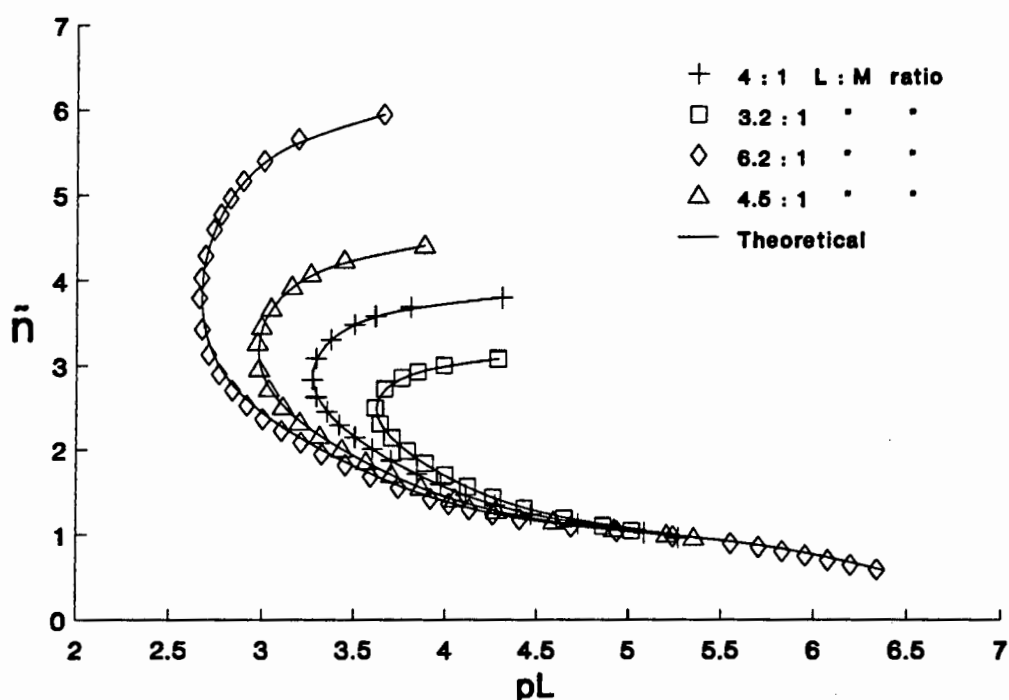


**Figure 3.11** : Experimental (symbols) and theoretical (solid line) complexation curves for various ligand to metal ratios of the copper(II)-6UM system.

Therefore not many data points were obtained in the region of 110 complexation, resulting in mathematical correlation of variables. One method of circumventing this problem would have been to use a copper(II) ion sensitive electrode. Since such an electrode was not available, another approach was adopted, namely of carrying out

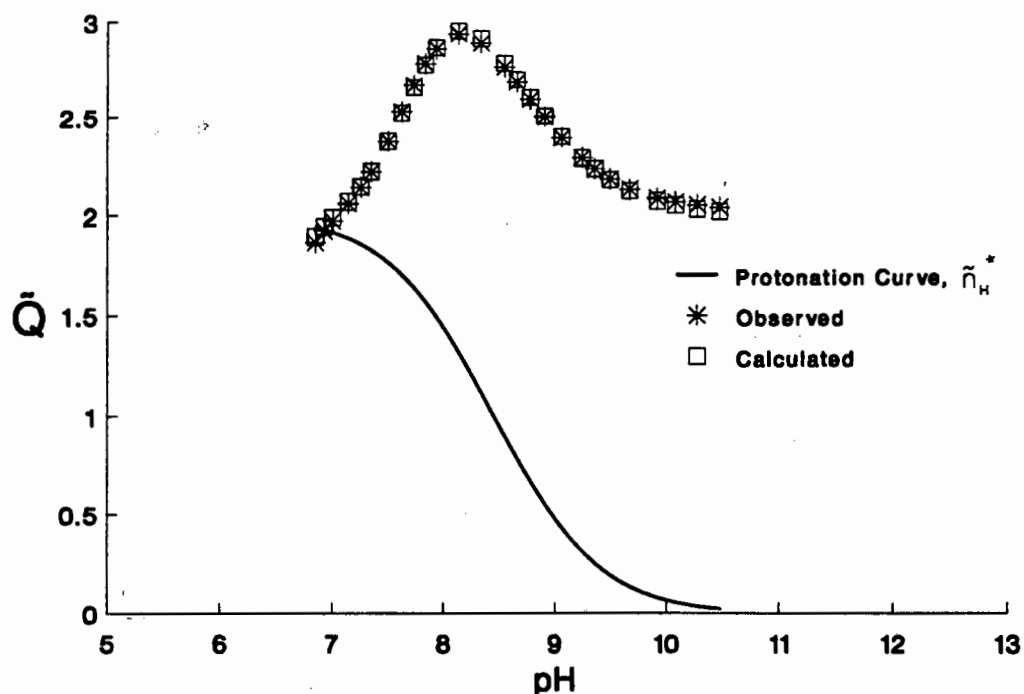


**Figure 3.12** : Observed and calculated deprotonation curves for a 4.5 : 1 ligand to metal ratio titration of the copper(II)-6UM system together with the calculated curve using the refined constants from Table 3.4

titrations with very high ligand to metal ratios and small increments in the titrant in order to extend this region of complexation to the limit and obtain a greater number of data points. The latter method was successful resulting in an analysis without correlation, from which the constant for the 110 species was obtained. This was fixed in the refinement over all the titrations, including those with lower ligand to metal ratios, and resulted in the three constants for the copper(II)-6UM system reported in Table 3.4, which gave quite a good theoretical fit with the experimental points as can be seen from Figures 3.11 and 3.12 for  $\bar{n}$  and  $\bar{Q}$  respectively.

Using the refined constants from Table 3.4 the speciation diagram, given in Figure 3.13, for a 4 to 1 ligand to metal titration of the copper(II)-6UM system was constructed. Even though this distribution curve is calculated for a ligand to metal concentration ratio

**Table 3.4** : Logarithms of the overall stability constants,  $\beta_{pqr}$  of copper(II) with 6UM, determined at 25°C and 0.15 mol dm<sup>-3</sup> (Na)[Cl].

Species p q r	$\log \beta_{pqr}$	SDEV in $\log \beta$	$n_T$	$n_p$	pH range	conc. range mmol dm <sup>-3</sup>	$R^H, (R_{lim})$
1 1 0	6.51	.01	12	817	6.4 – 11.0	[L] : 8.0 – 19.1	.00790 (.00536)
1 1 -1	-1.54	.005				[M] : 1.7 – 3.6	
1 1 -2	-8.94	.002					

that is double that employed for Figures 3.8 and 3.10, it is immediately evident that the ligand 6UM is not as effective in complexing copper(II) as either 5UM or 5UE. Compared to the distribution diagram of 5UM, the curve for the copper(II) aqua ion is noticeably shifted towards higher pH resulting in an appreciable free copper(II) concentration up to a pH of about 7. This causes the ionic product to be exceeded and results in copper(II) hydroxide precipitation as observed during the titrations.

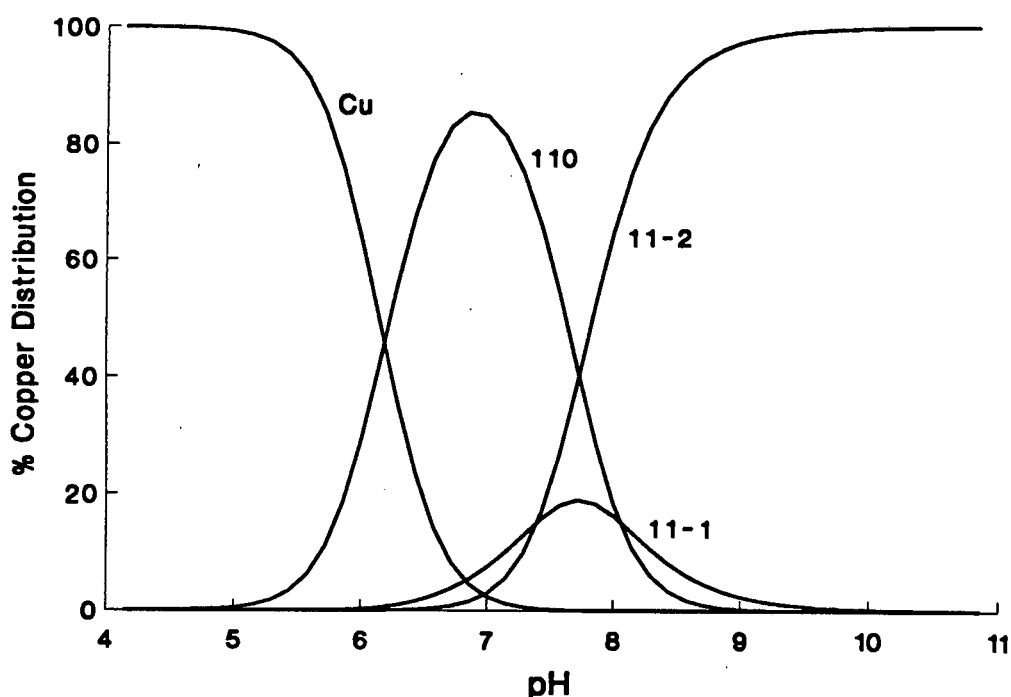


**Figure 3.13** : Species distribution of the copper(II)-6UM system for a 4 : 1 ligand to metal ratio.

The experimental solutions were even less intensely coloured than in the 5UE system with copper(II). Furthermore the colour change on titrating with acid proceeded only from a very faint violet to light blue.

#### 3.4.2.4 N,N' bis [3-(dimethylamino)propyl] ethanediamide (656UM)

In order to complete the homologous series, titrations with the ligand 656UM were carried out for various ligand to metal ratios from 2.7 : 1 to 4 : 1. No unexpected difficulties such as undue precipitation were encountered during the experimental investigation nor were there any problems experienced with the refinement of the titration data. As can be seen from Figure 3.14 the formation curves are quite well-behaved meeting the X-axis at a value for pL of about 10 and showing the characteristic fanning-back at higher pH.

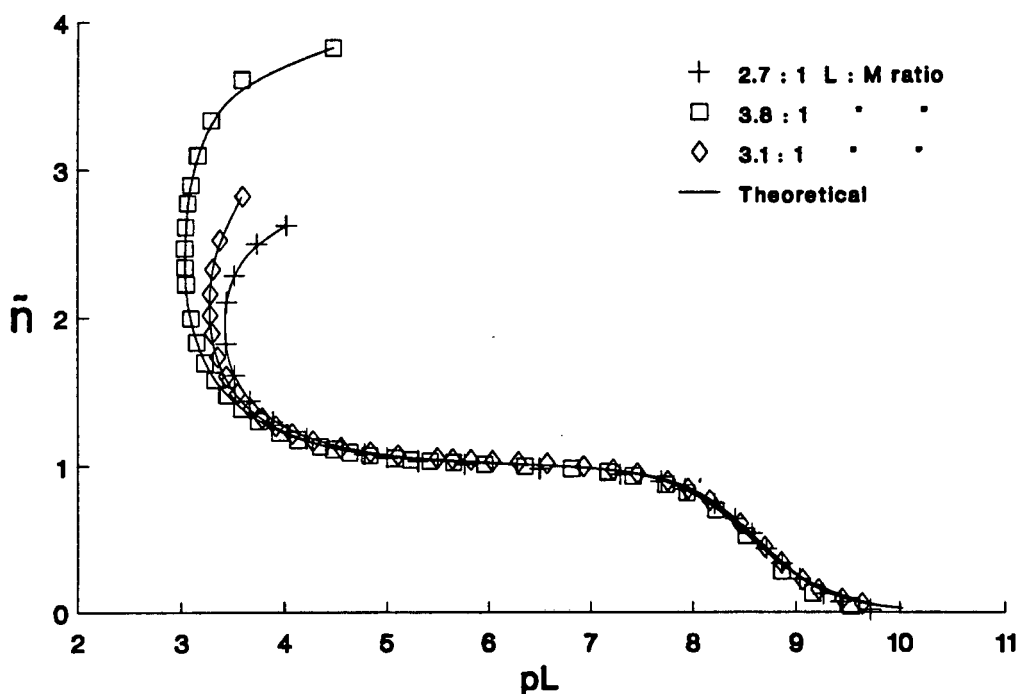


**Figure 3.14** : Experimental (symbols) and theoretical (solid line) complexation curves for various ligand to metal ratios of the copper(II)-656UM system.

Using the refined constants presented in Table 3.5 the theoretical formation curves were again calculated and plotted in Figure 3.14 on the same set of axis as solid lines. These superimpose very well with the experimental curves giving some confidence to the proposed model and the refined constants.

**Table 3.5** : Logarithms of the overall stability constants,  $\beta_{pqr}$ , of copper(II) with 656UM, determined at 25°C and 0.15 mol dm<sup>-3</sup> (Na)[Cl].

Species p q r	log $\beta_{pqr}$	SDEV in log $\beta$	$n_T$	$n_p$	pH range	conc. range mmol dm <sup>-3</sup>	$R^H$ , ( $R_{lim}$ )
1 1 0	8.39	.01	7	524	5.0 – 11.5	[L]: 4.7 – 14.7	.00591 (.00378)
1 1 -1	-0.17	.005				[M]: 1.7 – 3.8	
1 1 -2	-9.80	.005					
1 1 -3	-21.87	.01					
2 1 -2	-1.23	.02					

In contrast to the other three systems this model, describing the copper(II)-656UM system, includes a 11-3 complex for the first time, as reported by Ojima and Nonoyama [44] for the ligand 5UH. As can be seen from the speciation diagram for the copper(II)-656UM system, calculated using the constants in Table 3.5, the 11-3 species becomes increasingly important accounting for about 25% of bound copper at a pH of 11.5. Apart from this additional species and the absence of the 21-3 complex the speciation diagram is again quite similar to that of the copper(II)-5UM system, although the curves have all been shifted to a higher pH by between one and two log units. Even so this ligand is better able to solubilize copper(II) than 6UM, as is evident on comparing the positions of the copper aqua ion curves in the two speciation diagrams, represented in Figures 3.13 and 3.15. This is probably due to the stronger 110 complex and the existence of the 21-2 species in the case of the ligand 656UM. The colour of the experimental solutions again changed during

the course of the titrations but was far less intense and of a lighter shade of blue (i.e. shifted towards longer wavelength) than observed for any of the other three systems.

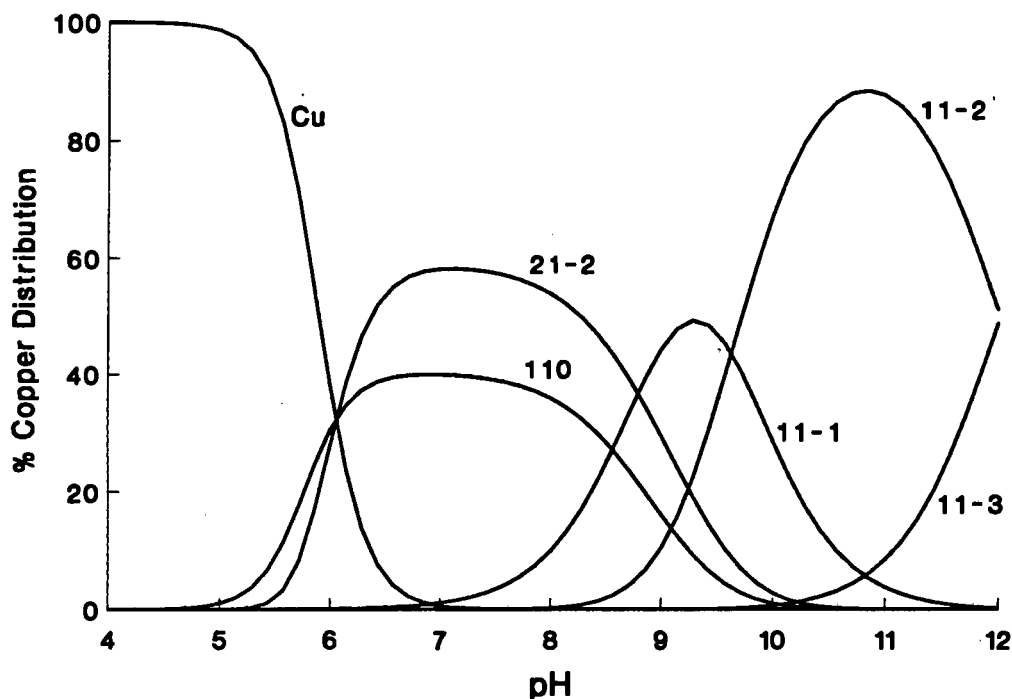


**Figure 3.15** : Species distribution of the copper(II)-656UM system for a 2 : 1 ligand to metal ratio.

This then concludes the potentiometric study of the series of copper(II) chelators, with some rather unexpected results being observed. Before addressing these problems however, what needs to be determined next are the actual structures of the various species in solution since for some of the complexes a number of different possibilities exist, between which potentiometry cannot distinguish. As the solutions of all four ligands with copper(II) exhibited a change in colour and intensity during the course of the titrations it seemed appropriate to use UV/VIS spectrophotometry for this structure elucidation.

## 3.5 UV/VIS ANALYSIS

### 3.5.1 THEORY AND PROCEDURE

In order to elucidate the structures of the various species formed in solution a number of spectroscopic techniques can potentially be used, i.e. NMR, Infrared, Raman or UV/VIS spectroscopy. The use of Infrared is precluded owing to the fact that this technique cannot be used for work in aqueous solutions as well as not being suitable in any event because of the relatively low molar absorption coefficients in this spectral region, requiring very high species concentrations, and limited accuracy of the absorbance values. NMR was also not suitable due to the presence of the paramagnetic metal ion copper(II) in the systems under investigation. An attempt was made to analyze the solutions using Raman spectroscopy. However the necessarily high species concentrations resulted in test solutions that were too intensely coloured for any meaningful results to be obtained. Thus as a change in the visible spectrum of the solutions had already been observed during the course of the titrations the use of UV/VIS spectrophotometry was indicated.

This experimental technique can in fact be used in much the same way as potentiometry for the quantitative analysis of equilibrium reactions, thereby determining formation constants. This is due to the fact that the absorbance  $A$  of a solution is a linear function of the concentration of the absorbing species, which is given by the Beer-Lambert law

$$A = \log I_0 / I = \epsilon c l$$

where  $I_0$  and  $I$  are the intensities of the incident and emergent light

beams respectively

$\epsilon$  is the molar absorption coefficient

$c$  is the species concentration in  $\text{mol dm}^{-3}$  and

$l$  is the optical path length.

As the species concentration is a function of its formation constant and the reactant concentrations, the former can essentially be evaluated. In a review on the subject, McBryde discusses various experimental techniques as well as several graphical and computational methods for the evaluation of the data obtained [97].

In systems where an overlap of absorbing species occurs the treatment of the data is more complicated and is susceptible to error. For systems of more than one absorbing species the Beer-Lambert law can be expanded to give the following linear combination in terms of individual concentrations and molar absorption coefficients of the species involved

$$\begin{aligned} A^\lambda &= l(\epsilon_1^\lambda c_1 + \epsilon_2^\lambda c_2 + \dots + \epsilon_i^\lambda c_i) \\ &= l \sum \epsilon_i^\lambda c_i \end{aligned} \quad 3.26$$

If the path length is given in cm,  $\epsilon_i^\lambda$  is the molar absorption coefficient of the  $i$ th species in solution at a wavelength of  $\lambda$  and has the units  $\text{mol}^{-1} \text{dm}^3 \text{cm}^{-1}$ .

Thus a set of simultaneous equations can be set up which can be solved for the stability constants by some iterative refinement procedure. The use of UV/VIS spectroscopy is especially indicated for the study of equilibria that do not directly or indirectly involve protons, thereby precluding the use of glass electrode potentiometry, or for which ion sensitive electrodes are not available. It has the further advantage over potentiometry that the properties of more than one reactant or product can be directly measured. Furthermore as the absorbance is a measure of the concentration and not the

activity of the species, and since stoichiometric formation constants are expressed in terms of concentration no further mathematical manipulation is therefore required although again a constant ionic strength needs to be maintained.

An obvious requirement of the absorptiometric method is that the reaction being investigated should be accompanied by appreciable changes in the absorption of light at one or more convenient wavelengths. This was not exactly satisfied in the case of the copper(II)-656UM system. A further drawback of the technique is the fact that owing to experimental limitations the absorbance cannot be widely varied without decreasing the precision of the measurement. The readings are therefore effectively confined to a range covering about one order of magnitude which does not allow for a wide spread of reactant concentrations to be employed. Furthermore, each complex contributes two unknowns to the system of simultaneous equations, namely  $\epsilon$  and  $\beta$  thus doubling the number of parameters requiring evaluation from the experimental results compared to potentiometry [97]. Problems can arise when more than one species absorb at very similar wavelengths. In proceeding from one species to another only small changes in  $\epsilon$  at a given wavelength are expected for complexes with the same number of nitrogens coordinated to the central metal ion thus making the technique unreliable. Lastly, significant parameter correlation has been reported due to band overlap in electronic spectra.

UV/VIS spectroscopy can be used diagnostically for the determination of the number of absorbing species present in solution by carrying out a graphical or computer based rank analysis of the wavelength absorbance matrix [59]. Secondly the occurrence of isosbestic points in a set of superimposed absorbance spectra for solutions of constant metal ion and increasing ligand concentrations, is usually an indication of the presence of only two absorbing species in equilibrium. However, a fortuitous combination of circumstances could give rise to pseudo-isosbestic points with more than two absorbing species in solution.

Due to the complexity of the copper(II)-ligand systems under investigation, consisting of overlapping species with potentially very similar absorption coefficients, together with the several other limitations of the absorptiometric method discussed above, UV/VIS spectroscopy was not used for the purposes of obtaining quantitative results. This technique was used solely for reasons of structure elucidation as the strength of complexation had already been successfully determined by the more sensitive and accurate method of glass electrode potentiometry.

Therefore we are more interested in the wavelength of maximum absorption of each species, i.e.  $\lambda^{\max}$ , which is related to the energy of the absorbed radiation by the well-known expression

$$E = h \nu = h c / \lambda$$

where  $h$  is Planck's constant and

$c$  is the speed of light,

and is a measure of the ligand field stabilization energy. This does not give a direct measure of the strength of bonding, but only of the amount by which the degenerate d-orbitals of the metal ion have been split due to the crystal field or more precisely in the case of solutions due to the ligand field experienced by the central metal ion. The theory involved is given in two very good accounts by Kettle [98] and Nicholls [99].

In particular the copper(II) ion has the  $d^9$  electronic configuration which is the hole equivalent of the  $d^1$  configuration. Arising from these configurations is only the one Russel-Saunders term or free ion ground state, namely  $^2D$ , which has the  $E_g$  and  $T_{2g}$  crystal field components. In essentially an octahedral field the 5 degenerate d-orbitals are split, due to their spatial arrangement, into 2 higher energy  $e_g$  and 3 lower energy  $t_{2g}$

orbitals or electron wave-functions with an energy difference of  $10Dq$ . For the  $d^9$  electronic configuration the ground state of the complex is given by  ${}^2E_g$  and the excited state, at an energy of  $10Dq$  above this, by  ${}^2T_{2g}$ , which is the inverse of the  $d^1$  case. Thus essentially only one absorption band occurs in the visible region of copper(II) complexes due to d-d transitions, of which  $\lambda^{\max}$  is an indication of the ligand field stabilization energy,  $10Dq$  [100]. Band broadening is however observed for copper(II) complexes due to the presence of several overlapping bands as a result of Jahn-Teller distortion.

Different ligands affect the size of orbital splitting to a greater or lesser extent and can therefore be classified in a spectrochemical series. According to Orgel this is given by  $Cl^- < H_2O < \text{pyridine} < NH_3 < \text{ethylenediamine}$  for the metal ion copper(II), in the order of an increasing effect on the size of  $10Dq$  which in turn affects the wavelength of the absorbed light. For example the  $[Cu(H_2O)_6]^{2+}$  species has a  $10Dq$  of only  $12600\text{ cm}^{-1}$  compared with the species  $[Cu(NH_3)_6]^{2+}$  which has a much larger  $10Dq$  of  $15100\text{ cm}^{-1}$  [101].

Furthermore, not only does the nature of the ligand but also the number of ligands in the coordination sphere of the metal ion affects the size of  $10Dq$ . For example, the series of ammine aqua cupric complexes,  $[Cu(H_2O)_{6-n}(NH_3)_n]^{2+}$ , shows absorption maxima at 790, 745, 680, 645, 590 and 640 nm for  $n = 0$  to 5, respectively [20, 101]. Therefore based on this trend it was thought that by evaluating  $\lambda^{\max}$  of the individual species this would indicate the particular coordination involved.

The titration apparatus and the experimental solution conditions were identical to those employed during the potentiometric work except that the titrations were carried out manually allowing for the readings of absorbance versus wavelength to be taken after each addition of titrant. Duplicate titrations of the four copper(II) systems were carried out with ligand to metal concentration ratios ranging from 1 : 1 to 4.5 : 1. The solutions were

continuously circulated through a standard flow-through quartz cuvette with a 1 cm path length. The absorbance readings were taken with a PYE UNICAM 1700 analogue machine at 10 nm intervals between 400 and 800 nm for about 15 different pH values per titration and were adjusted according to calibration curves determined immediately before and after each set of experimental measurements.

The systems were found to obey the Beer-Lambert law, although only a cursory check was carried out as mainly qualitative results were sought from the absorbance data in this study. In any event variations of this law generally do not occur when working with dilute solutions and are nearly always caused by shifts in the equilibria of the absorbing species due to the effects of dilution.

The analysis using a spectrophotometer has the added advantage over visual observations of being able to discern the onset of precipitate formation more precisely, as this is accompanied by unstable absorbance readings.

Using the analytical concentrations or the measured emf readings together with the formation constants determined in the previous section, the concentrations of the various species were calculated at each titration point by the subroutine ERR% of the program ESTA which had been specifically modified for this purpose. Since the absorption coefficients are based on the copper concentration these species concentrations were adjusted in the case of the polynuclear complexes 21-2 and 21-3 by the stoichiometric coefficients of copper. These concentrations were imposed on the linear absorption matrix, resulting from equation 3.26, which was then quite easily solved for the various  $\epsilon_i^\lambda$ 's by the method of Gaussian elimination with partial row pivoting using a simple BASIC program written especially for this purpose. The results are presented as the electronic spectra of the individual species plotted in the form of absorption coefficients versus wavelength.

### 3.5.2 RESULTS

The results of the UV/VIS analysis of the four copper(II)-diamino diamide systems are presented in Figures 3.16 to 3.19 and are given in the form of calculated absorption coefficients versus wavelength for the various species in solution. In each case the absorption coefficients are given in units of  $10^3 \text{ dm}^3 \text{ mol}^{-1} \text{ cm}^{-1}$  and the wavelengths in nm.

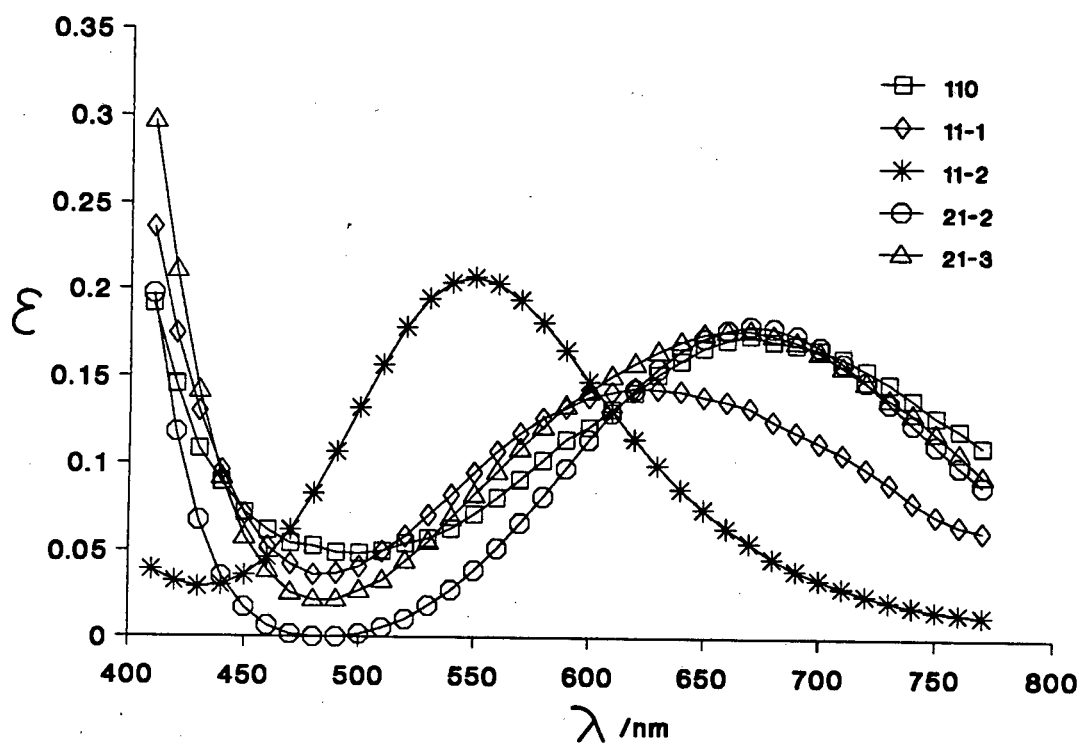


**Figure 3.16** : Calculated electronic spectra of the individual copper(II)-SUM species in aqueous solution. The absorption coefficients are given in units of  $10^3 \text{ dm}^3 \text{ mol}^{-1} \text{ cm}^{-1}$ .

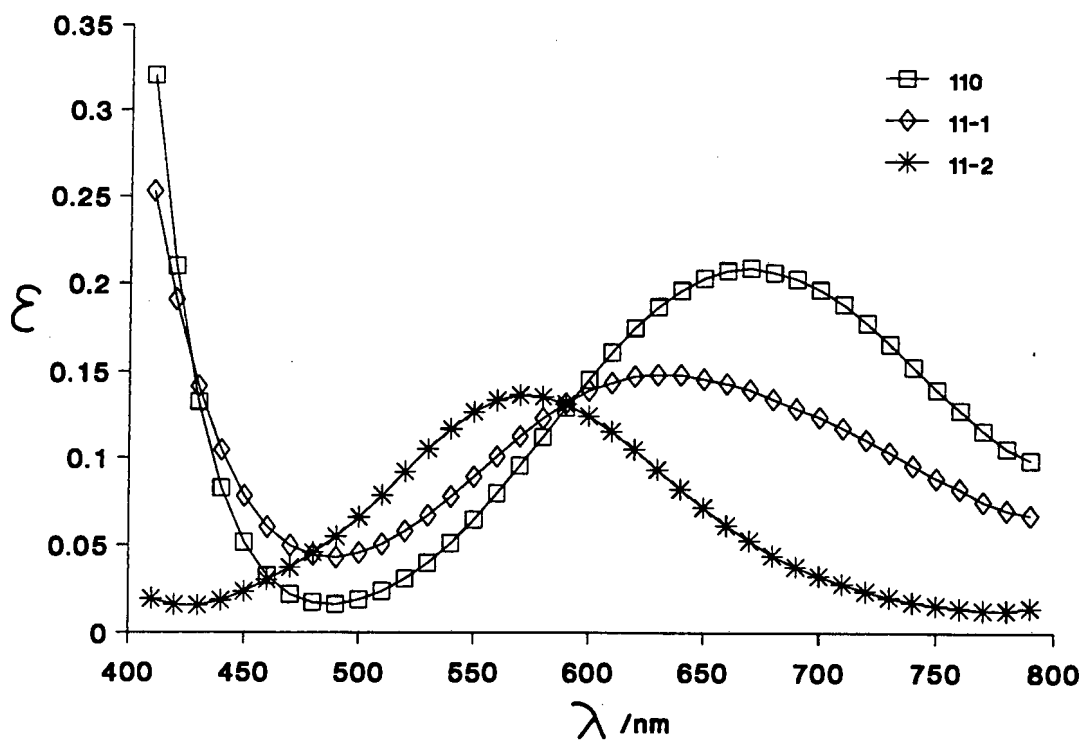


**Figure 3.17** : Calculated electronic spectra of the individual copper(II)-5UE species in aqueous solution. The absorption coefficients are given in units of  $10^3 \text{ dm}^3 \text{ mol}^{-1} \text{ cm}^{-1}$ .

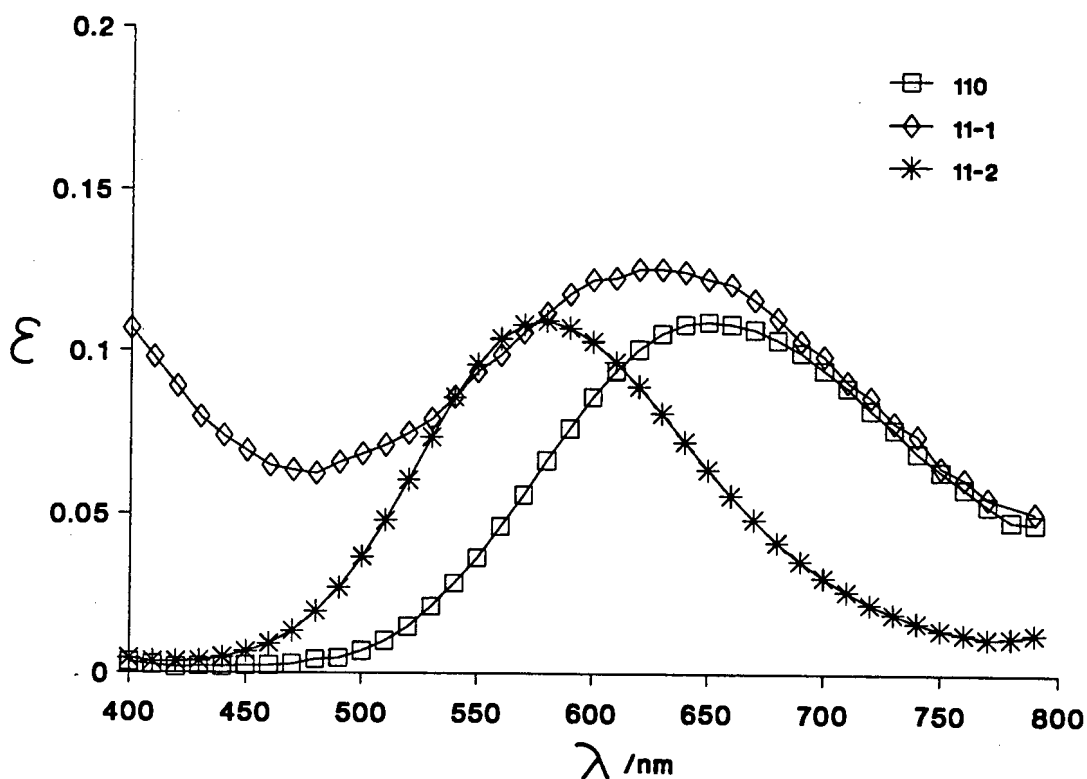


**Figure 3.18** : Calculated electronic spectra of the individual copper(II)-6UM species in aqueous solution. The absorption coefficients are given in units of  $10^3 \text{ dm}^3 \text{ mol}^{-1} \text{ cm}^{-1}$ .

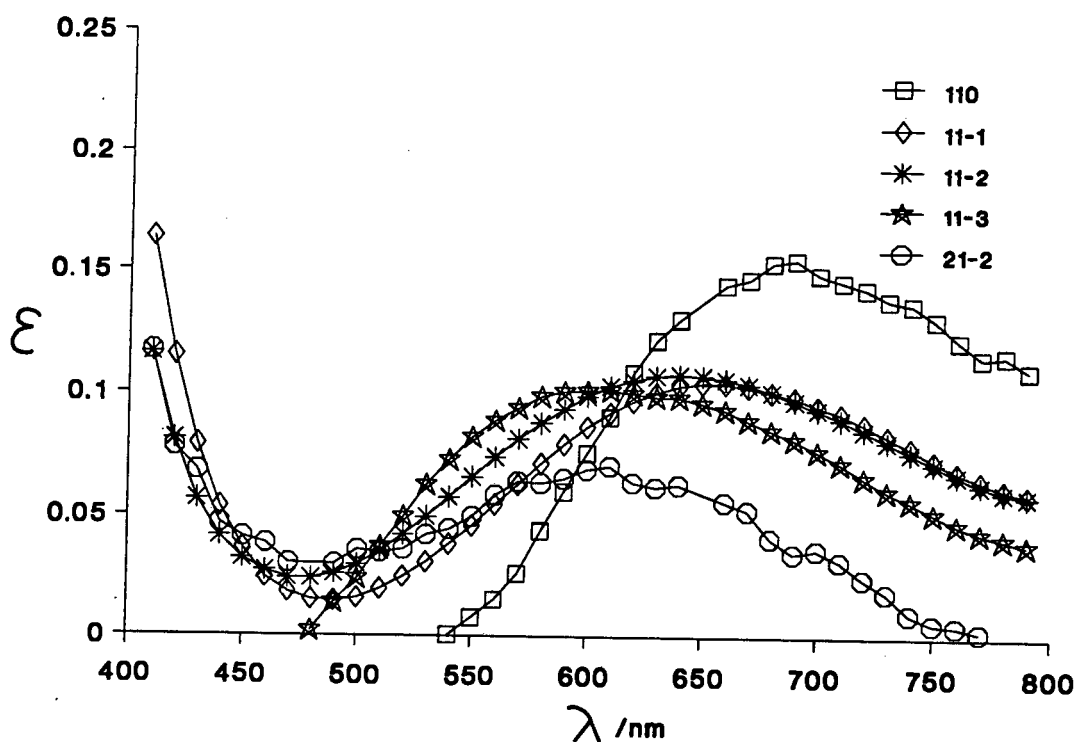


**Figure 3.19** : Calculated electronic spectra of the individual copper(II)-656UM species in aqueous solution. The absorption coefficients are given in units of  $10^3 \text{ dm}^3 \text{ mol}^{-1} \text{ cm}^{-1}$ .

As can be seen from the above figures most of the species have quite smooth curves of absorption coefficients versus wavelength, with a distinct shift in their position along the X-axis being observed for the different complexes.

In the case of the copper(II)-5UE system, the spectrum of the 21-2 species has not been shown as its curve was very uneven, oscillating wildly with no observable trend. Although this complex is quite important in the 2:1 ligand to metal titrations (see Figure 3.10), in the case of the 4 : 1 ligand to metal ratio employed in the UV/VIS titrations it is present to a much smaller extent. The high ligand to metal ratios were necessary in order to avoid copper hydroxide precipitation so that the analysis could be carried out over the entire pH region resulting in a greater number of data points. Furthermore, as the concentration profile follows that of the 110 species very closely and it is expected, c/o the

analogous 5UM species, that the electronic spectra of these two complexes are also very similar, considerable error is associated with the calculation of the absorption coefficient of the 21-2 species, which could explain the uneven curves. Possibly the use of greater differences in the concentration ratios might have solved this problem, but the ligand 5UE is not of major importance in this study and therefore no further titrations were carried out.

The wavelengths corresponding to the maximum absorption coefficients,  $\lambda^{\max}$ , were determined from the above calculated electronic spectra and are given in Table 3.6 together with literature values of the ammine aqua copper(II) species for the purposes of comparison.

**Table 3.6 :** Wavelengths in nm corresponding to the maximum absorption coefficients,  $\lambda^{\max}$ , of the various copper(II) species formed in solution with the ligands 5UM, 5UE, 6UM and 656UM. For comparison literature values of  $\lambda^{\max}$  for 5UM and mono5UM [93, 102], as well as for the  $[\text{Cu}(\text{H}_2\text{O})_{6-n}(\text{NH}_3)_n]^{2+}$  species where  $n = 1$  to 4 are also given [101].

Ligand	p q r					
	1 1 0	1 1 -1	1 1 -2	2 1 -2	2 1 -3	1 1 -3
5UM	675	620	550	670	665	-
5UE	670	630	570	N/C	-	-
6UM	650	625	575	-	-	-
656UM	690	660	640	600	-	610
	Literature Values					
5UM	650	630	550	660	670	
mono5UM	690	670	(570)			
NH <sub>3</sub>	n = 1	n = 2	n = 3	n = 4	in $[\text{Cu}(\text{H}_2\text{O})_{6-n}(\text{NH}_3)_n]^{2+}$	
	745	680	645	590		

As can be seen from this table, or directly from the spectra, there is in most cases a very marked shift in  $\lambda^{\max}$  with species type. Based on the results for the ammine aqua complexes of Cu(II) [101], this indicates a change in the number of nitrogen atoms in the coordination sphere of the copper(II) ion, in going from one species to the next, i.e. from 110 to 11-1 to 11-2. As the curves of the 21-2 and 21-3 species for the copper(II)-5UM system virtually overlap with that of the 110 complex this suggests that an equal number of nitrogen atoms are coordinated per metal ion in each of these cases.

The smallest shifts in  $\lambda^{\max}$  are observed for the copper(II)-656UM system which also showed the least colour change during the course of the titrations. The largest shifts are observed for the copper(II)-5UM system and parallel the data of the  $[\text{Cu}(\text{H}_2\text{O})_{6-n}(\text{NH}_3)_n]^{2+}$  species quite well although the  $\lambda^{\max}$  of the 11-2 complex is considerably lower than even the species with  $n = 4$ . Considering the spectrochemical series for copper(II) in which  $\text{NH}_3$  has a smaller effect on  $10Dq$  than the ligand ethylenediamine, this enhanced shift in  $\lambda^{\max}$  is quite acceptable. Apart from the 656UM ligand, large shifts in  $\lambda^{\max}$  corresponding to those of the  $[\text{Cu}(\text{H}_2\text{O})_{6-n}(\text{NH}_3)_n]^{2+}$  system, are also observed for the species of the copper(II)-5UE and -6UM systems.

Therefore, based mainly on the data of the  $[\text{Cu}(\text{H}_2\text{O})_{6-n}(\text{NH}_3)_n]^{2+}$  series for  $n = 2$  to 4, it seems likely that the UV/VIS analysis in this study can be used to determine the number of nitrogen atoms in the coordination sphere of the copper(II) ion, thereby indicating the most likely structures of the various copper(II)-ligand species present in solution. This will be further discussed in the next section.

An attempt was made to use the UV/VIS electronic spectra to help distinguish between the two models given for the copper(II)-5UM system in section 3.4.2.1. Thus concentrations calculated using the formation constants of the 2nd model were imposed on the mathematical analysis of the UV/VIS data. This unfortunately once again resulted in

smooth curves for the various species with reasonable and very similar  $\lambda^{\max}$  values to those obtained using model one. The method could therefore not be used to distinguish between the two models. In retrospect this is probably not very surprising as the 21-3 species has been replaced by the spectrochemically very similar 21-4 complex in going from model one to model two.

In the case of the copper(II)-656UM system however, the UV/VIS analysis was instrumental in the determination of an improved model. Initially this consisted of the species 110, 11-1, 11-2, 21-2 and the binary complex 120, and had an R-factor of .00832. The electronic spectra obtained using this model to calculate the species concentration, resulted in very jagged curves for virtually all of the species, with no discernable trends. Thus further refinement of the potentiometric data incorporating additional species was carried out, resulting in the present model given in Table 3.5 which has a significantly improved R-factor of .00591. The existence of a 11-3 species had not been previously checked as it had not been found for any of the other systems and according to Ojima and Nonoyama [44] was in fact less likely to form in the case of 6,5,6 type ligands.

### 3.6 DISCUSSION

In this section the various possible structures of the different species in solution as well as their relative strengths of complexation will be discussed using the results from the preceding experimental sections and relevant literature data. In each of the proposed structures it is assumed that water molecules occupy any unfilled coordination sites. For easier comparison of the stability constants of the various species these are presented once again in Table 3.7, together with the literature data of some related ligands with copper(II).

**Table 3.7 :** Logarithms of the equilibrium constants with copper(II) and protons for the ligands investigated in this study as well as selected values calculated from the literature for some related ligands for the purposes of comparison.  $K_n^H$  refers to stepwise protonation constants and  $\beta_{pqr}$  to the overall stability constants. See text for structure types.

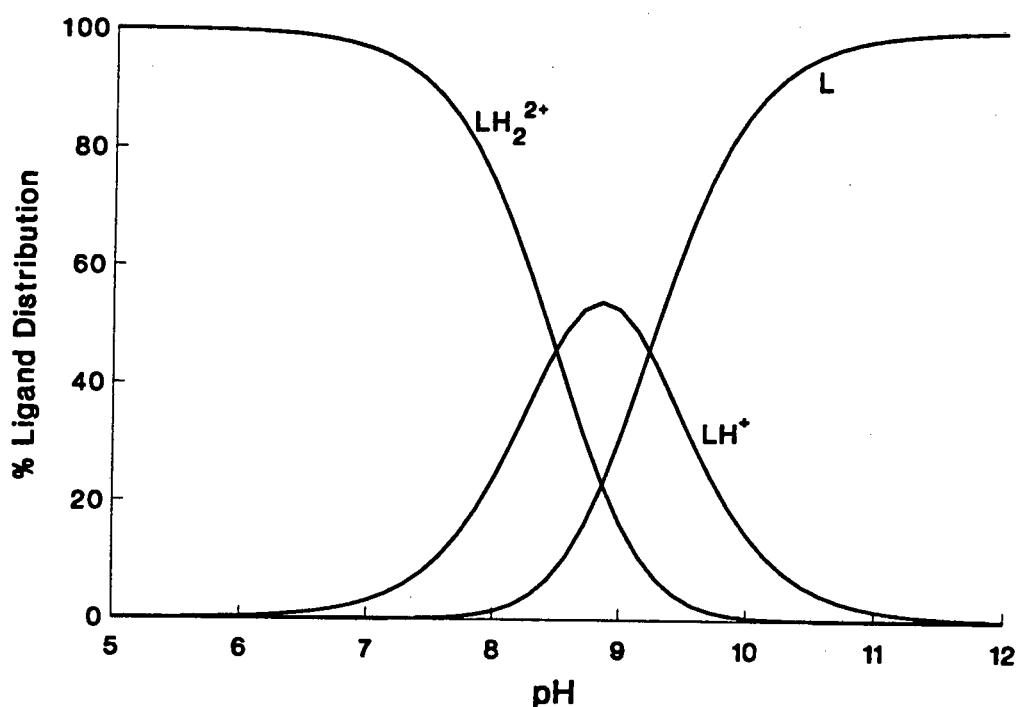
Ligand	$\log K_n^H$		$\log \beta_{pqr}$					
	n = 1	n = 2	110	11-1	11-2	21-2	21-3	11-3
5UM	8.72	7.91	8.33	1.06	-7.06	0.79	-6.89	-
6UM	8.83	8.07	6.51	-1.54	-8.94	-	-	-
656UM	9.52	8.86	8.39	-0.17	-9.80	-1.23	-	-21.9
5UE	9.23	8.49	8.16	0.35	-8.49	-1.72	-	-

	$\log K_n^H$		$\log \beta_{pqr}$ of structure type				medium / mol dm <sup>-3</sup>	Literature source	
	n = 1	n = 2	-	1a	1b	2d			3a
mono5UM	8.65	-	-	-	-0.38	-8.84	-	.5 KCl, 23°C	[102]
glycinamide	7.93	-	5.41	-1.44	-	-	-	.1 -, 25°C	[39]
$\beta$ -alaninamide	9.19	-	5.1	-	-	-	-	" , "	"
glyglyNH <sub>2</sub>	7.79	-	4.8	-	-0.25	-8.21	-	.1 KNO <sub>3</sub> , 25°C	[51]
glyalaNH <sub>2</sub>	7.83	-	5.22	-	-0.20	-9.19	-	" , "	"
5UH	9.31	8.43	-	-	9.42	1.91	-6.19	.1 KNO <sub>3</sub> , 22°C	[91]
5MH	8.22	7.48	-	-	7.50	-	-6.30	" , 25°C	[50]
656DH	8.78	5.82	-	-	12.58	4.50	-4.83	.1 Na(ClO <sub>4</sub> ), "	[103]

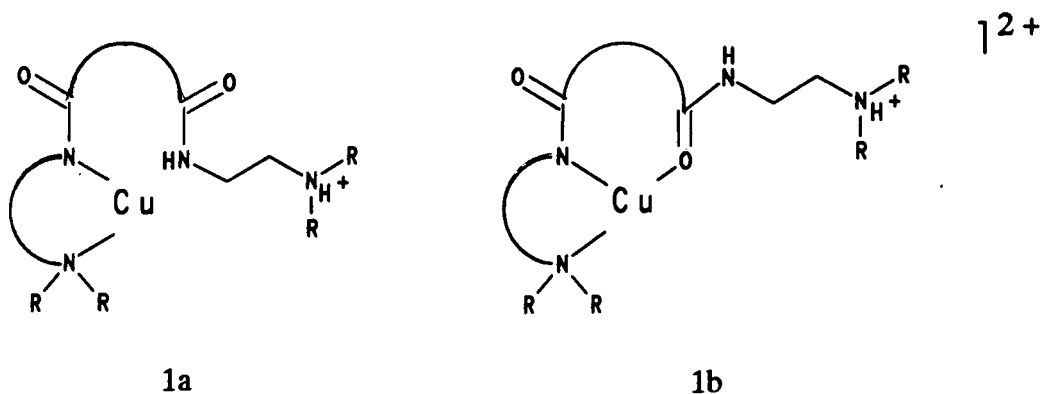
Common to all four copper(II)-diamino diamide systems investigated are the species 110, 11-1 and 11-2, the possible structures of which will therefore be discussed together.

Considering firstly the UV/VIS data given in Table 3.6, the  $\lambda^{\max}$  values of between 650 and 690 nm for the 110 species of the various systems clearly indicate the presence of two nitrogen atoms in the coordination sphere of the copper(II) ion. Secondly the strength of copper(II) binding suggests the presence of at least bidentate complexation. Thirdly any unbound nitrogens would most certainly be protonated (see Figure 3.20) in the pH region in which the complexes occur, i.e. pH 4 – 10. This would lead to protonated complexes, e.g. MLH, if solely mono-coordinate binding to the metal ion took place.



**Figure 3.20** : Species distribution of the ligand 5UE with protons indicating the state of protonation of the ligand with pH. Ligand 5UE was chosen as example, since its protonation constants are the most representative of the series of ligands studied.

It is therefore very likely that the 110 species involve complexation by two nitrogen atoms. Complexation through the amide nitrogens only, with the amine groups remaining unbound, is however very improbable. Thus the most likely structures for the 110 species are the following, which essentially differ in the number of chelate rings formed.



A further possibility is the structure in which both amine nitrogens only are bound to the metal ion, as was proposed by Desseyn *et al* [104] for the ligand 656UH with copper(II), in the solid state. The main reason for attempting the Raman study, was to determine the possible existence of this structure in solution, as the observed intensity of the characteristic N-H stretch might have indicated its presence or absence. Unfortunately this investigation was not successful for the reasons already described. However we do not believe this structure to be very plausible for the systems in solution due to the size of the chelate ring.

In order to decide between the two structure 1a and 1b, knowing the stability constants for the ligand  $\text{H}_2\text{N}-\text{CH}_2-\text{CH}_2-\text{NH}-\text{C}(=\text{O})\text{H}$  with copper(II) would have been very useful but these are unfortunately not available. The closest alternative ligands that can be used as models for the binding in the 110 species are glycineamide and  $\beta$ -alanineamide, i.e.  $\text{H}_2\text{N}-\text{CH}_2-\text{C}(=\text{O})-\text{NH}_2$  and  $\text{H}_2\text{N}-\text{CH}_2-\text{CH}_2-\text{C}(=\text{O})-\text{NH}_2$ , in which

however the  $-C(=O)-N-$  group has been interchanged relative to the position of the amine group. Therefore, in contrast to the ligands investigated in this study, the possibility of the formation of two distinctly different 5-membered chelate structures, in the case of the glycineamide for example, exists. Indeed these ligands are known to complex through the oxygen of the carbonyl group in preference to the amide nitrogen, with constants for  $\log \beta$  of 5.41 and 5.1 for glycineamide and  $\beta$ -alanineamide, respectively. This reflects the greater stability of the 5-membered versus 6-membered chelate rings, especially as the values of  $\log K_1^H$  for the two ligands are 7.93 and 9.19, respectively.

Good evidence for binding through the carbonyl oxygen is also given by the diethyl derivatives of the above ligands, i.e.  $H_2N-CH_2-C(=O)-NEt_2$  and  $H_2N-CH_2-CH_2-C(=O)-NEt_2$ , (with  $\log \beta$  values of 6.18 and 5.51 respectively [105]), as the ethyl groups effectively block coordination through the amide nitrogens.

This type of complexation, i.e. coordination through the amine and the adjacent carbonyl oxygen is however not expected in the case of the diamino diamide ligands investigated here as this would lead to the less stable 7 and 8-membered chelate rings which furthermore incorporate two  $sp^2$  centers.

On proton loss from the copper(II)-glycineamide complex, rearrangement in the chelate ring occurs which results in coordination through the amide nitrogen similar to that of structure 1a and for which a value of  $\log \beta$  of -1.44 can be calculated from data given in Smith and Martell [39] or -1.49 from Yamauchi *et al* [105]. This is roughly 2 log units lower than in the case of the ligand 5UM for which a value of 0.42 is calculated from  $\log \beta_{110} - \log K_2$  and strongly suggests the presence of a second chelate ring such as in the case of structure 1b. This type of complexation has also been suggested by Kaden and Zuberbühler for the very similar mono-substituted ligand N-[2-(dimethylamino)ethyl] ethanediamide, i.e.  $Me_2N-CH_2-CH_2-NH-C(=O)-C(=O)-NH_2$  [102].

Secondly, as the ligands 5UM and 6UM have very similar  $\log K^H$  values, the constants of their 110 species would be quite invariant, if complexation took place through only the one chelate ring (structure 1a), as this would lead to identical coordination for both ligands.

Therefore owing to the large difference between the constants of the 110 species of the ligands 6UM and 5UM or 5UE, of more than 1.5 log units, together with the enhanced stability observed for the 110 species of the ligands 5UM, 5UE and 656UM, the most likely coordination for the 110 complexes of the latter three ligands is therefore given by structure 1b with two contiguous 5,5 or 5,6-membered chelate rings.

Considering the two constants for the 110 species of the ligands 5UM and 6UM it would be easy to make the deduction that a complex with two contiguous 5-membered rings is more stable than one with contiguous 5 and 6-membered rings. However the 110 complex in the case of the ligand 6UM could have either of the two proposed structures and is therefore not necessarily directly comparable with the 110 species of the other ligands. In fact comparing the 110 constants of the ligands 5UM and 656UM which represent the 5,5 and 5,6-membered ring configurations respectively, it is seen that these complexes have quite similar stability. Only on making allowance for the larger  $\log K^H$  values of the ligand 656UM, is the greater stability of the 5,5-membered ring system apparent. This is in contrast to the analogous series of triamine ligands for which the order of stability for the copper(II) complexes of 56tri > 55tri > 66tri has been determined [37]. Literature constants for these and some tetramine ligands are given in Table 3.8.

**Table 3.8** : Logarithms of the protonation and equilibrium constants with copper(II) of the analogous series of tetramine as well as triamine ligands at 25°C reported in the literature.  $K_n^H$  refers to stepwise protonation constants and  $\beta_{pqr}$  to the overall stability constants.

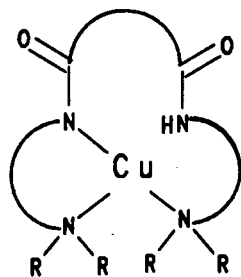
Ligand	log $K_n^H$				log $\beta_{110}$	medium / mol dm <sup>-3</sup>	Literature source
	n = 1	n = 2	n = 3	n = 4			
55tri	9.79	8.98	4.25	-	15.8	.1 KCl	[37] <sup>a</sup>
56tri	10.44	9.36	6.37	-	16.6	.5 KNO <sub>3</sub>	[37]
66tri	10.65	9.57	7.72	-	14.2	.1 KCl	[37] <sup>a</sup>
5tet	9.74	9.08	6.56	3.25	20.1	.1 -	[39]
6tet	10.08	9.26	6.88	5.45	23.2	"	[40]
"	10.25	9.50	7.28	6.02	23.9	.5 KCl	[38]
656tet	10.53	9.77	8.30	5.59	21.7	.1 -	[40]

<sup>a</sup> Values quoted in reference [37]

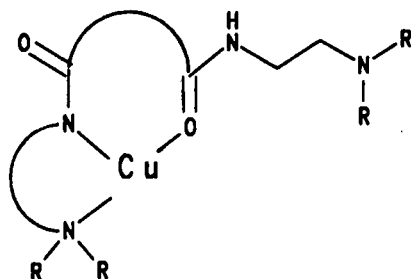
The unexpectedly large difference in the stability of the 110 complexes of the ligands 6UM and 656UM, which after all both have the ability of forming only the 5,6-membered ring configurations, could be explained on the basis of a destabilizing effect of the 6-membered ring when this contains a large number of sp<sup>2</sup> centers thereby increasing the 'bite size' even more, as is the case for the ligand 6UM. In contrast the 6-membered ring of the 110 complex formed with the ligand 656UM, contains only one sp<sup>2</sup> center which possibly causes less destabilization. Furthermore, the formation of the second ring containing the two carbonyl moieties results in only a small loss in entropy on complexation when this ring is of the 5-membered type as, according to Kaden and Zuberbühler [102], the planarity of the -N-C(=O)-C(=O)-N- system is maintained without loss of resonance.

In the limiting situation which is possibly the case for the ligand 6UM with copper(II), the destabilization of the 6-membered ring could lead to its not being formed at all, resulting in a complex of structure 1a with accompanying lower stability.

Deciding on the structure of the 11-1 species is somewhat more problematic. The most likely coordination schemes for this species are given by the following four structures.

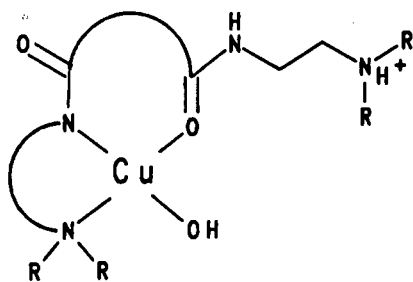


2a

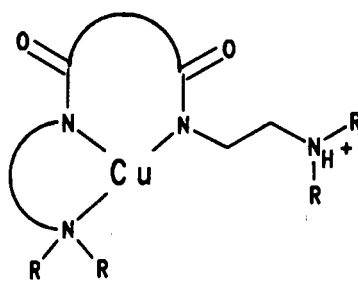


2b

] 1 +



2c



2d

] 1 +

As can be seen these essentially differ according to the number of nitrogen atoms present in the coordination sphere of the copper(II) ion. Structure 2a, suggested by Grieser and Fallab for the ligand 5UH with copper(II), seems unlikely due to the large chelate ring. Of the two structures 2b and 2c which both have only 2 nitrogen atoms in the coordination sphere of the copper(II) ion, the former is improbable due to the fact that the complex occurs in a pH region in which most of the unbound ligand is doubly protonated and hence the uncoordinated amino group is likely to be protonated. The structure 2c had been proposed by Zuberbühler and Kaden [93] for the ligand 5UM based on the equivalent type of complexation of copper(II) with the ligand mono5UM. They furthermore observed an

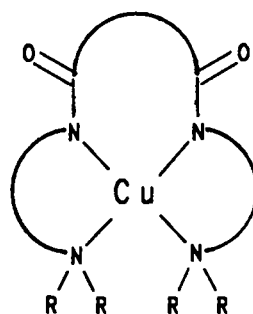
absorption in the UV region of the latter species which was apparently due to hydroxo complexation and which was absent in the 110 and 11-2 species of 5UM. Also, a shift of only 20 nm in going from the 110 to the 11-1 species was determined for both mono5UM and 5UM with copper(II).

In contrast we observed a shift of 55 and 40 nm for the same change in species for the ligands 5UM and 5UE respectively (see Table 3.6). Secondly, the  $\lambda^{\max}$  values of 620 and 630 nm respectively are even below that of the ammine aqua cupric species with 3 ammonia groups coordinated to the copper(II) ion. Furthermore the  $\lambda^{\max}$  of the equivalent mono5UM species, on which Zuberbühler and Kaden had based their argument, has a value of 690 nm, which is substantially different from the disubstituted ligands. Thus it seems very probable that the 11-1 species, particularly of the ligands 5UM and 5UE, has the corresponding structure 2d in solution, although structure 2c cannot be ruled out completely.

Even more so than before in the case of 110 complexation, the 11-1 constants clearly indicate the greater stability of the 5,5-membered ring system over that of the 5,6-membered chelate systems, which is again in contrast to the analogous series of triamine ligands. Enhanced stability of the system with two contiguous 5-membered rings was also observed by Yamauchi *et al* [51] for the similar glyglyNH<sub>2</sub> and glyalaNH<sub>2</sub> ligands with copper(II) undergoing the type of coordination as in structure 2d. However, for the alternative binding type, such as in structures 1b or 2c, they found the stability of the complexes of the above two ligands with copper(II) to be very similar, which further indicates the 11-1 species to have structure 2d. As before the large difference in stability between the 11-1 complexes of 6UM and 656UM can be partly explained by the greater loss in entropy of the former ligand on complexation.

Comparisons with the very similar hydrogen analogs of the ligands investigated in this study or with the M and D-type of diamino diamide ligands could have been made but these ligands are beset by the same problems of too many binding options and are therefore in this respect of not much use.

According to Zuberbühler and Kaden [93] and based on the absorption maximum at 590 nm of the species  $[\text{Cu}(\text{H}_2\text{O})_2(\text{NH}_3)_4]^{2+}$ , the  $\lambda^{\text{max}}$  values for the 11-2 species of the ligands 5UM, 5UE and 6UM indicate the presence of four nitrogen atoms in the coordination sphere of the copper(II) ion. Coordination through the amide nitrogens invariably indicates displacement of the amide protons which therefore results in the uncharged species. Thus the most likely structure for the 11-2 species of these ligands with copper(II) consists of three contiguous chelate rings all in the same plane and is given by the following.



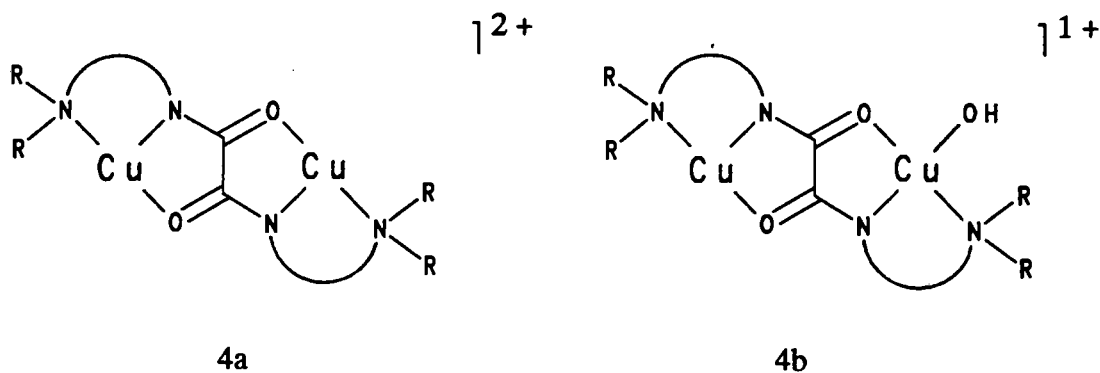
3a

Unfortunately these conclusions as to the most probable structure are not supported by the UV/VIS data of the copper(II)-656UM system. However, as the electronic spectra of this system are the most ill-defined of the four investigated not too much weight should possibly be placed on these results. Therefore, we believe by analogy, that the most likely structure of the 11-2 species of this system is also represented by structure 3a. Further evidence supporting this conclusion is given by several other studies [44], in particular the

crystallographic structure determination of the four coordinate 656UH complex with nickel(II) as the metal ion [106]. The order in stability of the 11-2 species is slightly altered, compared with that previously observed for the 110 and 11-1 complexes, as the 656UM ligand was found to be the least stable in this case. However the 11-2 species of the copper(II)-5UM system is once again the most stable by about 2 log units, which is in marked contrast to the order in stability of the analogous series of tetramine ligands with copper(II), i.e. 6tet > 656tet > 5tet (see Table 3.8).

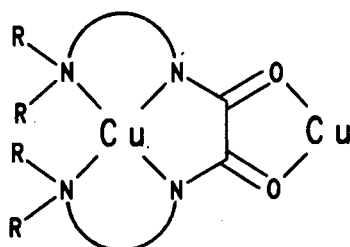
Ojima and Nonoyama have proposed a structure for the 11-3 species of the ligand 5UH with copper(II) in which a hydroxyl ion has displaced one of the amine nitrogens from the coordination sphere. However we believe this structure to be rather unlikely considering the shift in  $\lambda^{\max}$  to a lower wavelength by 30 nm from that of the 11-2 species. Therefore a structure in which an axial water molecule of the 11-2 complex has been replaced by a hydroxyl ion seems the most likely structure.

The  $\lambda^{\max}$  values of the 21-2 and 21-3 species of the copper(II)-5UM system are again virtually the same as that of the 110 species, indicating the coordination of two nitrogen atoms per metal ion. Furthermore only one absorption maximum is observed in the electronic spectra of these species, indicating a similar environment for both of the copper(II) ions. Therefore the most probable structures representing the species 21-2 and 21-3 are given by 4a and 4b, respectively.



Further evidence supporting the proposed structures of these species is given by the crystallographic determination of the  $\text{Cu}_2(5\text{UM})(\text{NCS})_2(\text{DMF})_2$  complex according to Yoshino and Nowacki [107].

In the case of the copper(II)-656UM system an additional structure may be suggested for the 21-2 species, but once again the electronic spectrum is rather poorly defined. As the  $\lambda^{\text{max}}$  for this species lies at 600 nm and the curve in Figure 3.19 could be construed as having a shoulder at about 700 nm, a structure with the copper(II) ions in two chemically different environments may be indicated. Such a structure is given by the following, where one copper(II) ion is coordinated by four nitrogen atoms and the other by the two carbonyl oxygens, with the remaining coordination sites being occupied by water molecules.



] 2 +

4c

Structures of this type have led to the notion of the 11-2 complexes being termed 'metal chelate ligands', as for example, in the formation of complexes with bis (2,2'-bipyridine) nickel(II) [108] or 2,2'-bipyridine copper(II) and pentaethyldiethylenetriamine copper(II) [109]. This is due to the initial complexation of the four nitrogen atoms fixing the carbonyl oxygens in a favorable position for further coordination to another metal ion. However, strong evidence supporting a structure such as 4a above for the 21-2 species of the copper(II)-656UM system is given by the crystallographic determination of  $[\text{Cu}_2(656\text{UH})](\text{NO}_3)_2$  according to Dessey *et al* [104].

In conclusion the most astonishing result of this experimental investigation was the fact that the ligand 5UM is not only much better at solubilizing copper(II), which could have been explained solely by its ability to form the 21-2 species, but that it is also a stronger complexor than the ligand 6UM, as is evident from the formation constants and the visual observations during the potentiometric and UV/VIS titrations. This was rather unexpected on considering the analogous tri- and tetramine ligands. The much stronger complexing ability of the 5UM ligand is immediately evident on considering the species distribution with pH of a copper(II) solution containing equal concentrations of the ligands 5UM and 6UM, such as is given in Figure 3.21, for example.

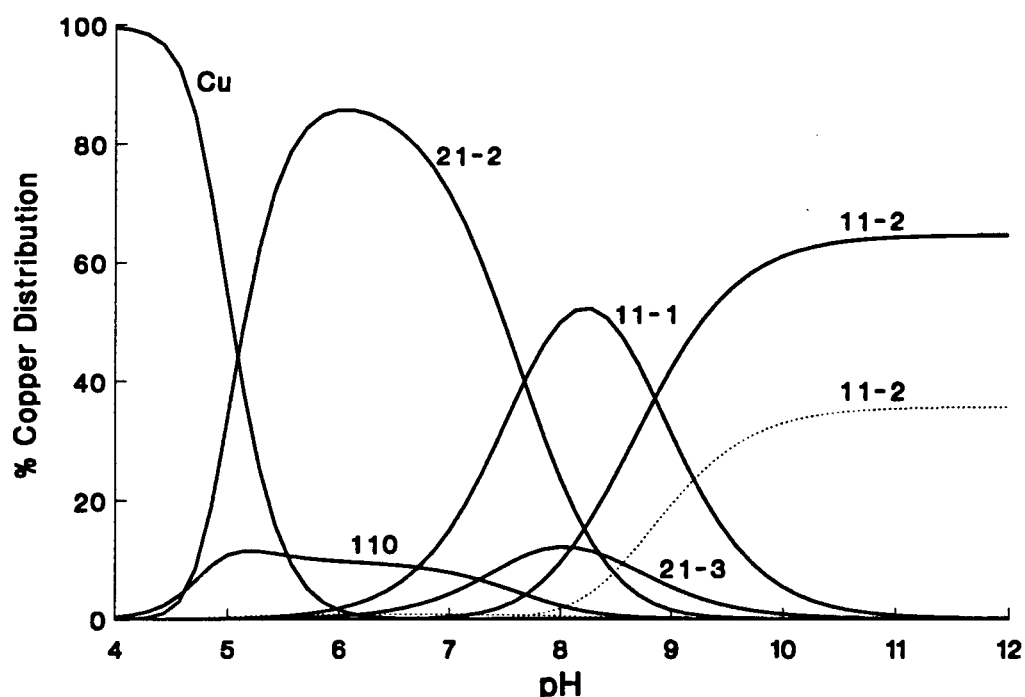


**Figure 3.21** : Species distribution of a  $10 \text{ mmol dm}^{-3}$  copper(II) solution containing an equal concentration of the ligands 5UM and 6UM of  $7.5 \text{ mmol dm}^{-3}$  each. Copper(II)-5UM species are represented as solid lines, whereas 6UM species are depicted by the broken lines.

Unfortunately, neither of the two experimental techniques employed could explain this reversal in the order of the stability of the diamino diamide ligands with copper(II). Therefore some other technique had to be applied to try and account for this anomaly. As

it had been suggested that the greater stability of the 6tet complex versus that of 5tet is due to the steric constraints of the three linked 5-membered chelate rings of the latter which are alleviated by the presence of a 6-membered ring, it therefore seemed pertinent to carry out strain energy calculations. Hence it was decided to carry out a molecular mechanics investigation on these and related systems in order to gain a better understanding of the energetics involved.

**CHAPTER FOUR**  
**COMPUTER MODELLING**

## 4.1 INTRODUCTION

This section is based on the general assumption that a direct relationship exists between the structure and energy of a molecule. It can furthermore be assumed, to a first approximation, that the molecule is described by a conformation that corresponds to the deepest energy minimum or, to a more refined approximation, that the molecule is described by an equilibrium mixture of conformers corresponding to all of the minima in a Boltzman distribution.

In order to calculate the energy and structure of a molecule the most direct and fundamental way would be to solve the Schrödinger equation for the particular nuclear configuration. Using the Born-Oppenheimer approximation which states that the Schrödinger equation can be separated into a part describing the motions of electrons and another describing the motions of the nuclei and that these two sets can be studied independently, this gives rise to essentially two different methods of performing these calculations.

The first of these is the quantum mechanical (usually molecular orbital) approach in which the nuclei of the system are fixed and the wave function of the three dimensional electronic structure is formulated and solved by standard approximations. Only in the simple case of the hydrogen molecule is an exact solution of the function possible. The imposed positions of the nuclei are then changed and the process repeated until the total energy minimum as a function of the internuclear positions has been found [110].

Although various approximations are employed in the *ab initio* calculations which are necessary for situations more complex than the hydrogen molecule, this method requires a great deal of computational time, even on truncating the infinite series of terms of the wave function resulting in a smaller more manageable basis set. This is due to the

fact that the number of calculations involved is a function of approximately the fourth power of the number of basis orbitals of which there are several per atom. Therefore several semi-empirical quantum mechanical alternatives have been employed in order to reduce the computational requirements with a concomitant increase in the uncertainty of the obtained results. However as the calculations need to be repeated for a number of different nuclear positions, as in the case of structure optimization, the process is still quite lengthy.

In the second approach, known as the force-field or molecular mechanics method, the other part of the Born-Oppenheimer approximation is involved, i.e. the motions of the nuclei are studied whereas the electrons are not explicitly considered. They are simply regarded as the cause of the potential field in which the nuclei find themselves, the effects of which are taken into account indirectly.

Thus the potential energy surface of the molecule in the ground electronic state is a function of its nuclear positions and can be calculated using empirically derived potential functions which are of the form of the classical equations of motion. This set of functions, which constitute the force field, contains adjustable parameters, i.e. the force constants, which are optimized to obtain the best fit between several calculated and experimental properties of a number of molecules. The successful application of the method therefore relies on the assumption that the force field and the constants are transferable, if not amongst all compounds, at least amongst those of the same class.

Although the *ab initio* method does not require experimental data, it was decided to use the molecular mechanics method in order to calculate the structure and energy of the ligands and complexes in this study as these are quite large and include a third row atom, which would have required substantial computational time. In addition force field

methods have been extensively used for a number of years with much success and the theory on which the method is based is relatively well understood.

The molecular mechanics method has been used primarily to calculate the most predominant conformations of organic molecules, based on the principle of the minimum energy structures being the most stable. In some cases these calculations have been further refined to give activation energies of conformational interconversions as well as to determine chemical reactivities, properties of molecular crystals, frequencies of vibrational spectra and various thermodynamic parameters [110, 111].

In a similar fashion the intention was to use force-field calculations to explain the anomalous order of stability of the series of diamino diamide ligands with copper(II) observed in this study. Much less work has been done however on calculations involving coordination compounds, for which the method is also less well understood. This is due to the problems associated with coordination about the metal ion, as well as the difficulty of applying the technique to complex heteronuclear systems. The calculations are therefore generally not carried out to such a degree as those for organic molecules. Furthermore, most of the work on coordination compounds has been performed on complexes involving the metal ions Ni(II) and Co(III) [112, 113, 114, 115, 116, 117, 118] for which a reasonable number of force-field parameters are thus available. However, calculations have only been performed on a small number of copper(II) complexes and therefore very few reliable parameters for the various interactions involving this metal ion exist [118, 119, 120]. Most of these studies center around the hole size best fit theory of Drew et al [119] and Hancock et al [121, 122].

Several molecular mechanics programs are available to carry out the necessary calculations of which three were considered, i.e. MM2 [123], MacroModel [124, 125] and a program originally coded by Boyd [126] and modified by Snow [127].

## 4.2 THEORY

The molecular mechanics approach has been extensively reviewed in the literature [110, 111, 118, 128, 129, 130], thus only a short summary of the relevant theory involved will be given here. The potential energy expressions making up a particular force field have their origin in vibrational spectroscopy. The potential energy of a molecule with  $n$  atoms, whose structure is defined by  $3n$  coordinates,  $x_i$ , and is deformed from its geometry of minimum energy, can be given by a Taylor-series expansion [129]. On making various simplifying assumptions, it can be shown that, to a first approximation, the potential energy depends only on the third term of this series and can be given by the following expression

$$E_{\text{pot}} = \frac{1}{2} \sum (\partial^2 E / \partial x_i \partial x_j) \Delta x_i \Delta x_j$$

where the derivatives can be replaced by the force constants,  $f_{ij}$ . Thus a simple harmonic force field is obtained, which describes a system of coupled harmonic oscillators. Considering only the terms with  $i = j$ , which implies that the oscillators are not coupled, a diagonal force field with Hook's law harmonic potentials results. In practise however, a number of off-diagonal terms corresponding to a simultaneous displacement in two coordinates must be included for the force field to have transferable constants as it was found that these cross-terms are significant especially in the case of 1,3 and 1,4-interactions.

At present two types of force fields are commonly used in molecular mechanics calculations, namely the Urey-Bradley and the generalized valence force field, which essentially differ in their treatment of the above interactions. As all of the molecular mechanics programs used in this study are based on the latter type of force-field, this will be mainly discussed here.

In the classical valence force-field the atoms of a molecule can be thought of as being joined by mutually independent springs restoring bond lengths and angles to their 'natural' values, i.e. elastic or harmonic forces are operative [128]. Thus a Hook's law function can be considered as a first approximation for the bond stretching potential which is given by

$$E_s = 1/2 k_s (l - l^0)^2$$

where  $E_s$  is the energy contribution to the total strain energy of the molecule, due to the bond being stretched from its natural value,  
 $k_s$  is the bond stretching force constant (restoring the deformation)  
 $l$  is the actual bond length of the energy minimized structure and  
 $l^0$  is the 'natural' bond length of the particular interaction, i.e. the strain-free value.

For large deformations it would be more accurate to substitute a Morse potential for the bond stretching interactions, however as simple potential functions are generally used it is preferable just to add a cubic term to the above expression which thus becomes the anharmonic function as used in MacroModel and MM2

$$E_s = 1/2 k_s (l - l^0)^2 + 1/2 k_s' (l - l^0)^3 \quad 4.1$$

where  $k_s'$  is simply a factor of  $k_s$ .

The cubic term causes the function to become inverted at large distances and is therefore only introduced after several refinement cycles of the calculations have been completed.

Similarly the potential function describing bond angle bending (in-plane) consists of a harmonic potential with additional higher order terms. The particular function used in this study, employing a sextic term, is given by

$$E_b = 1/2 k_b (\theta - \theta^\circ)^2 + 1/2 k_b' (\theta - \theta^\circ)^6 \quad 4.2$$

where  $k_b$  is the bending force constant with  $k_b'$  a factor of this,

$\theta$  is the bond angle and  $\theta^\circ$  the strain-free value.

Thus the energy associated with both the stretching and bending of bonds from their natural values is to a first approximation proportional to the square of the deviation. Furthermore, as  $k_s$  is generally about 10 times greater than  $k_b$ , molecular distortions are apparent to a greater extent in angle bending than in the stretching of bonds.

In opposition to the in-plane bending potential given above, which could lead to distortion in the pi bonding and a concomitant enormous increase in the double bond energy of  $sp^2$  hybridized atoms [129], is the out-of-plane bending potential given by

$$E_{opb} = 1/2 k_{opb} \theta^2 + 1/2 k_b' \theta^6 \quad 4.3$$

where  $k_{opb}$  is the out-of-plane bending constant and

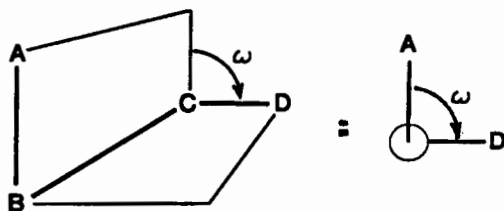
$\theta$  is the angle between the atoms and their projection in the plane described by the three atoms bound to the  $sp^2$  center.

The torsional energy associated with rotation about a usually covalent bond either single or double can be described by the Fourier-series expansion

$$E_\omega = 1/2 V_1 (1 + \cos \omega) + 1/2 V_2 (1 - \cos 2\omega) + 1/2 V_3 (1 + \cos 3\omega) \quad 4.4$$

where  $\omega$  is the torsional angle defined in the figure below and

$V_1$ ,  $V_2$  and  $V_3$  are one, two and three fold torsional energy parameters.



The torsional energy is a difficult concept to interpret for situations involving other than double bonds and many rationalizations have been given, e.g.  $V_1$  is thought to originate from dipole-dipole interactions,  $V_2$  from hyperconjugation in saturated and conjugation in unsaturated systems and  $V_3$  from steric interactions. The latter is not a result of 1,4 van der Waals interactions, i.e. these two are separate contributions to the steric energy as has been shown by *ab initio* calculations. Attempts have been made to design a molecular mechanics force-field excluding torsional contributions but these have failed to give even approximately correct results.

The final energy contributions to the total strain energy of the molecule originate from non-bonded interactions of which there are several different types. Some of these can essentially be thought to approximate the cross-terms mentioned previously.

The most important non-bonded interactions are the van der Waals interactions between all pairs of atoms not bonded to one another or to a common atom, i.e. only 1,4 and higher interactions are considered. The former two cases are excluded as these interactions are partly allowed for by the bond stretching and angle bending potentials, respectively. The general shape of the van der Waals function is well established [131] and results from two opposing forces, an attractive part due to electron correlation which is inversely proportional to the sixth power of the distance separating the two atoms and a

repulsive component at shorter distances which is generally inversely dependent on the distance to the 12th power (Lennard-Jones 6/12 potential). The repulsive part is often replaced by an exponential term resulting in a Buckingham potential. This is similar to the Hill equation which was used in this study and is given by the following expression.

$$E_{\text{vdw}} = \zeta^* [ -c_1(r^*/r)^6 + c_2 \exp(-c_3 r/r^*) ] \quad 4.5$$

where  $\zeta^*$  characterizes the depth of the potential energy-well for an atom pair and

is calculated from  $\sqrt{\zeta_k \zeta_l}$ ,

$c_1$ ,  $c_2$  and  $c_3$  are universal constants,

$r$  is the interatomic distance and

$r^*$  is the sum of the van der Waals radii of the two atoms which is somewhat larger than the distance of closest approach on which the van der Waals radii are usually based.

This function has an energy minimum at an interatomic distance equal to  $r^*$ , a very steeply repulsive portion for  $r < r^*$  and a flat region which asymptotically tends to zero at larger distances.

One of the main assumptions made in the use of equation 4.5 is that the van der Waals potentials, which have been derived from intermolecular interactions, are also applicable to intramolecular interactions. Furthermore it is also assumed that the interactions are additive and are not affected by other atoms in the vicinity.

The inclusion of 1,3-nonbonded interactions in the Urey-Bradley force-fields using a harmonic potential is the major difference to the molecular mechanics force-field described here. Clearly a harmonic potential for the non-bonded interactions of atom pairs that are further apart than 1,3 is not suitable. Therefore from the notion that compressing

of the bond angle leads to lengthening of the bond distances, and vice versa, a stretch-bend cross term is introduced, especially if the parameters of the force field are to be transferable, as the 1,3 interactions are only partly taken care of by the angle bending potential in cases where these interactions are severe. This potential function is given by the expression

$$E_{sb} = 1/2 k_{sb} (l_i - l_i^\circ + l_j - l_j^\circ) (\theta_{ij} - \theta_{ij}^\circ) \quad 4.6$$

where  $k_{sb}$  is the stretch-bend force constant

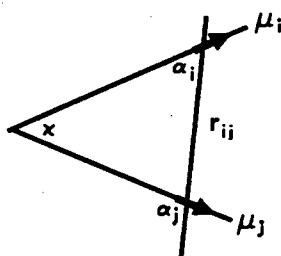
$l_i^\circ$  and  $l_j^\circ$  are the strain-free bond lengths to the central atom and

$\theta_{ij}^\circ$  is the strain-free bond angle.

A further non-bonded term to be considered is that of the electrostatic interactions. In contrast to MM2 which calculates a standard dipole-dipole electrostatic energy from bond dipole moments using the equation

$$E_{dipole} = \mu_i \mu_j / D r_{ij}^3 (\cos \chi - 3 \cos \alpha_i \cos \alpha_j)$$

where the geometric terms are as defined in the figure below.



MacroModel calculates the electrostatic energy using partial point charges according to the equation

$$E_{elec} = q_i q_j / D r_{ij}$$

where  $q_i$  and  $q_j$  are the partial charges on the atoms calculated from the bond dipole moments by the expression  $\theta = \mu \times 0.2082 / l$ ,  
(where  $l$  is the bond length in Ångström)  
 $r_{ij}$  is the distance between the point charges and  
 $D$  is the bulk dielectric constant.

Replacing the bulk dielectric constant by a distance dependent one, the above expression for the electrostatic energy becomes

$$E_{elec} = q_i q_j / D r_{ij}^2 \quad 4.7$$

which was the potential function used in this study.

The final 'non-bonded' interaction considered was that of hydrogen bonding between acidic hydrogens and electronegative acceptor atoms. Several angle and/or distance dependent functions have been proposed [132], later versions of MM2 use a Buckingham type function similar to that employed for the van der Waals interactions, whereas MacroModel uses an angle independent 10/12 Lennard-Jones potential given by the following

$$E_{hb} = C/r^{12} - D/r^{10} \quad 4.8$$

where  $C$  and  $D$  are empirical constants depending on the donor and acceptor atom types and  
 $r$  is the interatomic distance H...acceptor as opposed to the donor...acceptor distance.

As can be seen from the above the force-field method uses potential functions from classical mechanics (which is in fact the only reason why it is often referred to as the

classical approach). This is a further reason for its use in preference to *ab initio* calculations, as these functions are conceptually easier to understand than the Fock matrix elements, eigen vectors and eigenvalues of the quantum mechanical methods.

The total energy of the molecule in the force-field is thus given by the sum of the above energy contributions which are themselves summed over all possible interactions (apart from certain restrictions mentioned) resulting in the following expression for the steric energy

$$E_{\text{tot}} = \sum E_s + \sum E_b + \sum E_{\text{opb}} + \sum E_{\omega} + \sum E_{\text{vdw}} + \sum E_{\text{sb}} + \sum E_{\text{elec}} + \sum E_{\text{hb}} \quad 4.9$$

This represents the difference in energy between the real molecule and one in which all structural parameters are at their strain-free values. Once suitable parameters have been chosen from experimental data or *ab initio* calculations, the energy can be calculated for a particular molecular geometry. At the energy minimum the derivatives of the above expression with respect to each degree of freedom of the molecule must all equal zero. Therefore, by optimizing the molecular geometry, the energy can be minimized, using one of many gradient search or analytical methods, e.g. Newton-Raphson and variants thereof, resulting in a minimum energy structure.

The steric energy so calculated is specific to the particular force field used and will therefore differ from one to another. However it can be related to the enthalpy of formation on knowing the various force field dependent group increments. Then, using experimentally determined strain-free group increments the enthalpy of formation of a strain-free molecule can be calculated and subtracted from the actual heat of formation to give the strain energy of the molecule.

This calculated energy is that of a discrete molecule and not that of the system as a whole. As it is expected that several conformations of similar energy may exist in solution, particularly for the more flexible structures, the mean energy of the system,  $U$ , needs to be calculated. This can be obtained from a Boltzman distribution which is given by the following expression [133]

$$N_i = g_i N_0 \exp(-e_i / kT)$$

where  $N_0$  is the number of particles or molecules in any given energy state,

$N_i$  is the number of particles in an energy state whose potential

energy is  $e_i$  above that of the given state,

$g_i$  is known as the degeneracy of the  $i$ th energy level,

$k$  is the Boltzman constant and

$T$  is the absolute temperature.

To calculate the fraction of the total number of particles that have a potential energy  $e_i$  above that of the given state, the total number of particles,  $N$ , in the system needs to be determined. This is given by

$$N = \sum N_i = N_0 \sum g_i \exp(-e_i / kT)$$

where  $\sum g_i \exp(-e_i / kT)$  is known as the partition function,  $f$ . The fraction of particles with energy  $e_i$  is then given by

$$N_i / N = [g_i \exp(-e_i / kT)] / f$$

from which  $N_i$ , representing the population distribution, is easily determined for the various energy states on calculating the partition function. Thus the weighted mean energy of the system can be determined from

$$U = [ \sum N_i E_i ] / N$$

assuming that the kinetic energy is sufficient to populate all of the energy levels correctly.

### 4.3 COMPUTATIONAL PROCEDURE

The particular approach used in this study, although not exactly novel, needs to be explained in slightly greater detail and discussed together with the various additional assumptions made. Unfortunately, the discrete steric energies calculated for different complexes cannot be used directly to obtain a measure of their relative stabilities as these energies can only be compared for complexes with precisely the same binding, i.e. those involving the same number and type of interactions, and which differ only with respect to conformation. This is due to the fact that group increments are not available for coordination compounds and hence enthalpies of formation cannot be calculated. Furthermore these open-ended ligands do not lend themselves to the study of hole or cavity sizes as has frequently been performed on macrocyclic compounds [117, 119, 121, 134, 135, 136, 137, 180, 181]. Thus a more subtle method of comparisons needs to be made.

If it is assumed that the difference in steric energy between the free ligand and its copper(II) complex reflects the stability of the complex, then in order to obtain a measure of the relative stabilities of different complexes, with the same type of binding, it is merely necessary to compare the differences in energy on complexation of one ligand to a metal ion to that of another ligand to the same metal ion, i.e. the difference in energy is the increase in strain energy on complex formation. We can thereby assume that contributions from additional group increments in going from one ligand to the next are effectively cancelled out.

Furthermore as we are comparing structurally very similar ligands forming structurally very similar complexes we assume that the entropy of complexation is constant across the series. Hence any change in  $\Delta G$  reflects a change in  $\Delta H$  which in turn reflects a change in strain energy.

Using equation 3.8 and replacing  $\Delta H$  by  $\Delta(\Delta U)$ , where  $\Delta U$  is the strain energy change on complexation ( $\Delta H_{\text{complex}} - \Delta H_{\text{ligand}}$ ), this results in the expression

$$\Delta \log \beta = - \Delta(\Delta U) / 2.303 RT \quad 4.10$$

from which the difference in the logarithm of the stability constants of one complex to another can be calculated.

As the ligands are all nitrogen donor ligands and are all quite similar, forming part of a homologous series, and since the metal ion is the same in each case, the assumption of constant  $\Delta S$  of complexation seems quite reasonable. For ligands with very similar  $pK_a$ 's the above is even more reasonable, as is the assumption that the change in  $\Delta H$  (and therefore the relative stability) is mainly due to a change in the strain energy and not the binding energy. This is further supported by the fact that there is also no change in the type of amine present. Thus we feel reasonably justified in using molecular mechanics results to try and explain the anomalous order in the stability of the copper(II) complexes.

Needless to say this approach would have to be verified. This was in fact done by performing similar calculations on an analogous series of copper(II) tetramine complexes, for which  $\Delta H$  and  $\Delta S$  results were available. Also a similar technique has been used by other workers in the field of molecular modelling [113, 116, 138].

In order then to perform these calculations, first the steric energies of the free ligands needed to be determined followed by those of the various types of complexes that are formed. Since it was expected that several conformers of similar energy existed in solution, especially for the flexible ligand structures, the mean energies of the systems were calculated from a Boltzman distribution of the various populated states. For this purpose a simple BASIC computer program was written. Furthermore, initial energy

calculations were carried out on simplified forms of the complexes, i.e. ignoring water molecules occupying the unfilled coordination sites of the copper(II) ions. Thus square planar coordination about the copper(II) ions was assumed, which is after all the limit of tetragonal distortion.

Electrostatic interactions have presented serious problems in molecular mechanics calculations as they frequently overshadow all other interactions. Whilst the need for including these type of interactions in hydrocarbon force-fields appears to be debatable [111, 139] the situation is much more complicated for molecules containing more than one appreciably charged atom and therefore the solvation of charges and dipoles should possibly be dealt with explicitly.

As has already been pointed out in the previous section there are two basic ways in which electrostatic interactions are currently modelled by molecular mechanics methods. These lead essentially to the same results. More advanced approaches have been employed [125, 140], but require a substantial increase in effort and therefore one of the simpler techniques, in particular the method of partial charges, was chosen.

Both of the above techniques require a value for the dielectric constant. The effective constant actually operative in close proximity to the molecules may be substantially different from the bulk value but can unfortunately not be measured. Therefore the technique of using such a constant, although it was investigated, was finally not used.

Since the stabilities of the complexes were measured in aqueous solution, a dielectric constant of 78.3 (with distance dependence), which represents the bulk value of water, was used in this study. This is however also quite meaningless and should only be seen as an arbitrary value used to scale the electrostatic potentials. Increasing the

dielectric constant has the effect of reducing the numerical value of the electrostatic interactions. Whilst this approach is not very satisfactory many workers have neglected electronic effects altogether, especially in work involving metal ions [119].

Unfortunately *ab initio* calculations of the partial charges could not be carried out due to non-availability of the computer programs and hardware. Thus all formal charges were ignored in the molecular mechanics calculations, which seems reasonable at least for the uncharged 11-2 complexes.

#### 4.3.1 CHOICE OF PROGRAM

Initially an old version of the force-field program attributed to Boyd [126, 127] was used for molecular modelling. This program had been specifically written for calculations involving metal coordination. However the program was found to be lacking in its parametrization and more seriously in the functions employed. This was true especially for the organic part of the modelling study, a conclusion that Drew *et al* had also arrived at in their studies [135].

Molecular modelling was also carried out using the well-known program MMP2(85) [141]. In order to use this for calculations involving metal ion coordination of at least the square planar type, the coding of various subroutines had to be rewritten. The amended program was thus used with relative success incorporating constants for copper(II) interactions from Drew *et al* [119] (see later). Even though MM2 has been extensively used for all types of organic compounds, several parameters for purely organic interaction were still found to be missing and had to be included.

Unfortunately, MM2 was not always successful in minimizing the energy of some of the complexes investigated and therefore the more advanced program MacroModel was finally used. This program incorporates a number of additional convenient features which make it very attractive to use.

Firstly, it includes several force-fields together with their potential constants allowing the user a choice appropriate to the type of problem that is to be solved, i.e. the particular classes of compounds that are to be modelled. One of these is the MM2 force-field together with an updated set of potential constants taken from MM2(87). This allows for direct comparison of the results from MM2 and easy transfer of the constants that had already been parametrized in the initial stages of this study. Secondly, the program has an interactive stage allowing for a convenient on-screen structure minimization and visualization. Thirdly, MacroModel incorporates a Monte Carlo Multiple conformer energy Minimization technique [125, 142] which is well suited to find local minima and thereby hopefully also the global minima. This is especially useful for modelling of very flexible ligand species. Lastly, the program also includes a number of different mathematical solving routines which allowed the successful minimization of even some difficult structures which MM2 had been unable to refine.

#### 4.3.2 FORCE-FIELD PARAMETRIZATION

In the case of organic molecules, force constants and ideal or strain-free dimensions have become quite well established over the past few decades. These have been obtained mainly by empirical methods, the parameters having been refined so that a number of experimental variables, i.e. structural and energetic, of as many molecules as possible are correctly modelled. Although this was generally done by trial and error

methods, linear least-squares procedures for the systematic optimization of potential constants have also been employed [129, 143].

In the past starting values for the constants were obtained from several sources, e.g. vibrational spectra (stretching and some bending constants), microwave, far-infrared and NMR spectra (torsional barriers) and thermodynamic measurements (torsional barriers, as well as non-bonded interactions) [111, 125]. Natural bond lengths and angles were obtained from structural data of strain-free compounds by microwave, electron diffraction or crystallographic techniques.

The parametrization of force-fields is therefore an ongoing process involving continual refinement of the constants which has so far taken many years. None the less several parameters of purely organic interactions, especially torsional constants, were surprisingly absent from the force field of the MMP2(85) program. However, virtually all of these constants were found to be present in the updated MM2(87) force-field obtained with the program MacroModel. Using mainly data from the Cambridge Structural Database [144], time was spent parametrizing these missing interactions. However, in order to maintain as consistent a force-field as possible these parameters were not transferred to the updated MacroModel force-field, except for the C(=O)-C(=O) stretching and the C-C(=O)-N bending interactions which will be discussed later. Underlining the ongoing nature of force-field development, many publications on the parametrization of the amine and amide functional groups have only recently appeared in the literature [145, 146, 147, 148, 149, 150] and thus the constants supplied with MacroModel were frequently compared to these. Several other inconsistencies became apparent in the course of this study especially during the process of model validation. These will be discussed at a latter stage.

Obtaining parameters for interactions involving metal ions, especially copper(II), is considerably more difficult. Much less work has been performed on coordination compounds and most of this work has been on cobalt(III) and nickel(II) [118]. Furthermore most metal complexes can hardly be expected to yield any strain-free values as is the case for small organic molecules. Thus various parameters involving metal ion interactions have not been very well refined or are simply not available. The parameters used in this study for interactions involving the copper(II) metal ion were mainly obtained from three sources, i.e. Drew *et al* [119, 120], Brubaker and Johnson [118] and Hancock *et al* [113, 151], or alternately, were approximated by analogy with constants for similar interactions. Thus values of 0.89 mdyn Å<sup>-1</sup> for the stretching force constant and 2.00 Å for the natural bond lengths were used for both of the interactions Cu-N and Cu-O. These were taken from Brubaker and Johnson [118], having also been used by Drew *et al* [119]. Copper(II) is usually assigned a small value for the force constant so that its coordination sphere can be easily distorted. In this way an attempt is made to allow for the Jahn-Teller effect of copper(II).

The angle deformation constant for the N-Cu-N bending interaction is 0.30 mdyn Å rad<sup>-2</sup>, according to Drew *et al* [119], with natural bond angles of 90 and 180° as appropriate. Thus an ideal square planar geometry about the metal atom is assumed for most of the complexes as a first approximation.

In order to include both of the N-Cu-N bending interactions, i.e. with natural angles of either 90 or 180°, which occur simultaneously in many of the complexes modelled, use was made of the special substructure input feature of MacroModel [125] (see Appendix B). This bending interaction had presented severe problems in the preliminary modelling using MM2, eventually requiring additional coding, as this program cannot distinguish between the actual strain-free value to use for this bending interaction. The inclusion as a substructure in MacroModel is also not completely straight forward as

atom numbering is not unique for square-planar coordination and therefore the specific input order required can only be determined by the method of trial-and-error and had to be frequently changed to suit different input schemes.

The constants and strain-free angles used for all other bending interactions involving copper(II), i.e. X-N-Cu, were derived from analogous X-N-H or X-N-C interactions. The final values used will be discussed in a later section, as will the constants for the C-O-Cu interaction.

The non-bonded interaction parameters for copper(II) were obtained from Drew *et al* [119] and have values of 0.165 kcal mol<sup>-1</sup> and 2.35 Å for  $\zeta_{\text{Cu}}$  and the van der Waals radius, respectively. In line with current trends torsional interactions about coordinate bonds were assumed to be negligible, i.e. the torsional force constants for all X-Cu-X-X interactions were set equal to zero [120]. All other torsional parameters involving copper(II), i.e. of the type X-X-X-Cu, were estimated from the analogous X-X-X-C or other more general interactions.

The final force constants used throughout this study, which together with the potential functions 4.1 to 4.8 make up the force-field, are given in Appendix B. The bond and atom symbols used to describe the various interactions are defined at the beginning of the appendix. This force-field is however not intended to be definitive by any means, as much more work is required in order to obtain accurate parameters for the terms involving the metal ion.

### 4.3.3 MODEL VALIDATION

In the following discussion atom numbering in italics refers to specific interactions of the structures in the relevant figures, whereas standard print refers to general interaction types as in the molecular mechanics force-field.

#### 4.3.3.1 Structural comparisons

The molecular model was essentially validated by comparison of structural features such as bond lengths and angles of several energy minimized structures with those obtained from X-ray crystallographic data. Obviously a comparison with crystal structures that are very similar to the complexes being investigated is desirable and therefore the crystal determinations that were considered from the literature included the following: 1. the copper(II) complex with the ligand 5tet involving tetradentate binding [152], 2. the 11-2 complex of the ligand 6UH with nickel(II) [106], 3. the 656UH ligand involved in 11-2 binding to copper(II) [109], 4. the copper(II)-5UM complex with 21-2 coordination [107], 5. the 21-2 complex of copper(II) with the ligand 656UH [104]. In each case any additional ligands occupying coordination sites not filled by the ligands of interest, as well as counter-ions and possible crystal lattice effects, were ignored and therefore not modelled. This could be a rather severe simplification in some instances, especially in the case of the 11-2 structure of 656UH with copper(II), which also involved the ligand bipyridine, together with a second copper(II) ion.

The reasons for comparing the energy minimized structures with those determined by X-ray crystallography were mainly to decide on the set of bending parameters to be used for the X-X-Cu interactions (see before), as well as to ascertain the goodness of fit resulting from the Cu-X and X-Cu-X parameters used and furthermore to check on any

inconsistencies which might indicate possible errors in the force-field or require the use of more refined parameters.

The crystal structures were obtained from a QUEST search of the Cambridge Structural Database (CSD) as were the corresponding crystal coordinates. An exception was the structure determined by Desseyn *et al* [104] which had not as yet been deposited in the database. The CSD coordinates were transformed to MacroModel format by a FORTRAN program written specifically for this purpose and used as input to the molecular mechanics calculations. In this way the structural coordinates from before, i.e. as in the crystal, and after energy minimization could be easily compared and the goodness of fit determined by the method of least squares of residuals of the predicted minus the actual values. This was followed by Monte Carlo Multiple conformer energy Minimization (MCMC) [142] in order to determine whether the crystal structures were in fact representative of the minimum energy conformations. As expected this was generally not the case and is probably due to the presence of the additional ligands which were not considered in the molecular mechanics approach in this study.

Whilst modelling the copper(II)-5tet complex obtained from the structure determined by Marongiu *et al* [152] (actual crystal: thiocyanato triethylenetetramine copper(II) thiocyanate, i.e.  $[\text{Cu}(\text{trien})\text{SCN}][\text{NCS}]$ ) it became apparent that the attached atoms, namely H1, connected to the central atom in the three C3-N5-C3 bending interactions were incorrect (see Appendix B for atom symbols used). These were therefore replaced by the correct atom type, i.e. H4. Of greater concern however was the observation that the strain-free angles of the C3-C3-N5 interactions had the rather small values of about  $103^\circ$ . As it was intuitively felt that these values should be somewhat larger, a fact which is also borne out by Terui [153], attempts were made to trace the origins of these parameters. This however proved unsuccessful. Thus a search of acyclic strain-free molecules occurring in the CSD containing this fragment was undertaken. This

resulted in 60 'hits' with an average angle of about 113° as determined by the program GSTAT. Nonetheless, the fact that there are three separate entries with different strain-free values for these interactions in the MM2 force-field of MacroModel, suggests that these parameters have been well researched and therefore a more conservative value of 109° was eventually used, although the CSD average was also tried. This markedly improved the correspondence between the actual and energy minimized structures, especially with respect to several of the torsion angles. The best fit was thus obtained using the 'soft' constants for X-N5-Cu analogous to the X-N5-H interactions and a strain-free value of 109° for the C3-C3-N5 interaction.

As can be seen from Table 4.1, which gives the values of selected interactions of the energy minimized and crystal structures, as well as the corresponding strain-free parameters used, the fit is quite acceptable especially since Burkert and Allinger have claimed that parametrization of the amine functional group is extremely difficult [139]. Comparisons of bond lengths are not presented in the table as the agreement was generally very good.

The structure corresponding to that of the crystal is given in Figure 4.1. It has both of the central amine hydrogens *H1* and *H2*, situated on the same side above the plane, and the carbon atoms *C2* and *C5* situated below the plane of the four nitrogen atoms. This seemed a bit strange as this conformer corresponds to the energetically less stable  $\lambda\delta\delta$  diastereomer [94]. On carrying out a global minimum energy search it was found that this structure is indeed only the second most stable, with an energy of about 10 kJ mol<sup>-1</sup> above that of the structure which has the central amine hydrogens on opposite sides of the plane, i.e. the  $\lambda\delta\lambda$  diastereomer. This could be explained by the presence of the additional NCS<sup>-</sup> ligand, which occupies the 5th coordination site. Although rather interesting, this was however not investigated further. The very similar structure of the

**Table 4.1** : Comparison of selected bond and torsional angles of the crystal structure with those predicted by the energy minimization calculations, together with the strain-free parameters of the 'soft' force-field used for the corresponding interactions. The atom numbering relates to Figure 4.1.

Bond angle	crystal	minimized	strain-free	Torsion angle	crystal	minimized
N1-Cu-N4	98.8	97.3	90.0	C2-C1-N1-Cu	41.5	40.0
N1-Cu-N2	84.6	87.3	90.0	C3-C4-N3-Cu	-22.3	-18.8
N2-Cu-N3	84.3	87.0	90.0	C1-C2-N2-Cu	40.5	44.1
N3-Cu-N4	84.8	87.3	90.0	C4-C3-N2-Cu	-50.4	-51.1
Cu-N1-C1	107.8	106.5	109.5	N1-C1-C2-N2	-54.9	-56.2
N1-C1-C2	106.8	106.9	109.3	N2-C3-C4-N3	48.7	-46.8
C1-C2-N2	109.2	105.8	109.3	N3-C5-C6-N4	54.9	56.1
Cu-N2-C2	107.1	107.0	109.5	C1-C2-N2-C3	155.4	160.3
Cu-N2-C3	104.1	104.0	109.5	C4-C3-N2-C2	-167.0	-168.9
C2-N2-C3	114.4	117.0	111.2	C6-C5-N3-C4	-172.2	-172.8
N2-C3-C4	108.4	106.4	109.3	C6-C5-N3-Cu	-48.2	-53.3
C3-C4-N3	108.8	110.0	109.3	C5-C6-N4-Cu	-33.9	-29.4
Cu-N3-C4	110.8	108.4	109.5	C3-C4-N3-C5	98.8	97.8
Cu-N3-C5	105.3	102.8	109.5			
C4-N3-C5	117.7	118.5	111.2			
N3-C5-C6	107.0	104.9	109.3			
C5-C6-N4	107.0	108.3	109.3			
C6-N4-Cu	109.9	107.2	109.5			

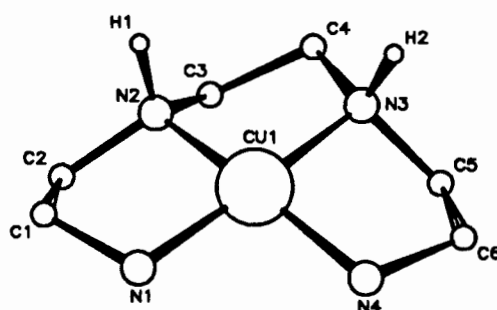


**Figure 4.1** : Energy minimized  $\lambda\delta\delta$  conformer of 5tet with copper(II), analogous to that of the crystal structure. For clarity all hydrogen atoms except those bound to the two central nitrogens have been omitted.

dimethyl derivative of 5tet, in the form of the diperchlorate monohydrate copper(II) complex, has also been determined but was not modelled in this study [154].

An attempt was made to model the 11-2 complex of the nickel(II)-656UH system obtained from the crystal structure determined by Lewis *et al* [106] (actual crystal: N,N'-bis (2-aminoethyl)propanediamidato nickel(II) trihydrate, i.e. Ni(6UH)•3H<sub>2</sub>O ). The stretching ( $k_s = 2.0 \text{ m dyn } \text{Å}^{-1}$  and  $l^\circ = 1.86 \text{ Å}$ ) and van der Waals parameters ( $\zeta_{\text{Ni}} = 0.165 \text{ kcal mol}^{-1}$  and radius =  $2.35 \text{ Å}$ ) for interactions involving the metal ion nickel(II) were taken from Drew *et al* [119], all other constants being the same as those for copper(II).

On minimizing the energy it was immediately apparent that large discrepancies exist between the energy minimized conformation and crystal structure. Although a not very thorough investigation was carried out on our part, we nevertheless feel that some peculiarities are associated with the crystal structure. This conviction stems from the fact that in the crystal structure the central 6-membered ring is virtually planar, as can be seen in Figure 4.2, which is highly strained and energetically very unfavourable. This is even evident from a Dreiden model of the crystal conformation. Furthermore the crystal does not incorporate any other ligands which could have caused this large deviation from the energy minimized structure. There are three water molecules involved in intermolecular hydrogen bonding, but we feel that the associated energy stabilization is not nearly sufficient to bring about this strained conformation. A re-evaluation of the crystal structure might therefore be in order, especially as the authors discuss only the position of the nickel(II) ion in the plane of the four nitrogen atoms but do not comment on the planarity of the central 6-membered ring.

Thus we could unfortunately not use this crystal structure for evaluation of calculated structural coordinates. It would have been ideal as it is quite closely related to those structures investigated in this study apart from the presence of the nickel(II) ion. As this was the only structural determination of the 5,6,5 ring configuration found in the literature, an attempt was made to solve the structure of 6UM with copper(II), a crystal of

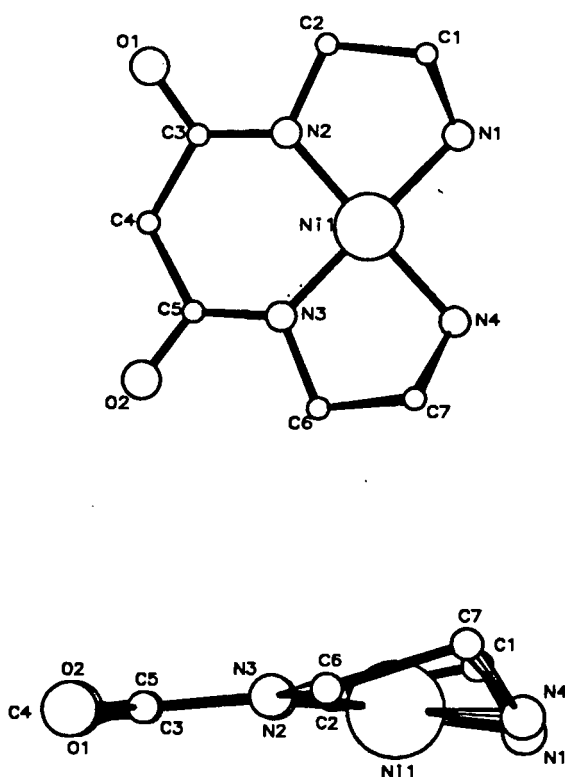


**Figure 4.2** : Perpendicular and side view of the crystal structure  $N,N'$ -bis (2-aminoethyl)propanediamidato nickel(II) trihydrate showing the flat central 6-membered ring. For clarity all hydrogen atoms and water molecules of hydration have been omitted.

which was available in the department. The details of the structure determination by X-ray crystallography are presented in Appendix C. Unfortunately the structure does not show any metal ion complexation by the ligand of interest and could therefore also not be used in the validation process. It is simply an ionic crystal consisting of a diprotonated derivative of the ligand acting as the cation with hexa- $\mu_2$ -chloro- $\mu_4$ -oxo-tetra[chlorocuprate(II)] as the anion. The polynuclear cluster is however of some interest as it involves tetrahedral coordination of the central oxygen atom in the anion.

An attempt was made to model the structure of the 11-2 complex of 656UH with copper(II) as determined by Journaux *et al* [109] (actual crystal:  $\mu N,N'$ -bis (3-aminopropyl) ethanediamidato 2,2'-bipyridyl copper(II) dichlorate, i.e.  $[\text{Cu}(656\text{UH})\text{Cu}(\text{bipy})] (\text{ClO}_4)_2$ ). The essentially symmetrical crystal structure however

shows large differences in bond lengths, i.e. 1.516 compared to 1.313 Å, for the same C3-C3 interactions, which are just in opposite chelate rings (see Figure 4.3). The authors in fact comment on the problem of the unresolved disorder and concomitant low accuracy of the structural parameters in this part of the crystal. Furthermore the actual crystal is much more complicated than the fragment which is of interest in this study making it unsuitable for purposes of model validation. Therefore this crystal determination was also not used for the evaluation of calculated structural parameters.

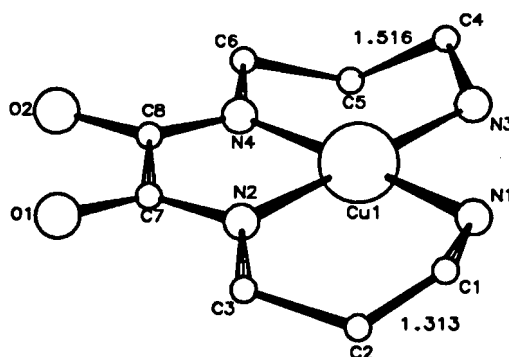


**Figure 4.3** : The 11-2 fragment of copper(II) with the ligand 656UH of the crystal structure according to Journaux *et al.* Bond lengths are given in Ångström. For clarity all hydrogen atoms have been omitted.

The model was next validated against the 21-2 complex of copper(II) with 5UM, the structure of which was determined by Yoshino and Nowacki [107] (actual crystal:  $\mu$ N,N'-bis [2-(dimethylamino)ethyl] ethanediamidato diisothiocyanato bis dimethylformamide copper(II), i.e.  $\text{Cu}_2(5\text{UM})(\text{NCS})_2 \cdot (\text{DMF})_2$ ). Similarly to the problem with the C3-N5-C3 interactions, it was found that the atoms attached to the central atom of the three bending interactions C3-C3-N2 were in fact missing from the MM2 force-field supplied with MacroModel and the correct H1 atom types thus had to be added.

Although the minimum energies were somewhat different using the 'hard' or 'soft' force-fields (see the results section) there appeared to be little difference between the goodness of fit of the crystal and either of the two energy minimized structures. Table 4.2

gives structural values of selected stretching, bending and torsional interactions, as well as the corresponding strain-free parameters of the 'soft' force-field used in these calculations. As can be seen from the table the agreement between the energy minimized and crystal structures, is once again quite good. This is particularly borne out by the good correspondence of the torsional angles which should show the largest deviations having the smallest force constants.

Initially the largest discrepancy in bond length (not shown in the table) was observed for the bond between the two carbonyl carbons, i.e. the C2(O2)-C2(O2) interaction. The MM2 force-field of MacroModel has several entries for this interaction with strain-free lengths ranging from 1.334 to 1.477 Å, all indicating a significant amount of double bond character and quite different from the value in the crystal. Thus a search was carried out on 'strain-free' diketone and diamide fragments contained in the CSD. This resulted in 37 'hits' with a mean value of 1.517 Å ( $\pm 0.022$ ) as determined by the program GSTAT. Therefore the strain-free bond length of this interaction was adjusted to a value of 1.520 Å and used for all subsequent calculations resulting in a fairly good correlation. As can be seen from the table the largest remaining discrepancy between the crystal and energy minimized structures is in the C1 to N1 bond distance, the former being .084 Å shorter. The strain-free length of 1.343 Å used in this study is already somewhat shorter than the MacroModel value of 1.385 Å and was obtained on applying a dielectric constant reduction as per MM2. Furthermore, as the GSTAT calculation on uncomplexed strain-free fragments in the CSD gave a mean bond length of 1.330 Å and for complexed species a value of 1.314 Å, the reduced strain-free value therefore seems justified. The crystal structure according to Yoshino and Nowacki has in fact the shortest C2(O2)-N2 bond length of all CSD complexes found, therefore no further adjustments were made with respect to this interaction. Similarly, the elongated

**Table 4.2** : Comparison of selected bond lengths, angles and torsional interactions of the crystal structure with those predicted by the energy minimizations, together with the respective 'soft' strain-free parameters used in the calculations. Atom numbering relates to Figure 4.4, below.

Bond Length	crystal	$E_{\min}$	strain-free	Bond angle	crystal	$E_{\min}$	strain-free
Cu1-N1	1.909	1.948	2.000	N1-Cu1-N2	82.4	82.2	90.0
Cu1-N2	2.093	2.036	2.000	O1-Cu1-N1	83.1	85.4	90.0
Cu1-O1	2.015	2.015	2.000	O1-Cu1-N2	164.0	167.6	180.0
C1-N1	1.259	1.343	1.343*	N1-C1-C6	112.5	109.9	114.0*
C1-C6	1.544	1.532	1.520*	N1-C1-O2	130.4	126.5	124.3
C2-C3	1.514	1.541	1.523	N1-C2-C3	106.2	103.9	109.3
C2-N1	1.482	1.442	1.437	N2-C3-C2	110.9	110.9	109.3*
C3-N2	1.484	1.504	1.480	C1-N1-Cu1	117.0	113.7	119.0
C4-N2	1.465	1.495	1.480	C2-N1-Cu1	118.4	119.7	124.0
C5-N2	1.466	1.494	1.480	C1-N1-C2	124.6	126.5	119.9
C6-O1	1.271	1.249	1.244*	Cu1-N2-C3	104.5	105.7	109.5
				C6-O1-Cu1	110.3	107.4	109.5
				O1-C6-C1	117.1	123.6	123.0
				Cu1-N2-C4	108.9	108.4	109.5
				C4-N2-C3	112.2	111.3	107.7
				Cu1-N2-C5	112.3	110.4	109.5
				C5-N2-C3	108.3	110.4	107.7
				C5-N2-C4	110.5	110.0	107.7
Torsion angle	crystal	minimized					
C6-C1-N1-Cu1	-0.2	0.6					
O2-C1-N1-Cu1	-178.9	-179.5					
C3-C2-N1-Cu1	-15.3	-19.8					
C2-C3-N2-Cu1	-44.8	-44.3					
C1-C6-O1-Cu1	-1.3	-0.4					
C2-C3-N2-C4	73.0	73.2					
C2-C3-N2-C5	-164.7	-164.0					
C6-C1-N1-C2	-180.0	-178.3					
O2-C1-N1-C2	1.3	1.6					
N1-C1-C6-O1	1.1	-0.1					
N1-C2-C3-N2	40.0	41.4					
O1-C6-C1-O2	-180.0	-180.0					

\* Adjusted strain-free values, see text

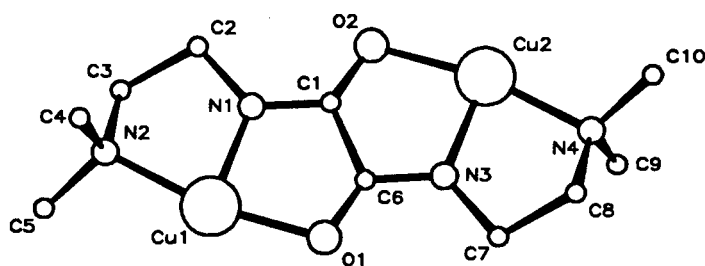


**Figure 4.4** : Energy minimized conformer of the 21-2 complex of the copper(II)-SUM system, analogous to that of the crystal structure. For clarity all hydrogen atoms have been omitted.

C2=O2 strain-free bond length of 1.244 Å, according to MM2, was used throughout this study in preference to the MacroModel value of 1.218 Å. This resulted in a better fit.

In the case of the bond angles a large difference was initially observed for the C2(O2)-C2(O2)-N2 interactions, i.e. angle *N1-C1-C6* in Figure 4.4, as the MM2 force-field supplied with MacroModel has a strain-free value of 120° for this bond angle. Carrying out GSTAT calculations on 21 'strain-free' fragments obtained from a search of the CSD, indicated instead a mean value of 114° which was thus used throughout. Even calculations on complexed fragments contained in the CSD gave a very similar value to this, with however, a much larger standard deviation.

Initially values of 0.3 mdyn Å rad<sup>-2</sup> and 120° were used respectively for the bending constant and strain-free angle of the C-O-Cu interactions according to Boeyens *et al* [155]. However finally, values of 0.3 mdyn Å rad<sup>-2</sup> and 109° were used, based on the parameters of Brubaker and Johnson [118] for the Cu-O-H bending interaction. This resulted in a more reasonable fit.

As can be seen from Table 4.2, the largest discrepancy of the bending interactions is for the bond angle *O1-C6-C1* for which the strain-free value is 123°. Even though GSTAT calculations on complexed structures gave a mean value of 117° for this interaction, the strain-free value was not adjusted as a search of uncomplexed fragments contained in the CSD resulted in 37 'hits' with a mean value of 122°. A further refinement should possibly be introduced into the force-field for the case in which this angle forms part of a chelate ring.

Lastly, as can be seen from the angle *N2-C3-C2* in Table 4.2, the strain-free value of 109.3° used for the C3-C3-N5 interactions (discussed previously), models the crystal structure very well, i.e. neither 103 nor 113° seems to be correct.

Finally the model was checked against the structure of the 21-2 complex of copper(II) with 656UH determined by Desseyn *et al* [104] (actual crystal:  $\mu$ N,N'-bis (2-aminopropyl)ethanediamidato dinitrato copper(II), i.e.  $\text{Cu}_2(656\text{UH})(\text{NO}_3)_2$ ). Unfortunately the crystal coordinates were not yet available from the CSD and therefore the input structure was 'built up' using the interactive mode of MacroModel. The energy of this was minimized by the MCMM technique resulting in several minimum energy structures of which the second most stable, lying energetically only slightly above the global minimum, was analogous with the crystal structure reported by Desseyn *et al*. The fit between the experimentally determined and energy-minimized structural features was again relatively good, although in this case using the strain-free angle of  $113^\circ$  for the C3-C3-N5 interactions resulted in a better agreement especially with respect to some of the torsional angles.

#### 4.3.3.2 Energetic Comparisons

In order to validate the molecular mechanical approach employed in this study, i.e. of using the calculated increase in strain energy on complexation as a measure of complex stability, the homologous series of tetramine ligands namely 5tet, 6tet and 656tet, was modelled with copper(II) as the metal ion. Several reasons exist for choosing this homologous series for the purposes of validating the specific approach used in this study.

Firstly, these ligands make up the series against which the analogous diamino diamides were initially compared with respect to the order of stability of their copper(II) complexes. Secondly, the stated reason for the increased stability of 6tet with copper(II) was relief of ring strain [38], which lends itself very well to the investigation by the molecular mechanics technique. Thirdly, the ring sizes of corresponding complexes of the two series are the same and at least one of the functional groups, namely the amine group,

which has been one of the most difficult to parametrize [139], is common to both series of ligands. Lastly, if the force-field calculations could successfully model the reversed order of stability observed for the copper(II) complexes of the two series of ligands, this would lend additional credence to the use of the intended force-field approach. Furthermore, as has already been discussed, a crystal structure of one of the tetramine ligands with copper(II) is available in the literature and could be used for comparison of structural parameters.

Thus the interactive mode of MacroModel was used to create input coordinates of the three tetramine ligands. Using these literally thousands of starting geometries were then randomly generated and energy minimized by the MCMM method, in order to obtain the global minima in each case. As the free ligands are rather flexible, many different conformers of similar energy were acquired. Therefore in order to obtain a better estimate of the energies of these systems as a whole, Boltzman distribution calculations were carried out as described in section 4.2. In each case a sufficient number of conformers were used such that the one of highest energy contributed just less than 1 percent to the weighted mean total energy.

Similarly, input coordinates of the copper(II) complexes of the three tetramine ligands were generated, the minimum energy conformers obtained using the MCMM technique of MacroModel and the Boltzman mean energies of the systems calculated. As had previously been observed to some extent during the calculations involving the copper(II)-5tet crystal structure, the copper(II)-656tet complex remained completely 'trapped' in the higher energy conformations, i.e. with the central amine hydrogens located on the same side of the plane of the four nitrogen atoms similar to Figure 4.1. This was even after several thousand starting geometries had been generated and minimized by the MCMM technique. Therefore the input coordinates were manually adjusted to give the lower energy conformers with the hydrogens on opposite sides of the plane. This

illustrates the care that needs to be taken in order to obtain global minima even with such 'powerful' programs such as MacroModel.

The calculated strain energies of the ligands and complexes, together with the energy changes on complexation,  $\Delta U$ , as well as  $\Delta(\Delta U)$ , from which the differences in stability constants were determined using equation 4.10, are given in Table 4.3. Also given in the table, for the purposes of comparison, are potentiometric data taken from the literature. As can be seen from Table 4.3, a surprisingly large variation in the Boltzman mean energies was observed for the free ligand species. It was found that one interaction alone, namely the N3-C3-C3-N3 torsion angle, was virtually entirely responsible for these large energy differences. This interaction has V1, V2 and V3 terms of -0.4, -1.1 and 1.2 kcal mol<sup>-1</sup> respectively, which results in a very large energy minimum of roughly -4.7 kJ mol<sup>-1</sup> per interaction, at a torsion angle of 60°. Since there are a different number of these interactions in each ligand, decreasing along the series in the order 5tet > 6tet > 656tet, this causes the unexpected differences in energy. This might therefore be a rather unsatisfactory situation, especially as these interactions do not appear in the complexes, allowing for no cancellation of a possibly bad parameter. This could be a reason for the poor correlation of observed differences in the stability constants and the differences calculated using  $\Delta(\Delta U)$  of (C1 - F1).

The N3-C3-C3-N3 interaction seems to be quite well researched however, having also been parametrized by other workers [145, 149] resulting in very similar constants to those supplied with MacroModel. However in related calculations on coordination compounds using the molecular mechanics program according to Boyd, a more general 00-C3-C3-00 interaction with V1, V2 and V3 of 0.0, 0.0 and 0.35 kcal mol<sup>-1</sup> respectively, has been used [113]. This also has an energy minimum at 60° but with a much smaller negative value than before. Using this in the calculations, i.e. the 'general' force-field, resulted in the free ligands having a much more similar energy (see Table 4.3).

**Table 4.3** : Strain energies, in  $\text{kJ mol}^{-1}$ , determined by a Boltzman distribution of the minimum energy conformers of the free and complexed tetramine species in solution. These were calculated using the program MacroModel with different MM2 force-fields (see text).  $\Delta U$  is the energy change on complexation and  $\Delta(\Delta U)$  is the difference in the energy change on going from one ligand to another. The differences in  $\log \beta_{110}$  were calculated from  $\Delta(\Delta U)$  using equation 4.10. Stability constants were taken from the literature.

Force-field	Species					
	5tet	Cu(II)-5tet	6tet	Cu(II)-6tet	656tet	Cu(II)-656tet
(F1) Specific	16.4	-	23.8	-	32.0	-
(F2) General	30.1	-	32.2	-	36.2	-
(C1) Soft 109°	-	49.9	-	34.0	-	41.1
(C2) Hard 109°	-	57.9	-	38.9	-	38.4
(C3) Soft 103°	-	46.4	-	38.2	-	52.1
$\Delta U$ (C1 - F1)	33.5		10.2		9.1	
$\Delta U$ (C1 - F2)	19.8		1.8		4.9	
$\Delta U$ (C2 - F2)	27.8		6.7		2.2	
$\Delta U$ (C3 - F1)	15.6		5.8		20.2	
$\log \beta_{110}^a$		20.1		23.2		21.7

5tet → 6tet				
F-F Combination	C1 - F1	C1 - F2	C2 - F2	C3 - F1
- $\Delta(\Delta U)$	23.3	18.0	21.1	15.6
calc $\Delta \log \beta_{110}$	4.1	3.2	3.7	2.7
actual $\Delta \log \beta_{110}^a$		3.1		
5tet → 656tet				
F-F Combination	C1 - F1	C1 - F2	C2 - F2	C3 - F1
- $\Delta(\Delta U)$	24.4	14.9	25.6	9.8
calc $\Delta \log \beta_{110}$	4.3	2.6	4.5	1.7
actual $\Delta \log \beta_{110}^a$		1.6		
656tet → 6tet				
F-F Combination	C1 - F1	C1 - F2	C2 - F2	C3 - F1
- $\Delta(\Delta U)$	-1.1	3.1	-4.5	5.8
calc $\Delta \log \beta_{110}$	-0.2	0.6	-0.8	1.0
actual $\Delta \log \beta_{110}^a$		1.5		

<sup>a</sup> Data from reference [39]

Furthermore, the fit between calculated  $\Delta \log \beta_{110}$  and those determined from potentiometric data was greatly improved as can be seen from the results for the (C1 - F2)

combination obtained using the 'soft' force-field with a strain-free angle of  $109^\circ$  for the C3-C3-N5 interactions (Table 4.3). This predicts the copper(II)-6tet and copper(II)-656tet complexes to be respectively 3.2 and 2.6 log units more stable than the copper(II)-5tet complex, which compares well with the actual differences of 3.1 and 1.6 log units.

Considering the entropy changes of complex formation, which have so far been ignored but are in fact not identical, even better agreement between observed and calculated differences in stability constants is obtained. The  $\Delta S$  of copper(II)-5tet formation is about  $4 \text{ cal mol}^{-1} \text{ K}^{-1}$  larger than the entropy changes of the other two complexes [39]. This has the effect of reducing the calculated differences in the logarithms of the stability constants to 2.4 and 1.8 respectively. These results therefore support the hypothesis of Weaton *et al* that the increased stability of 6tet with copper(II) is due to relief of ring strain.

Lastly, the copper(II)-6tet complex is predicted to be 0.6 log units more stable than copper(II)-656tet, which compares quite well with the actual difference in stability constants of 1.5 log units. The calculated value is unaffected by any  $\Delta S$  contributions since the entropy changes are identical for these two complexes.

As can also be seen from the table for the combination (C2 - F2), using the 'hard' force-field, with parameters for the Cu-X-X bending interactions analogous to those of the C3-X-X interactions, results in the worst correspondence. In this case the calculated energy differences in fact predict the copper(II)-656tet complex to be the most stable by 0.8 log units which is clearly not correct.

For interests sake the results using the 'soft' force-field with a strain-free angle of  $103^\circ$  for the C3-C3-N5 interaction have also been presented in Table 4.3. This resulted in

quite good agreement of predicted versus actual differences in the stability constants, but gave the poorest correspondence of structural features and was therefore not considered.

Overall, the best agreement was thus obtained with the 'soft' force-field incorporating a strain-free angle of  $109^\circ$  for the C3-C3-N5 bending interaction. This is therefore the force-field of choice for the modelling of the diamino diamide complexes investigated in this study. The problem regarding the use of the 'specific' as opposed to the 'general' force-field in the modelling of the free tetramine ligands does not arise as the N3-C3-C3-N3 torsional interaction is not present in the diamino diamide ligands.

## 4.4 RESULTS AND DISCUSSION

As is evident from the previous sections, molecular modelling and, in particular, the molecular mechanics method employed, can be used quite successfully to calculate the structure and stability of metal complexes. Therefore an identical approach could now be applied to the various diamino diamide copper(II) systems to try and explain the anomalous order of stability which had been observed potentiometrically.

Thus the input coordinates of the three diamino diamide ligands and of the various copper(II) complexes, as determined in the spectrophotometric study, were generated using the interactive mode of MacroModel. Minimum energy conformers were then obtained by the MCMM method of MacroModel as before, using the 'soft' force field with a strain-free angle of  $109^\circ$  for the C3-C3-N5 bending interactions. Since in most cases several different conformers with similar strain energy were obtained, the Boltzman mean energies were again calculated. These results, together with the energy changes on complex formation,  $\Delta U$ , are presented in Table 4.4.

**Table 4.4** : Boltzman mean energies,  $U$ , in  $\text{kJ mol}^{-1}$  of the free diamino diamide ligands and their various copper(II) complexes, calculated using the program MacroModel with the 'soft' MM2 force-field. The changes in strain energy on complexation,  $\Delta U$ , are given in parenthesis.

	Species				
	Free Ligand	110	11-1	11-2	21-2
5UM	73.0	74.8 (1.8)	71.6 (-1.4)	89.1 (16.1)	76.9 (3.9)
6UM	55.6	86.8 (31.2)	77.2 (21.6)	109.8 (54.2)	-
656UM	72.7	81.7 (9.0)	77.8 (5.1)	154.8 (82.1)	86.4 (13.7)

In order to discuss the origins of some of the values listed in Table 4.4, separate or individual energy terms contributing to the total energy of, for example, the most stable conformers of each system are given in Table 4.5.

**Table 4.5 :** Separate energy terms in  $\text{kJ mol}^{-1}$  contributing to the total energies of the most stable conformers of the free ligands and their copper(II) complexes. (Molecular mechanics calculations were carried out using the force field in Appendix B.)

Species	Stretch	Bend	Str-Bend	v.d.Waals	Torsion	Electro.	Total
5UM	5.4	16.7	2.1	42.7	4.6	0.0	71.0
6UM	5.5	17.0	2.0	31.8	-1.7	-1.4	53.1
656UM	6.0	19.3	2.4	34.6	6.8	0.2	69.0
5UM110	6.2	27.2	2.0	30.9	7.7	-0.4	73.4
6UM110	5.4	25.1	1.3	38.8	15.5	-1.7	84.7
656UM110	5.5	23.7	2.0	38.5	10.5	-0.3	79.8
5UM11-1	5.9	26.5	2.1	27.9	7.9	0.0	70.2
6UM11-1	5.4	23.3	1.4	31.8	13.6	-1.3	74.5
656UM11-1	5.5	24.7	2.1	32.9	10.5	0.1	75.8
5UM11-2	10.1	48.3	1.9	16.9	11.2	0.2	88.6
6UM11-2	12.2	40.2	0.5	33.2	21.5	-1.1	107.1
656UM11-2	14.2	55.3	2.0	52.5	28.5	0.1	153.6
5UM21-2	6.7	38.5	1.7	20.0	10.9	-0.9	76.9
656UM21-2	5.1	28.7	1.5	40.0	12.2	-0.9	86.4

A peculiar result, apparent in Table 4.4, is that the 11-1 copper(II) complex of 5UM has a lower strain energy than the free ligand itself, which has the effect of causing a decrease in the strain energy on complex formation ( $\Delta U = -1.4 \text{ kJ mol}^{-1}$ ). This could be explained by the introduction of a favourable metal ion interaction whose potential function has a negative energy minimum. A more likely explanation is the loss of interactions involving the amide protons and the amine lone electron pairs on

complexation. These contribute significantly to the van der Waals energy, especially in the case of the short ligand 5UM (Table 4.5). The force-field parameters of these interactions should possibly be further investigated.

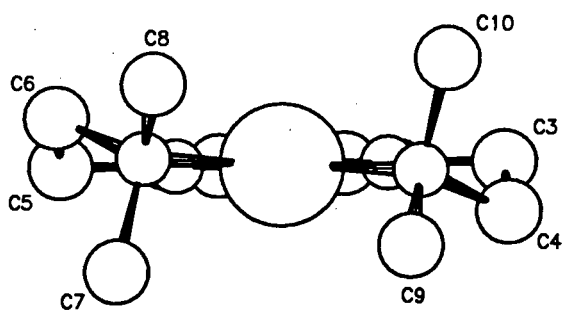
As is indicated in Table 4.4, very large changes in strain energy on complexation of 52.2 and 82.1 kJ mol<sup>-1</sup> are observed for the 11-2 species of 6UM and 656UM respectively, compared to only 16.1 kJ mol<sup>-1</sup> for the 5UM complex. In the case of the 6UM system this is due to a combination of a low energy free ligand together with a relatively high energy 11-2 complex, whereas for the 656UM system the large  $\Delta U$  results from the complex having a very high energy.

The 5UM complex shows virtually no distortion of the nitrogen atoms from square planarity about the copper(II) ion. The central 5-membered ring, containing four sp<sup>2</sup> centers, is completely planar and the outer rings are able to take on the low energy puckered configurations represented by the  $\lambda\lambda$  enantiomer in Figure 4.5.

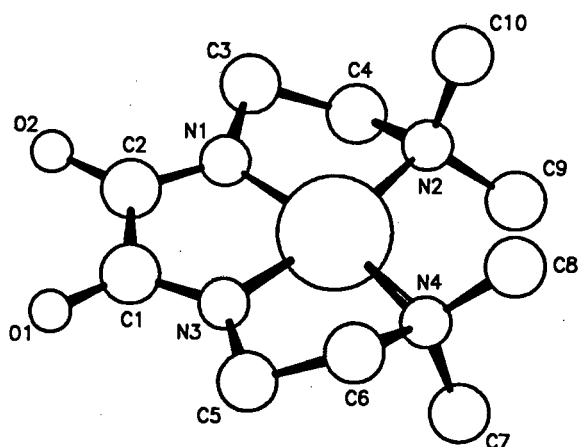
In the case of the 6UM complex the nitrogen atoms are not completely planar. Furthermore, as can be seen from Figure 4.6(b & c), the central 6-membered ring is in a distorted boat conformation. This has the consequence that both methylene carbons C2 and C8, are on the same side, below the plane of the nitrogens. Therefore only one of the outer 5-membered rings is in a stable puckered  $\lambda$  configuration, whereas the other is severely distorted with both methylene carbons C2 and C3, below the plane of the nitrogens as can be seen from Figure 4.6(a & c).

Figure 4.7(a) clearly indicates that the planarity of the nitrogen atoms about the copper(II) ion is severely distorted in the 656UM11-2 complex. As in the case of the 5UM complex the central 5-membered ring is completely planar. However, both outer 6-membered rings are severely distorted having neither a chair nor a boat conformation.

(a)



(b)



(c)

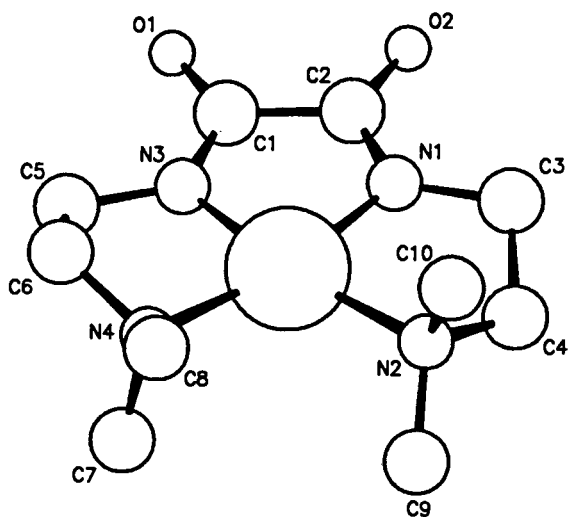
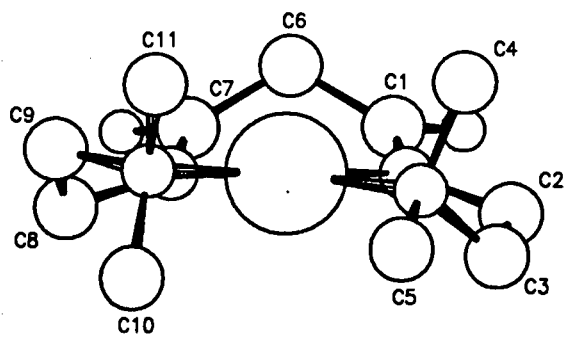
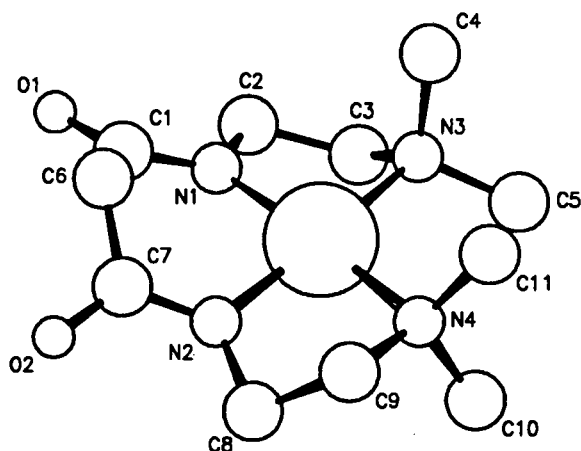


**Figure 4.5** : Pluto representations of the lowest energy 5UM11-2 conformer, viewed (a) from the open end, (b) and (c) from the side and the open end at 45° to the plane of the four nitrogens. Only the  $\lambda\lambda$  diastereomer is shown. For clarity hydrogen atoms have been omitted.

(a)



(b)



(c)

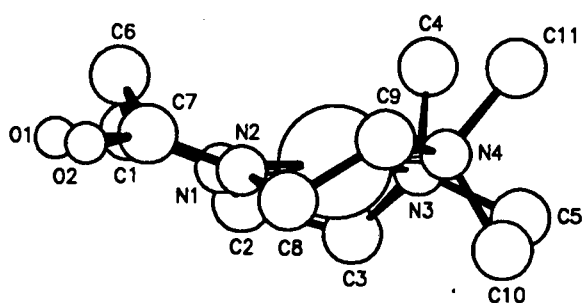
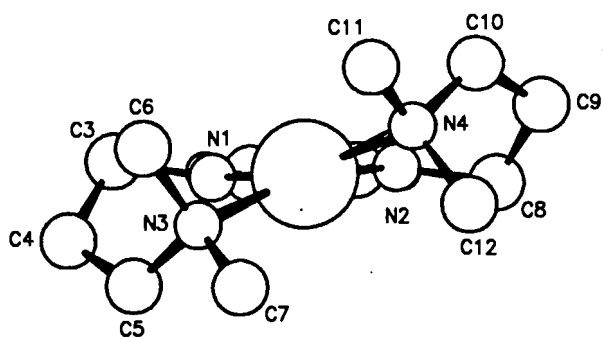
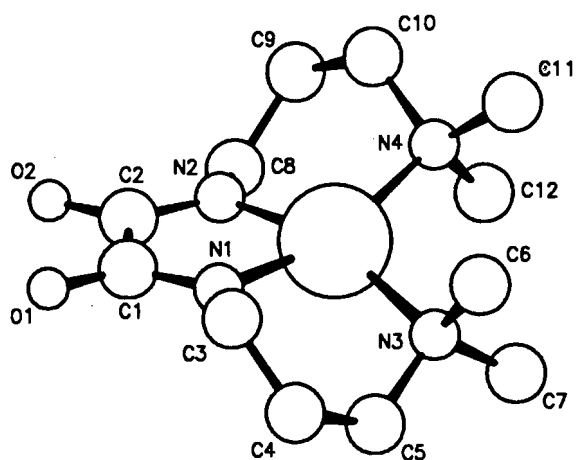


**Figure 4.6** : Pluto representations of the lowest energy 6UM11-2 conformer, viewed (a) from the open end, (b) from the side rotated down by 30° from the plane of the four nitrogens and (c) directly from the side. For clarity hydrogen atoms have been omitted.

(a)



(b)



(c)

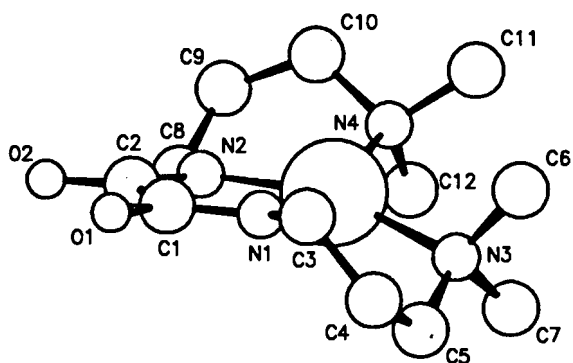


**Figure 4.7 :** Pluto representations of the lowest energy 656UM11-2 conformer, viewed (a) from the open end, (b) from the side rotated down by 25° from the Cu-N1-N2 plane and (c) essentially from the side to best show the configuration of the outer ring. For clarity hydrogen atoms have been omitted.

Therefore compared to the 11-2 complex of 5UM, both the 6UM11-2 and 656UM11-2 complexes show quite severe distortions from ideal 5 and 6-membered ring configurations. This is also indicated by the increasing torsional energy terms given in Table 4.5 and, based on the van der Waals energy contributions, is probably due to the increased crowding of the terminal methyl groups.

Finally the results from Table 4.4 were used to determine the differences in the strain energy changes, i.e.  $\Delta(\Delta U)$ , on formation of equivalent complexes in going from one ligand to another. These values, together with the differences in the logarithms of the stability constants calculated using equation 4.10, are presented in Table 4.6. Also given in the table are the actual differences in stability constants obtained from the potentiometric study.

**Table 4.6** : Differences in the strain energy changes on complex formation,  $\Delta(\Delta U)$ , going from one ligand to another, in  $\text{kJ mol}^{-1}$ . The differences in  $\log \beta_{pqr}$  are calculated using equation 4.10, whereas the actual differences are obtained from the potentiometric results.

	p q r			
	110	11-1	11-2	21-2
<b>6UM → 5UM</b>				
$-\Delta(\Delta U)$	29.4	23.0	38.1	—
calc $\Delta \log \beta_{pqr}$	5.2	4.0	6.7	—
actual $\Delta \log \beta_{pqr}$	1.82	2.6	1.92	—
<b>656UM → 5UM</b>				
$-\Delta(\Delta U)$	7.2	6.5	66.0	9.8
calc $\Delta \log \beta_{pqr}$	1.3	1.1	11.6	1.7
actual $\Delta \log \beta_{pqr}$	-0.06	1.23	2.74	2.02
<b>6UM → 656UM</b>				
$-\Delta(\Delta U)$	22.2	16.5	-27.9	—
calc $\Delta \log \beta_{pqr}$	3.9	2.9	-4.9	—
actual $\Delta \log \beta_{pqr}$	1.88	1.37	-0.86	—

As can be seen from Table 4.6, with the exception of one structure molecular mechanics predicts the correct order of stability. In the case of the 110 complexes of 5UM and 656UM the molecular mechanics calculations predict the former to be 1.3 log units more stable than the latter, whereas the potentiometric study in fact shows the 5UM complex to be 0.06 log units less stable. However, in all other instances the order of stability is correctly predicted by the molecular mechanics calculations, although sometimes far greater differences in stability are indicated by the results than is actually observed experimentally.

In these diamino diamide copper(II) systems the differences in stability constants can largely be attributed to three main factors, i.e. differences in the strain energy, the entropy and the metal-ligand bond strength. The molecular mechanics calculations essentially only model differences in the strain energy which are however expected to play a major role, as the systems have very different ring configurations. Thus, for the calculations to give meaningful results the latter two factors need to be negligible or quantifiable.

In the case of the tetramine complexes, entropy contributions were found to be negligible and were only introduced as a further refinement of the results. Unfortunately, the entropy changes for the diamino diamide systems are not known and therefore no quantitative adjustments can be made. However the ligands are very similar, having the same functional groups and differing only in chain length. Furthermore the metal ion, i.e. hydration, and types of coordination are identical. Therefore to a first approximation, entropy contributions can be ignored as they effectively cancel out.

For the molecular mechanics calculations to successfully model these systems, the metal-ligand bond strengths in the different complexes must also be sufficiently similar. Using the protonation constants as an indication of amine basicity and hence as a measure

of metal-ligand bond strength, this assumption seemed quite reasonable in the case of the tetramine ligands (see Table 3.8). The protonation constants of the diamino diamide ligands lie even closer together and therefore the assumption of similar bond strengths is even more valid in this case (see Table 3.1). However, the same cannot be said for the amide protonation constants and hence the metal-amide bond strengths. These protonation constants cannot be measured as the amide protons are only displaced on metal ion complexation. However, they are probably quite similar for the 5UM and 656UM ligands, which have the same central configuration of amide groups, but might be somewhat different for the 6UM ligand. This is because the amide functional groups are separated by a methylene group in the latter ligand and therefore do not influence each other to the same extent. Having either two or three methylene groups attached on the outside of the amide groups is not expected to make much difference to the protonation constants.

Assuming the metal-amide bond strength of the ligand 6UM to be different to that of the other ligands cannot, however, be used to consistently explain the differences between observed and calculated differences in stability.

In conclusion therefore, neither entropy nor metal-ligand bond strengths are expected to contribute significantly to the differences in the observed stability of the complexes. Since the molecular mechanics calculations model the potentiometric results quite well in most respects we maintain that the differences in stability are due to differences in steric energy. This is not to say that the 5,5,5 contiguous ring system is necessarily the most stable, in fact the bending interactions indicate the 5,6,5 system to be the least strained. However, in the systems investigated in this thesis, with the central chelate ring containing four  $sp^2$  centers and the terminal amine groups fully substituted the order of stability of 5,5,5 > 5,6,5 > 6,5,6 found in the potentiometric study has been successfully modelled by molecular mechanics calculations. The same comments can be

made about the stability order  $5,5 > 6,5 > 5,6$  where the second number refers to the ring containing the carbonyl carbons.

The problem of the extremely large stability predicted for the 5UM11-2 complex thus still remains. The possibility exists that the global minima of the corresponding 6UM and 656UM complexes were not found even though an exhaustive search in which literally thousands of starting geometries were generated and minimized by the MCMM method of MacroModel, was carried out. This required substantial amounts (several days) of CPU time.

**CHAPTER FIVE**  
**ANIMAL EXPERIMENTS**

## 5.1 INTRODUCTION

Unfortunately, any drug showing promise as a therapeutic agent ultimately has to undergo some form of clinical testing, no matter how thoroughly the preliminary investigations have been carried out.

In this study it was decided to initially determine the bio-distribution of the copper(II) complexes which would also indicate their *in vivo* stability. If the drugs had a favourable bio-distribution further experiments could be carried out to investigate their anti-inflammatory activity as well as determine their mammalian toxicity. Thus in order to determine the efficacy of these diamino diamide ligands in transporting copper(II) through the body to possible sites of inflammation, tissue distribution studies using white mice were performed.

Furthermore only the strongest of the diamino diamide copper(II) complexors, i.e. 5UM, was studied. For comparison the ligands TTDA and DTDA were also investigated. These have been shown, by computer modelling of blood plasma [41], to be excellent mobilizers of copper(II) *in vivo*.

Due to the small size of the laboratory animals the copper distribution was monitored by radio-active labelling, which also allowed for very rapid analysis of the excised samples. For this purpose  $^{67}\text{Cu}$  was used in the present study since it has a relatively long half-life of 61.9 hrs. Although decay is by release of beta particles, this isotope also has moderately abundant 93 and 184 keV gamma emissions which are usually monitored [156].

## 5.2 EXPERIMENTAL PROCEDURE

The experimental approach used in this study was similar to that of other workers in the field of nuclear medicine [157, 158]. Male Balb/c mice were used throughout the study, with food and water being allowed *ad libitum*. Approximately  $1 \text{ mmol dm}^{-3}$  copper(II) solutions of the three ligands, as well as a cupric chloride control, were made up using sterile saline and adjusted to physiological pH. These solutions were spiked with  $^{67}\text{CuCl}_2$  (radiochemical purity > 98%) to give solutions of about  $12 \text{ kBq ml}^{-1}$ . Groups of 10 mice were injected intraperitoneally with  $200 \mu\text{l}$  of these  $^{67}\text{Cu}$  solutions. This approximated to a  $2.4 \text{ kBq}$  dose of radioactivity per mouse. The mice were then individually placed in polycarbonate cages which contained paper towelling for urine absorption.

After 6 or 24 hours groups of 5 mice were lightly anesthetized by ether inhalation and then sacrificed by cervical dislocation. Aliquots of blood were taken from the inferior vena cava and various organs were excised and weighed. The urine impregnated towelling was extracted with  $100 \text{ ml}$  of  $20\% \text{ v/v HCl}$ . Radioactive counting was carried out in a Minaxi Autogamma 5000 Series  $\gamma$  counter using a window set for  $^{67}\text{Cu}$  and a counting time of 10 minutes. Samples of the injected solutions were used as counting standards.

### 5.3 IN VIVO MODELLING

Computer modelling of the *in vivo* copper(II) speciation was carried out using the program ECCLES [159]. The calculations were based on an updated model of blood plasma [160] with the relevant constants taken from the potentiometric results (section 3.4.2.1) and from references by Jackson and Kelly [41, 161]. Of particular interest is the computed increase in low-molecular-weight copper(II) concentration caused by the individual drugs in the presence of competing endogenous ligands. The key function in this respect is the plasma mobilization index (p.m.i.) [162] which is defined, for example, for copper(II) by the following equation.

$$\text{p.m.i.}_{\text{Cu}} = \frac{\text{total conc. of low-molecular-weight copper(II) complexes in the presence of the drug}}{\text{total conc. of low-molecular-weight copper(II) complexes in normal plasma}}$$

Thus a strong and specific copper(II) chelator would have high p.m.i. values at low drug concentrations, which would indicate a potentially useful therapeutic agent.

## 5.4 RESULTS AND DISCUSSION

The bio-distribution results are given in Table 5.1(a & b). The readings were corrected for background noise and adjusted according to the half-life of  $^{67}\text{Cu}$  since the samples were counted at different times. Section (a) of the table shows the degree of copper(II) retention by the body for the various ligands, whereas part (b) indicates into which organs copper(II) has been concentrated.

**Table 5.1 :** (a) Tissue distribution of  $^{67}\text{Cu}$  in white mice for various ligands (% radioactive dose, mean  $\pm$  sdev). Similarly for (b) except the units are in % dose / g of tissue.

(a)		<u>% DOSE</u>		
LIGAND	TIME/hrs	Carcass	Urine	Whole Body
TTDA	6.0	26.41 $\pm$ 4.48	64.31 $\pm$ 5.61	35.69 $\pm$ 5.61
	24.0	20.96 $\pm$ 5.28	72.85 $\pm$ 6.03	27.15 $\pm$ 6.03
SUM	6.0	46.36 $\pm$ 3.85	17.38 $\pm$ 5.57	82.62 $\pm$ 5.57
	24.0	45.60 $\pm$ 4.13	28.85 $\pm$ 3.84	71.15 $\pm$ 3.84
Control	6.0	43.12 $\pm$ 3.35	21.16 $\pm$ 3.86	78.84 $\pm$ 3.86
	24.0	41.54 $\pm$ 6.60	34.44 $\pm$ 7.71	65.56 $\pm$ 7.71
DTDA	# 6.0	13.60 $\pm$ 5.45	70.88 $\pm$ 6.87	29.13 $\pm$ 6.88
	24.0	18.25 $\pm$ 7.30	71.80 $\pm$ 7.63	28.20 $\pm$ 7.63

(b)		<u>% DOSE / g</u>				
LIGAND	TIME/hrs	Whole Body	Blood	Kidney	Liver	Muscle
TTDA	6.0	1.91 $\pm$ 0.37	1.28 $\pm$ 0.79	3.64 $\pm$ 0.59	9.73 $\pm$ 1.63	0.04 $\pm$ 0.09
	24.0	1.59 $\pm$ 0.52	1.40 $\pm$ 0.14	2.31 $\pm$ 0.38	4.50 $\pm$ 1.08	0.02 $\pm$ 0.05
SUM	6.0	4.26 $\pm$ 0.39	4.36 $\pm$ 0.43	7.27 $\pm$ 2.13	35.61 $\pm$ 3.83	0.78 $\pm$ 0.60
	24.0	4.56 $\pm$ 0.61	5.29 $\pm$ 0.66	6.68 $\pm$ 0.47	25.27 $\pm$ 4.64	0.55 $\pm$ 0.17
Control	6.0	4.60 $\pm$ 0.26	4.02 $\pm$ 0.74	6.96 $\pm$ 0.57	36.20 $\pm$ 3.43	0.77 $\pm$ 0.12
	24.0	4.05 $\pm$ 0.61	3.57 $\pm$ 0.93	6.03 $\pm$ 0.90	23.42 $\pm$ 3.27	0.42 $\pm$ 0.17
DTDA	# 6.0	1.64 $\pm$ 0.31	0.15 $\pm$ 0.10	2.27 $\pm$ 0.70	17.68 $\pm$ 2.50	-0.17 $\pm$ 0.15
	24.0	1.70 $\pm$ 0.46	0.53 $\pm$ 0.73	1.60 $\pm$ 0.26	10.05 $\pm$ 1.16	-0.08 $\pm$ 0.05

# Averages and SDEV's are for 4 mice only

Unfortunately the results of the  $^{67}\text{CuCl}_2$  control at 24 hrs do not agree well with the results in fibrosarcoma-bearing mice injected with  $^{64}\text{CuCl}_2$  obtained by Pastakia *et al.* The latter results show much smaller uptake in the liver, kidneys, blood and muscles at 24 hrs. This could however be due to the intraperitoneal, as apposed to intravenous, injection method used in this study resulting in a slow release of radioactivity into the blood. Alternatively hydrolysis of the  $^{67}\text{CuCl}_2$  to colloidal  $^{67}\text{Cu}(\text{OH})_2$  could have occurred prior to injection due to the relatively high pH ( $\approx 7.4$ ) of the solution, which would have been phagocytosed and taken up in the liver.

The results of the control do however compare quite well with those of Owen who studied the bio-distribution of copper in rats injected intravenously with  $^{64}\text{Cu}$ -acetate [163]. Although the clearance rate in mice should be faster by a factor of

$$\left( \frac{\text{weight}_{\text{rat}}}{\text{weight}_{\text{mouse}}} \right)^{0.33}$$

according to McAfee and Subramanian [164], this is probably compensated for by the different means of injection.

The results for the  $^{67}\text{Cu}$ -5UM complex are quite similar to those of the control, i.e. good retention of the radioactive label, as is evidenced by the high whole body and low urine % dose values (Table 5.1(a)). The elevated liver concentrations however support the hypothesis that on injection, the  $^{67}\text{Cu}$ -5UM complex dissociates immediately into its components, indicating a low *in vivo* stability of the complex. The liberated copper(II) ions then follow the normal metabolic pathway of ionic copper. This consists of binding to serum albumin and rapid uptake by the liver, followed by a slow release back into the blood as ceruloplasmin or excretion into the gut as biliary copper [21]. Only a small fraction appears to be eliminated in the urine. Protein binding in the blood would also account for the elevated levels of  $^{67}\text{Cu}$  in the muscle.

Based on the modelling results given in Figure 5.1, which show 5UM to be a far weaker copper(II) mobilizer than DTDA, TTDA or DTPA, by several orders of magnitude, the *in vivo* results are not very surprising. In fact serum stability studies of  $^{67}\text{Cu}$ -DTPA have indicated that the metal is readily transferred, even from this relatively strong chelator, to the plasma protein serum albumin [165].

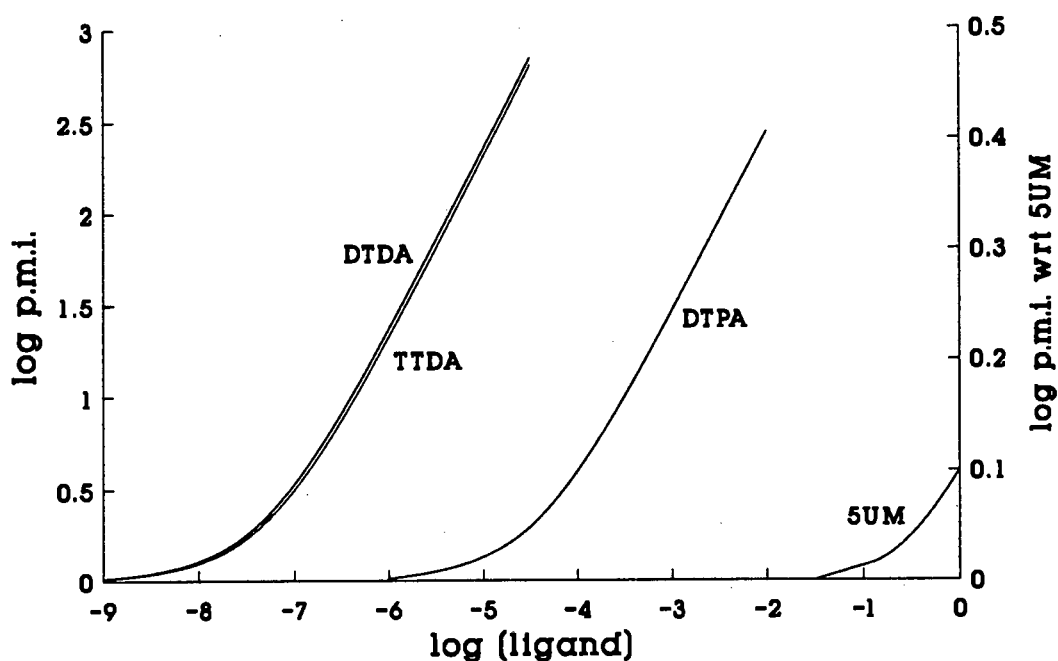


**Figure 5.1 :** Logarithms of the plasma mobilization index of copper(II) for various ligands. The right hand y-axis relates to 5UM only. Calculations were carried out using the updated constants from Jackson and Kelly [41, 161].

In contrast to the results of the copper(II)-5UM complex, the distribution of the  $^{67}\text{Cu}$ -DTDA and TTDA complexes is completely different. The whole body retention is unfortunately quite low even after only 6 hrs post injection as the complexes are rapidly eliminated in the urine with only a small amount of copper excreted via the liver. This is probably due to the fact that although the complexes are uncharged at physiological pH they are presumably too hydrophilic for efficient reabsorption from the urine. In a

previous animal study carried out on rats with adjuvant arthritis, renal excretion of the intensely coloured copper(II) complexes had been observed [42].

As predicted from the speciation modelling results (Figure 5.1), both DTDA and TTDA are quite stable *in vivo*, being able to prevent loss of copper to serum albumin and therefore ultimately to ceruloplasmin. This is indicated by the low levels of  $^{67}\text{Cu}$  in the blood 6 hrs post injection. In this respect the two ligands appear to be not dissimilar to the macrocycle p-nitrobenzyl-TETA which is known to form stable complexes with copper(II) in mice [156, 165], but undergoes even more rapid renal elimination due to being charged.

Finally the  $^{67}\text{Cu}$ -TTDA complex appears to be more stable *in vivo* than the DTDA complex based on the liver results of these two ligands. Thus the loss in radioactivity with time for TTDA from 9.7 to 4.5%  $\text{g}^{-1}$  corresponds to a whole body loss of about 8%  $\text{g}^{-1}$ . For DTDA the corresponding liver loss is from 17.7 to 10.0%  $\text{g}^{-1}$  and is accompanied by very little change in whole body retention, indicating some loss of  $^{67}\text{Cu}$  to ceruloplasmin.

Future work of interest would be to measure the comparative *in vitro* serum stability of the copper(II)-DTDA and TTDA complexes using the technique described by Cole *et al* [165]. It is however apparent that neither of the three drugs investigated is particularly suitable as an injected anti-arthritic agent. This is clearly the case for the administration of copper by injection of the complexes copper(II)-TTDA and DTDA. Whilst they are sufficiently stable to avoid breakdown in the low pH environment of the stomach, oral administration of these complexes would suffer the same fate of rapid renal excretion.

In contrast, as is evident from the speciation diagram in Figure 3.8, the copper(II)-SUM complexes are not formed below pH 4.5 and hence are not suitable for oral administration. However, topical application at the sites of inflammation, might be a

viable proposition in the case of this ligand. At a pH > 8 most of the copper would be present as the uncharged SUM complex, allowing for absorption through the skin in a manner similar to that reported by Walker *et al* [27]. Once in the body, the copper(II) ion would be readily given up due to the low stability of the complex. This would increase the labile body pool of copper(II) which could then elicit the desired anti-arthritis response. Topical application of the copper(II)-TTDA and DTDA complexes is not expected to be successful as they are quite polar and would therefore not easily perfuse through the skin.

**CHAPTER SIX**  
**CONCLUDING REMARKS**

The aim of this thesis was not to investigate the pathogenesis of RA nor to contribute to the on-going discussion of the aetiology of this disease, but rather to try and develop a series of copper(II) mobilizing agents which might be of use in the treatment of Rheumatoid inflammation. Although copper(II) is undoubtedly involved in the progression of this disease, we are making the assumption that control of the speciation of this metal at the site of inflammation can be of some use in the treatment of RA. This assumption is not altogether uncontentious, but we believe that the benefits of copper(II) administration have been sufficiently demonstrated to justify this line of research. Thus this thesis describes the steps that are required in an idealized approach for the development of new drugs, in particular copper(II) mobilizing agents.

Having determined a series of likely *in vivo* copper(II) mobilizing agents based on the computer modelling study of Jackson and Kelly [24] as well as taking into account the observations of Frausto da Silva and Williams [43] (see section 2.3), an unusual order of stability was obtained from the potentiometric results. Thus for the first time a system forming three contiguous 5-membered chelate rings with copper(II) was found to be substantially more stable than those which form the 5,6,5 or 6,5,6-membered configurations (see section 3.6).

In order to explain this anomalous stability pattern these systems were investigated by other experimental techniques. An attempt was made to account for the potentiometric observations by determining the actual structures of the complexes in solution using UV/VIS spectrophotometry. However, since there are several species present in solution at any given pH (see, for example, Figure 3.15) a mathematical evaluation of absorbance versus pH data was required (see section 3.5.2). Using this the actual structures of the complexes in solution were successfully determined (see section 3.6). However, as similar structures were formed by each of the ligands, this investigation could not be used on its

own to explain the apparently anomalous order of stability, referred to in the previous paragraph.

Accordingly, having determined the actual structures of the complexes in solution, molecular mechanics modelling was used to calculate the strain energies of the various species. By applying a novel approach in which the differences in strain energy on complexation were determined, the order of stability was then successfully explained. Thus it was shown that molecular mechanics calculations can be used to rationalize the stability of related complexes (see section 4.4).

Finally speciation modelling of blood plasma was found to be useful in order to explain the *in vivo*  $^{67}\text{Cu}$  tissue distribution results, obtained for the copper(II)-5UM complex in the animal experiments (see section 5.4). These computer simulations have however, to be used with caution as they do not take into account other factors such as hydrophilicity of the complexes. Thus the simulations could not predict the observed rapid urinary excretion of the stable and formally uncharged copper(II)-TTDA and DTDA complexes. Hence, it became evident only after the tissue distribution studies that neither of the three ligands investigated would be suitable as injected anti-inflammatory copper(II) mobilizers.

The 5UM complex may however be of some use as a topically applied anti-arthritis agent and therefore further studies should be directed along these lines. Alternatively, another interesting series of diamino diamide ligands is one in which the amide functional groups occupy the terminal positions, i.e. the series of ligands 5DH, 6DH and 656DH. Although the first of these ligands has not been studied, the latter two are known to be good complexors of copper(II) [103, 166]. Thus their potential as anti-inflammatory agents should be investigated in a study similar to the one presented in this thesis.

In addition preliminary potentiometric results have shown that the dioximo diamide ligand, analogous to 5UM and able to form a similar contiguous 5-membered ring system, is a very strong copper(II) chelator over a wide pH range. This is presumably due to the terminal oxime groups sharing a proton by hydrogen bonding on complexation, thus conferring macrocyclic like stability on the complex. The ligand however, loses three protons on complexation with copper(II), namely one oxime and two amide protons, which results in a negatively charged complex. This problem could be eliminated by replacing one of the amide groups by an amine, thereby again forming an uncharged complex which could be a potentially useful *in vivo* copper(II) mobilizer. This is therefore a further area of investigation.

In conclusion, although this thesis has not lead to the successful development of a new anti-arthritis agent for use in the treatment of RA, it is hoped that it has contributed to the understanding of some of the aspects and problems involved in such a project. Furthermore, apart from introducing some new ideas that can be successfully applied in the field of solution chemistry, it is hoped that this thesis has clearly outlined the approach to be followed in the development of new metal ion based drugs. This approach can be summarized by the following steps: 1. computer assisted design of potential ligands, 2. *in vitro* experimental evaluation in the laboratory, 3. speciation modelling of blood plasma and 4. *in vivo* verification by animal experiments.

## APPENDIX A : LIGAND SYNTHESIS

All starting materials were purified by distillation and checked by boiling point and proton NMR. Organic solvents were similarly purified and invariably had to be dried by standard methods. Dry HCl gas was generated by dropping conc. HCl into conc. H<sub>2</sub>SO<sub>4</sub> using a capillary system. All ligands whether synthesized in this study or obtained from other sources, were checked for purity by micro analysis, as well as proton and carbon-13 NMR. NMR spectra were recorded on a Varian VXR 200 spectrometer. Only the NMR results of selected ligands are presented here.

Essentially two relatively straightforward synthetic routes exist for the synthesis of this series of compounds, i.e. reaction of the N,N-dialkyl diamines with either the acyl chlorides or with the corresponding esters. Due to availability of the esters the latter approach was used throughout this study.

No mechanistic precautions against further substitution reactions needed to be taken as the amino precursors were all completely alkylated at one end. However only in one instance, i.e. in the case of N,N'-bis [3-(dimethylamino)propyl] ethanediamide, could the desired product be isolated. Due to the extremely hygroscopic nature of the other ligands, sometimes only obtainable in the form of an oil, these were reacted further to give their corresponding hydrochlorides. The hydrochlorides were also severely hygroscopic but were at least obtained as solids that could be purified sufficiently for the purposes of the potentiometric investigations.

### **A1. N,N' bis [2-(dimethylamino)ethyl] propanediamide (6UM)**

3.21 g diethylmalonate (0.020 mole) was slowly added to 3.78 g N,N-dimethyl ethylenediamine (0.043 mole) and stirred under high purity nitrogen for 3 hours at 80°C.

The volume of the dark pink reaction mixture was then reduced on a rotary evaporator at a temperature of about 50°C thereby removing unreacted amine and the by-product ethanol. On allowing the reaction mixture to cool to room temperature, white radiating crystals in a hard pink matrix formed almost immediately. These were taken up in dry THF, the solution titrated with n-hexane and left to stand overnight, resulting in the formation of conglomerate, needle-shaped crystals. These were found to be very hygroscopic and it was thus decided to convert the product to its hydrochloride.

The supernatant was decanted and the crystals dissolved in dry THF. Dry HCl gas was slowly bubbled through this solution, resulting in the formation of a hard white precipitate. This was filtered off under nitrogen and recrystallized from a hot mixture of dry methanol and absolute ethanol titrated with THF. The large opaque crystals thus formed were washed with absolute ethanol followed by THF, and dried under high vacuum and stored over P<sub>2</sub>O<sub>5</sub>.

Microanalysis :	C	H	N
Calc. for C <sub>11</sub> H <sub>24</sub> O <sub>2</sub> N <sub>4</sub> •2HCl :	41.6%	8.2%	17.7%
Found :	41.6%	8.0%	17.6%

Spectral data : The proton NMR of the ligand was run in D<sub>2</sub>O. The following chemical shifts (ppm) are given relative to dioxane at  $\delta = 3.55$  ppm.

2.72 (12H, s, CH<sub>3</sub>); 3.11 (4H, t,  $J = 6.0$  Hz, MeNCH<sub>2</sub>); 3.17 (2H, s, COCH<sub>2</sub>CO) and 3.42 (4H, t,  $J = 6.1$  Hz, CONHCH<sub>2</sub>)

The methylene assignments were done by analogy with the ligands 6UE and 656UM (see below). The singlet for the central methylene protons was observed to undergo slow deuterium exchange with the solvent.

## A2. N,N' bis [2-(diethylamino)ethyl] propanediamide (6UE)

3.2 g diethylmalonate (0.02 mole) was added to 5.1 g N,N-diethyl ethylenediamine (0.044 mole) and stirred under nitrogen for about 40 hours at 70 to 80°C. Even though the volume of the pink reaction mixture was reduced first on a rotary evaporator at about 60°C and then under high vacuum at 50°C, the product could only be isolated as a viscous oil and was therefore converted directly to the hydrochloride.

The conversion to and subsequent isolation of the hydrochloride product posed many more problems than in the synthesis of the previous ligand. The oil was taken up in dry THF and HCl gas allowed to bubble slowly through the solution. A rather sticky, pale yellow precipitate was formed with the evolution of much heat. This could however not be recrystallized from a number of dry organic solvents, reverting in each case to a yellow oil. Eventually recrystallization from very dry MeCN, titrated with THF, was successful, resulting in a chunky white precipitate. This was filtered off under nitrogen, washed with THF and dried under high vacuum over P<sub>2</sub>O<sub>5</sub>. The percentage yield obtained was 81%. The product is quite hygroscopic.

Microanalysis :	C	H	N
Calc. for C <sub>15</sub> H <sub>32</sub> O <sub>2</sub> N <sub>4</sub> •2HCl :	48.3%	9.1%	15.02%
Found :	48.0%	9.0%	15.1%

Spectral data : The proton and carbon-13 NMR of the ligand were initially run in D<sub>2</sub>O. However, a signal for the protons of the central methylene group, expected at about  $\delta = 3.1$  ppm cf. the previous ligand, was not observed (see Figure A2.1a). Furthermore, only 5 of the expected 6 signals were apparent in the carbon-13 NMR. The NMR were thus rerun in CDCl<sub>3</sub>, a problem due to low ligand solubility, whereupon the proton and carbon-13

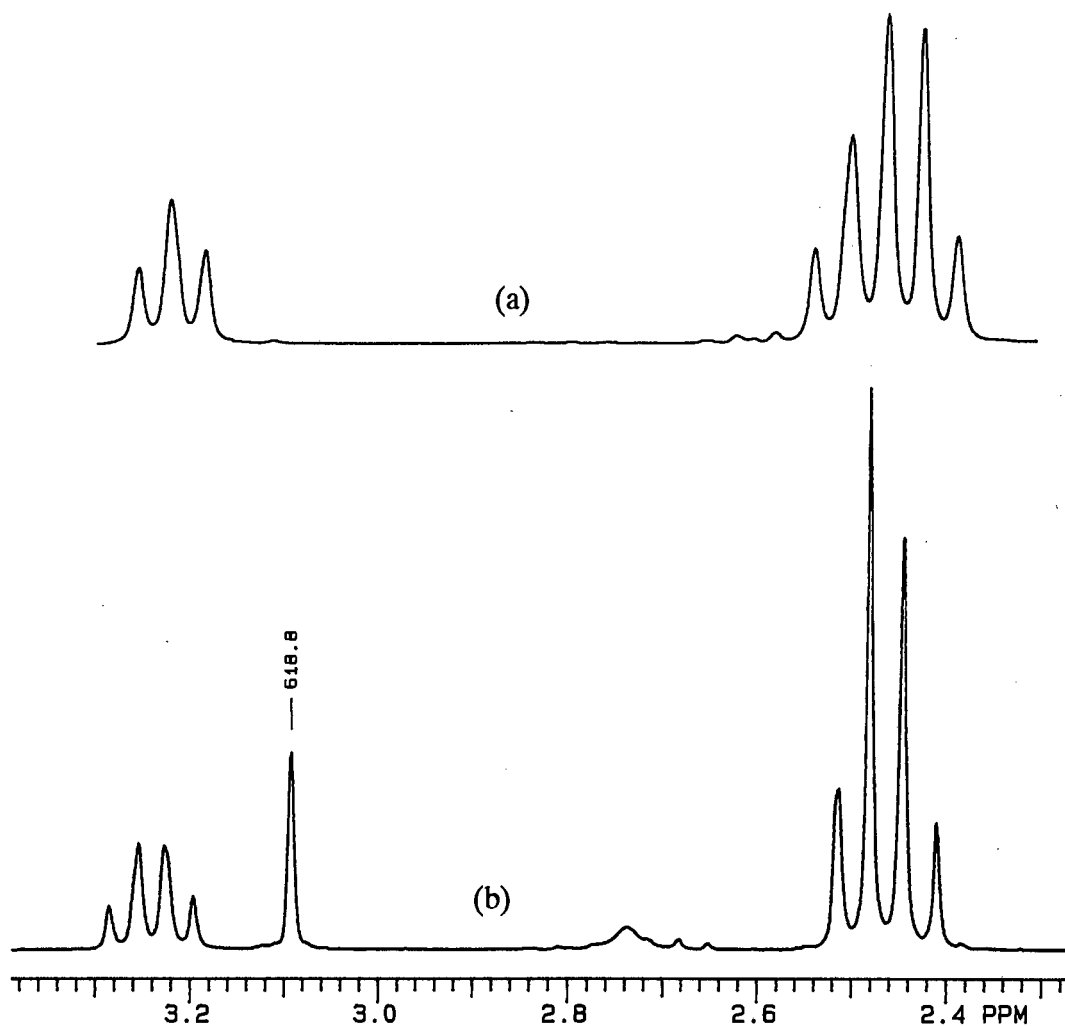


**Figure A2.1** : Comparison of the proton NMR of 6UE in D<sub>2</sub>O (a) and CDCl<sub>3</sub> (b) showing only the region in which the signals due to the methylene protons appear. The singlet at  $\delta = 3.09$  ppm in the CDCl<sub>3</sub> spectrum is assigned to the COCH<sub>2</sub>CO protons (see text).

spectra showed all the expected signals as can be seen in Figures A2.1(b) and A2.2 respectively. This suggests that deuterium exchange of the methylene protons may have occurred. The carbon-13 NMR was furthermore run in H<sub>2</sub>O. This gave a spectrum very similar to that obtained in CDCl<sub>3</sub>, showing all 6 signals as expected. By running the carbon-13 NMR in D<sub>2</sub>O immediately after dissolution of the ligand as well as at various

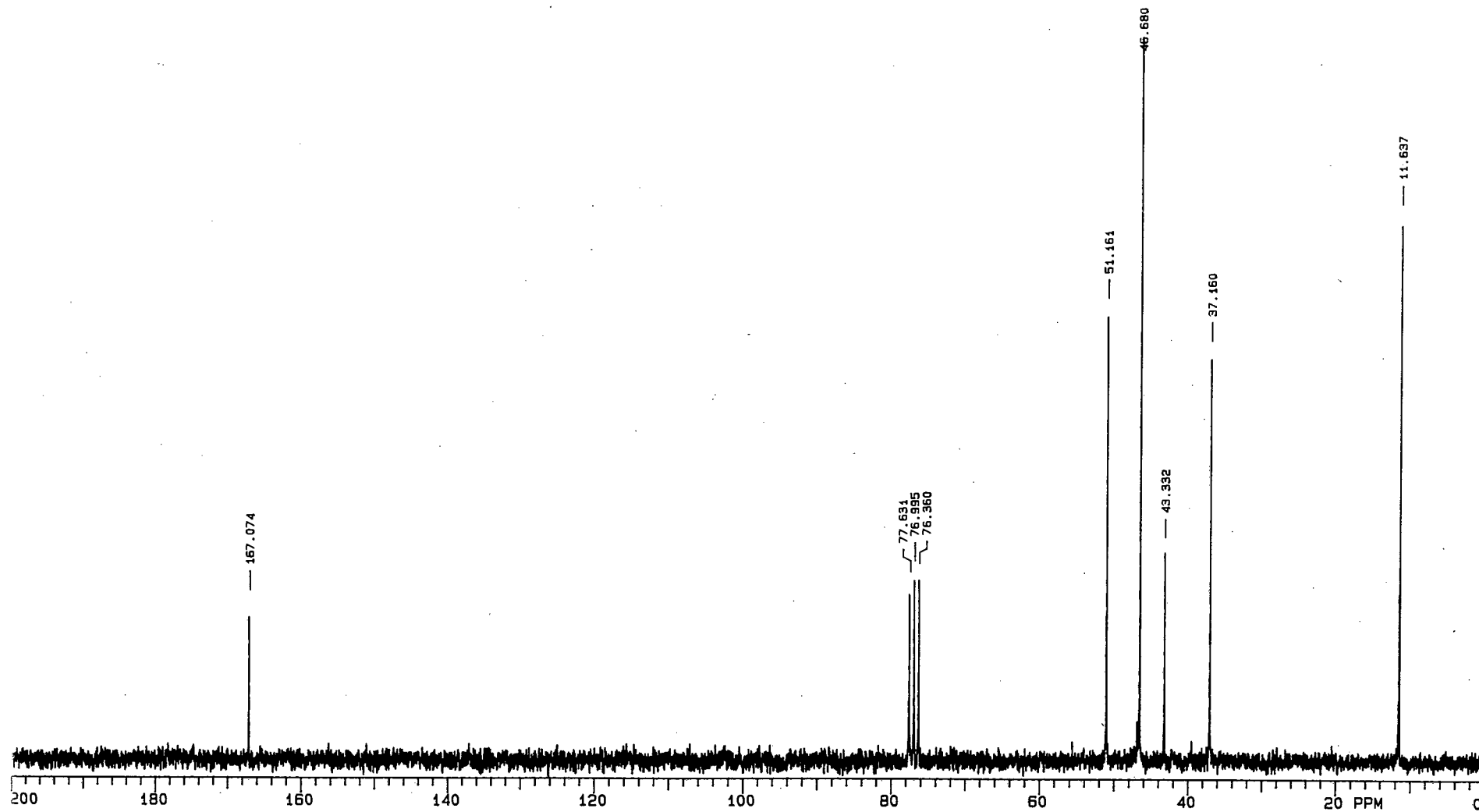


**Figure A2.2** : Carbon-13 NMR of 6UE in  $\text{CDCl}_3$  showing all the expected signals. The signal at  $\delta = 43.3$  ppm is assigned to the methylene carbon  $\text{COCH}_2\text{CO}$  and decays with time in  $\text{D}_2\text{O}$ . See text for other assignments.

intervals thereafter, the decrease in the intensity of the methylene signal with time was clearly observed, which is further evidence for deuterium exchange. The central methylene hydrogens are thus quite labile, undergoing keto-enol tautomerism with the amide groups and subsequent proton abstraction by the basic amine nitrogens.

Finally, as can be seen from Figure A2.1, on running the spectrum in  $\text{CDCl}_3$ , deuterium exchange of the amide protons also no longer takes place resulting in further splitting of the triplet at  $\delta = 3.24$  ppm into a doublet of triplets.

Thus the following proton chemical shifts (ppm) are given relative to  $\text{CDCl}_3$  at  $\delta = 7.24$  ppm.

.95 (12H, t,  $J = 7.1$  Hz,  $\text{CH}_3$ ); 2.43 (12H, t + q,  $\text{MeCH}_2\text{NCH}_2$ ); 3.09 (2H, s,  $\text{COCH}_2\text{CO}$ ) and 3.24 (4H, d of t,  $\text{CONHCH}_2$ )

The following carbon-13 chemical shifts (ppm) are given relative to  $\text{CDCl}_3$  at  $\delta = 77.0$  ppm.

11.6 ( $\text{CH}_3$ ); 37.2 ( $\text{CH}_2$ ); 43.3 ( $\text{COCH}_2\text{CO}$ ); 46.7 ( $\text{MeCH}_2$ ); 51.2 ( $\text{CH}_2$ ) and 161.7 (CO)

Further NMR experiments to definitively assign the methylene signals at  $\delta = 37.2$  and 51.2 ppm were not carried out.

**A3. N,N' bis [2-(dimethylamino)ethyl] - and N,N' bis [2-(dimethylamino)ethyl] ethanediamide (5UM and 5UE)**

The hydrochloride derivatives of these two ligands were synthesized as part of K. Voyi's Ph.D thesis [167]. Their purities were determined by NMR and micro analysis.

Microanalysis :	C	H	N
Calc. for $C_{10}H_{22}O_2N_4 \cdot 2HCl$ :	39.6%	7.9%	18.5%
Found :	39.4%	7.7%	18.5%

Microanalysis :	C	H	N
Calc. for $C_{14}H_{30}O_2N_4 \cdot 2HCl$	46.8%	9.0%	15.6%
Found :	47.0%	9.0%	15.6%

The compounds were used without further purification.

**A4. N,N' bis [2-(dimethylamino)propyl] ethanediamide (656UM)**

4.2 g N,N-dimethyl propylenediamine (0.041 mole) was added dropwise to 2.9 g diethyloxalate (0.02 mole) in 15 ml dry THF with the evolution of some heat. The solution was stirred and allowed to reflux under nitrogen for about 24 hours at 65°C. The volume of the pale yellow solution was then reduced to dryness on a rotary evaporator whereupon a bulky white precipitate formed. This was eventually recrystallized from cold n-hexane being very soluble in water and most other organic solvents. The product is not hygroscopic and it was therefore decided to use the ligand in this form. The percentage yield was greater than 90%.

Microanalysis :	C	H	N
Calc. for C <sub>12</sub> H <sub>26</sub> O <sub>2</sub> N <sub>4</sub> :	55.8%	10.1%	21.7%
Found :	55.2%	10.4%	21.7%

**Spectral data** : The proton NMR of the ligand was run in D<sub>2</sub>O. The following chemical shifts (ppm) are given relative to dioxane at  $\delta = 3.55$  ppm.

1.69 (4H, t of t, CH<sub>2</sub>CH<sub>2</sub>CH<sub>2</sub>); 2.14 (12H, s, CH<sub>3</sub>); 2.32 (4H, dist. t, MeNCH<sub>2</sub>) and 3.25 (4H, t,  $J = 7.0$  Hz, CONHCH<sub>2</sub>)

In order to determine the methylene assignments unequivocally, the proton NMR was rerun with the addition of a small amount of DCl. As expected, this had the effect of shifting all the signals progressively downfield according to their proximity to the positively charged amine nitrogens. Thus the triplets at  $\delta = 2.32$  and 3.25 ppm showed the largest and smallest downfield shifts, .54 and .07 ppm respectively, which allowed the above methylene assignments to be made. The signal at  $\delta = 1.96$  ppm was shifted an intermediate amount of only .18 ppm, which together with its observed multiplicity, provided evidence for its assignment. As expected, the singlet assigned to the protons of the methyl groups, also showed a large downfield shift of .47 ppm.

## APPENDIX B : MOLECULAR MECHANICS FORCE FIELD

### MacroModel - Atom and Bond Type Description and Numbering

---

#### BONDS:

No	Symbol	Description
0	.	Zero order bond
1	-	Single Bond
2	=	Double Bond
3	&	Triple Bond
4	*	Bond of Undefined Order

#### ATOMS:

No	Symbol	Description	MM2 Equivalent
2	C2	C - SP2	2,3
3	C3	C - SP3	1
15	O2	Oxygen - Double Bond	7
25	N2	N - SP2	9
26	N3	N - SP3	8
32	N5	N+ - SP3	39
41	H1	H-Electroneut (e.g. C,S)	5
43	H3	H-N(Neut)	23
44	H4	H-Cation	28
62	Z0	Special Atom to be defined	
63	Lp	Lone Electron Pair	20
64	00	Any Atom	0

Note: 00 atoms stored as type 0 in atom connection table.

Note: All current force fields require explicit hydrogens on heteroatoms.

Allinger MM2(87) Force Field

N.L. Allinger, JACS, 99, 8127 (1977); Parameters from NLA (6/87)

C  
C  
C  
C

Copyright Columbia University 1989  
All rights reserved

C Energy Functions and Conversion Factors in Use

C -----  
-1  
0 STR 2 601.99392  
0 BND 2 601.99392  
0 S-B 1 601.99392  
0 TOR 1 2.09200  
0 IMP 1 60.19939  
0 VDW 4 4.18400  
0 ELE 2 1389.50000  
0 HBD 1 418.40000  
0 V14 4 1.00000  
0 FIX 1 4.18400  
0 HYD 1 0.00000  
0 SEL 1 O Original MM2 Parameters  
0 SEL 1 M Modified MM2 Parameters  
0 SEL 1 A Added parameters  
0 SEL 2 1 High quality parameters  
0 SEL 2 2 Tentative value parameters  
0 SEL 2 3 Low quality parameters  
0 ALT 1 a MM2 hydrocarbon params  
0 ALT 2 b Kroon-Battenburg Lp params  
C END

C Field 1 (Origin): O = Original MM2, M = Modified Parameter, A = Additional Parameter

C Field 2 (Quality): 1 = Final Values, 2 = Tentative Values, 3 = Low Quality Value

C Field 3

C Field 4

C Field 5

C Alternate 001: a = Original MM2, b = Osawa (Tet, 2769 (83)) MM2' modification of C and H parameters.

C Alternate 002: a = Original MM2, b = Kroon-Battenburg (JMolStr, 417 (83)) special Lp-H interaction  
to give proper hydrogen bonding geometries and energies.

C  
C

C Stretching Interactions (STR) Opt. Descriptor Parameter Referencing

C -----  
C Bond Length Constant Bond Moment Atm1 Atm2 Select Altrn  
C (ang) (mdyn/ang) (debye) 1 2 3 4 5 S A Comment  
-2  
1 C3 - C3 1.5230 4.4000 0.0000 0000 0000 O 1 1 a C-C  
1 C3 - C3 1.5260 4.4000 0.0000 0000 0000 M 1 1 b C-C, MM2', Tet, 2769(83)  
1 C3 - H1 1.1130 4.6000 -0.7500 N500 0000 A 2 H-C(-N+), WCS(CU)  
1 C3 - H1 1.1130 4.6000 0.0000 0000 0000 O 1 H-C(sp3)  
1 C2 - C3 1.5090 4.4000 -0.3000 O200 0000 O 1 C-C(=O)  
1 C2 - C3 1.4970 4.4000 -0.3000 0000 0000 O 1 C-C(sp2)  
1 C3 - N2 1.4470 3.5200 1.4700 0000 H300 O 2 C-N(sp2), JCompChem,503(89)  
1 C3 - N2 1.4370 3.5200 1.4700 0000 0000 O 2 C-N(sp2), JCompChem,503(89)  
1 C3 - N3 1.4380 5.1000 0.0400 0000 0000 O 2 C-N(sp3)  
1 C3 - N5 1.4800 5.1000 1.3000 0000 0000 M 1 C-N+(sp3), JACS, 7141(87)  
1 C2 - C2# 1.5200 5.0000 0.0000 O2N2 O2N2 A 1 C(sp2)-C(sp2), WCS(CU), Lo AVoye  
1 C2 - C2 1.3340 9.6000 0.0000 O200 O200 O 2 C(=O)-C(=O)  
1 C2 - C2 1.4700 6.0000 0.0000 0000 O200 M 2 C=C-C=O, JACS, 14(87)  
1 C2 = O2# 1.2440 9.9000 2.8000 N200 0000 O 2 O=C(-N), JCompChem,503(89)

1	C2 = O2	1.2080	10.8000	2.6000	0000 0000	O 1	O=C, ketone/ald
1	C2 - N2#	1.3430	6.4000	-0.2900	0200 0000	O 2	N-C(=O), JCompChem,503(89)
1	C2 - N2	1.3300	6.3000	1.0000	0000 0000	A 2	C(sp2)-N(sp2), enamine, WCS(CU)
1	C2 - N5	1.4800	5.5000	1.3000	0000 0000	A 3	C(sp2)-N+(sp3), WCS(CU)
1	O2 - Lp	0.5000	4.6000	0.6000	0000 0000	A 2	Lp-O(=C), WCS(CU)
1	N3 - Lp	0.6000	6.1000	0.6000	0000 0000	O 2	N(sp3)-Lp
1	N3 - H3	1.0200	6.1000	-0.7600	0000 0000	O 2	N(sp3)-H
1	N2 - H3	1.0220	5.9000	-1.3100	0000 0000	O 2	N(sp2)-H
1	N2 - Lp	0.6000	6.1000	0.6000	0000 0000	A 2	N(sp2)-Lp, WCS(CU)
1	N5 - H4	1.0450	6.1000	-1.6000	0000 0000	A 2	H-N+(sp3), WCS(CU)
1	Z0 * O2	2.0000	0.8900	0.0000	0000 0000	A 3	Cu-O(sp2), according to Drew
1	Z0 * N2	2.0000	0.8900	1.3100	0000 0000	A 3	Cu-N(sp2),
1	Z0 * N5	2.0000	0.8900	1.6000	0000 0000	A 3	Cu-N+(sp3), AVoye

C		Bending Interactions (BND)		Opt. Descriptors					
C		-----		-----					
C		Angle	Bending Constant	Atm1	Atm2	Atm3			
C		(deg)	(mdyn/rad**2)						
-2	2	H1 - C3 - H1	109.4700	0.3200	0000	H1H1	0000	O 1	H-C(H2)-H
	2	H1 - C3 - H1	109.0000	0.3200	0000	H100	0000	O 1	H-C(H)-H
	2	H1 - C3 - H1	109.4000	0.3200	0000	0000	0000	O 1	H-C-H
	2	C3 - C3 - C3	109.5000	0.4500	0000	H1H1	0000	O 1	C-C(H2)-C
	2	C3 - C3 - C3	109.5100	0.4500	0000	H100	0000	O 1	C-C(H)-C
	2	C3 - C3 - C3	109.4700	0.4500	0000	0000	0000	O 1	C-C-C
	2	C3 - C3 - H1	110.0000	0.3600	0000	H1H1	0000	O 1	C-C(H2)-H
	2	C3 - C3 - H1	109.4100	0.3600	0000	H100	0000	O 1	C-C(H)-H
	2	C3 - C3 - H1	109.3900	0.3600	0000	0000	0000	O 1	C-C-H
	2	C2 - C3 - H1	109.4700	0.3700	0200	H1H1	0000	O 1	C(=O)-C(H2)-H
	2	C2 - C3 - H1	108.8000	0.3700	0200	H100	0000	O 1	C(=O)-C(H)-H
	2	C2 - C3 - H1	107.9000	0.3700	0200	0000	0000	O 1	C(=O)-C-H
	2	C2 - C3 - H1	110.0000	0.3600	0000	H1H1	0000	O 1	C(sp2)-C(H2)-H
	2	C2 - C3 - H1	109.4100	0.3600	0000	H100	0000	O 1	C(sp2)-C(H)-H
	2	C2 - C3 - H1	109.3900	0.3600	0000	0000	0000	O 1	C(sp2)-C-H
	2	C2 - C3 - C2	110.2000	0.4700	0200	H1H1	0200	O 2	C(=O)-C(H2)-C(=O)
	2	C2 - C3 - C2	110.5100	0.4700	0200	H100	0200	O 2	C(=O)-C(H)-C(=O)
	2	C2 - C3 - C2	109.4700	0.4700	0200	0000	0200	O 2	C(=O)-C-C(=O)
	2	C2 - C3 - C2	110.2000	0.4700	0000	H1H1	0200	O 2	C(sp2)-C(H2)-C(=O)
	2	C2 - C3 - C2	110.5100	0.4700	0000	H100	0200	O 2	C(sp2)-C(H)-C(=O)
	2	C2 - C3 - C2	109.4700	0.4700	0000	0000	0200	O 2	C(sp2)-C-C(=O)
	2	C2 - C3 - C2	109.5000	0.4500	0000	H1H1	0000	O 1	C(sp2)-C(H2)-C(sp2)
	2	C2 - C3 - C2	109.5100	0.4500	0000	H100	0000	O 1	C(sp2)-C(H)-C(sp2)
	2	C2 - C3 - C2	109.4700	0.4500	0000	0000	0000	O 1	C(sp2)-C-C(sp2)
	2	C3 - C3 - N3	109.5000	0.5700	0000	H1H1	0000	O 2	C-C(H2)-N(sp3)
	2	C3 - C3 - N3	108.8000	0.5700	0000	H100	0000	O 2	C-C(H)-N(sp3)
	2	C3 - C3 - N3	109.4700	0.5700	0000	0000	0000	O 2	C-C-N(sp3)
	2	C3 - C3 - N2#	109.2800	0.5000	0000	H1H1	0000	O 2	C-C(H2)-N(sp2), JCompChem,503(89)
	2	C3 - C3 - N2#	110.7800	0.5000	0000	H100	0000	O 2	C-C(H)-N(sp2), JCompChem,503(89)
	2	C3 - C3 - N2	109.2800	0.5000	0000	0000	0000	O 2	C-C-N(sp2), JCompChem,503(89)
	2	N3 - C3 - H1	108.8000	0.5000	0000	0000	0000	O 2	N(sp3)-C-H
	2	N2 - C3 - N2	110.0000	1.0500	0000	0000	0000	A 2	N(sp2)-C-N(sp2)
	2	N2 - C3 - H1	109.0000	0.4200	0000	0000	0000	O 2	N(sp2)-C-H
	2	C3 - C3 - N5#	109.2800	0.5700	0000	H1H1	0000	O 2	C-C(H2)-N+(sp3), AVoye
	2	C3 - C3 - N5#	109.2800	0.5700	0000	H100	0000	O 2	C-C(H)-N+(sp3),
	2	C3 - C3 - N5#	109.2800	0.5700	0000	0000	0000	O 2	C-C-N+(sp3),
	2	N5 - C3 - H1	108.8000	0.5000	0000	0000	0000	O 2	H-C-N+(sp3)
	2	C3 - C2 = O2	122.5000	0.4600	0000	0000	0000	O 1	O=C-C same as 1-3-7 MH2
	2	C2 - C2 = O2	123.0000	0.4600	0000	0000	0000	O 2	O=C-C(sp2)



4	N3 - C3 - C3 - H1	-0.1500	0.0000	0.1500	0000	0000	0000	0000	0	2	N(sp3)-C-C-H
4	N2 - C3 - C3 - H1	0.0000	0.0000	0.4000	0000	0000	0000	0000	0	2	N(sp2)-C-C-H
4	N5 - C3 - C3 - C3	0.1000	0.4000	0.5000	0000	0000	0000	0000	0	2	N+(sp3)-C-C-C
4	N5 - C3 - C3 - H1	-0.1500	0.0000	0.1500	0000	0000	0000	0000	0	2	N+(sp3)-C-C-H
4	N3 - C3 - C3 - N3#	0.0000	0.0000	0.3500	0000	0000	0000	0000	0	2	N(sp3)-C-C-N(sp3), A Voyer
4	O2 = C2 - C3 - H1	0.0000	0.0000	0.0000	0000	0M00	0000	0000	A	2	O=C(-OH)-C-H, WCS(CU)
4	O2 = C2 - C3 - H1	-0.1670	0.0000	-0.1000	0000	0000	0000	0000	0	1	O=C-C-H
4	N2 - C2 - C3 - H1	0.0000	0.0000	0.4000	0000	0200	0000	0000	0	2	N-C(=O)-C-H
4	N2 - C2 - C3 - H1	0.0000	0.0000	0.2500	0000	0000	0000	0000	A	2	N(sp2)-C(sp2)-C-H, WCS(CU)
4	O2 = C2 - C3 - C2	0.0000	0.0000	-0.3500	0000	0000	0000	0000	0	2	O=C-C-C(sp2)
4	H1 - C3 - N3 - C3	0.0000	0.0000	0.5200	0000	0000	0000	0000	0	2	H-C-N(sp3)-C
4	C3 - C3 - N3 - C3	-0.2000	0.7300	0.8000	0000	0000	0000	0000	0	2	C-C-N(sp3)-C
4	C3 - C3 - N3 - Lp	0.2000	-0.2200	0.1000	0000	0000	0000	0000	0	2	C-C-N(sp3)-Lp
4	C3 - C3 - N3 - H3	0.0000	0.1200	0.1000	0000	0000	0000	0000	0	2	C-C-N(sp3)-H
4	H1 - C3 - N3 - H3	0.0000	0.0000	0.2500	0000	0000	0000	0000	0	2	H-C-N(sp3)-H
4	C3 - C3 - N5 - C3	-0.2000	0.4500	0.8000	0000	0000	0000	0000	M	2	C-C-N(+)-C, JACS, 7141(87)
4	H1 - C3 - N5 - C3	0.0000	0.0000	0.5200	0000	0000	0000	0000	0	2	H-C-N(+)-C
4	C3 - C2 - N2 - H3	0.0000	5.0000	0.0000	0000	0200	0000	0000	0	2	C-C(=O)-N-H, Amide
4	O2 = C2 - N2 - H3	1.1000	5.0000	0.0000	0000	0000	0000	0000	0	2	O=C-N-H, Amide
4	O2 = C2 - N2 - C3	0.0000	5.0000	0.0000	0000	0000	0000	0000	0	2	O=C-N-C, Amide
4	C3 - C2 - N2 - C3	1.1000	5.0000	0.0000	0000	0200	0000	0000	0	2	C-C(=O)-N-C, Amide
4	C2 - C2 - N2 - C3	0.0000	5.0000	0.0000	0000	0200	0000	0000	A	2	C(sp2)-C(=O)-N-C, WCS(CU)
4	C3 - C3 - N2 - H3	0.0000	0.0000	0.9100	0000	0000	0000	0000	0	2	C-C-N(sp2)-H
4	H1 - C3 - N2 - C2	0.0000	0.0000	0.0000	0000	0000	0000	0200	0	2	C-C-N-C(=O), JCompChem, 503(89)
4	H1 - C3 - N2 - H3	0.0000	0.0000	0.1600	0000	0000	0000	0000	0	2	H-C-N(sp2)-H
4	C3 - C3 - N2 - C2	0.0000	0.0000	0.0000	0000	0000	0000	0200	0	2	C-C-N-C(=O), JCompChem, 503(89)
4	C3 - C3 - N5 * Z0	-0.2000	0.4500	0.8000	0000	0000	0000	0000	A	3	analogous to C3-C3-N5-C3
4	H1 - C3 - N5 * Z0	0.0000	0.0000	0.5200	0000	0000	0000	0000	A	3	anal. to H1-C3-N5-C3
4	C3 - C3 - N2 * Z0	0.0000	0.0000	0.4000	0000	0000	0000	0000	A	3	anal. to 00-C3-N2-00
4	H1 - C3 - N2 * Z0	0.0000	0.0000	-0.2000	0000	0000	0000	0000	A	3	anal. to H1-C3-N2-C3
4	C3 - C2 - N2 * Z0	1.1000	5.0000	0.0000	0000	0000	0000	0000	A	3	anal. to C3-C2-N2-C3
4	C2 - C2 - N2 * Z0	0.0000	5.0000	0.0000	0000	0000	0000	0000	A	3	anal. to C2-C2-N2-C3
4	O2 * C2 - N2 * Z0	0.0000	5.0000	0.0000	0000	0000	0000	0000	A	3	anal. to O2=C2-N2-C3
4	00 - C2 = O2 - Z0	0.0000	10.0000	0.0000	0000	0000	0000	0000	A	2	anal. to *C(sp2)=O(sp2)*, WCS(CU)
4	O2 = C2 - N2 - 00	0.0000	4.5000	0.0000	0000	0000	0000	0000	A	3	-C(=O)-N(sp2)-
4	00 - C3 - N3 - Lp	0.0000	0.0000	0.0000	0000	0000	0000	0000	0	2	-C-N(sp3)-Lp
4	00 - C3 - N2 - Lp	0.0000	0.0000	0.0000	0000	0000	0000	0000	0	2	-C-N(sp2)-Lp
4	00 - C3 - C3 - 00	0.0000	0.0000	0.3500	0000	0000	0000	0000	A	3	-C(sp3)-C(sp3)-
4	00 - C2 - C3 - 00	0.0000	0.0000	0.2000	0000	0000	0000	0000	A	3	-C(sp2)-C(sp3)-
4	00 * C2 - C2 * 00	0.0000	1.2500	0.0000	0000	0000	0000	0000	A	3	*C(sp2)-C(sp2)*
4	00 - C2 - N2 - 00	0.0000	4.5000	0.0000	0000	0200	0000	0000	A	3	-C(=O)-N(sp2)-
4	00 * C2 - N2 * 00	0.0000	2.5000	0.0000	0000	0000	0000	0000	A	3	*C(sp2)-N(sp2)*
4	00 - C3 - N3 - 00	0.0000	0.0000	0.3500	0000	0000	0000	0000	A	3	-C(sp3)-N(sp3)-
4	00 - C3 - N2 - 00	0.0000	0.0000	0.4000	0000	0000	0000	0000	A	3	-C(sp3)-N(sp2)-
4	00 - C3 - N5 - 00	0.0000	0.0000	0.5000	0000	0000	0000	0000	A	3	-C(sp3)-N+(sp3)-
4	00 - 00 * Z0 * 00	0.0000	0.0000	0.0000	0000	0000	0000	0000	A	3	
4	00 = 00 * Z0 * 00	0.0000	0.0000	0.0000	0000	0000	0000	0000	A	3	
4	00 * C1 & C1 * 00	0.0000	25.0000	0.0000	0000	0000	0000	0000			Dummy maximum limit barrier

C	Out of Plane Bending	Angle	Const.	Opt. Descriptor	Atm1	Atm2	Atm3	Atm4		
-2										
5	C2 * O2 * 00 * 00	0.0000	0.8000		0000	0000	0000	0000	0	1
5	C2 * 00 * 00 * 00	0.0000	0.0500		0000	0000	0000	0000	0	1
5	N2 * H3 * 00 * 00	0.0000	0.0100		0000	0000	0000	0000	0	1
5	N2 * 00 * 00 * 00	0.0000	0.0500		0000	0000	0000	0000	0	1
5	Z0 * 00 * 00 * 00	0.0000	0.1000		0000	0000	0000	0000	A	3

AVoyer

Van der Waals Interactions				Opt. Descriptor		
Radius	Eps	Offset	Charge	Atm1 Lp		
(ang)	(kcal/mole)	(ang)				
-6						
C2	1.9400	0.0440	0.0000	0200	O 1	
C2	1.9400	0.0440	0.0000	0000	O 1	
C3	1.9000	0.0440	0.0000	0000	O 1	1 a
C3	2.0000	0.0440	0.0000	0000	M 1	1 b Osawa MM2', Tet, 2769(83)
H1	1.5000	0.0470	-0.0850	0000	O 1	1 a
H1	1.4260	0.0470	-0.0850	0000	M 1	1 b Osawa MM2', Tet, 2769(83)
H3	1.3250	0.0340	0.0000	0000	O 2	
H4	1.2000	0.0360	0.0000	0000	A 2	WCS(CU)
O2	1.7400	0.0660	0.0000	0000	O 1	
N2	1.8200	0.0550	0.0000	0000	O 1	
N3	1.8200	0.0550	0.0000	0000 Lp	O 1	
N5#	1.8200	0.0550	0.0000	0.0000	A 2	WCS(CU)
Lp	1.2000	0.0160	0.0000	0000	O 1	
Z0	2.3500	0.0165	0.0000	0000	A 3	according to Drew

END OF NONBONDED INTERACTIONS

Special Van der Waals Interactions				Opt. Descriptor		
Radius	Eps	Atm1 Atm2				
(ang)	(kcal/mole)					
-2						
6 C3 H1	3.3400	0.0460	0000 0000	O 1	Special C3-H1 part of MM2	
6 H3 Lp	2.5250	0.0233	0000 0000	O 1	2 a	
6 H3 Lp	2.4900	0.0187	0000 0000	A 2	2 b LKB (JMolStr,417(83)) HBonding	

Hydrogen Bond Interactions (function and params from AMBER modified for Lp-containing oxygens)						
Acceptor Donor	C/100	D/100	Atm1 Atm2 Atm3 Atm4			
-2						
7 H3 O2	42.5000	10.0000	0000	0000		
7 H4 O2	46.7500	11.0000	0000	0000		

Special Substructures						
Square Planar Tridentate Copper Amide						
N2-Z0(-N5)-N2						
-2						
2 1 2 3	180.0000	0.3000	0000	0000	0000	
2 1 2 4	90.0000	0.3000	0000	0000	0000	
2 3 2 4	90.0000	0.3000	0000	0000	0000	

Square Planar Copper Amide						
N2-Z0(-N5)(-N5)-N2						
-2						
2 1 2 5	90.0000	0.3000	0000	0000	0000	

2	1	2	3	90.0000	0.3000	0000 0000 0000
2	1	2	4	180.0000	0.3000	0000 0000 0000
2	3	2	5	180.0000	0.3000	0000 0000 0000
2	4	2	5	90.0000	0.3000	0000 0000 0000
2	3	2	4	90.0000	0.3000	0000 0000 0000

-3

C Square Planar Copper Tetra Amine

9 N5-E0(-N5)(-N5)-N5

-2

2	1	2	5	180.0000	0.3000	0000 0000 0000
2	1	2	3	90.0000	0.3000	0000 0000 0000
2	1	2	4	90.0000	0.3000	0000 0000 0000
2	3	2	5	90.0000	0.3000	0000 0000 0000
2	4	2	5	90.0000	0.3000	0000 0000 0000
2	3	2	4	180.0000	0.3000	0000 0000 0000

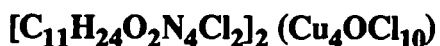
C

C

C NOTE : A # indicates interactions with altered parameters c/o the MM2 force-field  
 C supplied with MacroModel. See text for original values.

## APPENDIX C : CRYSTAL STRUCTURE DETERMINATION

### C1. Experimental Details, Solution and Refinement of the Structure



Red crystals of  $[\text{C}_{11}\text{H}_{24}\text{O}_2\text{N}_4\text{Cl}_2]_2 (\text{Cu}_4\text{OCl}_{10})$  were prepared by Dr K. Voyi by slow diffusion of chloroform into an aqueous solution of 6UM and copper(II) chloride.

Microanalysis :	C	H	N
Calc. for $\text{C}_{22}\text{H}_{48}\text{O}_5\text{N}_8\text{Cl}_{14}\text{Cu}_4$ :	21.05%	3.85%	8.9%
Found :	21.0%	4.0%	8.8%

#### C1.1 Crystal and Diffraction Data

Preliminary investigations were made by taking oscillation and Weissenberg photographs which provided the cell dimensions and showed the crystal to be monoclinic. Accurate X-ray diffraction data were then obtained using an Enraf-Nonius CAD4 diffractometer with graphite monochromated Mo- $K_{\alpha}$  radiation ( $\lambda = 0.7107 \text{ \AA}$ ). The intensities were collected at room temperature with an  $\omega - 2\theta$  scan and variable scan width. The data were corrected for absorption. Systematic absences of the reflections  $h k l$  with  $h + k$  odd and  $h 0 l$  with  $l$  odd indicated the presence of a c-glide plane perpendicular to the unique axis  $b$  which implies the space group to be either  $Cc$  or  $C2/c$ .

#### C1.2 Structure Solution and Refinement

The structure was solved by Patterson and difference Fourier heavy-atom direct methods using SHELXS-86 [168]. Inspection of the statistics of a Patterson determination indicated the crystal to be centric, establishing the space group as  $C2/c$ . Refinement was carried out by full-matrix least-squares techniques using SHELX-76 [169] with anisotropic thermal parameters for all non-hydrogen atoms except for the oxygen and chlorine atoms

lying on special positions. The thermal parameters of these atoms were fixed according to the method of Peterse and Palm [170]. The methyl hydrogens were treated as a rigid group whereas the methylene and amide hydrogens were placed in calculated positions, all with a single temperature factor. A weighting scheme was applied in the final refinement with the function  $w$  being adjusted to give constant variances with  $\sin \theta$  and  $|F_o|$ . Refinement converged at  $R = 0.049$  and  $R_w = 0.059$  with the average parameter shift less than 0.05 of the corresponding estimated standard deviations. The crystal data and full experimental details, together with parameters for the solution and final refinement of the structure, are given in Table C1.

**Table C1** : Summary of the crystal data, together with details of the data collection and the final refinement parameters for the structure determination of  $[\text{C}_{11}\text{H}_{24}\text{O}_2\text{N}_4\text{Cl}_2]_2 (\text{Cu}_4\text{OCl}_{10})$ .

*Crystal data*

Molecular formula	: $\text{C}_{22}\text{H}_{48}\text{O}_5\text{N}_8\text{Cl}_{14}\text{Cu}_4$
Molecular weight /g mol <sup>-1</sup>	: 1255.2
Crystal system	: Monoclinic
Space group	: C2/c
$a/\text{\AA}$	: 14.405(2)
$b/\text{\AA}$	: 15.805(2)
$c/\text{\AA}$	: 20.644(5)
$\beta/^\circ$	: 99.61(2)
$V/\text{\AA}^3$	: 4634(2)
Z	: 4
$D_c/\text{g cm}^{-3}$	: 1.799
$\mu(\text{Mo-K}\alpha)/\text{cm}^{-1}$	: 25.5
F(000)	: 2520

*Data collection*

Crystal dimensions /mm	: $0.28 \times 0.40 \times 0.43$
Scan mode	: $\omega - 2\theta$
Scan width / $^\circ$	: $(0.90 + 0.35 \tan\theta)$
Aperture width /mm	: $(1.13 + 1.05 \tan\theta)$
$\theta$ Range scanned / $^\circ$	: 1 – 25
Range of $h, k, l$	: $-17 \leq h \leq 17; 0 \leq k \leq 18; 0 \leq l \leq 24$

Intensity decay / %	: 5.5
Empirical absorption correction, max / min	: .995 / .939
No. of unique reflections collected	: 3708
No. of observed reflections, N, with $I_{\text{rel}} > 2\sigma(I_{\text{rel}})$	: 3209
<i>Final refinement</i>	
Average parameter shift / e.s.d.	: 0.05
Residual electron density / e Å <sup>-3</sup> (max/min)	: 1.28 / -0.59
No. of parameters, N <sub>p</sub>	: 255
$R = \Sigma   F_o  -  F_c   / \Sigma  F_o $	: 0.049
$R_w = \Sigma \sqrt{w}   F_o  -  F_c   / \Sigma \sqrt{w}  F_o $	: 0.059
Weighting scheme, w	: $1.538 / [\sigma^2(F_o) + 1.163 \times 10^{-3}(F_o)^2]$

---

Complex neutral scattering factors, corrected for anomalous dispersion where applicable, were taken from the International Tables for X-Ray Crystallography [171]. The observed and calculated structure factors are presented at the end of this appendix in section C3. The final atomic coordinates and thermal parameters are listed in Tables C2 and C3 respectively.

**Table C2** : Fractional atomic coordinates ( $\times 10^4$ ) and Thermal Parameters ( $\text{Å}^2 \times 10^3$ ) of the non-hydrogen atoms with estimated standard deviations in parentheses for the structure  $[\text{C}_{11}\text{H}_{24}\text{O}_2\text{N}_4\text{Cl}_2]_2 (\text{Cu}_4\text{OCl}_{10})$ . The atom numbering relates to Figures C1 and C2.

Atom	x/a	y/b	z/c	$U_{\text{iso}}/U_{\text{equiv}}$
Cu(1)	4574( 0)	3176( 0)	1752( 0)	42( 0)
Cu(2)	6027( 0)	4575( 0)	2337( 0)	40( 0)
Cl(1)	7270( 1)	5321( 1)	2110( 1)	50( 1)
Cl(2)	4168( 1)	2355( 1)	867( 1)	61( 1)
Cl(3)	3129( 1)	3956( 1)	1685( 1)	62( 1)
Cl(4)	5738( 1)	3980( 1)	1250( 1)	63( 1)
Cl(5)	5000( 0)	5766( 1)	2500( 0)	66( 1)
Cl(6)	5000( 0)	2062( 1)	2500( 0)	83( 1)
Cl(7)	5219( 1)	9856( 1)	8315( 1)	79( 1)

Cl(8)	4806( 2)	10845( 2)	9416( 1)	94( 1)
O(1A)	5000( 0)	3880( 3)	2500( 0)	31( 1)
C(1)	8354( 6)	7984( 5)	9128( 4)	74( 3)
C(2)	9731( 5)	8902( 5)	9283( 5)	78( 3)
N(1)	8683( 4)	8861( 3)	9238( 3)	53( 2)
C(3)	8429( 4)	9289( 4)	9840( 3)	53( 2)
C(4)	7429( 5)	9184( 4)	9935( 3)	53( 2)
N(2)	6716( 3)	9532( 3)	9410( 2)	45( 2)
C(5)	6547( 4)	10360( 4)	9371( 3)	49( 2)
O(1)	7011( 4)	10899( 3)	9675( 3)	78( 2)
C(6)	5644( 4)	10635( 4)	8897( 3)	53( 2)
O(2)	5258( 5)	12039( 4)	8527( 4)	109( 3)
C(7)	5802( 5)	11471( 4)	8525( 3)	54( 2)
N(3)	6470( 4)	11434( 3)	8169( 3)	62( 2)
C(8)	6672( 5)	12147( 4)	7754( 3)	61( 2)
C(9)	7536( 6)	12600( 5)	7973( 5)	80( 3)
N(4)	7614( 6)	13040( 6)	8605( 5)	121( 5)
C(10)	8467( 9)	13480(13)	8774(10)	332(17)
C(11)	6915(12)	13471(16)	8761( 8)	239(13)

**Table C3** : Anisotropic Thermal Parameters<sup>#</sup> ( $\text{\AA}^2 \times 10^3$ ) of the non-hydrogen atoms with estimated standard deviations in parentheses for the structure  $[\text{C}_{11}\text{H}_{24}\text{O}_2\text{N}_4\text{Cl}_2]_2 (\text{Cu}_4\text{OCl}_{10})$ . The atom numbering relates to Figures C1 and C2.

Atom	$U_{11}$	$U_{22}$	$U_{33}$	$U_{23}$	$U_{13}$	$U_{12}$
Cu(1)	57( 0)	34( 0)	32( 0)	-4( 0)	4( 0)	-3( 0)
Cu(2)	46( 0)	37( 0)	38( 0)	0( 0)	11( 0)	-5( 0)
Cl(1)	51( 1)	53( 1)	46( 1)	1( 1)	11( 1)	-11( 1)
Cl(2)	90( 1)	48( 1)	40( 1)	-9( 1)	0( 1)	-14( 1)
Cl(3)	57( 1)	81( 1)	44( 1)	-9( 1)	-4( 1)	12( 1)
Cl(4)	92( 1)	64( 1)	38( 1)	-8( 1)	24( 1)	-30( 1)
Cl(5)	83( 2)	34( 1)	90( 2)	0( 0)	37( 1)	0( 0)
Cl(6)	169( 3)	33( 1)	41( 1)	0( 0)	0( 2)	0( 0)
Cl(7)	83( 1)	66( 1)	76( 1)	2( 1)	-19( 1)	-16( 1)
Cl(8)	89( 1)	99( 2)	108( 2)	39( 1)	59( 1)	30( 1)
O(1A)	39( 3)	27( 2)	27( 2)	0( 0)	4( 2)	0( 0)
C(1)	94( 5)	56( 4)	76( 5)	-15( 4)	21( 4)	2( 4)
C(2)	65( 4)	72( 5)	99( 7)	1( 4)	19( 4)	8( 4)
N(1)	57( 3)	56( 3)	45( 3)	0( 2)	7( 2)	6( 2)

C(3)	60( 4)	60( 4)	36( 3)	1( 3)	0( 3)	7( 3)
C(4)	70( 4)	52( 4)	37( 3)	3( 3)	8( 3)	2( 3)
N(2)	52( 3)	38( 3)	46( 3)	1( 2)	8( 2)	5( 2)
C(5)	60( 4)	48( 3)	40( 3)	-4( 3)	8( 3)	-2( 3)
O(1)	93( 4)	51( 3)	80( 4)	-21( 3)	-14( 3)	-3( 3)
C(6)	56( 4)	47( 3)	56( 4)	4( 3)	12( 3)	5( 3)
O(2)	140( 5)	63( 3)	146( 6)	42( 4)	87( 5)	45( 4)
C(7)	72( 4)	40( 3)	54( 4)	3( 3)	23( 3)	10( 3)
N(3)	80( 4)	40( 3)	77( 4)	8( 3)	40( 3)	8( 3)
C(8)	83( 5)	57( 4)	45( 4)	4( 3)	19( 3)	0( 3)
C(9)	82( 5)	63( 5)	100( 7)	9( 5)	32( 5)	-3( 4)
N(4)	105( 6)	114( 7)	151( 9)	-72( 7)	41( 6)	-22( 5)
C(10)	80( 8)	474(36)	449(32)	372(30)	71(14)	-93(15)
C(11)	208(18)	364(30)	149(15)	160(18)	46(13)	45(20)

# These are in the form of  $\exp(-2\pi^2(U_{11}h^2(a^*)^2 + \dots + 2U_{12}hk(a^*)(b^*) + \dots))$ .

## C2. Results and Discussion

The structure of the garnet-red crystal thus determined was found to incorporate the very interesting  $(\text{Cu}_4\text{OCl}_{10})^{4-}$  polynuclear cluster shown in Figure C1. This has the oxide ion in a rather unusual environment, i.e. tetrahedrally coordinated to four copper(II) ions. The anion can be thought of as a member of the series of compounds with the general formula  $\text{Cu}_4\text{OCl}_6\text{L}_4$ . Structures with L = triphenylphosphine oxide, pyridine or N,N - diethylnicotinamide, for example, have been reported previously in the literature [172, 173, 174, 175, 176]. Furthermore, structure determinations of polynuclear anions with L =  $\text{Cl}^-$ , essentially identical to this study, have also been reported, and occur together with different quaternary ammonium cations in, for example, the tetramethyl- [175, 177], diethyl- [178] and N,N,N',N'-tetramethylethylenediammonium [179] salts.

As in the case of the crystal structure determined by Belford *et al* [179], the space group is C2/c with only four formula units in the monoclinic unit cell. This requires symmetry for the anion which therefore lies on a crystallographic two-fold axis, running through the atoms Cl(5), O(1A) and Cl(6).

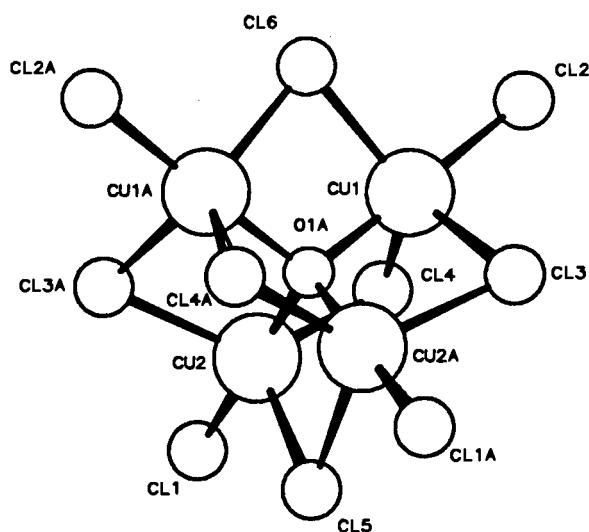


**Figure C1** : Pluto representation of the anion  $(\text{Cu}_4\text{OCl}_{10})^{4-}$ . The atoms Cl(5), O(1A) and Cl(6) lie on a crystallographic two-fold axis, indicated by the arrows.

**Table C4** : (a) Bond lengths ( $\text{\AA}$ ) and (b) bond angles (degrees) with estimated standard deviations in parentheses for the  $(\text{Cu}_4\text{OCl}_{10})^{4-}$  anion. The atom numbering relates to Figure C1 and the type of interactions are furthermore as indicated.

(a) axial :	Cu(1) - Cl(2)	2.238( 2)	Cu(2) - Cl(1)	2.257( 2)
	Cu(1) - O(1A)	1.919( 3)	Cu(2) - O(1A)	1.917( 3)
equatorial :	Cu(1) - Cl(3)	2.403( 2)	Cu(2) - Cl(3A)	2.384( 2)
	Cu(1) - Cl(4)	2.466( 2)	Cu(2) - Cl(4)	2.404( 2)
	Cu(1) - Cl(6)	2.355( 1)	Cu(2) - Cl(5)	2.452( 1)
(b)	Cu(1) - O(1A) - Cu(2)	110.1( 1)	Cu(1) - O(1A) - Cu(2A)	108.7( 1)
	Cu(1) - O(1A) - Cu(1A)	109.1( 1)	Cu(2) - O(1A) - Cu(2A)	110.1( 1)
	Cu(1) - Cl(4) - Cu(2)	80.4( 1)	Cu(1) - Cl(3) - Cu(2A)	81.3( 1)
	Cu(1) - Cl(6) - Cu(1A)	83.2( 1)	Cu(2) - Cl(5) - Cu(2A)	79.7( 1)
eq. to eq. :	Cl(3) - Cu(1) - Cl(6)	123.3( 1)	Cl(3A) - Cu(2) - Cl(5)	115.7( 1)
	Cl(4) - Cu(1) - Cl(6)	122.7( 1)	Cl(4) - Cu(2) - Cl(5)	114.5( 1)
	Cl(3) - Cu(1) - Cl(4)	110.8( 1)	Cl(3A) - Cu(2) - Cl(4)	127.8( 1)
ax. to eq. :	Cl(2) - Cu(1) - Cl(6)	96.1( 1)	Cl(1) - Cu(2) - Cl(5)	98.4( 1)
	Cl(2) - Cu(1) - Cl(4)	93.4( 1)	Cl(1) - Cu(2) - Cl(4)	91.7( 1)
	Cl(2) - Cu(1) - Cl(3)	98.4( 1)	Cl(1) - Cu(2) - Cl(3A)	94.6( 1)
eq. to ax. :	Cl(4) - Cu(1) - O(1A)	83.7( 1)	Cl(4) - Cu(2) - O(1A)	85.5( 1)
	Cl(6) - Cu(1) - O(1A)	83.8( 1)	Cl(5) - Cu(2) - O(1A)	85.1( 1)
	Cl(3) - Cu(1) - O(1A)	84.6( 1)	Cl(3A) - Cu(2) - O(1A)	85.2( 1)
ax. to ax. :	Cl(2) - Cu(1) - O(1A)	176.5( 1)	Cl(1) - Cu(2) - O(1A)	176.3( 1)

Interatomic distances and angles of the anion are given in Table C4. The Cu-O distances, 1.917 and 1.919  $\text{\AA}$ , agree well with those reported for the three structures mentioned above, i.e. 1.92 to 1.95  $\text{\AA}$  [175], 1.917  $\text{\AA}$  [179] and 1.903 to 1.917  $\text{\AA}$  [178], and

with the value for copper(II) oxide of 1.95 Å. The Cu-O-Cu angles, varying by only .82° from the ideal value, together with the very similar Cu-O distances, indicate that the tetrahedron of copper atoms about the central oxygen is only slightly distorted from perfect  $T_d$  symmetry.

The copper atoms are essentially in a trigonal bipyramidal environment with the terminal Cl-Cu bond lengths of 2.238 and 2.257 Å significantly shorter than the bridging Cl-Cu bond lengths which range from 2.355 to 2.466 Å. These distances compare well with the values of 2.25 and 2.38 to 2.45 Å, reported by Bertrand and Kelly [175], and 2.242 and 2.409 Å of Belford *et al* [179], for the axial and equatorial interactions respectively. The O-Cu-Cl<sub>ax</sub> arrangements are virtually linear with angles of about 176.4°. The Cl<sub>eq</sub>-Cu-Cl<sub>eq</sub> bond angles show quite large variations but agree well with the corresponding values reported by Belford *et al*. Considering the O-Cu-Cl<sub>eq</sub> angles, which have an average value of about 85°, and the Cl<sub>ax</sub>-Cu-Cl<sub>eq</sub> angles, which are all greater than 90°, it is apparent that the copper atoms are displaced out of the equatorial plane away from the oxide towards the axial chlorides, as has also been observed in previous structures [175].

Bertrand and Kelly have attributed the differences in Cu-Cl distances to a shortening of the axial bonds by back-donation from the copper into the vacant 3d orbitals of the chloride, rather than lengthening of the equatorial bonds as a result of bridging. This arises from a comparison of the Cu-Cl distances with those of the CuCl<sub>5</sub><sup>3-</sup> ion, having no bridging equatorial chlorides, but showing similar differences in bond lengths. The back-donation is thought to be similar to the proposed  $\pi$  bonding with back-donation from copper to the phosphine oxide in the triphenylphosphine oxide complex mentioned above, resulting in the linear P-O-Cu arrangement [175].

Unlike the structure studied by Bertrand and Kelly, the octahedron of chloride ions is quite distorted. Although the Cu-Cl<sub>eq</sub> distances are spread over a similar range of

values (see above), the  $\text{Cl}_{\text{eq}}\text{-Cu-Cl}_{\text{eq}}$  angles show a much greater variation than the 118 to 120° spread observed for the non-origin anion of their structure.

Furthermore, Holt *et al* report  $\text{Cl}_{\text{eq}}\cdots\text{O}\cdots\text{Cl}_{\text{eq}}$  angles with values of 90°(±1.02) for the non-origin polynuclear anion [177]. The oxide in the anion of this study is however distorted out of the Cl(3)-Cl(4)-Cl(3A)-Cl(4A) plane towards Cl(6), as is indicated by the  $\text{Cl}_{\text{eq}}\cdots\text{O}\cdots\text{Cl}_{\text{eq}}$  angles in the above plane, having values of 85.8°, and the Cl(6)···O···Cl<sub>eq</sub> angles having values of 92.3 and 93.2°. This distortion could be due to N-H···Cl hydrogen bonding of only two of the terminal chlorides i.e. Cl(1) and its symmetry related partner Cl(1A).

The cation is shown in Figure C2 with bond lengths and angles tabulated in Table C5. Most bond lengths are within the normal ranges, except for the apparently quite short N(4)-C(10) and the very short N(4)-C(11) distances. The angles about the N(4) nitrogen also indicate this amine to be in quite a distorted tetrahedral environment, which is not the case for the second amine, even though the cation is chemically symmetrical.

The environment about the N(4) amine nitrogen was the one area of concern in the crystallographic structure refinement. As can be seen from Table C2, the atoms involved all have very large thermal parameters indicating substantial disorder. This might be due to the fact that, in contrast to N(1), the nitrogen is not involved in hydrogen bonding and is therefore not held so rigidly in position. N(1) makes a close contact of 3.166(6) Å with Cl(1) in a tetrahedral position, which indicates the existence of N-H···Cl hydrogen bonding. The N-H···Cl angle is 167.2° which is very close to the distribution peak for such interactions of about 165°. Other close contacts were observed but these have very unfavourable angles making any additional hydrogen bonding unlikely.

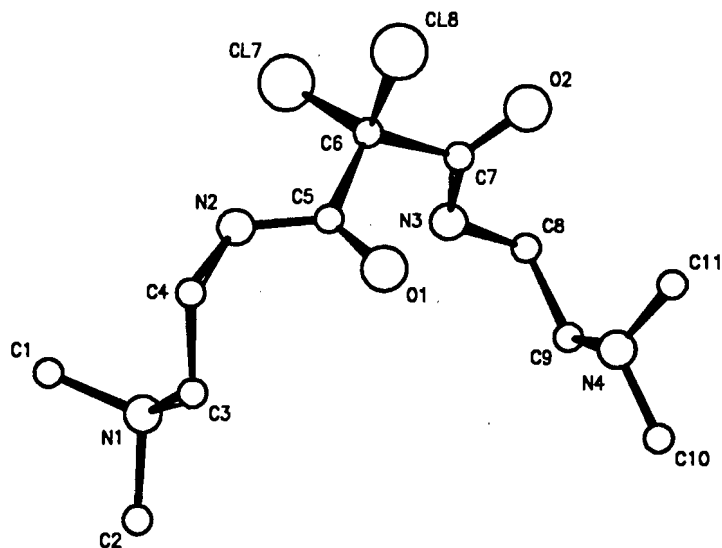


**Figure C2** : Pluto representation of the cation  $[\text{C}_{11}\text{H}_{24}\text{O}_2\text{N}_4\text{Cl}_2]^{2+}$  projected down the  $c$  axis, showing the designation of the atoms. For clarity all hydrogen atoms have been omitted.

**Table C5** : (a) Bond lengths ( $\text{\AA}$ ) and (b) angles (degrees) with estimated standard deviations in parentheses for the cation  $[\text{C}_{11}\text{H}_{24}\text{O}_2\text{N}_4\text{Cl}_2]^{2+}$ . The atom numbering relates to Figure C2.

(a)	C(1) - N(1)	1.470( 9)	N(4) - C(11)	1.300(22)
	C(2) - N(1)	1.498( 9)	N(4) - C(10)	1.405(17)
	N(1) - C(3)	1.513( 9)	C(9) - N(4)	1.466(14)
	C(3) - C(4)	1.495(10)	C(8) - C(9)	1.442(11)
	C(4) - N(2)	1.470( 7)	N(3) - C(8)	1.473( 9)
	N(2) - C(5)	1.331( 8)	C(7) - N(3)	1.306(10)
	C(5) - O(1)	1.194( 8)	O(2) - C(7)	1.193(10)
	C(5) - C(6)	1.554( 8)	C(6) - C(7)	1.563( 9)
	Cl(7) - C(6)	1.759( 6)	C(6) - Cl(8)	1.774( 7)
(b)	C(1) - N(1) - C(2)	110.2(5)	C(10) - N(4) - C(11)	111.1(14)
	C(2) - N(1) - C(3)	108.0(6)	C(9) - N(4) - C(10)	113.0(10)
	C(1) - N(1) - C(3)	115.6(5)	C(9) - N(4) - C(11)	121.4(11)
	N(1) - C(3) - C(4)	115.4(5)	C(8) - C(9) - N(4)	116.7( 7)
	C(3) - C(4) - N(2)	115.6(5)	N(3) - C(8) - C(9)	116.2( 6)
	C(4) - N(2) - C(5)	120.7(5)	C(7) - N(3) - C(8)	121.9( 6)
	N(2) - C(5) - C(6)	116.1(5)	C(6) - C(7) - N(3)	114.9( 5)
	N(2) - C(5) - O(1)	126.1( 6)	O(2) - C(7) - N(3)	125.6( 7)
	O(1) - C(5) - C(6)	117.8( 6)	C(6) - C(7) - O(2)	118.9( 7)
	Cl(8) - C(6) - C(5)	104.7( 4)	Cl(7) - C(6) - C(7)	108.6( 4)
	Cl(7) - C(6) - C(5)	113.1( 4)	Cl(8) - C(6) - C(7)	108.1( 4)
	Cl(7) - C(6) - Cl(8)	110.4( 4)	C(5) - C(6) - C(7)	111.8(5)

The crystal structure of  $[\text{C}_{11}\text{H}_{24}\text{O}_2\text{N}_4\text{Cl}_2]_2$  ( $\text{Cu}_4\text{OCl}_{10}$ ) thus consists of discrete  $(\text{Cu}_4\text{OCl}_{10})^{4-}$  ions, each associated with only two independent cations, which are not further connected by hydrogen bonding to other anions. This is unlike the structures of

Belford *et al* and Harlow and Simonsen which consisted of hydrogen bonded networks of anions and cations. The hydrogen bonding in the formula unit is indicated in Figure C3 and the packing of the ions in the unit cell is shown in Figure C4.

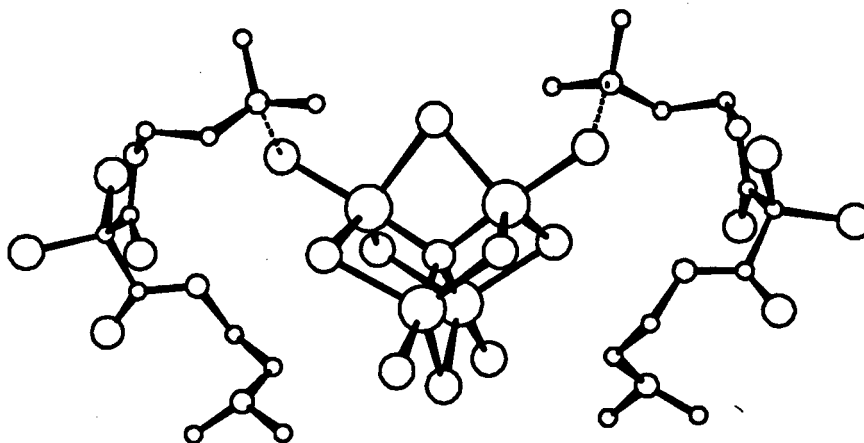


**Figure C3** : A formula unit of  $[\text{C}_{11}\text{H}_{24}\text{O}_2\text{N}_4\text{Cl}_2]_2 (\text{Cu}_4\text{OCl}_{10})$  with the N-H...Cl hydrogen bonding indicated by the broken lines.

An interesting feature of the cation is the displacement of the central methylene protons by chlorine during synthesis of the crystal. As has been previously observed for this ligand (see Appendix A), these protons are quite labile because they are situated between two electron withdrawing amide groups. Any source of positive chlorine could therefore readily bring about this substitution.

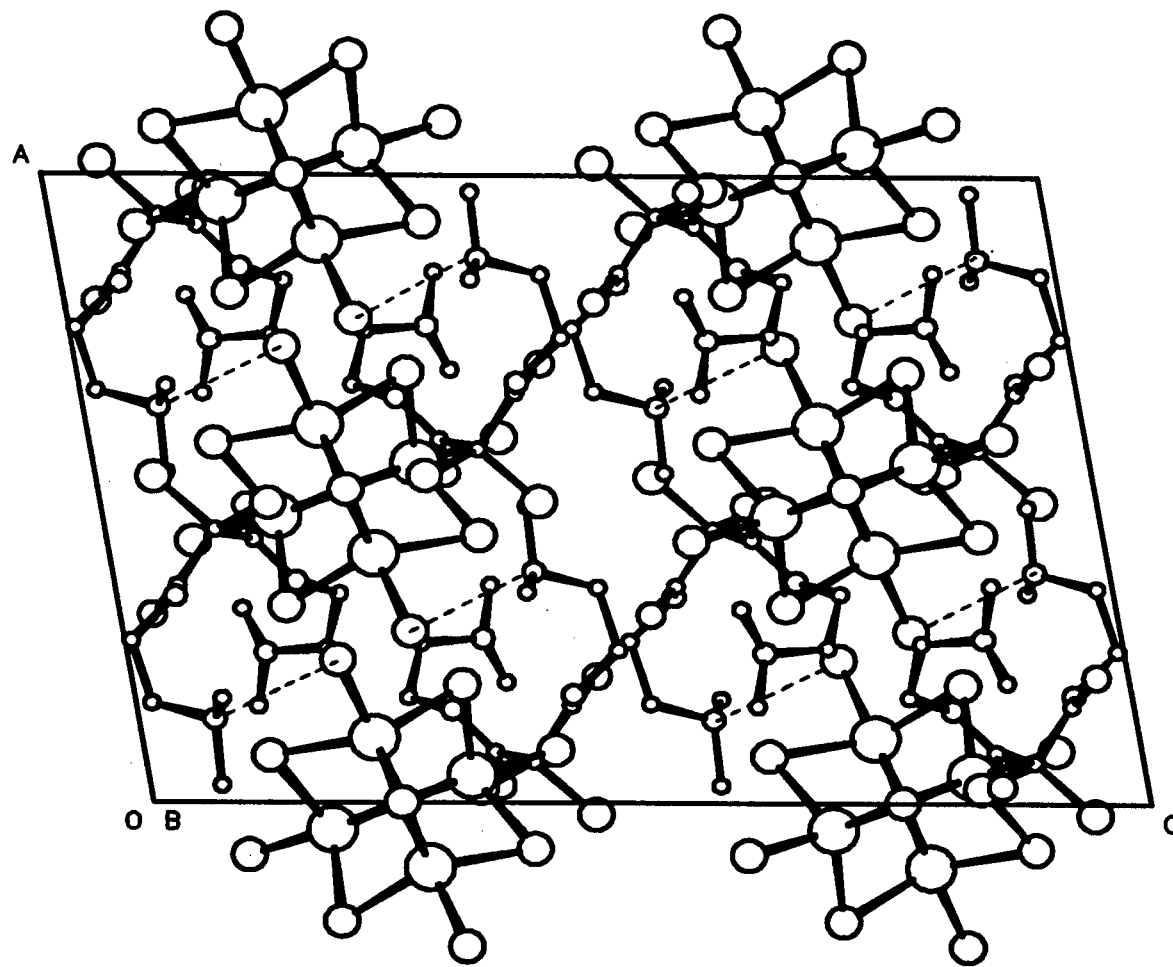


**Figure C4** : Projection down the *b* axis of [C<sub>11</sub>H<sub>24</sub>O<sub>2</sub>N<sub>4</sub>Cl<sub>2</sub>]<sub>2</sub> (Cu<sub>4</sub>OCl<sub>10</sub>) in the unit cell. The broken lines indicate the N-H...Cl hydrogen bonds.

### C3. Observed and Calculated Structure Factors for $[C_{11}H_{24}O_2N_4Cl_2]_2 (Cu_4OCl_{10})$

H	K	L	FO	FC	H	K	L	FO	FC	H	K	L	FO	FC	H	K	L	FO	FC	H	K	L	FO	FC
2	0	0	300	325	6	4	0	144	-145	3	9	0	112	-110	8	14	0	24	27	0	2	1	340	333
4	0	0	172	184	8	4	0	80	80	5	9	0	33	29	10	14	0	17	-14	2	2	1	42	43
6	0	0	42	40	10	4	0	19	14	7	9	0	11	7	1	15	0	54	-59	6	2	1	83	-88
10	0	0	40	36	12	4	0	17	15	9	9	0	55	-58	7	15	0	32	32	8	2	1	171	-169
12	0	0	30	28	14	4	0	22	-24	11	9	0	19	15	9	15	0	26	-26	14	2	1	24	-22
14	0	0	54	-57	16	4	0	40	-37	13	9	0	17	21	0	16	0	21	-21	-15	3	1	20	-20
16	0	0	30	-30	1	5	0	156	-145	0	10	0	74	77	2	16	0	51	52	-13	3	1	23	-18
1	1	0	177	165	3	5	0	20	-14	2	10	0	103	104	4	16	0	19	20	-11	3	1	132	136
3	1	0	159	-166	5	5	0	48	-47	4	10	0	196	199	6	16	0	24	21	-9	3	1	108	111
5	1	0	165	-173	7	5	0	74	-75	6	10	0	139	144	1	17	0	41	43	-7	3	1	48	43
7	1	0	143	-141	11	5	0	104	-99	8	10	0	38	-38	3	17	0	31	32	-5	3	1	182	-177
9	1	0	98	102	13	5	0	34	-33	10	10	0	36	-37	5	17	0	30	30	-3	3	1	387	-386
11	1	0	21	21	15	5	0	47	-44	12	10	0	18	-11	7	17	0	28	27	-1	3	1	51	38
13	1	0	31	-28	0	6	0	194	-166	14	10	0	18	10	0	18	0	30	-28	1	3	1	58	-35
15	1	0	36	-35	2	6	0	62	65	1	11	0	87	87	4	18	0	35	-34	3	3	1	11	-13
0	2	0	171	192	4	6	0	57	47	3	11	0	63	57	-15	1	1	25	-26	5	3	1	99	-101
2	2	0	43	-44	6	6	0	10	7	5	11	0	31	34	-13	1	1	37	-38	7	3	1	74	-78
4	2	0	25	-24	8	6	0	10	8	7	11	0	30	-29	-11	1	1	15	15	9	3	1	104	-110
6	2	0	23	15	10	6	0	87	-89	9	11	0	158	-163	-7	1	1	41	-42	11	3	1	52	54
8	2	0	107	103	12	6	0	63	-66	11	11	0	45	-41	-3	1	1	251	262	13	3	1	73	-70
10	2	0	117	125	14	6	0	24	-22	0	12	0	64	-60	-1	1	1	252	269	-16	4	1	23	21
12	2	0	25	28	1	7	0	21	-23	2	12	0	61	54	1	1	1	216	180	-14	4	1	27	-23
16	2	0	20	-15	3	7	0	28	27	4	12	0	100	100	5	1	1	94	-94	-12	4	1	41	42
1	3	0	134	-132	5	7	0	41	44	6	12	0	33	35	7	1	1	160	-173	-10	4	1	91	89
3	3	0	206	-200	7	7	0	67	-58	8	12	0	32	-32	9	1	1	71	-64	-8	4	1	40	-38
5	3	0	184	-186	15	7	0	12	5	10	12	0	52	-48	11	1	1	24	-25	-6	4	1	196	-199
7	3	0	29	-35	0	8	0	163	-185	1	13	0	175	-179	13	1	1	60	-62	-4	4	1	393	-397
9	3	0	174	182	2	8	0	115	-111	5	13	0	67	66	-14	2	1	67	-71	-2	4	1	131	-139
11	3	0	59	59	4	8	0	66	-59	7	13	0	88	83	-12	2	1	35	-35	0	4	1	28	27
13	3	0	71	65	6	8	0	14	-20	9	13	0	41	-39	-10	2	1	28	29	2	4	1	37	-37
15	3	0	17	-18	10	8	0	52	51	0	14	0	129	-145	-8	2	1	58	-64	4	4	1	84	-87
0	4	0	8	-14	12	8	0	50	50	2	14	0	12	-11	-6	2	1	35	-36	6	4	1	37	-38
2	4	0	13	-12	14	8	0	39	43	4	14	0	34	32	-4	2	1	233	-229	8	4	1	117	121
4	4	0	10	7	1	9	0	161	-155	6	14	0	81	79	-2	2	1	377	372	10	4	1	171	169
12	4	1	77	79	1	7	1	185	210	-12	10	1	46	45	-9	13	1	44	-46	-3	17	1	49	51
-11	5	1	79	82	3	7	1	157	151	-10	10	1	118	113	-5	13	1	58	56	-1	17	1	17	-19
-9	5	1	55	56	5	7	1	184	-186	-8	10	1	46	44	-3	13	1	67	68	1	17	1	36	-37
-5	5	1	248	-251	13	7	1	59	-59	-6	10	1	14	-4	-1	13	1	89	88	5	17	1	21	23
-3	5	1	102	-84	15	7	1	32	-33	-4	10	1	182	-189	1	13	1	64	68	-4	18	1	60	61
-1	5	1	167	177	-14	8	1	14	-11	-2	10	1	96	-103	5	13	1	14	-20	0	18	1	29	-29
3	5	1	135	-129	-12	8	1	25	-27	0	10	1	111	-103	7	13	1	37	-35	4	18	1	34	37
5	5	1	219	-222	-10	8	1	35	35	2	10	1	12	-14	9	13	1	83	-86	-16	0	2	23	26
7	5	1	27	33	-8	8	1	39	38	4	10	1	59	-57	11	13	1	29	-31	-14	0	2	87	88
9	5	1	78	81	-6	8	1	65	-67	6	10	1	47	46	-10	14	1	18	-23	-12	0	2	20	-15
11	5	1	105	107	-4	8	1	26	-24	8	10	1	31	30	-8	14	1	46	-43	-10	0	2	38	-38
13	5	1	50	-51	-2	8	1	130	129	10	10	1	66	59	-6	14	1	13	9	-8	0	2	174	-198
15	5	1	43	-41	0	8	1	52	43	12	10	1	48	49	-4	14	1	52	-58	-6	0	2	106	-112
-16	6	1	31	-27	2	8	1	107	105	-13	11	1	20	-18	-2	14	1	75	-71	-4	0	2	170	-172
-14	6	1	57	-60	4	8	1	258	-255	-11	11	1	65	62	0	14	1	85	-84	-2	0	2	345	-348
-12	6	1	73	-73	6	8	1	77	-79	-9	11	1	22	20	2	14	1	18	-18	0	0	2	396	-440
-10	6	1	23	25	8	8	1	70	72	-7	11	1	40	42	4	14	1	51	54	2	0	2	32	17
-8	6	1	23	23	10	8	1	39	44	-5	11	1	20	16	6	14	1	61	56	4	0	2	28	-29
-6	6	1	34	-39	12	8	1	40	41	-3	11	1	41	45	-5	15	1	21	22	6	0	2	276	277
-4	6	1	172	-170	14	8	1	34	-35	-1	11	1	108	110	-3	15	1	20	-20	8	0	2	61	65
-2	6	1	123	124	-13	9	1	20	-18	1	11	1	116	110	-1	15	1	116	-118	10	0	2	113	-116
0	6	1	29	-26	-11	9	1	86	92	3	11	1	101	101	1	15	1	83	-84	12	0	2	59	62
2	6	1	173	174	-9	9	1	21	23	5	11	1	37	37	3	15	1	21	19	-17	1	2	20	-20
4	6	1	230	-221	-7	9	1	15	17	11	11	1	33	32	5	15	1	30	32	-15	1	2	79	78
6	6	1	97	-100	-5	9	1	63	-66	-8	12	1	49	-46	7	15	1	42	40	-13	1	2	15	14
14	6	1	71	-66	-3	9	1	21	-21	-6	12	1	39	37	9	15	1	17	-12	-11	1	2	71	-72
-15	7	1	47	-51	-1	9	1	19	22	-4	12	1	18	22	-8	16	1	46	-46	-9	1	2	142	-146
-13	7	1	95	-99	1	9	1	31	28	-2	12	1	118	117	-6	16	1	24	-20	-7	1	2	26	23
-11	7	1	31	-29	3	9	1	15	13	0	12	1	78	77	-2	16	1	35	-40	-5	1	2	14	18

-9	7	1	23	22	5	9	1	98	-94	2	12	1	43	47	0	16	1	100	-99	-3	1	2	252	262
-7	7	1	115	117	7	9	1	95	90	4	12	1	24	22	2	16	1	87	-89	-1	1	2	150	-140
-5	7	1	32	-30	9	9	1	115	117	6	12	1	32	-29	4	16	1	13	-14	1	1	2	427	-430
-3	7	1	127	130	11	9	1	93	94	8	12	1	70	-70	6	16	1	24	20	3	1	2	98	-91
-1	7	1	204	188	-14	10	1	12	12	10	12	1	16	-11	-5	17	1	59	60	5	1	2	59	-53

H	K	L	FO	FC	H	K	L	FO	FC	H	K	L	FO	FC	H	K	L	FO	FC	H	K	L	FO	FC
7	1	2	174	179	-4	4	2	336	-325	0	6	2	262	-249	-5	9	2	72	70	-2	12	2	53	-51
9	1	2	121	-125	-2	4	2	89	-78	4	6	2	103	106	-3	9	2	158	157	0	12	2	129	128
11	1	2	20	-23	0	4	2	180	-203	6	6	2	129	135	-1	9	2	158	162	2	12	2	39	40
-14	2	2	18	12	2	4	2	73	80	8	6	2	128	129	1	9	2	152	139	4	12	2	18	-15
-12	2	2	30	-31	4	4	2	137	132	10	6	2	110	110	3	9	2	130	-120	6	12	2	69	-65
-10	2	2	113	-122	6	4	2	56	53	12	6	2	23	22	5	9	2	156	-156	10	12	2	69	69
-8	2	2	110	-117	8	4	2	49	-51	-11	7	2	47	49	7	9	2	29	-28	-9	13	2	17	18
-6	2	2	239	253	10	4	2	22	-19	-9	7	2	105	101	13	9	2	17	-19	-7	13	2	14	7
-4	2	2	369	360	12	4	2	16	11	-7	7	2	20	21	-12	10	2	39	-41	-3	13	2	23	-24
-2	2	2	123	110	14	4	2	44	45	-5	7	2	23	20	-8	10	2	27	25	-1	13	2	69	63
0	2	2	71	-35	16	4	2	41	41	-3	7	2	13	11	-6	10	2	153	-152	1	13	2	60	62
2	2	2	119	-136	-15	5	2	49	46	-1	7	2	115	117	-4	10	2	67	-59	3	13	2	89	-89
4	2	2	112	-106	-13	5	2	65	63	1	7	2	157	154	0	10	2	31	34	5	13	2	84	-85
6	2	2	100	112	-11	5	2	110	115	3	7	2	80	73	2	10	2	95	-93	7	13	2	67	-67
8	2	2	20	-22	-9	5	2	21	16	5	7	2	35	-29	4	10	2	121	-125	9	13	2	25	25
10	2	2	143	-142	-7	5	2	124	125	7	7	2	17	-18	6	10	2	45	-44	-10	14	2	11	10
16	2	2	31	31	-5	5	2	91	96	9	7	2	25	-25	8	10	2	79	77	-8	14	2	41	39
-13	3	2	32	-28	-3	5	2	46	-40	11	7	2	19	-20	10	10	2	87	89	-6	14	2	30	-31
-9	3	2	42	-41	-1	5	2	98	81	13	7	2	33	-33	12	10	2	28	26	0	14	2	82	86
-7	3	2	108	114	1	5	2	54	57	-14	8	2	34	-39	-11	11	2	34	31	6	14	2	107	-109
-5	3	2	232	236	3	5	2	179	182	-12	8	2	57	-57	-9	11	2	63	61	8	14	2	58	-58
-3	3	2	189	189	5	5	2	308	302	-10	8	2	43	39	-7	11	2	72	-77	-9	15	2	41	41
-1	3	2	90	98	7	5	2	64	64	-8	8	2	74	72	-5	11	2	171	-168	-5	15	2	34	-35
1	3	2	216	-219	9	5	2	64	68	-4	8	2	55	57	-3	11	2	180	-179	-3	15	2	59	-60
3	3	2	250	234	11	5	2	39	38	-2	8	2	161	166	-1	11	2	82	-85	-1	15	2	41	48
5	3	2	37	-38	13	5	2	33	-36	0	8	2	123	119	1	11	2	85	95	1	15	2	89	89
7	3	2	112	-112	15	5	2	20	17	2	8	2	125	131	5	11	2	64	-67	7	15	2	45	-46
9	3	2	175	-185	-16	6	2	19	20	4	8	2	112	-105	9	11	2	82	80	9	15	2	12	10
11	3	2	82	-75	-12	6	2	16	21	6	8	2	108	-115	11	11	2	47	42	-6	16	2	63	-64
13	3	2	41	-38	-10	6	2	15	-16	8	8	2	53	-50	13	11	2	12	13	-4	16	2	74	-80
15	3	2	52	48	-8	6	2	109	-104	-13	9	2	33	-35	-10	12	2	53	52	-2	16	2	50	-54
-10	4	2	29	-27	-6	6	2	78	-77	-11	9	2	21	-19	-8	12	2	63	69	2	16	2	14	-13
-8	4	2	133	-138	-4	6	2	240	-249	-9	9	2	71	73	-6	12	2	66	-66	4	16	2	21	17
-6	4	2	92	80	-2	6	2	137	-141	-7	9	2	39	44	-4	12	2	64	-62	-7	17	2	35	-36

H	K	L	FO	FC	H	K	L	FO	FC	H	K	L	FO	FC	H	K	L	FO	FC	H	K	L	FO	FC
-5	17	2	25	-26	14	2	3	18	15	-9	5	3	31	-32	-1	7	3	195	-197	13	9	3	18	17
-3	17	2	29	-28	-15	3	3	33	30	-5	5	3	228	211	1	7	3	161	-156	-10	10	3	27	-30
-1	17	2	44	-49	-13	3	3	38	38	-3	5	3	120	121	3	7	3	119	113	-8	10	3	57	59
3	17	2	28	-27	-11	3	3	74	-75	-1	5	3	62	-51	5	7	3	430	432	-6	10	3	55	59
5	17	2	28	29	-9	3	3	32	-33	1	5	3	41	-59	7	7	3	130	138	-4	10	3	190	193
-4	18	2	29	30	-7	3	3	40	-36	3	5	3	63	-52	9	7	3	98	103	-2	10	3	50	-50
-15	1	3	43	44	-5	3	3	186	199	5	5	3	78	81	11	7	3	77	-69	0	10	3	117	-114
-13	1	3	62	67	-3	3	3	311	300	7	5	3	70	-68	13	7	3	11	-4	2	10	3	147	-152
-11	1	3	32	-33	-1	3	3	247	-256	9	5	3	46	-46	15	7	3	26	28	4	10	3	108	-108
-9	1	3	44	-41	1	3	3	222	-201	11	5	3	37	-36	-14	8	3	30	32	6	10	3	64	-56
-7	1	3	242	-256	3	3	3	198	-199	13	5	3	31	34	-12	8	3	59	58	8	10	3	65	-67
-5	1	3	186	-206	5	3	3	95	99	15	5	3	51	52	-10	8	3	72	-69	10	10	3	66	-69
-3	1	3	147	-138	7	3	3	38	36	-16	6	3	30	29	-2	8	3	171	-170	12	10	3	39	-40
-1	1	3	14	5	9	3	3	90	-90	-14	6	3	45	46	0	8	3	112	-115	-11	11	3	43	-42
1	1	3	190	-225	11	3	3	23	-19	-12	6	3	13	15	2	8	3	144	-132	-9	11	3	55	-49
3	1	3	74	-54	13	3	3	25	22	-10	6	3	109	-113	4	8	3	54	49	-7	11	3	83	-91
5	1	3	36	-31	15	3	3	16	8	-8	6	3	25	23	6	8	3	28	25	-5	11	3	27	-24
7	1	3	68	66	-14	4	3	36	40	-6	6	3	10	10	8	8	3	47	-53	-1	11	3	132	-141
9	1	3	19	-18	-10	4	3	52	-54	-4	6	3	162	159	10	8	3	72	-70	1	11	3	26	-23
11	1	3	53	57	-8	4	3	36	35	-2	6	3	8	4	12	8	3	69	-69	3	11	3	68	-68
15	1	3	27	-24	-6	4	3	145	149	0	6	3	114	-115	14	8	3	22	25	7	11	3	19	-22
-16	2	3	27	27	-4	4	3	421	421	2	6	3	30	-35	-15	9	3	28	-26	11	11	3	25	-22
-14	2	3	60	59	-2	4	3	189	182	4	6	3	285	297	-13	9	3	14	9	-10	12	3	16	-18
-10	2	3	34	-37	0	4	3	150	150	6	6	3	229	227	-11	9	3	33	-29	-8	12	3	34	-39
-8	2	3	140	-134	2	4	3	212	-209	8	6	3	52	55	-9	9	3	39	-38	-6	12	3	107	-106
-6	2	3	181	-185	4	4	3	60	-65	10	6	3	35	-35	-7	9	3	29	27	-4	12	3	33	-33

-4	2	3	241	243	6	4	3	29	-27	12	6	3	74	-76	-5	9	3	85	86	-2	12	3	44	-43
-2	2	3	13	10	8	4	3	156	-157	14	6	3	46	43	-3	9	3	119	115	0	12	3	38	39
0	2	3	70	-77	10	4	3	115	-117	-13	7	3	49	51	-1	9	3	33	31	4	12	3	32	-30
2	2	3	242	235	12	4	3	16	-10	-11	7	3	54	-54	1	9	3	12	-2	6	12	3	25	18
4	2	3	188	197	14	4	3	55	59	-9	7	3	120	-118	3	9	3	56	-62	8	12	3	19	15
6	2	3	146	154	16	4	3	19	20	-7	7	3	17	-12	5	9	3	107	106	10	12	3	30	26
8	2	3	71	62	-13	5	3	54	58	-5	7	3	25	18	7	9	3	56	-54	12	12	3	19	19
12	2	3	17	14	-11	5	3	19	-22	-3	7	3	91	-91	11	9	3	39	-40	-7	13	3	93	-90

H	K	L	FO	FC	H	K	L	FO	FC	H	K	L	FO	FC	H	K	L	FO	FC	H	K	L	FO	FC
-5	13	3	83	-83	3	17	3	42	45	-14	2	4	30	-28	0	4	4	187	171	-1	7	4	108	-105
-3	13	3	32	-33	-4	18	3	69	-73	-12	2	4	41	44	2	4	4	150	159	1	7	4	67	70
-1	13	3	17	-16	-2	18	3	28	-27	-10	2	4	36	37	4	4	4	133	-136	3	7	4	32	26
1	13	3	114	108	-14	0	4	62	-70	-8	2	4	69	68	6	4	4	70	-70	5	7	4	90	96
3	13	3	41	45	-12	0	4	77	80	-6	2	4	185	-173	8	4	4	90	-85	7	7	4	35	34
7	13	3	37	38	-10	0	4	193	204	-4	2	4	34	-18	-15	5	4	15	-11	9	7	4	20	-20
9	13	3	47	46	-8	0	4	526	558	-2	2	4	206	-191	-9	5	4	86	89	11	7	4	35	-32
11	13	3	21	18	-6	0	4	234	240	0	2	4	323	324	-7	5	4	74	-76	-12	8	4	13	-11
-10	14	3	18	16	-4	0	4	154	175	2	2	4	90	79	-5	5	4	45	44	-10	8	4	91	-92
-8	14	3	56	60	-2	0	4	18	-15	4	2	4	149	-146	-3	5	4	67	68	-8	8	4	95	-95
-6	14	3	51	57	0	0	4	49	-65	6	2	4	115	-115	-1	5	4	23	-26	-6	8	4	70	-71
-4	14	3	24	24	2	0	4	265	-238	8	2	4	48	43	1	5	4	154	152	-4	8	4	64	-66
0	14	3	63	59	4	0	4	109	-119	10	2	4	76	74	3	5	4	204	-201	-2	8	4	26	-29
2	14	3	20	-20	6	0	4	190	-199	12	2	4	29	-28	5	5	4	159	-167	0	8	4	137	-131
4	14	3	28	-31	8	0	4	110	-102	14	2	4	34	-30	7	5	4	142	-142	4	8	4	204	205
6	14	3	38	-36	10	0	4	42	42	16	2	4	63	-62	9	5	4	19	-20	6	8	4	111	110
-9	15	3	45	43	12	0	4	27	-30	-13	3	4	24	-28	11	5	4	42	41	8	8	4	22	19
-7	15	3	62	63	14	0	4	22	20	-11	3	4	49	-52	13	5	4	22	23	10	8	4	59	-62
-3	15	3	25	25	16	0	4	25	-26	-7	3	4	103	-103	-12	6	4	12	-12	12	8	4	48	-44
-1	15	3	52	54	-17	1	4	14	15	-5	3	4	275	-275	-8	6	4	50	-52	-11	9	4	25	-24
1	15	3	23	28	-15	1	4	79	-81	-3	3	4	127	-130	-6	6	4	41	-40	-9	9	4	109	-107
3	15	3	29	-30	-13	1	4	25	-23	-1	3	4	82	86	-4	6	4	62	59	-7	9	4	56	-61
5	15	3	67	-65	-11	1	4	23	-24	1	3	4	419	413	-2	6	4	71	75	-5	9	4	20	18
7	15	3	43	-42	-9	1	4	101	107	3	3	4	94	86	0	6	4	86	-84	-3	9	4	61	65
-8	16	3	55	57	-7	1	4	178	186	5	3	4	241	244	2	6	4	117	-119	-1	9	4	31	-33
-6	16	3	35	34	-5	1	4	217	-232	7	3	4	43	45	4	6	4	257	-256	1	9	4	154	-158
-2	16	3	64	64	-1	1	4	278	260	9	3	4	109	111	6	6	4	162	-161	3	9	4	89	93
0	16	3	100	103	1	1	4	115	112	11	3	4	70	69	8	6	4	95	-101	5	9	4	121	116
2	16	3	68	70	3	1	4	48	51	15	3	4	50	-46	12	6	4	17	16	7	9	4	99	94
6	16	3	56	-53	5	1	4	20	15	-14	4	4	31	-31	14	6	4	17	16	9	9	4	26	29
-5	17	3	60	-60	7	1	4	81	-83	-10	4	4	20	23	-11	7	4	18	23	11	9	4	49	-47
-3	17	3	51	-51	9	1	4	165	167	-6	4	4	106	-113	-9	7	4	29	-30	-14	10	4	43	40
-1	17	3	28	26	11	1	4	78	79	-4	4	4	138	-125	-5	7	4	44	47	-12	10	4	50	48
1	17	3	32	32	13	1	4	40	39	-2	4	4	307	-296	-3	7	4	18	-20	-8	10	4	18	19

H	K	L	FO	FC	H	K	L	FO	FC	H	K	L	FO	FC	H	K	L	FO	FC	H	K	L	FO	FC
-6	10	4	131	128	7	13	4	111	107	-9	1	5	94	103	1	3	5	390	-358	13	5	5	13	-11
-4	10	4	102	106	11	13	4	13	9	-7	1	5	118	133	3	3	5	43	-56	15	5	5	43	-39
-2	10	4	133	131	-10	14	4	24	-26	-3	1	5	18	-11	5	3	5	251	-260	-16	6	5	24	-21
0	10	4	130	-126	-8	14	4	67	-70	-1	1	5	135	-125	7	3	5	11	-6	-14	6	5	32	-29
2	10	4	136	-137	-6	14	4	15	-7	1	1	5	79	-94	9	3	5	71	71	-12	6	5	47	-41
4	10	4	23	28	-2	14	4	43	42	3	1	5	23	20	11	3	5	50	54	-10	6	5	124	121
8	10	4	20	-18	4	14	4	74	77	5	1	5	242	-240	15	3	5	42	-39	-8	6	5	60	54
10	10	4	45	-42	6	14	4	96	92	7	1	5	79	-87	-16	4	5	17	-19	-6	6	5	32	-27
12	10	4	29	-27	8	14	4	23	25	9	1	5	35	31	-14	4	5	34	-36	-4	6	5	221	-222
-9	11	4	13	-4	10	14	4	23	-26	11	1	5	46	43	-12	4	5	83	-87	-2	6	5	126	-117
-7	11	4	107	116	-9	15	4	27	-31	13	1	5	52	54	-10	4	5	16	14	0	6	5	80	80
-5	11	4	153	152	-7	15	4	20	-20	15	1	5	29	23	-6	4	5	44	-42	4	6	5	206	-199
-3	11	4	88	83	-5	15	4	34	34	-16	2	5	18	-19	-4	4	5	217	-213	6	6	5	188	-186
-1	11	4	68	-67	3	15	4	39	39	-14	2	5	20	-18	-2	4	5	236	224	8	6	5	22	-18
1	11	4	203	-210	5	15	4	25	24	-10	2	5	54	54	0	4	5	274	278	10	6	5	24	27
5	11	4	32	32	7	15	4	28	31	-8	2	5	164	166	2	4	5	385	374	12	6	5	56	56
7	11	4	48	53	9	15	4	39	-41	-6	2	5	144	148	4	4	5	225	220	14	6	5	36	-32
9	11	4	28	-26	-6	16	4	51	52	-4	2	5	26	-33	6	4	5	38	-33	-13	7	5	40	-42
11	11	4	30	-29	-4	16	4	22	20	-2	2	5	20	20	8	4	5	74	65	-11	7	5	114	116
-6	12	4	88	86	-2	16	4	30	28	0	2	5	212	-200	10	4	5	38	37	-9	7	5	183	180
-4	12	4	89	87	0	16	4	39	-41	2	2	5	218	-221	14	4	5	55	-55	-7	7	5	73	69
0	12	4	94	-101	2	16	4	28	-29	4	2	5	36	-37	-15	5	5	12	-13	-5	7	5	58	61
2	12	4	97	-94	4	16	4	29	-30	6	2	5	167	-168	-13	5	5	92	-96	-3	7	5	141	-139

6	12	4	18	17	6	16	4	25	-28	8	2	5	69	67	-9	5	5	79	78	-1	7	5	134	140
8	12	4	25	-20	-7	17	4	27	25	10	2	5	74	77	-7	5	5	58	-49	1	7	5	20	13
10	12	4	59	-55	-5	17	4	57	60	12	2	5	23	28	-5	5	5	220	-223	3	7	5	138	-132
-9	13	4	94	-98	-3	17	4	39	44	-15	3	5	23	-23	-3	5	5	250	-236	5	7	5	200	-200
-7	13	4	84	-86	-1	17	4	43	43	-13	3	5	39	-37	-1	5	5	78	66	7	7	5	64	-65
-5	13	4	37	37	1	17	4	34	-34	-11	3	5	88	-92	1	5	5	147	139	9	7	5	19	-20
-3	13	4	30	27	3	17	4	35	-33	-9	3	5	49	-51	3	5	5	124	120	11	7	5	100	99
-1	13	4	29	26	5	17	4	41	-40	-7	3	5	43	-48	5	5	5	139	-135	13	7	5	13	16
1	13	4	21	22	-4	18	4	39	-34	-5	3	5	159	-148	7	5	5	78	-79	-14	8	5	23	-24
3	13	4	66	65	0	18	4	21	-22	-3	3	5	171	-182	9	5	5	39	-36	-12	8	5	33	-35
5	13	4	40	37	-11	1	5	55	58	-1	3	5	16	-17	11	5	5	58	51	-10	8	5	116	120

H	K	L	FO	FC	H	K	L	FO	FC	H	K	L	FO	FC	H	K	L	FO	FC	H	K	L	FO	FC
-8	8	5	36	33	-5	11	5	75	76	6	14	5	74	71	-15	1	6	20	18	-1	3	6	163	-159
-6	8	5	20	-13	-3	11	5	68	67	8	14	5	34	32	-11	1	6	22	-21	1	3	6	414	-394
-4	8	5	178	-172	-1	11	5	51	46	-9	15	5	50	-50	-9	1	6	173	-183	3	3	6	261	-263
0	8	5	153	148	1	11	5	47	-43	-7	15	5	83	-83	-7	1	6	148	-155	5	3	6	106	-108
2	8	5	173	180	3	11	5	87	82	-1	15	5	11	-8	-3	1	6	229	-221	7	3	6	88	84
6	8	5	63	-60	5	11	5	36	-36	3	15	5	28	29	-1	1	6	119	107	13	3	6	43	41
12	8	5	61	60	7	11	5	43	39	5	15	5	29	26	1	1	6	370	-361	15	3	6	28	30
14	8	5	21	-20	9	11	5	22	22	7	15	5	29	26	3	1	6	47	50	-14	4	6	39	37
-13	9	5	31	-29	-12	12	5	25	26	-8	16	5	50	-48	5	1	6	195	190	-12	4	6	50	-47
-11	9	5	46	49	-10	12	5	34	37	-6	16	5	39	-39	7	1	6	35	36	-10	4	6	29	-30
-7	9	5	36	-34	-8	12	5	30	33	-2	16	5	24	-24	9	1	6	147	-153	-6	4	6	130	127
-5	9	5	79	-81	-6	12	5	89	87	4	16	5	38	38	11	1	6	61	-59	-4	4	6	225	219
-3	9	5	157	-153	-4	12	5	26	27	6	16	5	39	40	13	1	6	37	-32	-2	4	6	270	249
-1	9	5	137	129	-2	12	5	12	5	-1	17	5	48	-46	15	1	6	16	12	0	4	6	203	-197
1	9	5	207	202	0	12	5	38	-38	1	17	5	71	-62	-14	2	6	73	72	4	4	6	128	122
3	9	5	139	135	2	12	5	22	-21	3	17	5	53	-54	-12	2	6	46	51	6	4	6	82	78
7	9	5	45	-39	4	12	5	25	-26	0	18	5	40	-38	-10	2	6	66	71	8	4	6	167	173
9	9	5	19	-18	6	12	5	47	-45	2	18	5	47	-50	-8	2	6	95	-97	10	4	6	34	-32
-12	10	5	36	-33	8	12	5	33	32	-14	0	6	16	20	-6	2	6	68	76	-15	5	6	21	25
-10	10	5	29	-30	-9	13	5	28	29	-12	0	6	46	-46	-4	2	6	60	56	-13	5	6	26	20
-8	10	5	84	-83	-7	13	5	43	41	-10	0	6	61	-58	0	2	6	85	-74	-11	5	6	85	-88
-6	10	5	10	-13	-1	13	5	89	-87	-8	0	6	259	-266	2	2	6	155	-172	-9	5	6	61	-62
-4	10	5	60	-57	1	13	5	165	-173	-6	0	6	51	53	6	2	6	47	56	-7	5	6	49	-50
-2	10	5	66	75	3	13	5	78	-75	-4	0	6	279	285	8	2	6	42	38	-5	5	6	24	22
0	10	5	90	87	5	13	5	71	-71	-2	0	6	125	-115	10	2	6	46	-45	-3	5	6	163	166
2	10	5	131	130	7	13	5	23	-25	0	0	6	69	-72	12	2	6	43	39	-1	5	6	177	170
4	10	5	72	75	9	13	5	12	-13	2	0	6	107	-95	14	2	6	16	16	1	5	6	56	45
6	10	5	48	46	-10	14	5	29	-33	4	0	6	178	183	-15	3	6	42	40	3	5	6	85	92
8	10	5	84	81	-8	14	5	38	-38	6	0	6	140	137	-13	3	6	87	88	5	5	6	58	-57
12	10	5	14	18	-6	14	5	37	40	8	0	6	30	-30	-11	3	6	27	25	7	5	6	42	46
-13	11	5	12	7	-4	14	5	67	66	10	0	6	186	-187	-9	3	6	33	-29	9	5	6	12	-11
-11	11	5	18	19	-2	14	5	70	70	12	0	6	94	-91	-7	3	6	35	32	11	5	6	48	-49
-9	11	5	28	24	2	14	5	19	-16	14	0	6	60	-58	-5	3	6	117	110	-12	6	6	45	-47
-7	11	5	38	37	4	14	5	45	44	-17	1	6	38	-38	-3	3	6	77	-76	-10	6	6	59	-57

H	K	L	FO	FC	H	K	L	FO	FC	H	K	L	FO	FC	H	K	L	FO	FC	H	K	L	FO	FC
-8	6	6	59	-58	1	9	6	43	41	8	12	6	31	-32	-13	1	7	67	-64	-1	3	7	82	-78
-4	6	6	63	63	3	9	6	54	-53	10	12	6	22	24	-11	1	7	61	-63	1	3	7	102	-89
-2	6	6	347	342	5	9	6	84	-83	-9	13	6	44	46	-9	1	7	94	-94	3	3	7	40	-44
0	6	6	295	279	7	9	6	96	-94	-7	13	6	22	24	-7	1	7	34	-37	5	3	7	129	123
2	6	6	325	314	9	9	6	20	21	-5	13	6	108	-112	-5	1	7	30	28	7	3	7	68	70
4	6	6	130	132	11	9	6	77	69	-3	13	6	51	-52	-3	1	7	105	-92	9	3	7	16	20
8	6	6	74	82	-14	10	6	49	-48	-1	13	6	37	-39	-1	1	7	54	-54	13	3	7	28	-23
14	6	6	12	-6	-10	10	6	54	46	1	13	6	51	51	1	1	7	62	56	15	3	7	34	29
-13	7	6	19	-17	-8	10	6	53	54	3	13	6	43	-41	3	1	7	123	124	-16	4	7	14	19
-9	7	6	98	97	-6	10	6	82	-81	5	13	6	86	-88	5	1	7	149	157	-14	4	7	50	50
-7	7	6	30	29	-4	10	6	95	-101	7	13	6	57	-55	7	1	7	28	-31	-12	4	7	120	126
-5	7	6	40	41	-2	10	6	69	-67	9	13	6	30	31	9	1	7	105	-108	-10	4	7	23	29
-1	7	6	156	-147	0	10	6	150	157	-8	14	6	83	84	11	1	7	69	-71	-8	4	7	64	63
1	7	6	128	-115	2	10	6	127	121	-6	14	6	21	-18	13	1	7	58	-58	-6	4	7	22	21
3	7	6	88	-90	4	10	6	17	19	-4	14	6	54	-51	-12	2	7	22	22	-2	4	7	159	-158
5	7	6	91	-95	6	10	6	26	-27	-2	14	6	51	-47	-10	2	7	41	-41	0	4	7	369	-360
7	7	6	51	-48	8	10	6	89	-88	2	14	6	55	-50	-8	2	7	23	-23	2	4	7	296	-287
-12	8	6	19	17	10	10	6	39	33	4	14	6	117	-115	-6	2	7	196	197	4	4	7	72	61
-10	8	6	93	90	-13	11	6	67	-63	6	14	6	61	-61	-4	2	7	180	187	6	4	7	177	177
-8	8	6	89	92	-11	11	6	43	-41	-9	15	6	18	21	-2	2	7	78	72	8	4	7	16	17

-6	8	6	106	99	-7	11	6	28	-29	-7	15	6	21	14	0	2	7	236	225	10	4	7	68	70
-4	8	6	67	-60	-5	11	6	67	-70	-5	15	6	27	-26	2	2	7	22	-17	12	4	7	23	-27
-2	8	6	91	-95	-3	11	6	73	-78	-3	15	6	18	18	4	2	7	100	105	14	4	7	36	34
2	8	6	14	-10	-1	11	6	24	27	-1	15	6	26	-32	6	2	7	132	128	-15	5	7	24	25
6	8	6	17	18	1	11	6	164	160	1	15	6	18	21	8	2	7	67	-70	-13	5	7	86	84
10	8	6	71	68	3	11	6	76	74	5	15	6	15	-14	10	2	7	15	-12	-9	5	7	44	-49
12	8	6	44	42	5	11	6	21	-18	-6	16	6	14	-16	12	2	7	84	-87	-5	5	7	22	22
-13	9	6	13	-15	-10	12	6	24	-18	-2	16	6	34	34	-15	3	7	15	10	-3	5	7	110	112
-11	9	6	77	74	-8	12	6	69	65	0	16	6	54	54	-13	3	7	34	35	-1	5	7	105	-106
-9	9	6	108	105	-6	12	6	29	-26	2	16	6	52	52	-11	3	7	31	30	1	5	7	158	-156
-7	9	6	15	12	-4	12	6	74	-69	4	16	6	27	29	-9	3	7	87	-86	3	5	7	63	-52
-5	9	6	77	-75	-2	12	6	26	-27	-5	17	6	35	-34	-7	3	7	65	-67	5	5	7	161	167
-3	9	6	170	-162	0	12	6	126	130	1	17	6	77	78	-5	3	7	25	28	7	5	7	126	129
-1	9	6	72	-76	2	12	6	55	57	-15	1	7	42	-42	-3	3	7	91	80	9	5	7	18	-26

H	K	L	FO	FC	H	K	L	FO	FC	H	K	L	FO	FC	H	K	L	FO	FC	H	K	L	FO	FC
11	5	7	15	-15	-2	8	7	38	31	-7	11	7	24	23	6	14	7	20	-21	-9	1	8	101	105
-14	6	7	24	25	0	8	7	170	-164	-1	11	7	60	-60	-9	15	7	56	59	-7	1	8	166	171
-12	6	7	52	49	2	8	7	73	-72	3	11	7	93	-95	-7	15	7	35	34	-5	1	8	101	-103
-10	6	7	86	-87	4	8	7	71	-72	5	11	7	31	34	-5	15	7	56	-57	-3	1	8	46	-42
-8	6	7	60	-56	6	8	7	59	57	7	11	7	21	-18	-3	15	7	42	-43	-1	1	8	36	38
-6	6	7	43	-41	10	8	7	52	-52	11	11	7	26	-23	-1	15	7	29	-26	1	1	8	369	380
-4	6	7	303	295	12	8	7	31	-30	-12	12	7	22	-23	1	15	7	18	-17	3	1	8	69	70
-2	6	7	254	255	-13	9	7	40	39	-10	12	7	30	-31	5	15	7	18	-20	5	1	8	41	-41
0	6	7	52	-49	-11	9	7	39	33	-8	12	7	13	-10	-8	16	7	57	56	7	1	8	17	-14
2	6	7	12	6	-9	9	7	19	22	-6	12	7	23	22	-4	16	7	27	-27	11	1	8	75	79
6	6	7	74	79	-7	9	7	33	35	-4	12	7	15	-15	-2	16	7	22	-23	13	1	8	20	22
8	6	7	18	11	-5	9	7	63	58	-2	12	7	51	-53	0	16	7	22	23	-14	2	8	71	-69
10	6	7	52	-47	-3	9	7	86	95	0	12	7	49	50	2	16	7	31	34	-12	2	8	42	-44
12	6	7	48	-44	-1	9	7	138	-130	2	12	7	57	62	-3	17	7	23	22	-8	2	8	135	137
14	6	7	24	26	1	9	7	73	-73	4	12	7	66	59	-1	17	7	68	67	-6	2	8	122	-122
-15	7	7	17	18	3	9	7	52	-46	6	12	7	30	34	1	17	7	82	80	-4	2	8	101	-120
-13	7	7	28	29	5	9	7	71	73	8	12	7	49	-51	3	17	7	57	54	-2	2	8	91	-78
-11	7	7	40	-39	7	9	7	24	19	10	12	7	25	-25	-16	0	8	60	55	0	2	8	83	81
-9	7	7	135	-133	11	9	7	25	-21	-11	13	7	20	-21	-14	0	8	17	20	2	2	8	245	241
-7	7	7	65	-66	-14	10	7	15	12	-7	13	7	57	57	-12	0	8	36	32	4	2	8	86	-93
-5	7	7	73	73	-12	10	7	37	37	-5	13	7	20	19	-10	0	8	26	28	6	2	8	147	-149
-3	7	7	459	455	-10	10	7	53	-50	-3	13	7	19	17	-8	0	8	77	81	8	2	8	139	-139
-1	7	7	149	141	-8	10	7	58	-58	-1	13	7	52	51	-6	0	8	317	-316	10	2	8	17	22
1	7	7	128	132	-6	10	7	65	-64	1	13	7	79	80	-4	0	8	140	-129	12	2	8	24	23
3	7	7	73	-68	-4	10	7	31	-32	3	13	7	52	51	-2	0	8	206	-237	-15	3	8	53	-55
5	7	7	54	57	-2	10	7	131	-134	5	13	7	24	21	0	0	8	60	-73	-13	3	8	77	-79
9	7	7	68	-63	0	10	7	133	-142	7	13	7	30	-26	2	0	8	221	212	-11	3	8	27	-24
11	7	7	85	-82	2	10	7	100	-103	9	13	7	15	-16	4	0	8	106	-110	-9	3	8	33	30
13	7	7	23	-20	4	10	7	100	-102	-10	14	7	23	23	6	0	8	11	-5	-7	3	8	183	194
-14	8	7	14	15	6	10	7	29	27	-8	14	7	12	14	8	0	8	72	66	-5	3	8	51	53
-10	8	7	145	-151	8	10	7	29	30	-6	14	7	18	-17	10	0	8	168	169	-3	3	8	112	112
-8	8	7	77	-74	10	10	7	47	46	-4	14	7	48	-50	12	0	8	117	112	-1	3	8	244	232
-6	8	7	108	-108	-13	11	7	20	-16	-2	14	7	28	-25	14	0	8	23	21	1	3	8	283	270
-4	8	7	59	57	-9	11	7	59	-64	4	14	7	57	-52	-11	1	8	59	59	3	3	8	21	25

H	K	L	FO	FC	H	K	L	FO	FC	H	K	L	FO	FC	H	K	L	FO	FC	H	K	L	FO	FC
5	3	8	16	-17	-2	6	8	199	-188	-1	9	8	23	20	-8	12	8	78	-81	0	16	8	49	-47
7	3	8	140	-139	0	6	8	141	-133	3	9	8	55	56	-4	12	8	26	23	2	16	8	59	-65
9	3	8	77	-78	2	6	8	34	-33	5	9	8	51	-54	0	12	8	76	-71	4	16	8	15	15
13	3	8	39	-43	4	6	8	91	87	7	9	8	25	-24	2	12	8	132	-136	-3	17	8	50	-50
-14	4	8	62	-64	6	6	8	62	60	9	9	8	63	-60	6	12	8	69	66	-1	17	8	21	-25
-12	4	8	47	-46	8	6	8	41	44	11	9	8	60	-58	8	12	8	33	36	1	17	8	19	-17
-10	4	8	46	-51	10	6	8	74	67	-14	10	8	52	54	10	12	8	40	-40	3	17	8	28	29
-8	4	8	39	36	14	6	8	25	24	-12	10	8	39	35	-11	13	8	16	-14	-15	1	9	30	27
-6	4	8	65	68	-11	7	8	17	-21	-10	10	8	18	-19	-7	13	8	13	6	-11	1	9	26	-31
-4	4	8	78	-73	-9	7	8	54	-49	-8	10	8	76	-79	-5	13	8	112	107	-9	1	9	22	21
-2	4	8	75	64	-5	7	8	42	40	-6	10	8	59	-61	-3	13	8	68	77	-7	1	9	61	-62
0	4	8	23	-24	-3	7	8	110	108	-4	10	8	39	36	-1	13	8	111	111	-5	1	9	98	-108
2	4	8	70	-69	-1	7	8	25	28	-2	10	8	29	-30	1	13	8	29	-31	-3	1	9	215	-197
4	4	8	27	-24	1	7	8	44	-45	0	10	8	27	-30	3	13	8	53	55	-1	1	9	154	-167
6	4	8	26	28	3	7	8	81	-74	2	10	8	32	-34	5	13	8	64	60	1	1	9	56	51
10	4	8	79	85	11	7	8	19	-19	4	10	8	16	10	7	13	8	19	19	3	1	9	85	92
12	4	8	28	-28	13	7	8	19	-20	6	10	8	54	55	9	13	8	35	-33	5	1	9	97	102

-11	5	8	56	62	-12	8	8	15	-13	8	10	8	46	44	-10	14	8	22	-20	7	1	9	156	164
-7	5	8	50	44	-10	8	8	48	-46	10	10	8	33	-31	-8	14	8	27	-28	9	1	9	48	56
-5	5	8	151	-148	-8	8	8	88	-88	12	10	8	35	29	-6	14	8	71	70	11	1	9	27	29
-3	5	8	222	-209	-6	8	8	19	16	-13	11	8	57	58	-4	14	8	83	82	-16	2	9	13	17
-1	5	8	284	-268	-4	8	8	129	135	-11	11	8	32	33	-2	14	8	78	79	-14	2	9	42	41
1	5	8	131	-126	-2	8	8	152	143	-9	11	8	32	-29	0	14	8	63	60	-10	2	9	87	88
3	5	8	144	-138	0	8	8	24	-28	2	14	8	79	-79	2	14	8	43	-46	-8	2	9	18	20
5	5	8	20	20	2	8	8	20	-19	-5	11	8	29	34	4	14	8	49	50	-6	2	9	155	-154
7	5	8	22	-25	4	8	8	47	-48	-3	11	8	73	70	8	14	8	14	-13	-4	2	9	175	-186
9	5	8	21	22	8	8	8	38	-37	-1	11	8	18	-19	-5	15	8	58	61	-2	2	9	199	-195
13	5	8	19	-20	10	8	8	55	-54	1	11	8	121	-118	-3	15	8	28	27	0	2	9	80	76
-14	6	8	27	-31	12	8	8	34	-30	3	11	8	16	13	1	15	8	89	-89	2	2	9	176	180
-12	6	8	31	32	-13	9	8	21	24	5	11	8	57	64	3	15	8	37	-40	6	2	9	22	-23
-10	6	8	41	41	-9	9	8	13	-13	7	11	8	98	93	7	15	8	30	30	10	2	9	26	29
-8	6	8	10	-8	-7	9	8	88	-87	9	11	8	47	51	-6	16	8	16	13	12	2	9	44	44
-6	6	8	25	-24	-5	9	8	63	62	-12	12	8	24	22	-4	16	8	21	-21	14	2	9	14	-15
-4	6	8	198	-196	-3	9	8	150	151	-10	12	8	22	-20	-2	16	8	34	-31	-15	3	9	28	-21

H	K	L	FO	FC	H	K	L	FO	FC	H	K	L	FO	FC	H	K	L	FO	FC	H	K	L	FO	FC
-13	3	9	54	-56	1	5	9	52	42	-4	8	9	42	-48	3	11	9	29	32	1	15	9	51	-52
-11	3	9	67	-68	3	5	9	105	102	-2	8	9	55	-51	5	11	9	20	-19	3	15	9	19	-28
-9	3	9	89	91	5	5	9	65	-62	2	8	9	17	10	9	11	9	16	16	-6	16	9	20	21
-7	3	9	97	-99	7	5	9	81	-83	4	8	9	88	80	11	11	9	31	32	-4	16	9	50	53
-5	3	9	168	-172	-14	6	9	20	-17	6	8	9	93	-86	-10	12	9	33	35	0	16	9	75	-73
-3	3	9	191	-189	-12	6	9	46	-46	8	8	9	45	45	-6	12	9	25	-25	2	16	9	88	-87
-1	3	9	113	111	-8	6	9	24	24	10	8	9	30	31	-4	12	9	35	-30	4	16	9	27	-29
1	3	9	234	216	-6	6	9	20	13	12	8	9	18	15	-2	12	9	72	-75	-1	17	9	25	-24
3	3	9	160	158	-4	6	9	247	-239	-13	9	9	35	-37	2	12	9	23	28	1	17	9	67	-70
5	3	9	148	-147	-2	6	9	125	-120	-11	9	9	37	-34	4	12	9	38	33	-16	0	10	45	-44
7	3	9	46	-54	0	6	9	29	25	-9	9	9	80	75	6	12	9	74	76	-14	0	10	40	41
9	3	9	44	-45	2	6	9	80	-73	-7	9	9	118	116	8	12	9	57	55	-10	0	10	119	-123
11	3	9	38	36	4	6	9	50	49	-5	9	9	100	101	10	12	9	14	-14	-8	0	10	110	-116
13	3	9	33	37	6	6	9	127	-135	-1	9	9	76	68	-9	13	9	24	-23	-6	0	10	56	-54
-14	4	9	31	-29	8	6	9	11	-12	3	9	9	22	-22	-7	13	9	81	-82	-4	0	10	129	145
-12	4	9	74	-81	10	6	9	50	46	5	9	9	51	-41	-5	13	9	53	-53	-2	0	10	136	125
-10	4	9	86	84	12	6	9	34	32	7	9	9	59	-62	-3	13	9	57	-55	0	0	10	162	-163
-8	4	9	145	145	-9	7	9	65	62	-10	10	9	42	41	-1	13	9	42	-40	2	0	10	485	-497
-6	4	9	114	118	-7	7	9	39	-34	-8	10	9	67	62	1	13	9	36	-36	4	0	10	189	-197
-4	4	9	84	88	-5	7	9	95	-94	-6	10	9	52	53	3	13	9	42	42	6	0	10	221	-221
-2	4	9	10	8	-3	7	9	273	-270	-4	10	9	53	48	5	13	9	48	45	8	0	10	20	-19
0	4	9	167	160	-1	7	9	12	12	-2	10	9	59	58	7	13	9	58	53	10	0	10	77	-77
2	4	9	54	54	1	7	9	16	-5	0	10	9	156	154	-10	14	9	24	21	12	0	10	51	-48
4	4	9	66	-66	3	7	9	83	78	2	10	9	79	76	-8	14	9	23	-22	-15	1	10	25	-26
6	4	9	220	-217	5	7	9	28	26	4	10	9	16	-13	-6	14	9	16	-21	-13	1	10	57	58
8	4	9	104	-99	7	7	9	22	-20	6	10	9	127	-134	-4	14	9	57	55	-11	1	10	21	-22
10	4	9	36	-37	9	7	9	104	101	8	10	9	43	-42	-2	14	9	25	28	-9	1	10	99	-100
-15	5	9	29	-28	11	7	9	67	66	10	10	9	39	-41	0	14	9	34	33	-7	1	10	53	-49
-13	5	9	90	-88	13	7	9	27	27	-11	11	9	17	15	8	14	9	28	-28	-5	1	10	245	242
-11	5	9	46	-48	-14	8	9	27	-28	-9	11	9	63	61	-9	15	9	35	-33	-3	1	10	123	134
-9	5	9	76	76	-12	8	9	37	-38	-7	11	9	22	-17	-7	15	9	21	-16	-1	1	10	177	173
-7	5	9	19	19	-10	8	9	39	36	-3	11	9	39	-40	-5	15	9	49	47	1	1	10	184	-186
-5	5	9	31	29	-8	8	9	50	50	-1	11	9	53	58	-3	15	9	61	66	3	1	10	92	-93
-3	5	9	122	-115	-6	8	9	63	65	1	11	9	96	96	-1	15	9	42	37	5	1	10	22	20

H	K	L	FO	FC	H	K	L	FO	FC	H	K	L	FO	FC	H	K	L	FO	FC	H	K	L	FO	FC
7	1	10	45	49	-6	4	10	51	-50	-3	7	10	74	-70	0	10	10	35	-41	-2	14	10	106	-109
9	1	10	55	57	-4	4	10	124	124	-1	7	10	57	-49	2	10	10	27	26	2	14	10	82	84
11	1	10	50	-51	-2	4	10	15	20	1	7	10	77	64	4	10	10	103	-105	6	14	10	39	40
13	1	10	16	14	0	4	10	75	76	3	7	10	49	46	6	10	10	123	-122	-7	15	10	16	16
-14	2	10	67	63	2	4	10	67	-66	5	7	10	40	-34	8	10	10	62	-58	-5	15	10	36	-36
-10	2	10	57	-59	4	4	10	12	-10	7	7	10	18	14	-11	11	10	19	-23	1	15	10	66	67
-8	2	10	87	-90	10	4	10	47	-48	9	7	10	39	44	-9	11	10	56	51	-6	16	10	29	29
-6	2	10	108	-109	-15	5	10	13	-17	11	7	10	32	31	-7	11	10	118	120	-2	16	10	19	15
-2	2	10	22	28	-11	5	10	18	20	-10	8	10	24	-25	-5	11	10	13	15	2	16	10	22	18
0	2	10	125	-114	-9	5	10	100	100	-6	8	10	34	-32	-3	11	10	48	46	4	16	10	31	-32
2	2	10	148	-145	-7	5	10	20	19	-4	8	10	68	-65	-1	11	10	68	72	-1	17	10	39	-41
4	2	10	170	168	-5	5	10	135	136	-2	8	10	19	-19	1	11	10	26	29	-13	1	11	38	37
6	2	10	68	67	-3	5	10	69	65	0	8	10	52	53	3	11	10	16	-15	-7	1	11	84	79
8	2	10	53	54	-1	5	10	21	15	2	8	10	66	65	5	11	10	116	-112	-5	1	11	86	93

10	2	10	49	-53	1	5	10	94	91	4	8	10	44	45	7	11	10	104	-102	-3	1	11	197	190
12	2	10	46	-50	3	5	10	19	-20	8	8	10	60	59	-12	12	10	18	-20	-1	1	11	98	99
14	2	10	15	-14	5	5	10	56	49	10	8	10	51	48	-8	12	10	74	74	1	1	11	232	-231
-15	3	10	17	21	7	5	10	32	32	-13	9	10	15	-17	-4	12	10	28	-29	3	1	11	158	-158
-13	3	10	42	43	9	5	10	48	-50	-11	9	10	40	-41	-2	12	10	20	-20	5	1	11	151	-158
-11	3	10	31	-31	11	5	10	12	-9	-9	9	10	21	-19	0	12	10	40	37	7	1	11	23	-27
-9	3	10	65	-66	13	5	10	26	24	-7	9	10	49	49	2	12	10	44	40	9	1	11	21	22
-7	3	10	206	-207	-10	6	10	127	124	-5	9	10	83	-84	4	12	10	65	-62	-14	2	11	28	26
-5	3	10	62	-60	-8	6	10	126	130	-3	9	10	69	-68	6	12	10	51	-52	-12	2	11	64	59
-3	3	10	97	-104	-6	6	10	193	191	1	9	10	61	57	8	12	10	48	-47	-8	2	11	48	47
1	3	10	72	-71	-4	6	10	119	108	3	9	10	137	139	-9	13	10	35	36	-4	2	11	71	62
3	3	10	28	28	-2	6	10	20	17	5	9	10	64	60	-7	13	10	28	30	-2	2	11	215	214
5	3	10	160	164	4	6	10	33	-31	9	9	10	69	64	-5	13	10	98	-95	0	2	11	82	-76
7	3	10	160	170	6	6	10	32	-25	11	9	10	28	27	-3	13	10	84	-80	2	2	11	124	-131
9	3	10	41	41	8	6	10	73	-73	-12	10	10	22	-23	-1	13	10	57	-62	4	2	11	103	-100
11	3	10	13	-13	10	6	10	65	-61	-10	10	10	26	-26	1	13	10	42	46	6	2	11	52	-51
-14	4	10	50	53	-11	7	10	11	-4	-8	10	10	39	39	3	13	10	70	73	12	2	11	20	-19
-12	4	10	43	45	-9	7	10	20	-18	-6	10	10	63	56	5	13	10	18	19	-13	3	11	33	30
-10	4	10	87	88	-7	7	10	93	-96	-4	10	10	67	-61	-6	14	10	60	-57	-11	3	11	12	10
-8	4	10	51	-56	-5	7	10	65	-68	-2	10	10	74	-73	-4	14	10	116	-114	-9	3	11	74	-77

H	K	L	FO	FC	H	K	L	FO	FC	H	K	L	FO	FC	H	K	L	FO	FC	H	K	L	FO	FC
-7	3	11	46	-39	-8	6	11	52	-50	-11	9	11	26	25	0	12	11	34	-28	6	0	12	110	114
-5	3	11	71	-73	-6	6	11	46	47	-9	9	11	120	-124	2	12	11	47	-48	8	0	12	50	-51
-3	3	11	187	183	-4	6	11	129	127	-7	9	11	74	-78	4	12	11	93	-92	10	0	12	62	62
-1	3	11	124	120	-2	6	11	79	72	-5	9	11	53	-49	6	12	11	48	-50	12	0	12	29	25
1	3	11	14	-7	0	6	11	67	-68	-3	9	11	35	35	-7	13	11	52	52	-15	1	12	25	26
3	3	11	120	117	2	6	11	20	-17	-1	9	11	67	-64	-5	13	11	15	13	-13	1	12	79	-82
7	3	11	64	72	4	6	11	24	-20	3	9	11	76	-76	-3	13	11	29	31	-11	1	12	17	20
11	3	11	38	-41	6	6	11	116	114	5	9	11	50	53	1	13	11	19	-21	-9	1	12	44	41
-14	4	11	40	44	8	6	11	25	-19	7	9	11	87	86	3	13	11	35	-32	-7	1	12	155	158
-12	4	11	48	53	12	6	11	14	-13	11	9	11	20	-19	5	13	11	60	-60	-5	1	12	37	34
-10	4	11	82	-87	-13	7	11	25	24	-10	10	11	51	-47	7	13	11	24	-26	-3	1	12	146	-146
-8	4	11	173	-175	-11	7	11	97	100	-8	10	11	94	-89	-4	14	11	42	-37	-1	1	12	30	-37
-6	4	11	120	-118	-9	7	11	32	29	-6	10	11	59	-57	-2	14	11	31	-30	1	1	12	120	118
-4	4	11	39	36	-7	7	11	60	61	-4	10	11	73	-69	0	14	11	18	12	3	1	12	50	54
-2	4	11	201	189	-5	7	11	84	81	-2	10	11	44	44	2	14	11	86	85	7	1	12	29	-28
0	4	11	24	-19	-3	7	11	73	72	0	10	11	16	14	4	14	11	27	26	9	1	12	48	-49
4	4	11	42	39	-1	7	11	136	-132	2	10	11	99	100	-5	15	11	23	-26	11	1	12	56	56
6	4	11	112	117	1	7	11	115	-109	4	10	11	65	62	-3	15	11	43	-48	13	1	12	15	-17
8	4	11	51	46	3	7	11	165	-165	6	10	11	107	106	1	15	11	64	63	-16	2	12	19	21
12	4	11	56	-54	5	7	11	26	-30	8	10	11	37	39	3	15	11	67	65	-14	2	12	49	-44
-15	5	11	22	24	7	7	11	13	12	-9	11	11	51	-47	5	15	11	16	14	-12	2	12	42	-39
-13	5	11	25	26	9	7	11	76	-79	-7	11	11	20	15	0	16	11	35	39	-10	2	12	20	18
-9	5	11	85	-86	-14	8	11	18	-16	-5	11	11	77	-77	2	16	11	55	58	-8	2	12	146	150
-7	5	11	61	-65	-12	8	11	24	26	-3	11	11	16	-11	-16	0	12	19	22	-6	2	12	116	116
-5	5	11	11	9	-8	8	11	45	-47	1	11	11	57	-56	-14	0	12	60	-59	-4	2	12	87	-79
-3	5	11	209	202	-6	8	11	27	20	3	11	11	64	-61	-12	0	12	91	-85	-2	2	12	89	-94
1	5	11	93	-91	-4	8	11	69	65	5	11	11	63	-60	-10	0	12	60	-61	0	2	12	106	-99
3	5	11	28	-28	-2	8	11	54	48	7	11	11	41	-41	-8	0	12	55	55	2	2	12	21	26
5	5	11	85	86	0	8	11	110	-107	9	11	11	32	-29	-6	0	12	64	72	8	2	12	22	-25
7	5	11	137	128	2	8	11	94	-87	-10	12	11	18	-21	-4	0	12	155	-160	10	2	12	45	47
11	5	11	26	-27	4	8	11	26	-30	-8	12	11	22	18	-2	0	12	50	55	12	2	12	43	40
13	5	11	47	-44	6	8	11	102	104	-6	12	11	43	39	0	0	12	237	255	-11	3	12	72	69
-12	6	11	68	74	8	8	11	31	27	-4	12	11	51	53	2	0	12	342	350	-9	3	12	69	68
-10	6	11	31	30	-13	9	11	18	15	-2	12	11	77	71	4	0	12	156	160	-7	3	12	137	136

H	K	L	FO	FC	H	K	L	FO	FC	H	K	L	FO	FC	H	K	L	FO	FC	H	K	L	FO	FC
-5	3	12	31	-34	11	5	12	41	-38	-5	9	12	92	87	-5	13	12	36	41	8	2	13	70	-69
-3	3	12	40	-44	-10	6	12	50	-50	-1	9	12	64	-65	-3	13	12	70	69	12	2	13	26	-22
-1	3	12	144	-132	-8	6	12	69	-66	1	9	12	144	-138	1	13	12	122	-113	-13	3	13	54	-49
1	3	12	35	-40	-6	6	12	26	-27	3	9	12	147	-142	3	13	12	71	-73	-11	3	13	34	-35
3	3	12	56	-59	-4	6	12	40	39	5	9	12	40	41	-4	14	12	64	68	-9	3	13	100	99
5	3	12	182	-181	-2	6	12	104	107	7	9	12	41	43	-2	14	12	22	21	-7	3	13	120	122
7	3	12	82	-83	0	6	12	47	49	9	9	12	22	22	2	14	12	70	-70	-5	3	13	101	99
9	3	12	22	-18	2	6	12	117	115	-10	10	12	12	-12	-7	15	12	48	-50	-3	3	13	103	-106
11	3	12	57	55	4	6	12	67	65	-8	10	12	52	-49	-5	15	12	24	-27	-1	3	13	50	-48
13	3	12	44	40	6	6	12	27	32	-6	10	12	16	19	-1	15	12	29	28	1	3	13	75	-63
-12	4	12	15	11	8	6	12	11	13	-4	10	12	93	96	1	15	12	27	-27	5	3	13	44	44

-10	4	12	43	48	10	6	12	35	-30	-2	10	12	24	24	3	15	12	20	-23	7	3	13	68	-68
-8	4	12	62	59	12	6	12	40	-39	0	10	12	31	30	-2	16	12	15	17	11	3	13	13	20
-6	4	12	26	-20	-7	7	12	39	-42	2	10	12	36	-39	0	16	12	44	49	-12	4	13	20	-21
-4	4	12	120	-115	-5	7	12	86	-83	4	10	12	60	58	-13	1	13	53	-54	-10	4	13	52	50
-2	4	12	141	137	-3	7	12	21	20	6	10	12	129	122	-11	1	13	53	-55	-8	4	13	71	70
0	4	12	38	32	-1	7	12	20	-23	8	10	12	50	52	-9	1	13	38	-35	-6	4	13	17	18
2	4	12	153	154	5	7	12	17	-17	-9	11	12	42	-42	-7	1	13	22	-26	-4	4	13	90	-90
4	4	12	16	14	7	7	12	16	-19	-7	11	12	81	-78	-5	1	13	62	64	-2	4	13	230	-225
6	4	12	61	-66	9	7	12	16	-19	-5	11	12	23	20	-3	1	13	100	99	0	4	13	56	-49
8	4	12	54	-50	11	7	12	18	-15	-3	11	12	43	39	-1	1	13	226	226	2	4	13	77	-77
10	4	12	22	21	-12	8	12	28	29	-1	11	12	106	107	1	1	13	135	133	4	4	13	39	-39
12	4	12	34	29	-10	8	12	62	61	5	11	12	75	74	3	1	13	80	81	6	4	13	56	-53
-13	5	12	39	-39	-8	8	12	27	-24	7	11	12	21	23	5	1	13	32	36	8	4	13	31	-34
-11	5	12	65	-66	-6	8	12	46	47	-8	12	12	71	-69	7	1	13	25	-29	10	4	13	80	78
-9	5	12	124	-128	-4	8	12	52	51	-6	12	12	65	-62	-14	2	13	42	-38	12	4	13	58	57
-7	5	12	134	-134	-2	8	12	16	-17	-4	12	12	58	56	-12	2	13	79	-79	-11	5	13	51	-47
-5	5	12	182	-182	0	8	12	61	-60	-2	12	12	30	31	-10	2	13	60	-59	-9	5	13	77	80
-3	5	12	44	-46	2	8	12	103	-92	0	12	12	24	23	-8	2	13	27	-28	-7	5	13	57	56
-1	5	12	74	-78	4	8	12	107	-106	2	12	12	46	-44	-6	2	13	40	34	-5	5	13	35	32
1	5	12	32	33	6	8	12	26	-19	6	12	12	25	27	-2	2	13	64	-65	-3	5	13	99	-93
3	5	12	66	67	10	8	12	14	17	8	12	12	41	36	0	2	13	87	75	-1	5	13	32	-30
5	5	12	62	-66	-13	9	12	17	15	-9	13	12	35	28	2	2	13	31	-31	1	5	13	53	38
9	5	12	34	-37	-11	9	12	25	24	-7	13	12	14	3	4	2	13	41	46	5	5	13	88	-86

H	K	L	FO	FC	H	K	L	FO	FC	H	K	L	FO	FC	H	K	L	FO	FC	H	K	L	FO	FC
7	5	13	63	-65	4	8	13	45	44	-3	13	13	36	34	-2	2	14	131	134	5	5	14	33	38
9	5	13	41	44	6	8	13	69	-73	-1	13	13	70	68	0	2	14	68	66	7	5	14	17	19
11	5	13	37	37	-13	9	13	29	29	1	13	13	14	13	2	2	14	106	-115	9	5	14	84	88
-14	6	13	25	-21	-9	9	13	87	85	-2	14	13	28	-25	6	2	14	52	56	11	5	14	34	32
-12	6	13	65	-64	-5	9	13	23	-24	0	14	13	51	-49	8	2	14	48	47	-14	6	14	44	39
-10	6	13	21	-23	-3	9	13	93	-91	2	14	13	60	-57	12	2	14	36	-32	-12	6	14	50	46
-8	6	13	79	79	-1	9	13	69	-62	1	15	13	44	-46	-15	3	14	31	-29	-10	6	14	20	22
-6	6	13	80	-79	1	9	13	17	15	3	15	13	23	-23	-9	3	14	39	-39	-6	6	14	13	14
-4	6	13	103	-100	3	9	13	34	-35	-12	0	14	65	61	-7	3	14	112	-109	-2	6	14	32	-31
-2	6	13	143	-136	5	9	13	28	-29	-6	0	14	244	-254	-5	3	14	96	91	0	6	14	69	-66
0	6	13	28	26	7	9	13	49	-47	-4	0	14	113	-116	-3	3	14	172	172	2	6	14	127	-124
2	6	13	106	108	9	9	13	12	15	-2	0	14	176	-183	-1	3	14	126	126	4	6	14	25	-23
4	6	13	99	100	-10	10	13	49	45	0	0	14	104	-110	1	3	14	70	63	8	6	14	41	44
6	6	13	100	-97	-8	10	13	98	95	2	0	14	162	-161	3	3	14	31	-24	10	6	14	76	71
8	6	13	49	-49	-6	10	13	47	39	6	0	14	73	69	5	3	14	24	20	-13	7	14	24	-23
-13	7	13	35	-35	-2	10	13	121	-114	8	0	14	74	71	7	3	14	40	-43	-11	7	14	25	-23
-11	7	13	95	-98	0	10	13	43	-42	10	0	14	13	-15	9	3	14	19	-21	-7	7	14	57	61
-9	7	13	36	35	2	10	13	80	-72	12	0	14	19	23	11	3	14	77	-73	-5	7	14	32	30
-7	7	13	20	15	4	10	13	23	24	-13	1	14	84	85	-12	4	14	43	41	1	7	14	72	73
-5	7	13	48	-50	-7	11	13	30	29	-11	1	14	35	36	-10	4	14	25	-27	3	7	14	29	32
-3	7	13	48	-48	-5	11	13	57	60	-9	1	14	61	56	-8	4	14	34	-36	7	7	14	16	-17
-1	7	13	13	-11	-1	11	13	31	30	-7	1	14	117	-111	-6	4	14	14	14	-12	8	14	44	-44
1	7	13	218	210	1	11	13	54	56	-5	1	14	13	-17	-4	4	14	48	46	-8	8	14	35	35
3	7	13	189	180	3	11	13	27	22	-3	1	14	46	44	0	4	14	57	56	-6	8	14	15	12
5	7	13	18	16	5	11	13	80	80	-1	1	14	22	-34	2	4	14	116	-106	-2	8	14	14	8
7	7	13	82	-81	-8	12	13	29	-24	1	1	14	64	-58	4	4	14	21	18	0	8	14	82	79
9	7	13	38	-39	-6	12	13	16	-13	3	1	14	86	-90	10	4	14	26	24	2	8	14	157	156
11	7	13	46	-48	-4	12	13	55	54	7	1	14	52	54	-13	5	14	45	45	4	8	14	29	26
-12	8	13	23	-22	-2	12	13	51	53	9	1	14	17	17	-11	5	14	27	23	6	8	14	57	-54
-8	8	13	40	37	0	12	13	73	75	11	1	14	60	-58	-5	5	14	47	53	8	8	14	55	-52
-6	8	13	16	-8	4	12	13	17	17	-10	2	14	68	-74	-3	5	14	55	54	10	8	14	44	-45
-2	8	13	35	-39	-9	13	13	29	-30	-8	2	14	71	-69	-1	5	14	17	16	-11	9	14	39	-38
0	8	13	121	121	-7	13	13	16	-14	-6	2	14	79	-78	1	5	14	93	-83	-9	9	14	38	38
2	8	13	129	119	-5	13	13	34	36	-4	2	14	124	130	3	5	14	60	-61	-7	9	14	72	68

H	K	L	FO	FC	H	K	L	FO	FC	H	K	L	FO	FC	H	K	L	FO	FC	H	K	L	FO	FC
-5	9	14	17	21	1	13	14	12	8	9	3	15	19	-21	1	7	15	148	-140	-4	12	15	67	-68
-3	9	14	17	19	-6	14	14	38	35	11	3	15	23	-27	3	7	15	42	-48	-2	12	15	58	-59
-1	9	14	46	41	-2	14	14	26	26	-14	4	15	16	-18	5	7	15	16	20	0	12	15	56	-57
1	9	14	93	89	0	14	14	15	18	-10	4	15	18	20	7	7	15	99	99	4	12	15	13	-12
3	9	14	79	70	2	14	14	34	36	-8	4	15	48	-48	9	7	15	67	70	-3	13	15	55	-57
5	9	14	31	-28	-3	15	14	26	-26	-4	4	15	70	69	-12	8	15	52	50	-1	13	15	34	-31
7	9	14	25	-24	-15	1	15	26	25	-2	4	15	128	128	-10	8	15	12	11	1	13	15	18	16
9	9	14	40	-35	-13	1	15	33	36	2	4	15	18	-23	-8	8	15	86	-85	3	13	15	31	30

-12	10	14	34	-31	-11	1	15	52	54	4	4	15	82	-74	-6	8	15	30	-27	-6	14	15	39	33
-8	10	14	40	37	-9	1	15	43	44	8	4	15	32	-31	-4	8	15	34	-33	-12	0	16	45	-50
-6	10	14	13	-15	-7	1	15	56	-53	10	4	15	63	-59	-2	8	15	125	121	-8	0	16	136	140
-4	10	14	81	-76	-5	1	15	111	-117	-13	5	15	22	23	2	8	15	51	-50	-6	0	16	208	209
-2	10	14	116	-116	-3	1	15	83	-81	-11	5	15	68	70	4	8	15	27	-24	-4	0	16	16	-14
0	10	14	85	-79	-1	1	15	113	-109	-9	5	15	40	-37	-9	9	15	76	-78	-2	0	16	123	123
2	10	14	51	45	1	1	15	43	-51	-7	5	15	52	-51	-7	9	15	22	-22	0	0	16	55	57
4	10	14	31	-25	7	1	15	49	47	-3	5	15	152	146	-3	9	15	72	70	2	0	16	68	77
-11	11	14	31	34	9	1	15	23	21	-1	5	15	150	146	-1	9	15	102	96	4	0	16	72	68
-9	11	14	59	60	11	1	15	21	21	3	5	15	20	-15	1	9	15	29	25	6	0	16	109	-107
-7	11	14	60	61	-12	2	15	20	20	5	5	15	59	-61	3	9	15	21	-19	8	0	16	97	-95
-5	11	14	62	-66	-10	2	15	67	70	-12	6	15	60	58	5	9	15	34	-35	10	0	16	49	-50
-3	11	14	141	-137	-8	2	15	40	-42	-10	6	15	30	27	-6	10	15	60	54	-13	1	16	32	-31
-1	11	14	110	-103	-6	2	15	91	-95	-8	6	15	90	-84	-4	10	15	80	77	-9	1	16	23	24
3	11	14	46	47	-2	2	15	68	-71	-6	6	15	31	26	-2	10	15	108	107	-7	1	16	66	69
-8	12	14	28	29	0	2	15	142	-140	-2	6	15	129	121	2	10	15	23	-23	-3	1	16	25	-31
-4	12	14	56	-59	6	2	15	103	107	2	6	15	77	-74	4	10	15	46	-41	-1	1	16	48	55
-2	12	14	67	-68	8	2	15	55	54	6	6	15	67	71	6	10	15	25	-20	3	1	16	139	135
0	12	14	25	-28	-13	3	15	19	15	8	6	15	87	82	8	10	15	33	-27	5	1	16	37	-37
2	12	14	84	80	-11	3	15	46	44	10	6	15	22	24	-7	11	15	30	-25	7	1	16	55	-61
4	12	14	31	30	-9	3	15	44	45	-13	7	15	39	40	-5	11	15	29	-28	9	1	16	14	-15
-9	13	14	31	-31	-5	3	15	121	119	-11	7	15	41	41	-3	11	15	30	-27	-14	2	16	12	13
-7	13	14	36	39	-3	3	15	116	119	-9	7	15	104	-101	-1	11	15	76	-73	-12	2	16	12	-10
-5	13	14	17	19	-1	3	15	27	31	-7	7	15	86	-84	1	11	15	55	-51	-6	2	16	47	40
-3	13	14	19	-16	1	3	15	61	-57	-5	7	15	72	-69	7	11	15	29	32	-4	2	16	110	-114
-1	13	14	30	33	7	3	15	101	100	-3	7	15	19	-15	-6	12	15	21	-23	-2	2	16	36	-36

H	K	L	FO	FC	H	K	L	FO	FC	H	K	L	FO	FC	H	K	L	FO	FC	H	K	L	FO	FC
2	2	16	61	51	-4	6	16	35	35	-4	10	16	64	62	6	2	17	79	-80	-2	6	17	84	-81
6	2	16	30	-35	0	6	16	17	-17	-2	10	16	141	138	8	2	17	42	-43	4	6	17	40	-40
8	2	16	16	-20	2	6	16	53	-48	0	10	16	52	46	-13	3	17	28	30	6	6	17	21	-24
-13	3	16	33	-32	4	6	16	111	-111	2	10	16	28	-25	-7	3	17	13	10	8	6	17	48	-49
-11	3	16	35	-32	6	6	16	45	-45	6	10	16	31	-31	-5	3	17	57	-59	-11	7	17	49	-50
-5	3	16	61	-58	8	6	16	44	-44	-5	11	16	33	35	-3	3	17	18	-28	-9	7	17	33	30
-3	3	16	150	-147	-7	7	16	31	-28	-3	11	16	75	75	-1	3	17	47	-45	-7	7	17	98	92
-1	3	16	109	-105	-5	7	16	19	19	-1	11	16	71	68	3	3	17	72	73	-5	7	17	110	110
3	3	16	141	148	-3	7	16	15	16	1	11	16	16	-14	7	3	17	54	-59	-3	7	17	35	28
5	3	16	73	71	5	7	16	31	29	3	11	16	53	-51	9	3	17	21	25	-1	7	17	82	-80
7	3	16	74	77	7	7	16	50	53	-6	12	16	26	-27	-12	4	17	38	-35	3	7	17	97	-94
9	3	16	23	21	9	7	16	18	25	-4	12	16	65	60	-10	4	17	64	-64	5	7	17	37	-34
-12	4	16	51	-52	-12	8	16	37	33	-2	12	16	33	29	-6	4	17	63	-64	7	7	17	62	-58
-10	4	16	21	17	-10	8	16	17	17	2	12	16	31	-34	-4	4	17	85	-79	-8	8	17	99	101
-6	4	16	76	72	-8	8	16	52	-49	4	12	16	22	-25	-2	4	17	103	-101	-6	8	17	73	71
-4	4	16	25	-31	-6	8	16	81	-79	-7	13	16	61	-63	2	4	17	144	139	-4	8	17	42	40
-2	4	16	119	-117	-4	8	16	88	-84	-5	13	16	21	-21	4	4	17	129	123	-2	8	17	82	-79
0	4	16	89	-87	-2	8	16	47	-47	3	13	16	47	-43	6	4	17	45	44	0	8	17	44	44
2	4	16	29	39	0	8	16	43	-44	-4	14	16	26	22	-11	5	17	50	-50	2	8	17	22	19
6	4	16	16	18	2	8	16	32	-30	-11	1	17	38	36	-9	5	17	31	28	4	8	17	28	28
8	4	16	33	-34	4	8	16	24	23	-9	1	17	79	73	-7	5	17	26	29	-11	9	17	36	-34
10	4	16	30	-32	6	8	16	47	44	-7	1	17	77	78	-5	5	17	47	-47	-9	9	17	16	-14
-13	5	16	67	-64	8	8	16	35	36	-5	1	17	57	61	-3	5	17	125	-121	-5	9	17	39	-37
-11	5	16	29	-26	-11	9	16	34	33	1	1	17	27	21	-1	5	17	93	-88	-3	9	17	62	-57
-7	5	16	48	49	-9	9	16	45	-41	3	1	17	33	45	1	5	17	71	71	-1	9	17	77	-76
-5	5	16	81	82	-7	9	16	73	-73	5	1	17	43	-48	3	5	17	86	87	1	9	17	48	48
-3	5	16	25	30	-5	9	16	65	-65	7	1	17	79	-79	5	5	17	48	48	3	9	17	19	20
-1	5	16	28	-35	-3	9	16	15	16	9	1	17	24	-25	7	5	17	55	-52	5	9	17	40	41
3	5	16	26	-27	-1	9	16	71	70	-14	2	17	27	-22	9	5	17	21	-22	7	9	17	17	-19
5	5	16	62	-63	3	9	16	36	-34	-12	2	17	21	-17	-12	6	17	66	-62	-10	10	17	30	-24
9	5	16	35	-38	5	9	16	20	16	-10	2	17	17	-18	-10	6	17	38	-35	-6	10	17	28	-28
-12	6	16	27	-26	7	9	16	27	28	-8	2	17	59	63	-8	6	17	60	59	-4	10	17	20	-21
-10	6	16	30	30	-8	10	16	26	-26	0	2	17	51	-47	-6	6	17	55	56	0	10	17	26	29
-6	6	16	59	57	-6	10	16	59	-62	2	2	17	35	31	-4	6	17	71	71	2	10	17	35	33

H	K	L	FO	FC	H	K	L	FO	FC	H	K	L	FO	FC	H	K	L	FO	FC	H	K	L	FO	FC
4	10	17	56	55	-13	3	18	35	34	-7	7	18	42	39	-6	2	19	20	-23	-7	7	19	78	-75
6	10	17	27	25	-11	3	18	44	42	-5	7	18	20	18	-4	2	19	23	28	-5	7	19	45	-44
-7	11	17	38	34	-9	3	18	32	31	-1	7	18	41	-41	-2	2	19	79	84	-3	7	19	55	52
-3	11	17	28	28	-7	3	18	32	30	3	7	18	21	-26	0	2	19	107	101	-1	7	19	98	94
1	11	17	34	34	-3	3	18	52	52	5	7	18	15	-15	2	2	19	19	20	1	7	19	24	21

5	11	17	17	16	-1	3	18	35	-41	-8	8	18	41	41	-11	3	19	59	60	3	7	19	43	42
-12	0	18	24	29	1	3	18	102	-92	-6	8	18	85	83	-7	3	19	67	-71	-10	8	19	32	32
-10	0	18	64	-63	3	3	18	130	-129	-4	8	18	51	55	-5	3	19	13	20	-6	8	19	19	-20
-8	0	18	118	-121	5	3	18	61	-59	-2	8	18	24	-21	-3	3	19	28	25	-4	8	19	16	-15
-6	0	18	79	-79	7	3	18	27	-24	0	8	18	56	-50	-1	3	19	126	124	0	8	19	38	-35
-4	0	18	92	96	9	3	18	17	19	2	8	18	37	-36	1	3	19	22	-26	2	8	19	34	-33
-2	0	18	59	58	-12	4	18	37	36	-7	9	18	31	34	3	3	19	55	-65	-9	9	19	32	31
0	0	18	67	73	-8	4	18	27	29	-5	9	18	61	52	5	3	19	37	-37	1	9	19	44	-45
2	0	18	56	-64	-6	4	18	21	-18	-3	9	18	19	-19	7	3	19	13	-12	3	9	19	18	-19
4	0	18	16	-16	0	4	18	17	-15	-1	9	18	28	-28	-12	4	19	27	23	-4	10	19	24	-23
6	0	18	101	111	6	4	18	38	36	3	9	18	25	-28	-10	4	19	63	61	-2	10	19	20	-17
8	0	18	30	30	8	4	18	40	40	5	9	18	31	-31	-8	4	19	25	-26	0	10	19	17	-19
-13	1	18	12	6	-7	5	18	20	-21	-6	10	18	15	18	-2	4	19	45	42	2	10	19	77	-77
-9	1	18	40	-44	-5	5	18	79	-79	-4	10	18	24	-25	0	4	19	48	-46	-5	11	19	19	14
-7	1	18	120	-124	-3	5	18	30	30	-2	10	18	23	-22	2	4	19	110	-102	-1	11	19	30	28
-5	1	18	69	-72	1	5	18	88	86	2	10	18	27	27	4	4	19	81	-79	-10	0	20	52	51
-3	1	18	58	62	3	5	18	107	102	4	10	18	25	28	6	4	19	24	-25	-8	0	20	79	80
-1	1	18	24	26	5	5	18	40	36	-5	11	18	24	25	-11	5	19	57	55	-6	0	20	81	82
1	1	18	34	-32	7	5	18	14	17	-3	11	18	63	-63	-9	5	19	35	34	-4	0	20	51	52
3	1	18	122	-115	-10	6	18	21	-16	-1	11	18	19	-20	-1	5	19	22	13	-2	0	20	85	-87
5	1	18	21	27	-8	6	18	22	-23	3	11	18	33	35	1	5	19	83	-80	0	0	20	110	-120
-12	2	18	69	67	-6	6	18	67	-63	-9	1	19	43	-45	3	5	19	16	-19	2	0	20	13	-13
-10	2	18	19	21	-4	6	18	42	-40	-7	1	19	57	-59	5	5	19	15	-13	4	0	20	17	20
-6	2	18	40	-41	0	6	18	47	48	-1	1	19	51	47	7	5	19	32	35	-11	1	20	53	-51
-4	2	18	73	72	2	6	18	116	109	1	1	19	19	25	-10	6	19	33	32	-9	1	20	44	45
-2	2	18	75	79	4	6	18	63	59	3	1	19	33	35	-8	6	19	36	-36	-7	1	20	63	65
0	2	18	91	83	6	6	18	26	25	5	1	19	40	38	-6	6	19	47	-46	-5	1	20	56	62
2	2	18	49	-46	8	6	18	20	22	-10	2	19	31	-32	-2	6	19	98	96	-3	1	20	54	-56
4	2	18	65	-62	-11	7	18	14	12	-8	2	19	117	-115	0	6	19	62	62	-1	1	20	70	-74

H	K	L	FO	FC	H	K	L	FO	FC	H	K	L	FO	FC	H	K	L	FO	FC	H	K	L	FO	FC
1	1	20	61	-59	-6	6	20	27	-27	-5	3	21	20	26	-10	0	22	23	22	-4	6	22	56	57
3	1	20	59	62	-4	6	20	78	-78	-1	3	21	66	-65	-6	0	22	32	-35	-2	6	22	18	27
-6	2	20	56	58	-2	6	20	53	-54	1	3	21	25	26	-2	0	22	70	74	-4	8	22	41	-43
-4	2	20	25	-25	2	6	20	31	-28	-10	4	21	51	-54	0	0	22	29	31	-2	8	22	29	-34
-2	2	20	64	-65	-3	7	20	39	37	-8	4	21	28	29	2	0	22	14	-18	-7	1	23	20	15
2	2	20	67	66	-1	7	20	33	37	-6	4	21	71	70	4	0	22	60	-62	-5	1	23	20	28
4	2	20	63	65	1	7	20	25	21	-4	4	21	90	84	-9	1	22	20	-17	-3	1	23	32	36
6	2	20	21	-19	-8	8	20	36	-36	-2	4	21	21	21	-7	1	22	12	-9	1	1	23	45	-43
-11	3	20	60	-55	-6	8	20	30	-31	2	4	21	85	78	-5	1	22	69	-69	3	1	23	46	-41
-7	3	20	13	9	-4	8	20	27	26	-9	5	21	28	-27	-3	1	22	25	33	-8	2	23	55	52
-5	3	20	46	43	-2	8	20	64	63	-7	5	21	42	41	-1	1	22	49	52	-6	2	23	20	28
-3	3	20	21	23	0	8	20	19	21	-5	5	21	38	38	-6	2	22	58	-57	-2	2	23	36	36
-1	3	20	104	101	-7	9	20	24	-24	-1	5	21	42	-43	-4	2	22	28	-28	-7	3	23	15	-16
1	3	20	58	50	-3	9	20	33	30	3	5	21	18	19	0	2	22	37	-40	-5	3	23	31	-36
3	3	20	80	79	1	9	20	25	27	5	5	21	26	23	-9	3	22	17	-15	-3	3	23	42	-41
5	3	20	26	20	-4	10	20	22	20	-8	6	21	30	30	-7	3	22	39	-37	-6	4	23	66	-64
7	3	20	38	-37	-7	1	21	27	31	-4	6	21	50	-54	-5	3	22	85	-82	-4	4	23	39	-40
-10	4	20	25	-22	-3	1	21	36	-37	-2	6	21	73	-74	3	3	22	38	-35	-1	5	23	42	42
-8	4	20	49	-51	-1	1	21	89	-89	0	6	21	50	-49	-8	4	22	33	-34	-4	6	23	36	38
-6	4	20	18	18	1	1	21	51	-47	2	6	21	18	19	-6	4	22	30	-39	-2	6	23	48	46
0	4	20	23	25	3	1	21	20	-19	4	6	21	22	17	-4	4	22	33	33	-6	0	24	24	-24
6	4	20	19	-18	5	1	21	25	27	-7	7	21	34	33	-2	4	22	45	46	-2	0	24	36	-38
-11	5	20	36	33	-8	2	21	19	24	-5	7	21	66	-64	0	4	22	20	18	0	0	24	55	55
-9	5	20	13	13	-4	2	21	11	14	-3	7	21	71	-68	-7	5	22	26	31	-5	1	24	30	29
-5	5	20	13	-15	-2	2	21	64	-61	-1	7	21	62	-63	-5	5	22	56	58	-3	1	24	47	-47
-3	5	20	84	-87	0	2	21	77	-78	3	7	21	28	29	-3	5	22	95	94	-4	2	24	47	50
1	5	20	38	-38	2	2	21	15	19	-4	8	21	17	-19	-1	5	22	40	39	-2	2	24	24	-26
3	5	20	23	-24	4	2	21	25	-24	-2	8	21	25	-27	1	5	22	47	46	0	2	24	32	-28
-10	6	20	18	14	6	2	21	23	21	2	8	21	15	12	3	5	22	26	-24	-1	3	24	26	-25
-8	6	20	26	-27	-7	3	21	21	18	-3	9	21	24	25	-6	6	22	51	47					

## REFERENCES

1. N.J.Zvaifler in *Arthritis and Allied Conditions*. 11th Edition, D.J.McCarty (ed), Lea & Febiger, Philadelphia London (1989).
2. D.J.McCarty (ed), *Arthritis and Allied Conditions*. 11th Edition, Lea & Febiger, Philadelphia London (1989).
3. J.Morrow and D.Isenberg, *Autoimmune Rheumatoid Disease*. Blackwell Scientific Publications (1987).
4. M.Fischbach (ed), *Rheumatoid Arthritis*. Churchill Livingstone, New York Edinburgh London Melbourne (1991).
5. J.T.Scott (ed), *Copeman's Textbook of the Rheumatic Diseases*. 5th Edition, Churchill Livingstone, Edinburgh London New York (1978).
6. P.D.Utsinger, N.J.Zvaifler and G.E.Erich (eds), *Rheumatoid Arthritis: etiology, diagnosis, management*. JP Lippincott, Philadelphia (1985).
7. W.N.Kelley, E.D.Harris, S.Ruddy and C.Sludge (eds), *Textbook of Rheumatology*. 3rd Edition, W.B.Saunders Company, Philadelphia (1989).
8. E.D.Harris Jr in *Textbook of Rheumatology*. 3rd Edition, W.N.Kelley, E.D.Harris, S.Ruddy and C.Sludge (eds), W.B.Saunders Company, Philadelphia (1989).
9. H.L.F.Curry in *Copeman's Textbook of the Rheumatic Diseases*. 5th Edition, J.T.Scott (ed), Churchill Livingstone, Edinburgh London New York (1978).
10. J.C.Bennet in *Textbook of Rheumatology*. 3rd Edition, W.N.Kelley, E.D.Harris, S.Ruddy and C.Sludge (eds), W.B.Saunders Company, Philadelphia (1989).
11. D.A.Gerber in *Trace Elements in the Pathogenesis and Treatment of Inflammation*. K.D.Rainsford, K.Brune and M.W.Whitehouse (eds), Birkhäuser Verlag, Basel Boston Stuttgart (1981).
12. J.M.H.Moll, *Arthritis and Rheumatism*. Churchill Livingstone, Edinburgh (1983).
13. S.M.Krane in *Arthritis and Allied Conditions*. 11th Edition, D.J.McCarty (ed), Lea & Febiger, Philadelphia London (1989).
14. I.Sanz and D.Alboukrek in *Rheumatoid Arthritis*. M.Fischbach (ed), Churchill Livingstone, New York Edinburgh London Melbourne (1991).

15. I.L.Bonta, M.J.Parnham, J.E.Vincent and P.C.Bragt, *Progr. Med. Chem.* 1980, **17**, 186.
16. J.R.J.Sorenson, *J. Med. Chem.* 1976, **19**, 135.
17. G.E.Jackson, P.M.May and D.R.Williams, *J. Inorg. Nucl. Chem.* 1978, **40**, 1189.
18. J.R.J.Sorenson in *Metal Ions in Biological Systems*, Volume 14. H.Sigel (ed), Marcel Decker, New York (1982).
19. R.C.Weast (ed), *CRC Handbook of Chemistry and Physics*. 63rd Edition, CRC Press (1982).
20. F.A.Cotton and G.Wilkinson, *Advanced Inorganic Chemistry*. 4th Edition, John Wiley & Sons, New York Chichester Brisbane Toronto (1980).
21. H.W.Wahner, N.P.Goldstein and D.Jenkins in *Nuclear Medicine : Quantitative Procedures*. H.W.Wahner (ed), Little, Brown & Co., Boston (1983).
22. A.J.Lewis, *Agents Actions* 1984, **15**, 513.
23. T.L.Dormandy in *Trace Elements in the Pathogenesis and Treatment of Inflammation*. K.D.Rainsford, K.Brune and M.W.Whitehouse (eds), Birkhäuser Verlag, Basel Boston Stuttgart (1981).
24. G.E.Jackson and M.J.Kelly, *Inorg. Chim. Acta* 1988, **152**, 215.
25. S.C.R.Meacock, B.P.Swan and W.Dawson in *Trace Elements in the Pathogenesis and Treatment of Inflammation*. K.D.Rainsford, K.Brune and M.W.Whitehouse (eds), Birkhäuser Verlag, Basel Boston Stuttgart (1981).
26. J.R.J.Sorenson, *Chem. in Britain* 1984, **19**, 1110.
27. W.R.Walker, R.R.Reeves, M.Brosnan and G.D.Coleman, *Bioinorganic Chem.* 1977, **7**, 271.
28. W.R.Walker, S.J.Beveridge and M.W.Whitehouse in *Trace Elements in the Pathogenesis and Treatment of Inflammation*. K.D.Rainsford, K.Brune and M.W.Whitehouse (eds), Birkhäuser Verlag, Basel Boston Stuttgart (1981).
29. A.J.Lewis, W.E.Smith and D.H.Brown in *Trace Elements in the Pathogenesis and Treatment of Inflammation*. K.D.Rainsford, K.Brune and M.W.Whitehouse (eds), Birkhäuser Verlag, Basel Boston Stuttgart (1981).

30. D.H.Brown, J.Dunlop and W.E.Smith in *Trace Elements in the Pathogenesis and Treatment of Inflammation*. K.D.Rainsford, K.Brune and M.W.Whitehouse (eds), Birkhäuser Verlag, Basel Boston Stuttgart (1981).
31. J.C.Banford, D.H.Brown, R.A.Hazelton, C.J.McNeil, D.R.Sturrock and W.E.Smith, *Ann. Rheum. Dis.* 1982, **41**, 458.
32. A.Conforti, L.Franco, G.Menegale, R.Milanino, G.Piemonte and G.P.Velo, *Pharmacol. Res. Comm.* 1983, **15**, 859.
33. C.Furnival, P.M.May and D.R.Williams in *Trace Elements in the Pathogenesis and Treatment of Inflammation*. K.D.Rainsford, K.Brune and M.W.Whitehouse (eds), Birkhäuser Verlag, Basel Boston Stuttgart (1981).
34. N.A.Roberts and P.A.Robinson, *Br. J. Rheumatol.* 1985, **24**, 128.
35. D.A.Gerber, R.S.Pinals and E.D.Harris in *Histidine. Metabolism, Clinical Aspects, Therapeutic Use*. R.Kluthe and N.R.Katz (eds), Georg Thieme, Stuttgart (1977).
36. J.Burgess, *Ions in Solution*. Ellis Horwood, Chichester (1988).
37. R.Barbucci, L.Fabbrizzi and P.Paoletti, *Inorg. Chim. Acta* 1973, **7**, 157.
38. D.C.Weatherburn, E.J.Billo, J.P.Jones and D.W.Margerum, *Inorg. Chem.* 1970, **9**, 1557.
39. R.M.Smith and A.E.Martell, *Critical Stability Constants*. Volume 2 : Amines. Plenum Press, New York London (1975).
40. R.M.Smith and A.E.Martell, *Critical Stability Constants*. Volume 6 : 2nd Supplement. Plenum Press, New York London (1989).
41. G.E.Jackson and M.J.Kelly, *J. Chem. Soc. Dalton Trans.* 1989, 2429.
42. M.J.Kelly, Personal Communications.
43. J.J.R.Frausto da Silva and R.J.P.Williams, *The Biological Chemistry of the Elements*. Clarendon Press, Oxford (1991).
44. H.Ojima and K.Nonoyama, *Coord. Chem. Rev.* 1988, **921**, 857.
45. H.Ojima and K.Nonoyama, *Z. anorg. allg. Chem.* 1973, **401**, 195..
46. M-S.Chao and C-S.Chung, *J. Chem. Soc. Dalton Trans.* 1981, 683.

47. S-H.Liu and C-S.Chung, *Polyhedron* 1984, **3**, 559.
48. C-H.Len and C-S.Chung, *J. Chem. Soc. Dalton Trans.* 1990, 1755.
49. A.Zuberbühler and S.Fallab, *Helv. Chim. Acta* 1967, **50**, 889.
50. K.Sun Bai and A.E.Martell, *J. Amer. Chem. Soc.* 1969, **91**, 4412.
51. O.Yamauchi, Y.Nakao and A.Nakahara, *Bull. Chem. Soc. Jap.* 1973, **46**, 3749.
52. M.Kodama, T.Yatsunami and E.Kimura, *J. Chem. Soc. Dalton Trans.* 1979, 1783.
53. T.Murakami and K.Chiba, *Bull. Chem. Soc. Jap.* 1986, **59**, 3675.
54. S-J.Lau, T.P.A.Kruck and B.Sarkar, *J. Biol. Chem.* 1974, **249**, 5878.
55. M.Kodama and E.Kimura, *J. Chem. Soc. Dalton Trans.* 1979, 325.
56. J-P.Laussac and B.Sarkar, *Biochemistry* 1984, **23**, 2832.
57. T.Peters Jr and F.A.Blumenstock, *J. Biol. Chem.* 1967, **242**, 1574.
58. D.C.Neckers and M.P.Doyle, *Organic Chemistry*. John Wiley & Sons, New York London Sydney Toronto (1977).
59. F.R.Hartley, C.Burgess and R.Alcock, *Solution Equilibria*. Ellis Horwood, Chichester (1980).
60. A.E.Martell and R.J.Motekaitis, *The Determination and Use of Stability Constants*. VCH Publishers, Inc., New York (1988).
61. P.M.May, K.Murray and D.R.Williams, *Talanta* 1985, **32**, 483.
62. A.Sabatini, A.Vacca and P.Gans, *Talanta* 1974, **21**, 53.
63. P.Gans, A.Sabatini and A.Vacca, *J. Chem. Soc. Dalton Trans.* 1985, 1195.
64. M.T.Beck and I.Nagypal, *Chemistry of Complex Equilibria*. Ellis Horwood, Chichester (1990).
65. H.Rossotti, *The Study of Ionic Equilibria*. Longmans, New York (1978).
66. F.J.C.Rossotti and H.Rossotti, *The Determination of Stability Constants*. McGraw-Hill, New York (1961).
67. IUPAC recommendation I-10.3 in *Nomenclature of Inorganic Chemistry*. (1990).

68. N.Bjerrum, *Z. anorg. allg. Chem.* 1921, **119**, 179.
69. J.Kielland, *J. Amer. Chem. Soc.* 1937, **59**, 1675.
70. P.W.Linder and K.Murray, *Talanta* 1982, **29**, 377.
71. P.W.Linder, R.G.Torrington and D.R.Williams, *Analysis using Glass Electrodes*. Open University Press, Belfast (1984).
72. W.A.E.McBryde, *Can. J. Chem.* 1973, **51**, 3572.
73. G.K.R.Makar, M.L.D.Touche and D.R.Williams, *J. Chem. Soc. Dalton Trans.* 1976, 1016.
74. M.Filella and D.R.Williams, *Inorg. Chim. Acta* 1985, **106**, 49.
75. P.Gans, A.Sabatini and A.Vacca, *Inorg. Chim. Acta* 1976, **18**, 237.
76. P.M.May, K.Murray and D.R.Williams, *Talanta* 1988, **35**, 825.
77. P.M.May and K.Murray, *Talanta* 1988, **35**, 927.
78. A.M.Corrie, G.K.R.Makar, M.L.D.Touche and D.R.Williams, *J. Chem. Soc. Dalton Trans.* 1975, 105.
79. P.M.May and K.Murray, *Talanta* 1988, **35**, 933.
80. W.C.Hamilton, *Acta Crystal.* 1965, **18**, 502.
81. J.A.Ibers and W.C.Hamilton (eds), *International Tables for X-Ray Crystallography*, Volume 4, pp. 288. Kynoch Press, Birmingham (1974).
82. A.Vacca, A.Sabatini and M.Gristina, *Coord. Chem. Rev.* 1972, **8**, 45.
83. E.Teller, *The Pursuit of Simplicity*. Pepperdine University Press, Malibu, California (1980).
84. A.I.Vogel, *Vogel's Textbook of Quantitative Inorganic Analysis*. 4th Edition, J.Bassett, R.C.Denney, G.H.Jeffery and J.Mendham (eds), Longman, London New York (1978).
85. G.Schwarzenbach, *Complexometric Titrations*. Methuen, London (1957).
86. *Complexometric Assay Methods with Titriplex*. 3rd Edition, E.Merck, Darmstadt.
87. G.Biedermann and J.T.Chow, *Acta. Chem. Scand.* 1966, **20**, 2.

88. P.M.May, D.R.Williams, P.W.Linder and R.G.Torrington, *Talanta* 1982, **29**, 249.
89. D.Dyrssen and I.Hanson, *Marine Chemistry* 1972, **1**, 37.
90. E.Högfeldt (ed), *Stability Constants of Metal-Ion Complexes*. Part A : Inorganic Ligands. IUPAC, Pergamon Press, Oxford New York Toronto Sydney Paris Frankfurt (1982).
91. R.Grieser and S.Fallab, *Chimia* 1968, **22**, 90.
92. S.Cattoir, Personal Communications.
93. A.Zuberbühler and Th.Kaden, *Helv. Chim. Acta* 1968, **51**, 1805.
94. K.F.Purcell and J.C.Kotz, *Inorganic Chemistry*. W.B.Saunders Company, Philadelphia London Toronto (1977).
95. U.Kramer-Schnabel and P.W.Linder, *Inorg. Chem.* 1991, **30**, 1248.
96. C.F.Baes Jr and R.E.Mesmer, *The Hydrolysis of Cations*. John Wiley & Sons, New York (1976).
97. W.A.E.McBryde, *Talanta* 1974, **21**, 979.
98. S.F.A.Kettle, *Co-ordination Compounds*. Nelson, London (1969).
99. D.Nicholls, *Complexes and First-Row Transition Elements*. MacMillan, London (1974).
100. A.B.P.Lever, *Inorganic Electronic Spectroscopy*. Elsevier, Amsterdam (1968).
101. H.H.Jaffé and M.Orchin, *Theory and Applications of Ultraviolet Spectroscopy*. John Wiley and Sons, Inc., New York London Sydney (1962).
102. Th.Kaden and A.Zuberbühler, *Helv. Chim. Acta* 1968, **51**, 1797.
103. M-S.Chao and C-S.Chung, *Inorg. Chem.* 1989, **28**, 686.
104. F.J.Quaeyhaegens, H.O.Desseyn, S.P.Perlepes, J.C.Plakatouras, B.Bracke and A.T.H.Lenstra, *Transition Met. Chem.* 1991, **16**, 92.
105. O.Yamauchi, H.Miyata and A.Nakahara, *Bull. Chem. Soc. Japan* 1971, **44**, 2716.
106. R.M.Lewis, G.H.Nancollas and P.Coppens, *Inorg. Chem.* 1972, **11**, 1371.
107. A.Yoshino and W.Nowacki, *Z. Kristallogr.* 1974, **139**, 337.

108. H.Ojima and K.Nonoyama, *Z. anorg. allg. Chem.* 1977, **429**, 282.
109. Y.Journaux, J.Sletten and O.Kahn, *Inorg. Chem.* 1985, **24**, 4063.
110. U.Burkert and N.L.Allinger, *Molecular Mechanics*, ACS Monograph 177, Chapter 1. American Chemical Society (1982).
111. O.Ermer in *Structure and Bonding*, Volume 27. J.D.Dunitz *et al* (eds), Springer-Verlag, Berlin Heidelberg New York (1976).
112. D.A.Buckingham, I.E.Maxwell, A.M.Sargeson and M.R.Snow, *J. Amer. Chem. Soc.* 1970, **92**, 3617.
113. G.J.McDougall, R.D.Hancock and J.C.A.Boeyens, *J. Chem. Soc. Dalton Trans.* 1978, 1438.
114. T.W.Hambley, C.J.Hawkins, J.A.Palmer and M.R.Snow, *Aust. J. Chem.* 1981, **34**, 45.
115. T.W.Hambley, *J. Chem. Soc. Chem. Commun.* 1984, 1228.
116. V.J.Thöm, J.C.A.Boeyens, G.J.McDougall and R.D.Hancock, *J. Amer. Chem. Soc.* 1984, **106**, 3198.
117. K.Hendrick, L.F.Lindoy, M.McPartlin, P.A.Tasker, M.P.Wood, *J. Amer. Chem. Soc.* 1984, **106**, 1641.
118. G.R.Brubaker and D.W.Johnson, *Coord. Chem. Rev.* 1984, **53**, 1.
119. M.G.B.Drew, S.Hollis and P.C.Yates, *J. Chem. Soc. Dalton Trans.* 1985, 1829.
120. M.G.B.Drew and P.C.Yates, *J. Chem. Soc. Dalton Trans.* 1987, 2563.
121. V.J.Thöm, C.C.Fox, J.C.A.Boeyens and R.D.Hancock, *J. Amer. Chem. Soc.* 1984, **106**, 5947.
122. V.J.Thöm, G.D.Hosken and R.D.Hancock, *Inorg. Chem.* 1985, **24**, 3378.
123. N.L.Allinger, *J. Amer. Chem. Soc.* 1977, **99**, 8127.
124. F.Mohamadi, N.G.J.Richards, W.C.Guida, R.Liskamp, M.Lipton, C.Caufield, G.Chang, T.Hendrickson and W.C.Still, *J. Comput. Chem.* 1990, **11**, 440.

125. W.C.Still, F.Mohamadi, N.G.J.Richards, W.C.Guida, M.Lipton, R.Liskamp, G.Chang, T.Hendrickson, F.DeGunst and W.Hasel, *MacroModel V3.0 and V3.1*, Department of Chemistry, Columbia University, New York (1990).
126. R.H.Boyd, *J. Chem. Phys.* 1968, **49**, 2574.
127. M.R.Snow, *J. Amer. Chem. Soc.* 1970, **92**, 3610.
128. N.L.Allinger, *Adv. Phys. Org. Chem.* 1976, **13**, 1.
129. U.Burkert and N.L.Allinger, *Molecular Mechanics*, ACS Monograph 177, Chapter 2. American Chemical Society (1982).
130. D.B.Boyd and K.B.Lipkowitz, *J.Chem.Ed.* 1982, **59**, 269.
131. J.L.De Coen, G.Elefante, A.M.Liquori and A.Damiani, *Nature* 1967, **216**, 910.
132. A.Vedani and J.D.Dunitz, *J. Amer. Chem. Soc.* 1985, **107**, 7653.
133. W.J.Moore, *Physical Chemistry*. 4th Edition, Longmans, London (1963).
134. L.Martin, L.J.DeHayes, L.J.Zompa and D.H.Busch, *J. Amer. Chem. Soc.* 1974, **96**, 4046.
135. M.G.B.Drew, D.A.Rice, S.B.Silong and P.C.Yates, *J. Chem. Soc. Dalton Trans.* 1986, 1081.
136. M.G.B.Drew and D.G.Nicholson, *J. Chem. Soc. Dalton Trans.* 1986, 1543.
137. R.D.Hancock, S.M.Dobson, A.Evers, P.W.Wade, M.P.Ngwenya, J.C.A.Boeyens and K.P.Wainwright, *J. Amer. Chem. Soc.* 1988, **110**, 2788.
138. G.R.Brubaker and D.W.Johnson, *Inorg. Chem.* 1984, **23**, 1591.
139. U.Burkert and N.L.Allinger, *Molecular Mechanics*, ACS Monograph 177, Chapter 6. American Chemical Society (1982).
140. B.M.Pettitt and M.Karplus, *J. Amer. Chem. Soc.* 1985, **107**, 1166.
141. N.L.Allinger, *Q.C.P.E. Program No. MMP2(85)*, Quantum Chemistry Program Exchange, Indiana University Chemistry Department, Indiana (1985).
142. G.Chang, W.C.Guida and W.C.Still, *J. Amer. Chem. Soc.* 1989, **111**, 4379.
143. O.Ermer and S.Lifson, *J. Amer. Chem. Soc.* 1973, **95**, 4121.

144. Cambridge Structural Database. Version 4.4 Cambridge Crystallographic Data Center, University Chemical Laboratory, Cambridge (1991).
145. S.Profeta Jr and N.L.Allinger, *J. Amer. Chem. Soc.* 1985, **107**, 1907.
146. W.J.Colucci, R.D.Gandour and E.A.Mooberry, *J. Amer. Chem. Soc.* 1986, **108**, 7142.
147. D.M.Schnur, Y.H.Yuh and D.R.Dalton, *J.Org.Chem.* 1989, **54**, 3779.
148. J-H.Lii, S.Gallion, C.Bender, H.Wikström, N.L.Allinger, K.Flurchick and M.M.Teeter, *J. Comp. Chem.* 1989, **10**, 503.
149. L.R.Schmitz and N.L.Allinger, *J. Amer. Chem. Soc.* 1990, **112**, 8307.
150. J-H.Lii and N.L.Allinger, *J. Comp. Chem.* 1991, **12**, 186.
151. P.W.Wade, Personal Communications.
152. G.Marongiu, E.C.Lingafelter and P.Paoletti, *Inorg. Chem.* 1969, **8**, 2763.
153. Y.Terui, *J. Chem. Soc. Perkin Trans. II* 1975, 118.
154. F-J.Wu, S-L.Wang, Y-L.Liou and C-S.Chung, *J. Chim. Chem. Soc.* 1989, **36**, 101.
155. J.C.A.Boeyens, F.A.Cotton and S.Han, *Inorg. Chem.* 1985, **24**, 1750.
156. S.V.Deshpande, S.J.Denardo, C.F.Meares, M.J.McCall, G.P.Adams, M.K.Moi and G.L.DeNardo, *J. Nucl. Med.* 1988, **29**, 217.
157. B.Pastakia, L.M.Lieberman, S.J.Gatley, D.Young, D.H.Petering and D.Minkel, *J. Nucl. Med.* 1980, **21**, 67.
158. G.E.Jackson, M.J.Byrne, G.Blekkenhorst and A.J.Hendry, *Nucl. Med. Biol.* 1991, **18**, 855.
159. P.M.May, P.W.Linder and D.R.Williams, *J. Chem. Soc. Dalton Trans.* 1977, 588.
160. G.Berthon, B.Hacht, M.Blais and P.M.May, *Inorg. Chim. Acta* 1986, **125**, 219.
161. G.E.Jackson and M.J.Kelly, *J. Chem. Soc. Dalton Trans.* 1990, 1889.
162. P.M.May and D.R.Williams, *FEBS Lett.* 1977, **78**, 134.
163. C.A.Owen Jr, *Amer. J. Physiol.* 1965, **209**, 900.

164. J.G.McAfee and G.Subramanian in *Freeman and Johnson's Clinical Radionuclide Imaging*. 3rd Edition, L.M.Freeman (ed), Grune & Stratton, Inc., Orlando Florida (1984).
165. W.C.Cole, S.J.DeNardo, C.F.Meares, M.J.McCall, G.L.DeNardo, A.L.Epstein, H.A.O'Brien and M.K.Moi, *J. Nucl. Med.* 1987, **28**, 83.
166. Th.A.Kaden and A.D.Zuberbühler, *Helv. Chim. Acta* 1974, **57**, 286.
167. K.V.V.Voyi, Ph.D. Thesis, University of Cape Town (1988).
168. G.M.Sheldrick, *SHELX86 A Program for the Solution of Crystal Structures*. University of Göttingen (1986).
169. G.M.Sheldrick, *SHELX76 Program for Crystal Structure Determination*. University of Cambridge (1976).
170. J.A.M.Peterse and J.H.Palm, *Acta Cryst.* 1966, **20**, 147.
171. J.A.Ibers and W.C.Hamilton (eds), *International Tables for X-Ray Crystallography*, Volume 4, pp. 99 & 149. Kynoch Press, Birmingham (1974).
172. J.A.Bertrand and J.A.Kelley, *J. Amer. Chem. Soc.* 1966, **88**, 4746.
173. J.A.Bertrand, *Inorg. Chem.* 1967, **6**, 495.
174. B.T.Kilbourn and J.D.Dunitz, *Inorg. Chem.* 1967, **1**, 209.
175. J.A.Bertrand and J.A.Kelley, *Inorg. Chem.* 1969, **8**, 1982.
176. A.El-Toukhy, G-Z.Cai, G.Davies, T.R.Gilbert, K.D.Onan and M.Veidis, *J. Amer. Chem. Soc.* 1984, **106**, 4596.
177. E.M.Holt, S.L.Holt and M.Vlasse, *Cryst. Struct. Comm.* 1979, **8**, 767.
178. R.L.Harlow and S.H.Simonsen, *Acta Cryst.* 1977, **B33**, 2784.
179. R.Belford, D.E.Fenton and M.R.Truter, *J. Chem. Soc. Dalton Trans.* 1972, 2345.
180. R.D.Hancock and G.J.McDougall, *J. Amer. Chem. Soc.* 1980, **102**, 6551.
181. R.D.Hancock, *Prog. Inorg. Chem.* 1989, **37**, 187.